Modulation of microRNA processing by 5-Lipoxygenase

Dissertation

zur Erlangung des Doktorgrades

der Naturwissenschaften

vorgelegt beim Fachbereich Biochemie, Chemie und Pharmazie

der Johann Wolfgang Goethe Universität

in Frankfurt am Main

von

Carola Friederike Scholl

aus Staufenberg

Frankfurt am Main, 2015

(D30)

Vom Fachbereich Biochemie, Chemie und Pharmazie
der Johann Wolfgang Goethe Universität als Dissertation angenommen.

Dekan: Prof. Dr. Michael Karas

Gutachter: Prof. Dr. Dieter Steinhilber
Prof. Dr. Beatrix Süß

Datum der Disputation: 20. Oktober 2016

Live as if you were to die tomorrow.

Learn as if you were to live forever.

- Mahatma Gandhi

CONTENTS

1 ABBREVIATIONS

Δ	Knock-down
AA	Arachidonic acid
AEBSF	4-(2-Aminoethyl) benzenesulfonyl fluoride hydrochloride
Ago	Argonaute
APS	Ammonium persulfate
ATP	Adenosine triphosphate
B2M	β2-microglobulin
BSA	Bovine serum albumin
(c)AMP	(Cyclo)adenosinmonophosphate
(c)DNA	(Copy) desoxyribonucleic acid
CFTR	Cystic fibrosis transmembrane conductance regulator
CLP	Coactosin-like protein
$cPLA_2$	Cytosolic phospholipase A_2
DAG	Diacylglycerole
DEPC	Diethylpyrocarbonate
DMSO	Dimethyl sulfoxide
(d)NTP	(Deoxyribose) nucleoside triphosphate
DSMZ	Deutsche Sammlung von Mikroorganismen und Zellkulturen
DTT	Dithiothreitol
E.coli	*Escherichia coli*
EDC	1-Ethyl-3-(3-dimethylaminopropyl)carbodiimide
EDTA	Ethylenediaminetetraacetic acid
FCS	Fetal calf serum
FLAP	5-Lipoxygenase activating protein
(G)M-CSF	(Granulocyte-)macrophage colony-stimulating factor
GPCR	G protein coupled receptor
GPx-1	Glutathione peroxidase-1
HCV	Hepatitis C virus
HDAC	Histone deacetylase

HETE	Hydroxyeicosatetraenoic acid
HuR	Human antigen R
IFN	Interferon
IL	Interleukin
IP_3	Inositoltriphosphate
LO	5-Lipoxygenase
LOOH	Lipid hydroperoxides
LPS	Lipopolysaccharide
LT	Leukotriene
MAPEG	membrane-associated proteins in eicosanoid and glutathione metabolism
miRNA	microRNA
MM6	Mono Mac 6
MQ	Milli-Q
ND	Not detectable
NF-κB	Nuclear factor 'kappa-light-chain-enhancer' of activated B-cells
NMD	Nonsense-mediated mRNA decay
NP-40	Tergitol-type 40
Oe	Overexpression
ORP9	Oxysterol binding protein-like 9
PAGE	Polyacrylamide gel electrophoresis
PBMC	Peripheral blood mononuclear cell
PBS	Phosphate buffered saline
PFA	Paraformaldehyde
PG	Prostaglandin
PLC	Phospholipase C
PMA	Phorbol-12-myristat-13-acetate
PMSF	Phenylmethanesulfonylfluoride
PTC	Premature termination codons
RANKL	Receptor activator of NF-κB ligand
RNA	Ribonucleic acid
ROS	Reactive oxygen species
RXR	Retinoid X receptor

SDS	Sodium dodecyl sulfate
Ser	Serine
shRNA	Short hairpin RNA
STI	Soybean trypsin inhibitor
TBE	Tris/Borate/EDTA
TEMED	Tetramethylethylenediamine
TFA	Trifluoroacetic acid
TGF	Transforming growth factor
TGFRE	Transforming growth factor β responsive element
TNF	Tumor necrosis factor
TNFAIP	Tumor necrosis factor alpha induced protein
TNRC	Trinucleotide repeat-containing gene
TP53	Tumor protein 53
TRIM	Tripartite motif
VDRE	Vitamin D response element
VDR	Vitamin D receptor
Wt	Wild type

2 INTRODUCTION

2.1 5-Lipoxygenase

2.1.1 Leukotriene biosynthesis

5-Lipoxygenase (5-LO) is an inflammatory enzyme responsible for the first two steps in the biosynthesis of proinflammatory leukotrienes (LTs) from arachidonic acid [2]. LTs are important immune mediators which cause leukocyte chemotaxis and enhanced vascular permeability. They are formed from arachidonic acid (AA), a fatty acid and component of phospholipids in cell membranes. AA is liberated by cytosolic phospholipase A2 ($cPLA_2$) at high intracellular calcium concentrations [3]. A calcium increase is triggered, for example, by the activation of $G_{\alpha q}$ coupled receptors like H1 histamine receptors or by activation of the MAP kinase pathway. Both mobilize phospholipase C (PLC) which results in the release of inositoltriphosphate (IP3). This secondary

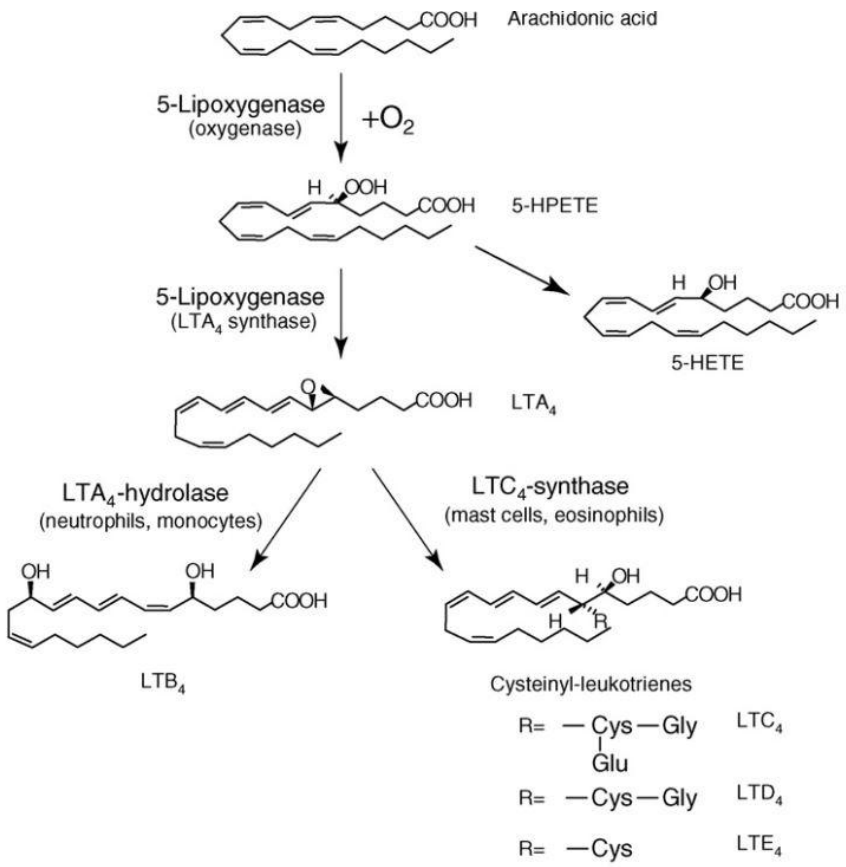

Figure 1: Leukotriene pathway
Conversion of AA to 5-HETE and LTs [1]

messenger causes the opening of Ca^{2+} channels and leading to an increase in calcium levels.

AA is transformed into LTs in a 5-LO dependent two step mechanism. The first step (see Figure 1) is the oxidation to 5-hydroperoxyeicosatetraenoic acid (5-HPETE). This intermediate can be reduced either 5-LO independently to the corresponding alcohol 5-hydroxyeicosatetraenoicacid (5-HETE) [4] or further metabolized by the LTA_4-synthase function of 5-LO into the unstable epoxide LTA_4. This product can be further hydrolysed by LTA_4-hydrolase to LTB_4 [5] or transformed into the glutathione conjugated slow response LTC_4, a cysteinyl-LT (cys-LT), by LTC_4-synthase [6].

Depending on the cell type, the formation pattern of LTB_4 and cys-LTs can vary. For example, neutrophils and monocytes express high level of LTA_4-hydrolase accompanied with dominating LTB_4 formation while mast cells and eosinophils exhibit increased level of LTC_4-synthase and cys-LTs, respectively. Besides LTC_4, LTD_4 and LTE_4 also belong to the family of cys- LTs.

As shown in Figure 1, they only differ in their amino acid substitution from LTC_4. Outside the cell LTC_4 can be converted either into LTD_4 or LTE4 by ubiquitously expressed enzymes. Their biological relevance is further discussed in chapter 2.2.

Two further human AA metabolizing LOs exist, 12-LO and 15-LO. The family members differ in their positional specificity of arachidonic acid oxygenation, indicated by their respective numbers (for review see [7]). 12-LO and 15-LO were not included in this study.

2.1.2 Transcriptional regulation of 5-LO

The 5-LO gene (ALOX5) is located on chromosome 10q11.2. Its putative promoter region contains multiple GC boxes but no TATA and CCAAT sequences, a characteristic common for house-keeping genes [8]. Several regulatory elements within the promoter region are identified by now (see Figure 2). Among them are vitamin D response elements (VDREs) [9, 10] and inhibitory methylation sites which prevent binding of the transcription factor Sp1 to the GC rich elements [11].

VDREs are activated by binding of a heterodimer, consisting of the vitamin D receptor (VDR) and the retinoid X receptor (RXR) [12]. Such heterodimers act as transcription factor and can

activate transcription. Their assembly is initiated by 1α,25-dihydroxy-vitamin D_3 (calcitriol), the biologically active form of vitamin D_3 [9]. In 2007, Seuter *et al.* showed that from 22 putative

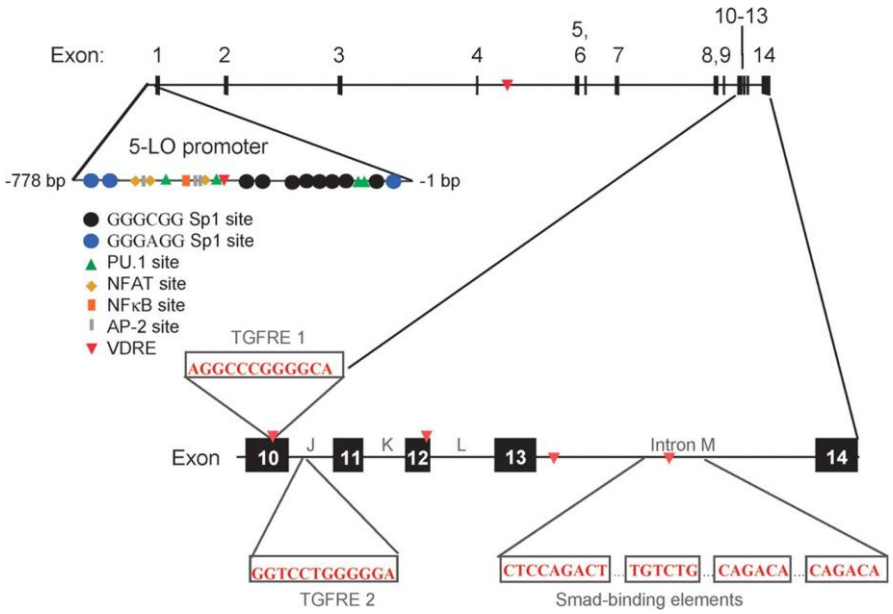

Figure 2: The human 5-LO gene

Several 5-LO promoter sites are described, but the main is shown here (adapted from [13]). It is located at position 0 and starts 65 nucleotides upstream of ATG. Regulatory elements within the transcription initiation side and the coding region of the gene are indicated. Abbr.: Specific protein 1, Sp1; nuclear factor of activated T-cells, NFAT; nuclear factor kappa-light-chain-enhancer of activated B cells, NF-κB; activating Protein 2, AP-2; Vitamin D response element, VDRE; transforming growth factor response element, TGFRE.

VDREs in the 5-LO gene at least two are functional VDREs and proved that the 5-LO gene is a calcitriol target gene [14]. Three years later three further VDREs in the distal part of the 5-LO gene have been identified. Activation of these regions with calcitriol and the cytokine transforming growth factor β (TGFβ) leads to histone modifications associated with open chromatin, resulting in transcription elongation [15]. Already in 1994, the combination of calcitriol and TGFβ was shown to induce 5-LO expression and activity [16]. But not until 2007 could this be attributed to specific regions inside the 5-LO gene. Besides VDREs, SMAD-binding elements and TGFβ responsive elements were identified to be involved in calcitriol/TGFβ dependent activation of 5-LO expression [17]. SMAD proteins are homologs of the protein SMA (small body size) in *Caenorhabditis elegans* and MAD (mothers against decapentaplegic) in *Drosophila melanogaster*, a portmanteau resulting in the name SMAD. They are transcription factors activated by the TGFβ pathway. In absence of this cytokine, SMADs are located in the

nucleus and the cytoplasm. Upon TGFβ release and activation of its corresponding receptors, they are phosphorylated and accumulate in the nucleus to enhance transcription [18].

In the monocytic cell line Mono Mac 6 (MM6) [19] a calcitriol/TGFβ independent low basal 5-LO mRNA expression exists. Upon differentiation with these mediators, 5-LO mRNA levels are induced up to 64 fold [16]. The DNA methylation and the promoter activity are not affected by calcitriol/TGFβ [17], instead differentiation has an effect on transcription elongation and maturation.

2.1.3 Post-transcriptional regulation of 5-LO

Besides regulatory events at the level of mRNA transcription, post-transcriptional control mechanisms at the level of splicing or translation influence 5-LO expression.

Alternative splicing is a cellular mechanism to generate several transcripts from one single gene. In the case of 5-LO, Boado *et al.* found several 5-LO isoforms in human brain tumors correlating with tumor malignancy [20]. In 2012, Ochs *et al.* published seven new alternatively spliced transcripts in MM6 cells. Most of the determined transcripts contain premature termination codons (PTC), which in consequence lead to nonsense-mediated mRNA decay (NMD) [21]. NMD is a quality control mechanism to degrade irregular mRNAs. Targets are next to the endogenous NMD substrates also mRNA emerging from mutated genes with PTCs 50 to 55 nt upstream of the final exon-exon junctions (50 to 55 nt rule). In case of 5-LO, the physiological role of NMD is still unclear, but is suggested to be involved in the regulation of wildtype (wt) 5-LO. Apart from this, the group around Marc E. Surette observed the 5-LOΔ13 isoform, which is lacking exon 13, in several cell lines. It was also identified in MM6 cells [21]. Interestingly, this isoform shows a negative correlation with 5-LO product formation [22] and is an indicator for the importance of alternative splicing on the regulation of 5-LO.

A recent work focused on 5-LO as a target of microRNAs (miRNA). These small non-coding RNAs are post-transcriptional regulators of protein biosynthesis and are further discussed in chapter 2.3. Two representatives, miR-19a-3p and miR-125b-5p, were confirmed to directly interact with 5-LO. Interestingly, 5-LO mRNA level were observed to be independent of miR-19a-3p and miR-125b-5p expression, but silencing of these miRNAs lead to an increase in

5-LO protein expression [23]. This indicates a role of miR-19a-3p and miR-125b-5p in translational repression rather than mRNA decay. However in contrast to the effect of miRNAs on 5-LO protein expression, 5-LO product formation is unaffected by miRNA silencing. This implies further elements exceeding miRNA regulation in 5-LO activity.

2.1.4 5-LO enzyme

The human 5-LO monomer contains 673 amino acids corresponding to 78 kDa. The enzyme is primarily located in the cytoplasm, but also acts in the nucleus [24]. It consists of two domains, the N-terminal domain and the catalytically active C-terminal domain. The N-terminal domain is able to bind Ca^{2+}, an important factor to activate 5-LO translocation to the nuclear membrane, while the C-terminal domain harbors a non-heme iron which changes oxidation state (Fe^{2+} /Fe^{3+}) during the catalytic cycle. Zileuton as 5-LO specific inhibitor, coordinates the iron and thereby blocks the transformation of AA [25]. Zileuton is a hydroxyurea derivative and the only licensed 5-LO inhibitor on the market. Its area of application is further covered in chapter 2.2.2. Another way to decrease 5-LO product formation is the application of inhibitors of the 5-LO activating protein (FLAP) like MK-886 [26]. FLAP was identified as an 18 kDa protein which specifically bound to the inhibitor and was necessary for LT biosynthesis [27, 28]. However, LT formation was only moderately reduced by MK-886 when exogenous AA was added to cells incubation. FLAP belongs to the membrane-associated proteins in eicosanoid and glutathione metabolism (MAPEG). It is the only member which does not exhibit any enzymatic activity (see [29] for review). FLAP is suggested to act as a scaffold for 5-LO at the nuclear membrane and may facilitate the transport of AA to the active side of 5-LO [30]. In absence of FLAP, 5-LO does not translocate to the nuclear membrane leading to an inhibition of LT biosynthesis [31]. Binding of 5-LO to FLAP occurs via its C-terminal domain [32]. In contrast binding of the other 5-LO scaffold protein Coactosin-like protein (CLP) [33] involves the N-terminal region of 5-LO. Three tryptophan residues in this region, in the ligand-binding loops of the C2-like domain to which hyperforin binds [34], were identified to be essential for binding of CLP. An exchange of W13, W75, and W102 to alanins resulted in the 5-LO W13/75/102A mutant which is incapable of interacting with CLP [35]. Furthermore, the mutant is not able to bind to Phosphatidylcholin

[36]. However, Esser *et al.* could show that the single 5-LO-W102 is essential for binding to CLP [37]. The C2-like domain of 5-LO is also involved in the interaction with Dicer, the W13/75/102A triple mutant did not bind to Dicer in vitro [38].

CLP is an F-actin binding protein [39, 40] and is suggested to comigrate with 5-LO upon stimulation with Phorbol-12-myristate-13-acetate (PMA). Compared to FLAP, this protein is not essential for cellular LT biosynthesis but CLP supports 5-LO activity in vitro [35, 37]. In intact cells both FLAP and CLP were required for efficient translocation of 5-LO to the nuclear membrane, and 5-LO activity [31].
Dicer in turn is involved in the maturation of miRNAs, further described in chapter 2.3. The involvement in the LT biosynthesis by binding to 5-LO is not well studied yet. Dicer had a weak upregulating effect on 5-LO activity in vitro, possibly similar to the effect of CLP [38].

2.1.5 5-LO activity

An increase of intracellular Ca^{2+} level leads to an activation of cPLA2 as shown in Figure 3. Dependent on its phosphorylation status [41] cPLA2 releases AA from membrane integrated phospholipids [42]. This fatty acid may bind to FLAP at the nuclear membrane [43]. Just as cPLA2, 5-LO gets also activated by increasing concentrations of intracellular calcium and translocates to the nuclear membrane from the cytoplasm or the nucleoplasm, respectively [44]. This action is supported by phosphorylations at Serine271 by MAPKAP kinases and Serine663 by ERK2 during cell stress [45-47]. Mutations at these sides or treatment with tyrosine kinase inhibitors lead to inhibition of 5-LO translocation and activity [45], while incubation with arachidonic acid leads to the opposite effect [48]. At the nuclear membrane, 5-LO is believed to interact with AA bound by FLAP. The fatty acid is subsequently transmitted to the active site of 5-LO [30], and transformed to the respective products as shown in Figure 1.

The localization of 5-LO in unstimulated cells is cell type dependent. For example, in MM6 cells 5-LO is located primarily in the cytoplasm. Upon stimulation and phosphorylation at Serine271 5-LO migrates to the nucleus [49]. In contrast, phosphorylation at Serine523 [50] prevents nuclear import and translocation [51]. The exact function of nuclear 5-LO is not well characterized yet, but an interaction with FLAP/LTC_4-synthase at the outer membrane and with FLAP/LTA_4-hydrolase at the inner nuclear membrane, are suggested [30].

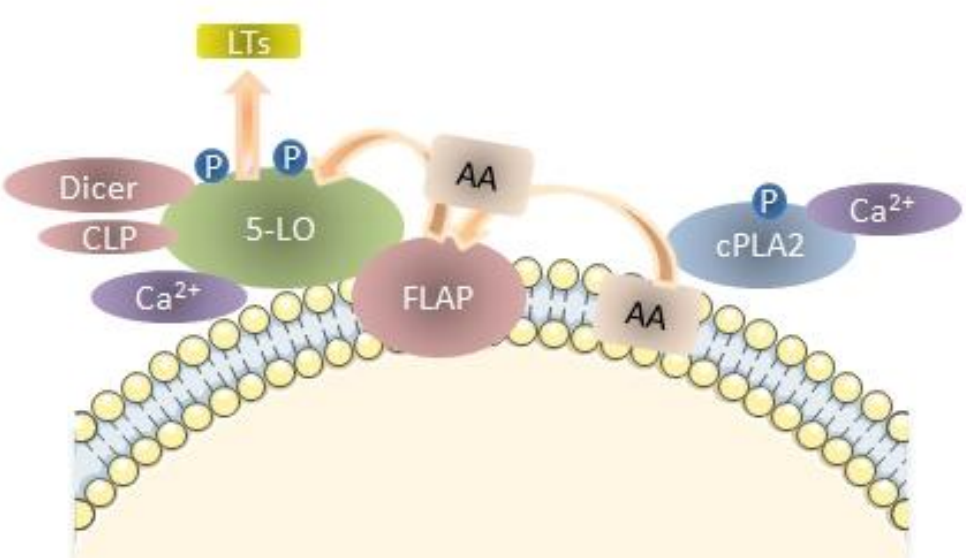

Figure 3: Regulation of 5-LO activity
Upon an increase of intracellular Ca^{2+} level and phosphorylation of cytosolic phospholipase A2 ($cPLA_2$), arachidonic acid (AA) is liberated from phospholipids. Free AA then binds to the membrane bound 5-LO activating protein (FLAP) which transfers the AA to the active center of 5-lipoxygenase (5-LO) where it is transformed to the respective LTs (see Figure 1).Phosphorylation and calcium binding supports 5-LO activity whereas the role of the 5-LO interacting proteins CLP and Dicer is still unclear (adapted from [13]).

Another regulatory element of 5-LO activity is the redox status, and glutathione peroxidase-1 (GPx-1). In general it reduces hydrogen peroxide to water and protects the organism from oxidative damage. Furthermore, GPx-1 is able to reduce lipid hydroperoxides (LOOH) levels. LOOHs are able to stimulate leukotriene biosynthesis by converting the non-heme iron in the active side of 5-LO from the inactive Fe^{2+} status to the active Fe^{3+} status. Hence, GPx-1 is capable of inhibiting leukotriene formation by decreasing the levels of 5-LO stimulating LOOHs. But

increased Ca^{2+} levels can protect 5-LO against the glutathione peroxidase action by binding of $Ca^{2+}$to the C2-like domain of 5-LO [52, 53].

In addition, it was shown in 2002, that treatment with lipopolysaccharides (LPS) affects 5-LO. LPS are part of the outer membrane of Gram negative bacteria. They act as antigen and activate toll-like receptor 4 (TLR4) signaling. Pacheco *et al.* showed that addition of LPS induces lipid body formation in mice, which contained eicosanoid-forming enzymes [54]. Additionally, LPS leads to an enhanced release of AA in monocytes associated with an increase in LT production [55]. To what extent the increased release of LTs is attributed to the different cytokines mobilized by activation of TLR4 is not yet known. Binding of LPS leads to an activation of the proinflammatory transcription factor nuclear factor 'kappa-light-chain-enhancer' of activated B-cells (NF-ϰB) and MAP kinases. Furthermore LPS controls the release of tumor necrosis factor (TNF) α and interleukin (IL) 6 (for detailed review of LPS activity see [56]). It was already shown in 1987 that TNFα enhances LT biosynthesis [57] and many publications followed showing the importance of this cytokine for 5-LO activity [58-60]. In addition, increasing levels of LTs accompany enhanced release of IL-4 [61, 62].

2.2 LTs

2.2.1 LTs in the immune system

LTs are mediators of inflammation and their biosynthesis is tightly regulated. They are involved in the regulation of the immune system, both in normal host defence, and in inflammatory diseases. The best explored LTs are LTB_4 and the cysteinyl LTs LTC_4, LTD_4, and LTE_4. LTB_4 is a potent chemoattractant for granulocytes [63-65], while cysteinyl LTs cause plasma extravasation and edema [66]. Cys-LTs are also involved in the activation and mobilization of dendritic cells [67, 68]. For LTB_4 two G-protein coupled receptors (GPCR) are described: BLT1 [65] and BLT2 [69]. They differ in their expression, their affinity, and their specifity towards LTB_4. BLT1 is mainly expressed on granulocytes, monocytes, macrophages, mast cells, dendritic cells and effector T-cells whereas BLT2 is ubiquitously expressed. BLT1 shows a high affinity towards LTB_4 while the activation of BLT2 needs higher LTB_4 concentrations [70]. The primary ligand

for BLT2 is 12-hydroxy-heptadecatrienoic acid, synthesized in activated blood platelets and macrophages and involved in wound healing [71].

Activation of BLT1 leads to decreased intracellular cAMP level [72] resulting in reduced protein kinase activity. Furthermore, binding of LTB_4 to this receptor activates PLC which in turn increases the turnover of phospholipids to inositoltriphosphate (IP_3) and diacylglycerol (DAG) [73]. As described in chapter 2.1.1, this results in elevated intracellular calcium level.

Cysteinyl LTs can also activate two receptors, $CysLT_1$ [74, 75] and $CysLT_2$ [76]. They are classified according to their sensitivity against CysLT receptor antagonists like montelukast or zafirlukast. $CysLT_1$ describes the receptor sensible for receptor antagonists while the $CysLT_2$ receptor is responsible for effects not inhibitable by these compounds. Both are GPCRs and increase intracellular calcium level by activating PLC [74-76]. $CysLT_1$ is mainly expressed in peripheral blood leukocytes, lung, and spleen tissue and LTD_4 has the highest affinity towards this receptor (EC_{50}= 0.4 nM). LTC_4, EC_{50}= 21 nM and LTE_4, EC_{50}= 212 nM respectively, need much higher expression levels to activate the $CysLT_1$ receptor [74]. $CysLT_2$ is also expressed in peripheral blood leukocytes and lung tissue but amongst others also in the heart, in vascular endothelial and in smooth muscle cells [77]. LTD_4, EC_{50}= 104 nM and LTC_4 with an EC_{50} of 67 nM respectively, have comparable affinities towards $CysLT_2$ although much weaker than towards $CysLT_1$. LTE_4, with an EC_{50} of 2300 nM, is even suggested as a partial agonist [78].

2.2.2 LTs in disease

LTs are by now identified to be dysregulated in several chronic diseases like asthma [79], cardiovascular diseases [80], and cancer [81]. Asthma is an inflammatory disease characterized by alternating level of bronchoconstriction, mucus secretion, and airway hyper-responsiveness. Worldwide approximately 300 million people suffer from this disease with divergent causes, however the prevalence to sicken rises with obesity and the exposure to smoke [82, 83]. In particular Th2 cytokines are suggested to be responsible for increased LT level in asthmatic patients. A combination of IL-3, IL-4, and IL-5 was shown to enhance cys-LT generation by increasing expression of LTC_4-synthase [84] and IL-4 together with IL-13 leads to an upregulation in $CysLT_1$ receptor expression [85].

Based on this knowledge, specific cys-LT receptor antagonists were developed for the treatment of asthma. As mentioned in chapter 2.2.1, Montelukast (Singulair®) is the only approved $CysLT_1$ receptor antagonist available on the German market [86]. Additionally, Zafirlukast (Accolate®), another $CysLT_1$ receptor antagonist, and a 5-LO inhibitor called Zileuton (Zyflo®) are on the US market for the treatment of asthma. Due to short half-life and side effects, Zileuton was never approved in Germany.

Cardiovascular diseases are notably spread in developed nations. In 2013 more than 350,000 people died in Germany alone as a consequence of cardiovascular diseases, according to the Statistisches Bundesamt [87]. This implies a need of action in the treatment of these diseases. Already in the early 1980s, Dahlén *et al.* showed an involvement of cys-LTs in the constriction of arterioles and the extravasation of macromolecules from postcapillary venules. In this context, LTB_4 induces a reversible leukocyte adhesion to these vessels [88].

Various cardiovascular diseases like the ischemic heart disease, stroke, and the peripheral artery disease involve atherosclerosis. An indication for this disease is the generation of so called foam cells. These cells originate from macrophages which uptake deposited oxidized LDL (oxLDL) which was deposited on blood vessels. In the year 2009 Silva *et al.* showed that lipid bodies in these foam cells are able to form LTs [89]. Apart from this, the 5-LO and the FLAP genotype seem to be relevant for the development of atherosclerosis and the risk to suffer from myocardial infarction or stroke [90-92]. A study was conducted by the University of Calgary to determine the effect of montelukast on the brachial artery's function in patients with coronary artery disease. Unfortunately the trial was terminated at the end of 2014 due to difficulties in recruiting suitable participants. But another phase II trial, completed in 2008, showed a reduced LT production within 12 weeks in patients suffering from acute coronary syndrome after treatment with VIA-2291(Atreleuton) [93]. This Zileuton follow-up 5-LO inhibitor, also known as ABT 761, exhibits a protective effect against bronchoconstriction in asthmatics [94]. However, a recently published study could not show a correlation between inhibition of LTs and reduction in vascular inflammation [95].

In the last 20 years more and more publications reveal elevated LT level in several forms of cancer. [96]. In case of prostate cancer cells, their growth is stimulated by 5-HETE but not by

other LTs [97]. Already in 1983 LTB_4 and 5-HETE were found to be dysregulated in some patients with chronic myeloid leukemia (CML). This abnormality was referred to the possible deficiency of 5-LO in the polymorphonuclear neutrophils of these patients [98]. Furthermore, ALOX5 deficient mice did not develop CML in a BCR-ABL dependent model. BCR-ABL is no longer able to induce formation of leukemia stem cells. This model is supported by the observation that Zileuton treatment suppresses leukemic stem cells and prolongs survival of CML mice compared to placebo treated mice [99]. Roos *et al.* could even expand these findings to acute myeloid leukemia (AML) [100]. They showed that 5-LO is involved in the regulation of the Wingless-related integration side (Wnt) signaling pathway and β-catenin, both implicated in growth of leukemia stem cells. A phase I study [NCT01130688] tried to determine the toxicity and safety profile of Zileuton in combination with Imatinib (Gleevec®) for CML, but the trial was terminated without mentioning reasons.

To summarize, it seems to be a promising approach to expand the application of 5-LO inhibitors and CysLT1 receptor antagonists to cardiovascular diseases and cancer therapies and thereby inhibiting excessed LT production. However, the search for novel, more effective 5-LO inhibitors is a current need.

2.3 MicroRNA

2.3.1 History and nomenclature

MicroRNAs (miRNA) are a class of noncoding RNAs. In 1989, Hodgkin *et al.* found the first evidence for a new control mechanism in the nematode *C. elegans* [101]. Four years later, the same group suggested a short noncoding RNA to interact with the 3' UTR of the *lin-14* mRNA via complementary sequences leading to a negative regulation of its expression [102]. Therefore, they published the first member of the new class of regulatory RNAs. However, it took further seven years to identify let-7, a second representative [103]. Shortly afterwards its sequence was found to be conserved among several species, including humans [104]. This started a whole new field of investigation and established the term "microRNA" [104].

In 2003, leading researchers in the field of miRNA research introduced a system for miRNA annotation [105]. They are named using the "miR" prefix, followed by a dash and a unique identifying number. MiRNAs having high sequence homologies are grouped in a family and often occur to have the same number with successive letters, for example miR-125a and miR-125b. As further described in 2.3.2, two miRNAs can originate from opposite arms of a common precursor. In this case they are denoted with the suffix -3p for the 3' strand and -5p for the 5' strand, respectively. The introduction of this suffix replaced the old labeling with an asterisk (*) for the less abundant mature miRNA.

2.3.2 MicroRNA biogenesis

The current miRBase version 21 [106] includes 2603 human mature miRNAs. MiRBase is a database of published miRNA sequences and is managed by the Griffiths-Jones lab at the Faculty of Life Sciences, University of Manchester. Many miRNA genes derive from independent transcription units [107], but about one third of human miRNA genes are located in introns of pre-mRNAs [108, 109]. In some cases related miRNA are located in close proximity to each other and are transcribed as a multi-cistronic primary transcript [107]. MiR-99b-5p, let-7e-5p, and miR-125a-5p, for example, represent such a cluster.

In general the miRNA genes are transcribed by RNA polymerase II and the resulting transcript, called pri-miRNA, is capped and polyadenylated [110]. One transcript can contain several miRNA precursors, also called pre-miRNA. These hairpin structures are ~65 nucleotides in length and are released by the nuclear RNAse III Drosha [111]. The pre-miRNAs have a two nucleotide overhang at their 3' ends by which they are recognized by Exportin-5. This protein is a member of the karyopherin protein family which is involved in nuclear ex- and import, and transports the pre-miRNA from the nucleus to the cytoplasm [112]. In this compartment the pre-miRNA is further processed by the RNase III enzyme Dicer (see Figure 4 for an overview of miRNA maturation) and yields to an imperfect miRNA:miRNA* duplex [113]. Dicer binds to a protein called human immunodeficiency virus-1 trans-activation response RNA-binding protein (TRBP) resulting in an enhanced RNA-binding capacity of Dicer [114, 115].

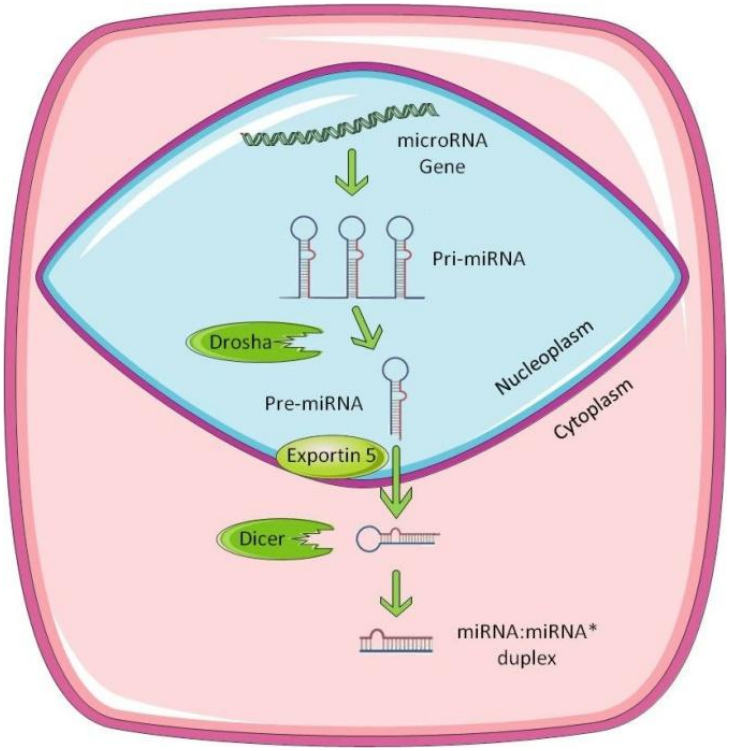

Figure 4: MicroRNA biogenesis
MicroRNA (miRNA) originate from long primary transcripts (pri-miRNA) consisting of one or several stem-loop structures. Inside the nucleus they are processed by the RNase III Drosha to form precursor miRNA (pre-miRNA) which are single stem-loop structures. In the next step, the pre-miRNA is exported to the cytoplasm by Exportin 5 and finally cleaved by Dicer to form miRNA duplexes.

TRBP in turn recruits Argonaute (AGO) proteins to form a complex which is called the pre-RNA induced silencing complex (pre-RISC) [115]. There are four human AGO proteins. They are able to incorporate miRNA duplexes without subtype specificity. Afterwards the miRNA guide strand is selected due to thermodynamic stability while the passenger strand is released and quickly degraded to generate the mature RISC [116]. Among human AGO proteins AGO2 has a special function as it exhibits a cleaving capacity for perfect match passenger strands and target mRNAs [117]. In general the incorporated miRNA leads the complex to the 3' UTR of the target mRNA by perfect match base pairing of nucleotides 2-8, the seed region of the miRNA [118]. The importance is further described in chapter 2.3.3.

2.3.3 RNA induced silencing complex assembly

Binding of RISC to mRNA, guided by the miRNA, leads to either translational inhibition or deadenylation followed by mRNA decay. It is suggested that in the majority of cases a combination of both mechanisms leads to silencing of protein biosynthesis, but the degree of participation is still in discussion [119-122]. As mentioned in 2.3.2, AGO proteins play an essential role in RISC formation and selection of the guide strand.The N-terminal end contains the N-terminal domain and the PAZ domain. They recognize the 3' overhang of the guide strand, while at the same time unwinding and releasing the miRNA duplex [123]. The C-terminal end contains the middle (MID) domain and a P-element induced wimpy testis (PIWI) domain. In their interface region the 5' phosphate of the miRNA guide strand is anchored [124, 125].

After accessing the target mRNA, AGO recruits further proteins to perform deadenylation or translational repression. One important interaction partner of AGO proteins belongs to the GW protein family. Members of this protein family exhibit multiple glycine-tryptophan (GW) repeats in their N-terminal domain by which they can bind to AGO proteins [124]. Trinucleotide repeat-containing gene 6A-C (TNRC6A-C) protein is the human paralog of the GW182 protein in *C. elegans*. TNRC6C was identified as negative regulator of translation [126] and initiator of deadenylation [127]. The deadenylation is performed by the CCR4-NOT complex although no direct association between RISC and this deadenylation complex was observed [128]. On the contrary, miRNA activity can be negatively regulated by tripartite motif 65 (TRIM65). This protein targets TNRC6 for ubiquitination and subsequent degradation [129]. This results in arrested deadenylation of the miRNA targeted mRNA.

Additionally, AGO stability can be altered by ubiquitination [130] or hydroxylation [131] and phosphorylation seems to determine localization and RNA binding [132, 133].

2.3.4 Regulation of Drosha

Drosha processes pri-miRNA to form pre-miRNA (see chapter 2.3.2). This is a complex process, including several regulatory elements. Essential for miRNA processing is the so called microprocessor complex [134, 135] containing Drosha and DGCR8 (DiGeorge syndrome

chromosomal/critical region 8). Drosha consists of an N-terminal part responsible for nuclear localization and a C-terminal part carrying a double-stranded RNA (dsRNA) binding region as well as a tandem RNAse III motif. These two motifs form a processing center and each RNAse motif cleaves one strand of the pri-miRNA [136]. The middle part of Drosha was identified to be responsible for binding of DGCR8. Mutational studies revealed that this interaction is essential for nuclear miRNA processing [137] and furthermore stabilize the Drosha protein. Drosha in turn regulates DGCR8 expression as it recognizes a loop in its mRNA and cleaves it as part of an autoregulatory mechanism [138]. DGCR8 is a nuclear protein without enzymatic activity. It interacts via its C-terminus with Drosha and increases pri-miRNA binding activity through two dsRNA binding regions. The N-terminal part is necessary for nuclear localization [139].

Beyond structural properties, the group of David Bartel identified regulatory motifs in the pri-miRNA specific for humans [140]. This includes a basal UG motif and a CNNC motif (N = any nucleotide) 17-18 nt downstream of the Drosha cleavage side. This region is able to interact with SRp20 resulting in enhanced pri-miRNA processing. SRp20 is known to be involved in splicing [141], nuclear export of mRNA [142], translational initiation [143], and alternative polyadenylation [144]. Thereby it reveals a multitude of potential regulatory mechanisms influencing the Drosha performance. Recently, the same CNNC motif was shown to interact with p73 [145], a tumor suppressor protein related to p53.

Additionally, the miRNA maturation can be modified by posttranslational modifications of the microprocessor. Phosphorylation of Drosha at Serine300 and Serine302 by glycogen synthase kinase 3 beta (GSK3β) maintains the enzyme inside the nucleus [146]. Phosphorylation of DGCR8 increases protein stability [147]. An acetylation at the N-terminus of Drosha has the same stabilizing effect [148], whereas acetylation of DGCR8 inhibits microprocessor activity due to a decreased affinity towards the pri-RNA [149]. Besides the interaction between Drosha and DGCR8, p68 and p72 are also able to bind to Drosha. These two members of the DEAD box family of RNA helicases are involved in RNA metabolism. They take part in unwinding RNA duplexes, catalyze RNA annealing and are able to remove proteins bound to RNA [150]. In general, DEAD box proteins are part of multi-protein complexes and are capable of regulating transcription. In 2008 it was shown by Davis *et al.* that p68 is involved in processing of

pri-miR-21 [151]. Two years later the same group expanded the group of p68/DGCR8/Drosha regulated miRNAs to 20. Amongst others, miR-199b-5p, let-7b, miR-424, miR-199a-3p, and miR-19a are upregulated upon TGFβ treatment in a SMAD 1-3 and SMAD 5 dependent manner.

Furthermore, it was found that among some representatives a conserved sequence motif exists, which is necessary to recruit Drosha/DGCR8 and SMAD 1 [152]. But besides p68 and p72, p53 is able to support miRNA maturation by binding to the p68/DGCR8/Drosha complex [153]. Concerning the regulation of Drosha expression, only minor knowledge is available. For example the transcription factor c-myc, known to be involved in the expression control of several miRNAs [154-156], was shown to activate the Drosha promoter [157]. On translational level, Drosha is regulated by an alternate reading frame (ARF) protein which is suggested to inhibit translation of Drosha mRNA [158]. However, so far no publication exists which indicates an involvement of miRNAs in posttranscriptional regulation of Drosha expression.

Taken all together, several interaction partners and posttranscriptional modulations are known to control Drosha RNA- cleavage. In contrast regulation of Drosha expression is less studied.

2.3.5 Regulation of Dicer

Upon export to the cytoplasm, Dicer recognizes the pre-miRNA, processes it and liberates short RNA duplexes. Analog to Drosha, the active center of Dicer is formed by two RNAse III motifs in the C-terminus [159]. The N-terminal helicase domain serves as recognition domain for the pre-miRNA loop and facilitates RNA-binding [160] whereas the so called PIWI-AGO-ZWILLE (PAZ) domain binds the termini of the pre-miRNA [161]. For an overview of the arrangement of the different loci see Figure 5.

The 3' overhang of the pre-miRNA is necessary for Exportin 5 recognition accompanied by nuclear export but also for specific recognition as a Dicer substrate [162]. Dicer RNA binding capacity is enhanced by an interaction partner, the trans-activation response RNA-binding protein (TRBP) [114, 115]. After interaction with the N-terminal domain of Dicer, this protein helps to determine the correct product length [163].

Protein activator of protein kinase R (PACT) is another dsRNA binding protein interacting with Dicer. Compared to TRBP, PACT increases RNA binding affinity in complex with Dicer to a less extent. Interestingly, TRBP-Dicer and PACT-Dicer complexes produce miRNA variants [165]. These variants or isomiRs origin from the same pre-miRNA but have different 3'/5' ends or differ in their length [166]. Furthermore isomiR composition is based on small differences in the dsRNA binding domains of TRBP/PACT. This suggests that structure and relative orientation of RNA substrates might be involved in determining the structure of the formed

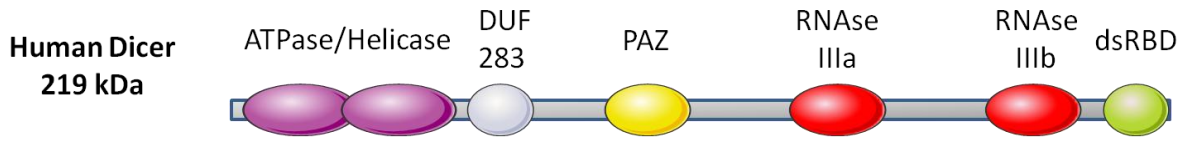

Figure 5: Domain structures of Dicer
Human Dicer consists of a C-terminal domain including two RNAse III domains and a binding region for double stranded RNA (dsRBD) and the N-terminal helicase domain. The latter one serves to facilitate RNA-binding and recognizes the pre-miRNA loop whereas the PIWI-AGO-ZWILLE (PAZ) domain binds the pre-miRNA termini. The role of the domain of unknown function (DUF) is still unclear (modified from [164]).

mature miRNA [165]. Besides increasing RNA binding affinity, the metabolic rate of pre-miRNAs can be increased by direct interaction of Dicer with adenosine deaminase acting on RNA 1 (ADAR1). ADAR proteins shuffle between the nucleus and the cytoplasm and are involved in A-to-I editing of dsRNAs [167]. As RNA editing primarily takes place in the nucleus, a function in the cytoplasm was assumed and a participation in RNAi was suggested. Confirmed by co-immunoprecipation experiments, the interaction was referred to the DUF283 and the RNA helicase domain in the N-terminal part of Dicer. Taking into account that this region is attributed to autoinhibition of human Dicer [168] this localization is a possible explanation for increased Dicer activity after binding to ADAR1, TRBP and PACT which all interact with the N-terminal domain. Apart from this ADAR1 was shown not to interfere with substrate RNA binding. This suggests ADAR1 to induce conformational changes of Dicer resulting in enhanced miRNA processing [169].

As indicated in chapter 2.1.4, Dicer is also able to interact with 5-LO. In contrast to the already mentioned binding partners, the C-terminal dsRNA binding region of Dicer is responsible for

this interaction. 5-LO turns the miRNA pattern towards longer (~55 nt) and shorter (~10-12 nt) RNA fragments in a dose dependant manner. But the mode of action as well as the biological role is still unknown.

Apart from regulation of Dicer activity, Dicer expression can be further controlled by the presence of various miRNAs via negative feedback loops. For example expression of let-7e family members correlates inversely with Dicer level [170, 171] and two conserved potential binding sides within the 3'UTR of Dicer were predicted by TargetScan 6.0. However, according to this prediction platform, the miRNA family possessing the highest probability of binding to Dicer is miR-29 which could be confirmed by the group of Cochrane *et al.* [172]. They further could show that miR-221 and miR-222 repress Dicer formation whereas miR-200c positively affects its expression. However, it is important to take into account that also many other miRNAs might be involved in Dicer regulation.

Taken together, 5-LO is assigned a particular role in regulation of Dicer as it binds in contrast to other Dicer-interacting proteins to its C-terminal domain. Moreover, the metabolic rate of Dicer is independent of 5-LO [38]. Apart from that, several proteins exist which interfere with the N-terminal region of Dicer and activate the miRNA turnover. Additionally, several miRNAs are known to regulate Dicer expression via a negative feedback loop.

2.3.6 MicroRNAs and the LT pathway

Only a few studies show the effect of miRNAs on the LT pathway. Among the target proteins are 5-LO and FLAP, but experimental data regarding LTA_4-hydrolase, LTC_4-synthase or CLP are still missing. In 2012, the group of Charles Serhan was the first to identify the 3'UTR of 5-LO to be a target of the precursor of miR-219-5p and miR-219-2-3p, miR-219-2, by reporter gene assay in macrophages [173]. Two years later Busch *et al.* found miR-19a-3p and miR-125b-5p to target 5-LO mRNA directly (see chapter 2.1.3) [23].

Apart from this, LTs, especially LTB_4, have been shown to influence miRNA expression. The group of Carlos Serezani showed that BLT1 activation by LTB_4 leads to a mobilization of NF-κB through increasing MyD88 expression [174]. A few years later, this protein was identified to be positively regulated by miR125b, miR-155, and miR-146a. These miRNAs inhibit expression of

suppressor of cytokine signaling-1 (SOCS-1) which in turn leads to an increase in MyD88 expression [175]. Interestingly the inhibition of LT biosynthesis by the 5-LO inhibitor AA-861 additionally decreases miR-19a and miR-125b expression. Considering these miRNA to regulate 5-LO expression, a negative feedback loop for 5-LO activation is likely.

Already in 2010, FLAP was published as a target of miR-135a and miR-199a-5p. Under hypoxic conditions, NF-κB and the hypoxia-inducible factor (HIF)-1α are activated and enhance the transcription of FLAP. Concurrent, HIF-1α decreases expression of miR-135a and miR-199a-5p which in turn reduces their inhibitory potential on translation of FLAP mRNA [176]. This double effect intensifies and accelerates the response to hypoxia.

2.3.7 MicroRNA family miR-125

The miRNA family miR-125 is highly conserved in diverse species and consists of three homologs: miR-125a, miR-125b-1 and miR-125b-2. They have manifold functions and are implicated in acting as tumor suppressors or as oncogenes (reviewed in [177]). Interestingly miR-125b was shown to be upregulated in several forms of leukemia [178-180] including AML [181-184]. Also, autoimmune diseases like eosinophilic chronic rhinosinusitis (accompanied by increased 5-LO activity) [185, 186] display miR-125b overexpression [187]. MiR-125a levels in turn, which are elevated in systemic lupus erythematosus, psoriasis, and multiple sclerosis [188-190], were shown to interfere with expression of chemokine (C-C motif) ligand 5 (CCL5), also known as RANTES. CCL5 is involved in recruiting leukocytes into inflammatory sides [191] and is decreased in 5-LO$^{-/-}$ mice [174]. Apart from this, both, miR-125a and miR-125b are involved in regulating the immune system development. Especially miR-125b is highly expressed in hematopoietic stem cells (HSCs) [192] and overexpression leads to increased self-renewal [193]. Also miR-125a is enriched in HSCs, but its expression decreases upon differentiation [194].

The seed region of miR-125a and miR-125b are identical which suggests similar targets and activities. However, more and more publications show a specific involvement of either miR-125b or miR-125a. For example, miR-125b was shown to be highly expressed in naïve T-cells [195], while miR-125a is present in activated T-cells [190]. Besides varying expression levels in different cell types, interaction of the 5' ends of the miRNAs with their target mRNAs can slightly differ

between family members, but certainly many common implications exist. Focusing further on inflammatory events and cancer, both miRNAs target p53 [196, 197]. This transcription factor acts as a tumor suppressor. It activates DNA repair and stops the cell cycle after DNA damage [198]. Interestingly several publications exist describing p53 in relation to 5-LO. In 2006, p53 was found to upregulate 5-LO expression in prostate cancer cells [199] and recently Gilbert *et al.* showed that 5-LO is a direct target gene of p53 [200]. Moreover, in cancer cell lines 5-LO antagonizes p53 mediated apoptosis [201]. On the other hand, in normal fibroblasts 5-LO stabilizes p53 through phosphorylation and increases expression of the p53-transcriptional target p21 [202].

5-LO is further implicated in the release of NF-κB (purple circle in Figure 6, [203]) and the TNFα pathway (blue circle in Figure 6), as 5-LO inhibition blocks the TNFα induced synthesis of reactive oxygen species [58]. In turn miR-125b was identified to block TNFα biosynthesis [204] whereas data for miR-125a are inconsistent. In mouse macrophages derived from bone-marrow cells, miR-125a is supposed to decrease TNFα expression [205], while human THP-1 cells, a cell line derived from an acute monocytic leukemia patient [206], exhibit increased, but not significantly changed, TNFα level after treatment with miR-125a-5p mimics [207] (yellow box in Figure 6). Additionally both miRNAs target tumor necrosis factor alpha-induced protein 3 (TNFAIP3) also called tumor necrosis factor-inducible zinc finger protein A20 (green circle in Figure 6) [208]. This protein is implicated in controlling diverse inflammatory responses. It is activated by TNFα and blocks TNFα mediated NF-κB activation [209]. TNFα is released upon contact with an inflammatory stimulus like LPS (red circle in Figure 6). This endotoxin down-regulates miR-125b expression in mouse macrophages [210] while a study with human cord and adult blood revealed that the miR-125b level in neonatal monocytes decreases after LPS stimulation but adult monocytes show an increased expression of miR-125b [211]. Though miR-125a shows a consistent increase after LPS stimulation in mouse macrophages, human macrophages, and THP-1 cells [205, 207, 212]. Interestingly, miR-125a was also found to be involved in differential activation of mouse macrophages [205, 207]. A distinction is made between classical activation, leading to M1 macrophages, and alternative activation, leading to

M2 macrophages. M1 macrophages can initiate inflammatory response and act as effector cells in TH1 cellular immune responses involving high level of IL-12, IL-23, and TNFα.

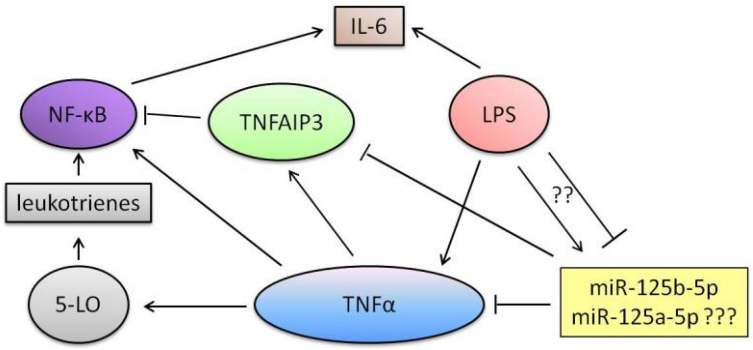

Figure 6: Overview of the inflammatory interplay of 5-LO and LPS

Stimulation with LPS (red circle) increases the release of the cytokines IL-6 (brown box) and TNFα (blue circle). The latter cytokine can directly activate NF-ϰB (purple circle) or activates 5-LO (grey circle) to increase the level of NF-ϰB activating LTs (grey box). Besides, TNFα induces TNFAIP3 (green circle) to inhibit and control NF-ϰB activity. In contrast, miR-125b-5p and potentially miR-125a-5p (yellow box) inhibit TNFAIP3 expression. The effect of LPS on expression of miR-125b-5p and miR-125a-5p is still in question.

Apart from this they are characterized by their cluster of differentiation (CD80/86 and CD163). M2 macrophages have repair functions as they suppress adaptive immunity and are involved in tissue repair. They release, amongst others, IL-10 and TGFβ and are characterized by CD206 [213].

2.3.8 MicroRNA cluster miR-99b/let-7e/miR-125a

MiR-125b-1 (located on chromosome 11) and miR-125b-2 (located on chromosome 21) are organized in clusters containing one member of the let-7 and one member of the miR-99 family. Their homolog miR-125a is located on chromosome 19 in a cluster containing miR-99b and let-7e (see Figure 7). MiR-100/let-7a-2/miR-125b-1 and miR-99a/let-7c/miR-125b-2 are considered clusters as they are highly conserved even if miR-125b-1 and miR-125b-2 are encoded approximately 50 kB downstream of miR-100/let-7a-2 and miR-99a/let-7c, respectively. Due to

the distant localization of the respective miRNAs, however, an alternative promoter for solely transcribing miR-125b is probable [214]. In contrast, the members of the miR-99b/let-7e/miR-125a cluster are located in close proximity (<1kb) and transcribed as one transcript. This suggests correlating expression profiles in different cellular contexts.

As mentioned in chapter 2.3.7, miR-125a is extensively studied while miR-99b and in particular let-7e are unattended. However, a few publications exist which deal with the expression and function of the whole miRNA-cluster.

According to the presence of miR-125a in HSCs, the whole miR cluster including miR-99b, let-7e, and miR-125a was identified to regulate primitive hematopoietic cells. Gerrits *et al.* studied the miRNA expression profiles in different mouse strains and observed a correlation between the presence of the miR-99b/let-7e/miR-125a cluster members and HSC frequency.

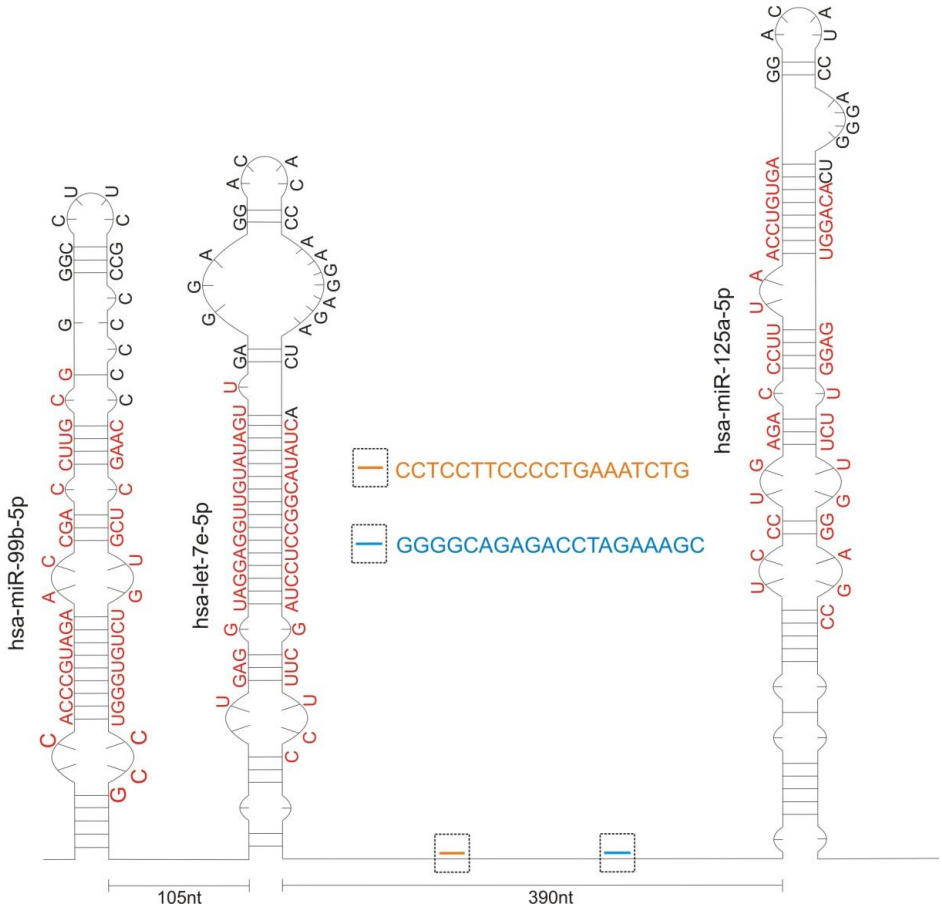

Figure 7: The miRNA-cluster containing miR-99b, let-7e, and miR-125a.
Stem-loop structures adopted from mirBase (5′→ 3′). Dicer products are displayed in red. Primer pairs for detection of the pri-miRNA are displayed in orange and blue.

However, overexpression experiments revealed that miR-125a is primarily responsible [194]. Besides hematopoietic cells, this cluster was also found to be overexpressed in patients with multiple myeloma, a cancer form of plasma cells [215]. Apart from this, the representatives of this cluster are involved in osteoclast differentiation of primary monocytes [216]. Osteoclasts resorb bone tissue and in cooperation with their opponents, the osteoblasts, are responsible for repairing and remodeling bones. Formation of osteoclasts is regulated by the cytokines TNFα, IL-1, and IL-6. They induce expression of receptor activator of NF-κB ligand (RANKL) which in turn activates NF-κB by binding to its receptor [217]. The NF-κB subunit p65 subsequently binds directly to the promoter of the miR-99b/let-7e/miR-125a cluster gene and enhances its transcription. Depletion of the individual miRNAs resulted in an inhibition of osteoclast differentiation which suggests a role in its negative regulation [216]. The miR-99b/let-7e/miR-125a cluster is further associated with the severity of cystic fibrosis [218]. This disease affects mostly the lungs and is associated with difficulties in breathing and coughing up sputum. The average life expectancy of patients suffer from cystic fibrosis is between 37 and 50 years in the developed world. It is caused by the presence of mutations in both copies of the gene for the protein CFTR (cystic fibrosis transmembrane conductance regulator). The most frequent mutation is a three base pair deletion, resulting in the loss of phenylalanine at position 508 (p.F508del). As a consequence, the CFTR protein retains inside the endoplasmatic reticulum [219]. CFTR knockout in mice is mostly lethal in the perinatal stage, but some mice survive due to a secondary genetic factor [220]. This factor could be attributed to the chromosomal region homolog to the region carrying the miR-99b/let-7e/miR-125a cluster in humans [221]. Interestingly only expression of miR-99b and miR-125a was increased in HeLa cells expressing the CFTR mutant compared to cells expressing the CFTR wild-type, let-7e level is unchanged. This suggests a role of the CFTR mutant in miRNA maturation rather than in transcription of the cluster [218].

Furthermore, miR-99b contributes to irradiation resistance in pancreatic cancer. Ionizing radiation decreases expression of miR-99b which in consequence leads to an enhanced expression and activity of its target, the mechanistic target of rapamycin (mTOR). This protein is a serine/threonine protein kinase and is particularly in tumor- and T-cells irreplaceable for normal

cell growth and proliferation. Reconstitution of pre-miR-99b in pancreatic carcinoma cells in turn reduces mTOR expression and results in an increased sensitivity upon radiation [222]. Apart from this miR-99b is used by *Mycobacterium tuberculosis* to adapt host immunity. Infected cells show a highly upregulated expression of miR-99b resulting in reduced level of host protective cytokines like IL-6, IL-12, IL-1β, and TNFα [223]. In epithelial NMuMG cells, originated from a mouse mammary gland, miR-99b is upregulated in response to TGFβ stimulation. TGFβ induces epithelial to mesenchymal transition [224] characterized by increased cell migration and invasion as well as decreased proliferation. Turcatel *et al.* could show that inhibition of miR-99b in TGFβ treated cells weakens and delays the transition to the mesenchymal phenotype by decreasing SMAD 3 phosphorylation which leads to an inhibition of TGFβ mediated implications (also see chapter 2.1.2) [225].

Let-7e is a member of the let-7 family. The first discovered human miRNA belongs to this family (also see chapter 2.3.1) and is conserved upon several organisms. The equivalent miRNA in *C. elegans* is essential for development [103], whereas let-7 in humans is primarily involved in differentiation processes [226-228]. In total, nine miRNAs belong to the let-7 family. Due to their sequence analogy, it is difficult to assign functions to specific family members. Nevertheless, let-7e is attributed to have implications in several forms of cancer. For example, Wu *et al.* could show that a specific mutation present in human cancers is located in the loop region of the pre-let-7e and affects let-7e expression [229]. Furthermore this miRNA is increased in ovarian cancer [230], colorectal carcinoma [231], and lung cancer [232]. Buechner *et al.* could even show a direct regulation of the proto-oncogene N-Myc by let-7e resulting in a proliferation stop [233]. This tumor suppressing activity is supported by the observation that suppression of let-7e by the histone demethylase Jumonji/JARID1 B (JARID1 B) increases cyclin D1 expression which in turn promotes cell cycle progression accompanied by increased proliferation [234]. Besides involvement of let-7e in cancer development, this miRNA was identified to be increased in a mouse model of multiple sclerosis and silencing of let-7e slowed down the course of disease [235]. In contrast to this, inflammation in the nasal mucosa upon allergic rhinitis is suggested to reduce let-7e levels [236] and similar results were obtained for asthma patients [237].

In summary, the miRNA cluster consisting of miR-99b/let-7e/miR-125a plays a role in many processes related to inflammation, hematopoiesis, and cancer development. The most prominent cluster member is miR-125a-5p, but in the last decade the number of let-7e and miR-99b related publications increased. At present, the interplay of the three clustered miRNAs comes into focus while the functions of the individual miRNAs are less frequently investigated.

2.3.9 Relevance of miRNAs in the regulation of protein biosynthesis

Since the discovery of miRNAs in the year 1993 by the group of Victor Ambros [102], miRNA research became one of the most promising fields in terms of developing new drugs and finding new biomarkers for various diseases. MiRNAs are involved in the posttranscriptional regulation of protein biosynthesis, as mentioned in chapter 2.3.2. The activity of miRNAs is essential for animal development and survival. The incapability of miRNA biosynthesis due to Dicer knockout is lethal in mice [238].

The significance of miRNAs further develops, when looking at the ratio of miRNA genes to protein coding genes. Up to now, more than 2,500 miRNAs are published and an estimated 20,000-25,000 human protein-coding genes. Moreover, each miRNA is predicted to control up to hundreds of targets. In practice, virtually every protein is regulated by miRNAs.

Many experiments have assigned miRNAs to be important during cell proliferation and differentiation [239-241]. Besides, miRNAs were attributed to crucial roles in homeostasis and disease. Almost every disease is somehow associated with miRNAs and, vice versa, nearly every dysregulation in miRNA biosynthesis correlates with a disease. This is a reason why interests in miRNAs as biomarkers are arising, especially in extracellular miRNAs which occur in serum or other body fluids. MiRNAs are stable, some are tissue specific and their level can be easily accessed by PCR [242]. MiR-125a-5p, for example is a potential biomarker in liver diseases [243]. However, miR-125a-5p can also be used as a biomarker in further diseases like breast cancer [244, 245], colorectal adenomas [246], gastric cancer [247], and non-small cell lung cancer [248]. Hence, the usage of miRNAs as biomarkers is manifold, but difficult to evaluate.

Currently, most of the *in vivo* data in respect of miRNAs were obtained in mice. However, up to now comparative studies are often missing, showing the applicability of miRNA data obtained in mice to humans.

In summary, miRNA research is a fast growing field with many future applications as biomarkers or even as drugs. However, data obtained from mice should be handled with care, as miRNA-binding sites and even functions can differ between different species.

3 AIM OF THE STUDY

MicroRNAs (miRNAs) are involved in posttranscriptional regulation of protein biosynthesis. Their maturation is initiated by the transcription of a pri-miRNA transcript which is further processed by two proteins, Drosha and Dicer. Finally, the mature miRNA directs the RNA induced silencing complex to the target mRNA and leads to translational repression or mRNA degradation [249]

Dicer, responsible for the last step of miRNA maturation, was shown to interact with 5-LO [33]. Due to the fact that 5-LO is responsible for LT formation [250] and its involvement in several inflammatory diseases, the question arose if 5-LO can influence the expression profile of miRNAs in the context of inflammatory processes.

This study intended to investigate if the loss of 5-LO protein in a monocytic cell culture model [251] influences its miRNA expression pattern by performing a miRNA-microarray. Furthermore, it anticipated to unravel which step of miRNA processing is affected by 5-LO knockdown. Therefore it was intented to select a couple of miRNAs showing an altered expression in 5-LO knockdown cells in the microarray and to detect their level of pri-, pre- and mature-miRNA.

Apart from that the role of the 5-LO protein itself and of its enzymatic products on regulation of miRNA processing by Dicer was intended to investigate. In this context, it was of further interest whether FLAP is involved in maturation of 5-LO regulated miRNAs, since it is a direct interaction partner of 5-LO and is required for cellular leukotriene biosynthesis.

In addition, the biological functions of miRNAs affected by 5-LO knockdown were investigated with regard to inflammatory events.

Thus, the compiled data should help to understand the role of 5-LO in miRNA maturation and the role of these miRNA in 5-LO related inflammatory events.

4 MATERIAL & METHODS

4.1 Cells and cell culture

4.1.1 Cell lines

Mono Mac 6 (MM6) is a human monocytic cell line. The cells were originally purchased from the German collection of microorganisms and cell culture (DSMZ) and transfected with lentiviral constructs expressing a shRNA against 5-LO, FLAP, and non-target control, respectively, by the group of Prof. O. Rådmark [31].

HEK-293T is a human cell line derived from an embryonic kidney. In contrast to HEK-293 cells, they express the SV40 large T antigen. This protein increases the amplification of the transfected plasmids by binding to p53 and other transcriptional co-activators. The advantage is enhanced transfection efficiency, increased vector production and elevated transduction efficiency [252].

BL41 is a Burkitt's lymphoma suspension cell line with high expression level of 5-LO [253].

U2OS is an adherent osteosarcoma cell line.

4.1.2 Cell culture

MM6 cells were maintained in glutamine containing RPMI 1640 medium, supplemented with 10% (v/v) heat inactivated FCS, 100 U/ml penicillin, 100 µg/ml streptomycin, 10 µg/ml insulin, 1x MEM non essential amino acids, 1 mM sodium pyruvate, and 1 mM oxaloacetate at 37°C, in a humidified atmosphere with 5% CO_2. The optimal growing density is 0.3×10^6 cells/ml and should not exceed 1×10^6 cells/ml. For differentiation experiments, the cells were stimulated with 1 ng/ml TGFβ and 50 nM calcitriol (isolated and purified by Dr. Ann-Kathrin Häfner and Sven George [254]) and kept at a cell density of 0.2×10^6 cells/ml with 6% CO_2. Untreated control cells were seeded at a density of 0.3×10^6 cells/ml at standard conditions. After 96 h cells were harvested by centrifugation (1000 rpm, 4 min at room temperature) and washed once with PBS pH 7.4.

HEK-293T cells were maintained in DMEM high glucose medium supplemented with 10% (v/v) FCS, 100 U/ml penicillin, and 100 µg/ml streptomycin at 37°C, in a humidified atmosphere with 5% CO_2.

BL41 cells were maintained in RPMI 1640 supplemented with 10% (v/v) heat inactivated FCS, 100 U/ml penicillin, and 100 µg/ml streptomycin. The optimal growing density is 0.5×10^6 cells/ml.

U2OS cells were maintained in DMEM supplemented with 100 U/ml penicillin and 100 µg/ml streptomycin. Their optimal growing density is 0.5-1 $\times 10^6$ cells/ml.

BL41 as well as U2OS cells were kept at 37° C, in a humidified atmosphere at 5% CO_2.

4.1.3 Isolation and polarization of peripheral blood mononuclear cells (PBMC)

PBMC were freshly isolated from buffy coats obtained from the German Red Cross Blood Donor Service Baden-Württemberg-Hessen in Frankfurt by Ficoll® (GE Healthcare) density centrifugation and maintained in Petri dishes. After 1 h non-adherent cells were removed. Adherent monocytes were incubated in RPMI 1640 supplemented with 5% (v/v) human plasma in tissue culture dishes (100 × 20mm cell+, Sarstedt). For polarization towards M1 macrophages, cells were stimulated with either 10 ng/ml GM-CSF for M1 or 10 ng/ml M-CSF for M2 macrophage polarization while control cells were kept unstimulated. After five days M1 cells were additionally to GM-CSF stimulated with 10 ng/ml IFNγ and M2 cells with 10 ng/ml IL-4 and M-CSF, respectively. After further two days, the macrophages were fully differentiated.

4.1.4 Substances involved in cell treatment

Table 1: Applied stimuli, drugs, chemicals, and antibiotics in cell culture

Substance	End concentration	Solvent	Source
TGFβ	1 ng/ml	25% acetonitrile, 1% BSA, 0,1% TFA	Dr. Ann-Kathrin Häfner, Sven George [254]
1α,25-dihydroxyvitamin D3 (calcitriol)	50 nM	Ethanol	Sigma Aldrich
LPS from *E.coli* 0111:B4	1 µg/ml	PBS	Sigma Aldrich
LTB_4	100 nM	Ethanol	Cayman Chemicals
LTC_4	100 nM	97% ethanol	Cayman Chemicals
5-HETE	100 nM	Ethanol	Cayman Chemicals
Zileuton	10 mM	DMSO	Cayman Chemicals
MK-886	1 µM	DMSO	Sigma Aldrich
Puromycin	8 µg//ml	MilliQ	Enzo Life Sciences
Geneticin G-418 Sulphate	400 µg/ml	MilliQ	Gibco
GM-CSF	10 ng/ml	PBS (BSA 0,1%)	PeproTech
M-CSF	10 ng/ml	PBS (BSA 0,1%)	PeproTech
IFNγ	10 ng/ml	PBS (BSA 0,1%)	PeproTech
IL-4	10 ng/ml	PBS (BSA 0,1%)	PeproTech
PMA	100 nM	DMSO	Calbiochem
Ionophore A23187	2 µM	methanol	Sigma Aldrich

4.2 RNA extraction and Microarray analysis

4.2.1 Extraction of cellular RNA with the hot phenol method

For extraction of total RNA, cells were harvested as described in chapter 4.1.2. The pellet of ~4 10^6 cells was kept on ice for direct extraction or at -80°C for later experiments. The

lysis was performed using 200 µl lysis buffer (10 mM sodium acetate, 150 mM sucrose, adjusted to pH 4.8 with acetic acid), 1% SDS and 200 µl 5 M guanidine thiocyanate. For extraction, the cell lysate was incubated for 5 min with 200 µl of pre-warmed aqueous phenol (pH 4.5-5; Roth) at 65°C followed by phase separation with 200 µl of a 1:25 mixture of chloroform and isoamyl alcohol, centrifuged at 4°C at 10,000 g for 5 min. MaXtract high-density tubes (Qiagen) were used for this step. The upper RNA containing aqueous phase was separated and extracted again with 300 µl phenol followed by two separation steps with 300 µl chloroform/isoamyl alcohol. The supernatant was transferred into a tube containing 1.5 ml ethanol and 60 mM sodium acetate pH 6.5 and kept at -80°C for 30 min for precipitation. Afterwards the samples were centrifuged at 4°C/10,000 g for 30 min and the supernatant was removed. The RNA pellet was subsequently washed with 100 µl 70% ethanol and centrifuged again under the same conditions. Finally, the supernatant was completely removed, the pellets were allowed to try for 5 min at room temperature, and dissolved in 40 µl MQ water. Quantification was performed using a NanoDrop 1000 (Thermo Scientific). In average 4×10^6 cells yield 40 µg RNA. For good quality RNA, $A_{260/280}$ and $A_{260/230}$, which determine RNA purity, should be 1.8 or higher. DNase digestion was performed using 1.7 µg RNA, 2 µl digestion buffer and 1 µl TURBO DNase (2 U/µl; Ambion). The samples were incubated at room temperature for 10 min and subsequently precipitated with 100 µl ethanol and 60 mM sodium acetate pH 6.5 at -20°C for 30 min. Centrifugation was performed at 4°C/10,000 g for 30 min. RNA quality was analyzed by 1% agarose gel electrophoresis performed with 1 µg RNA using GelPilot Loading Dye (Qiagen), denatured at 95°C for 5 min. Electrophoresis was performed at 110 V for 60 min.

4.2.2 Extraction of cellular RNA from primary cells

The miRNeasy® Mini kit (Qiagen) was used for RNA isolation from primary cells. Extraction was performed according to the manufacturer's protocol and RNA was eluted with 30 µl RNAse free water.

4.2.3 Microarray

The microarray was performed by Exiqon based on miRBase v19.0 to detect potential differences in miRNA expression between control and Δ5-LO cells. Undifferentiated and differentiated cells after 2 and 4 days were analyzed. 5-LO controlled miRNAs were chosen based on a fold change of <0.7 or >1.4 and p-values <0.05 and subsequently verified by qRT-PCR.

4.3 Reverse Transcription

4.3.1 Mature miRNA

DNAse digested RNA containing mature miRNAs were transcribed into cDNA by a specific cDNA synthesis for later analysis by qPCR. Therefore specific self-designed stem-loop primer as previously described were used (see Table 2 for sequences) [255]. 100 ng of total RNA was transcribed using 50 U SuperScript II (200 U/µl; Invitrogen), 2.5 pmol dNTPs (10 mM dNTP Mix; Invitrogen), 1 µl dithiothreitol (DTT; 0.1 M; Invitrogen), 2 µl 5 × First Strand buffer (Invitrogen), 0.5 pmol stem loop primer specific to the miRNA in demand, and 0.5 pmol stem loop primer specific to RNU48 (U48) as internal control in a final volume of 10 µl. The PCR was performed obeying the protocol listed in Table 3. The resulting cDNA was diluted 1:5 with MQ water.

Table 2: Applied stem loop primer
for Reverse Transcription PCR of mature miRNA

miRNA stem loop	**Sequence (5'-3')**
RNU48	GTTGGCTCTGGTGCAGGGTCCGAGGTATTCGCACCAGAGCCAACGGTCAG
miR-99b-5p	GTTGGCTCTGGTGCAGGGTCCGAGGTATTCGCACCAGAGCCAACCGCAAG
let-7e-5p	GTTGGCTCTGGTGCAGGGTCCGAGGTATTCGCACCAGAGCCAACAACTAT
miR-125a-5p	GTTGGCTCTGGTGCAGGGTCCGAGGTATTCGCACCAGAGCCAACTCACAG
miR-19a-3p	GTTGGCTCTGGTGCAGGGTCCGAGGTATTCGCACCAGAGCCAACTCAGTT

Table 3: Cycling conditions of Reverse Transcription
for mature miRNA

Time	Temperature	
30’	16°C	
30’’	30°C	60 ×
30’’	42°C	
1’	50°C	
15’	70°C	
∞	4-8°C	

4.3.2 Pre- and pri-miRNA

As the pri-miRNA includes the whole sequence of the pre-miRNA, it is not possible to detect the pre-miRNA alone. We performed Reverse Transcription with the miScript II RT (Qiagen) following the manufacturers protocol. The pri-miRNA is already polyadenylated while the pre-miRNA is polyadenylated by poly (A) polymerase simultaneously with Reverse Transcription using oligo-dT primers. For a 25 µl reaction we applied 1.5 µg DNAse digested total RNA.

4.3.3 Pri-miRNA & mRNA

As already mentioned, the primary transcript carries a Poly-A-tail corresponding to common mRNAs. Hence, in contrast to chapter 4.3.2 no polyadenylation is needed prior to reverse transcription of pri-miRNAs and mRNAs. By using the High Capacity RNA-to-cDNA Kit (Applied Biosystems) utilizing a combination of oligo-dT primers and random hexamers, unspecific reverse transcription was performed. Therefore 300 ng of DNAse digested total RNA was used, the resulting cDNA was diluted 1:2 with MQ water and further analysed by mRNA/pri-miRNA specific qPCR as described in chapter 4.4.3.

4.4 Quantitative Reverse Transcription PCR (qRT-PCR)

4.4.1 Mature miRNA

Quantitative RT-PCR for mature miRNAs was performed on a StepOne Plus device (Applied Biosystems), equipped with a 98-well reaction plate using Taqman as flourophor. 10 pmol of the universal reverse and the specific forward primer (designed as described in [255] and listed in Table 4) were used and mixed with 10 pmol Universal ProbeLibrary probe #21 (Roche Diagnostics), 2 × Taqman Universal PCR Mastermix, and MQ (Milli-Q) water to a final volume of 15 µl. U48 was used as endogenous control and 5 µl cDNA (prepared according to chapter 4.3.1) was used for each reaction performed in duplicates. For analysis the cycle number (C_t), at which the fluorescence signal starts to increase exponentially, was used. We used the $2^{-\Delta\Delta C_t}$ method for analysis [256].

Table 4: Applied primer for qRT-PCR of mature miRNA

miRNA fwd	Sequence (5'-3')
RNU48	GAGTGATGATGACCCCAGGTAA
miR-99b-5p	GGCACCCGTAGAACCGAC
Let-7e-5p	GCGGTGAGGTAGGAGGTTGT
miR-125a-5p	CGGTCCCTGAGACCCTTTAAC
miR-19a-3p	GCGGTGTGCAAATCTATGCAA

4.4.2 Pre- and pri-miRNA in combination

For simultaneous detection of pre- and pri-miRNA, quantitative RT-PCR was performed with the same device as used for detection of mature miRNA (see chapter 4.4.1), but following a different protocol (see Table 5). The runs were performed using the miScript precursor assay in combination with the miScript SYBR® Green PCR Kit (both Qiagen). 12.5 µl SYBR Green, 2.5 µl precursor primer mix and 2 µl cDNA (4.3.2) were supplemented to 25 µl with RNAse free water. RNU6-2 was used as endogenous control

and reactions were performed in duplicates. For analysis we again followed the $2^{-\Delta\Delta Ct}$ method [256].

Table 5: Cycling conditions for real-time PCR
Of pre- and pri-miRNA

Step	Time	Temperature	
Initial activation	15'	95°C	
Denaturation	15''	94°C	40 ×
Annealing	15''	55°C	
Extension	30''	70°C	

4.4.3 Pri-miRNA & mRNA

Quantitative RT-PCR for pri-miRNA and mRNA were performed using Power SYBR Green Universal PCR Mastermix (Applied Biosystems). Pri-miRNA primer pairs were designed to be located either in between let-7e and miR-125a or arranged behind miR-125a to target specifically the pri-miRNA, but not the pre-miRNA (see Figure 7 in chapter 2.3.8 for location). β-Actin was used as endogenous control. All reactions were

Table 6: Tested primer pairs for qRT-PCRof pri-miRNA and mRNA

Name	Sequence (5'-3')	Product length	
Pri-miRNA_A_fwd	CCTCCTTCCCCTGAAATCTG	130bp	Between let-7e and miR-125a
Pri-miRNA_A_rev	GGGGCAGAGACCTAGAAAGC		
Pri-miRNA_B_fwd	TGCTGTGTCTCTGTGGCTTC	181bp	
Pri-miRNA_B_rev	GTGGGGGTCAGAGATGGAG		
Pri-miRNA_C_fwd	AATTGCTGGCCTGACTTCTG	173bp	Behind miR-125a
Pri-miRNA_C_rev	CATCGTGTGGGTCTCAAGG		
Pri-miRNA_D_fwd	CCACCAACTGAAACCTGACC	111bp	
Pri-miRNA_D_rev	CCATCGTGTGGGTCTCAAG		
β-Actin_fwd	CGGGACCTGACTGACTACCTC	99bp	
β-Actin_rev	CTTCTCCTTAATGTCACGCACG		
5-LO_Exon 13-14_fwd	GAGCCAGTTCCAGGAAAACG	66bp	
5-LO_Exon 13-14_rev	GGCTTCTCGATAAAATGCTCTTCT		

performed in duplicates according to the manufacturer's protocol including a dissociation curve and the tested primer pairs are listed in Table 6.

4.5 Northern Blot

4.5.1 Preparation of RNA samples

A 1:1 mixture of sample extracted using the phenol method as prescribed in chapter 4.2.1 and RNA loading dye containing 90% (v/v) formamid, 0.025% (w/v) xylencyanol and 0.025% (w/v) bromphenol blue in 1 × TBE buffer was used. 10 µg of total RNA is dissolved in 15 µl MQ water and supplemented with 15 µl loading dye before denaturing the samples for 3 min at 95°C and immediately loading them to the gel.

4.5.2 Gel electrophoresis

According to GS Pall and AJ Hamilton [257] and in cooperation with Dr. Thomas Treiber from the group of Prof. Dr. Gunter Meister, University of Regensburg, the Northern Blot analysis was performed. Total RNA was separated on a 12% urea gel (Sequagel, National Diagnostics) of approximately 200 × 300 mm. Its polymerization was started by addition of 0.1‰ APS and 0.65 mg/ml TEMED. Prior sample loading, the gel was preheated by running in 1 × TBE at 350 V for approximately 20 min. For optimal separation the lower dye (bromphenol blue) should migrate 6 cm correlating with a running time of about 50 min at 400 V.

4.5.3 Blotting

The semi-dry technique was used for blotting [257]. Before packing the blot, all layers should be wetted with distilled water. From positive to negative electrode: three layers of Whatman 3 MM filter paper, followed by a Amersham Hybond-N membrane (nylon), the urea gel, and completed with another three sheets of Whatman 3 MM paper. Bubbles between the different layers should be avoided to ensure constant current flow. RNA was transferred from the urea gel to the membrane at 20 V for 60 min.

4.5.4 EDC-crosslink

The 1-ethyl-3- (3-dimethylaminopropyl)-carbodiimide (EDC) method was used for cross linking. EDC immobilizes the RNA via its 5' phosphate and thereby increases hybridization sensitivity up to 50 fold [258]. The cross linking solution for one gel consists of 128 mM 1-methylimidazol and 188 mg EDC in 6 ml water. The pH should be adjusted to 8.0 using 1 M HCL for improved EDC stability. The EDC solution was subsequently used to saturate a sheet of Whatman 3 MM paper which was laid on top of the membrane. The RNA containing side of the membrane should not face the filter paper to avoid direct contact of cross linking solution with the RNA. In the next step, the cling film was wrapped around the Whatman/membrane stack and kept in a hybridization oven for one hour at 50°C. Afterwards, the membrane was rinsed three times with distilled water for 20 sec. Unless continuing with hybridization, the membrane should be kept at -20°C, wrapped in cling film.

4.5.5 Preparation of the probes

For preparation of probes antisense to the respective mature miRNAs (**Table 7**), transcription of template DNA was performed using the T7-polymerase (Thermo Scientific; 20 U/µl). For 10 µl template (1 nmol) 10 µl T7-polymerase, 0.5 µl pyrophosphatase (Thermo Scientific; 0.1 U/µl), 50 µl DMSO, 12.5 µl NTPs (Thermo Scientific, 10mM), 15 µl 1M Tris buffer pH 8, 12.5 µl 1 M $MgCl_2$ solution, 5 µl 1% Triton X-100 solution, and 5 µl 1 M DTT were mixed and filled up to 500 µl by addition of DEPC treated water.

Table 7: Northern Blot probes

MiRNA	Sequence
MiR-99b-5p	GAAGGCCCCGCAAGGTCGGTTCTACGGGTG
Let-7e-5p	TTGGGTGTCCTCCTCAACTATACAACCTCCTACCTCA
MiR-125a-5p	ATGTCCTCACAGGTTAAAGGGTCTCAGGGA

The reaction was performed at 37°C over night and purified by urea polyacrylamide gel electrophoresis (PAGE) using a 15% Sequagel (250 V; 60 min). It was important to use RNA loading dye without xylene cyanol as the band runs at the same height as the transcript. Under UV light the DNA containing band is detected by putting the gel on top of a thin layer chromatography plate coated with a fluorescent molecule. The respective piece of gel was chopped out and the RNA is eluted in approximately 5 ml water for two hours using an overhead shaker. Next, the RNA was precipitated by adding 3.5 ml isopropanol and 400 mM NaCl. After ~30 min at -80°C, the samples were pelletized. The resulting pellet was washed once with 8 ml 70% ethanol and centrifuged again at 4°C/10,000 g for 30 min. Finally, the supernatant was discarded and the RNA pellet was resolved in 200 µl DEPC treated water.

For dephosphorylation, approximately 10 µg of the resulting RNA was mixed with 4 µl FAST AP Thermosensitive Alkaline Phosphatase (Thermo Scientific; 1 U/µl), 30 µl 10 × FAST AP buffer, 1 µl RiboLock RNAse Inhibitor (Thermo Scientific; 40 U/µl), filled up to 300 µl with DEPC treated water and kept for 1 h at 37°C. For RNA isolation the solution was supplemented with 18 µl of 5 M $NaCl_2$ and 500 µl of an aqua-phenol chloroform-isoamyl alcohol mixture (25:24:1, Roth) and centrifuged at 4°C/10,000 g for 30 min. The upper aqueous phase was separated and mixed with 900 µl ethanol for precipitation at -80°C. Afterwards the RNA was pelletized, washed with 70% ethanol and resolved in 50 µl DEPC-treated water.

4.5.6 Labeling of the probes

200 ng purified and dephosphorylated RNA transcript was incubated with T4 Polynucleotide Kinase (Thermo Scientific; 10 U/µl) and 2 µl g-^{32}P-ATP. The incubation should be performed while shaking for 1 h at 37°C and the reaction was stopped by addition of 30 µl 30 mM EDTA. The probes were further purified on a Sephadex G-25 (GE-Healthcare) gelfiltration column to remove free ATP.

4.5.7 Hybridization and Detection

The crosslinked RNA membrane (chapter 4.5.4) was incubated with to 50°C pre-warmed hybridization solution ($NaCl_2$, tri-Na-citrat, Albumin fraction V, polyvinylpyrrolidone K30, Ficoll 400, SDS, Na_2HPO_4, and NaH_2PO_4) for 1 h under rotation. The hybridization solution was next replaced by fresh hybridization solution containing additionally 25 µl labeled probe (chapter 4.5.6) and the membrane was incubated under rotation at 65°C over night. The following day, the membrane was washed with decreasing NaCl and tri-Na-citrat concentrations and wrapped in cling film. The wrapped membrane is finally exposed to a radioactive sensitive screen for three days. Scanning was performed using a Personal Molecular Imager (Biorad).

4.6 SDS PAGE and Western Blotting

4.6.1 Cell lysates and Bradford test

Approximately 4×10^6 cells were lysed in 100 µl 1% Triton-X 100 in PBS, supplemented with 10 µl of a PhosSTOP (Roche) stock solution of one tablet in 1 ml MQ water and 10 µl of a Protease Inhibitor Mix (Complete Mini, Roche) stock solution of one tablet in 1.5 ml MQ water. The protein concentration was determined by Bradford test [259]. Standard curves were generated by different dilutions of bovine serum albumin (BSA) solution and assessed with the Bradford reagent (BioRad) according to manufacturer's protocol. Absorption was measured with an Infinite 200 PRO Tecan reader. In average, 4×10^6 MM6 cells yield 20 µg/µl protein.

4.6.2 SDS-polyacrylamide gel electrophoresis (SDS-PAGE)

SDS-PAGE was performed using equal amounts of protein extracts (100 µg/15 µl) which are mixed with 5 µl loading buffer (250 mM Tris-HCl, 8% SDS, 40% glycerol, 20% β-mercaptoethanol and bromphenol blue) and heated up to 95°C for 5 min. Afterwards the samples can be stored at -20°C for later use or directly applied to a 10%

SDS-polyacrylamide gel. The Precision Plus Protein Standard (BioRad) was used as size marker.

4.6.3 Western Blotting

Proteins were electrophoretically blotted onto a nitrocellulose membrane (Thermo Scientific) which was further incubated with a 1:1 mixture of PBS:Odyssey Blocking buffer

Table 8: List of primary antibodies
Including target, dilution, and size

Target	Host species	Dilution	Provider	Size
5-LO [1551]	rabbit	1:200	Kind gift of Prof. Olof Rådmark	78 kDa
β-Actin [I-19]	goat	1:1000	Santa Cruz	42 kDa
Ago 2	rat	1:1500	Sigma-Aldrich	85 kDa
Dicer [13D6]	mouse	1:500	abcam	225 kDa
P53 [DO-1]	mouse	1:1000	eBioscience	43,7 kDa
Vinculin	mouse	1:250	R&D Systems	116 kDa
HDAC1	rabbit	1:200	abcam	65 kDa
Lamin A/C [4C11]	rabbit	1:1000	Cell Signaling	74 kDa (A) 63 kDa (C)

(Li-Cor Biosciences) for one hour at room temperature. Afterwards the membrane was incubated with the indicated primary antibodies over night at 4°C under rotation. All antibodies were diluted with PBS:Blocking buffer (1:1) supplemented with 0.1% Tween 20 (see Table 8 for a list of antibodies and the used dilution). Before incubating the membrane with either IRDye680 or IRDye800 conjugated secondary antibodies (Li-Cor Biosciences; 1:10,000 diluted) directed against the host species of the primary antibody, membranes were washed three times with PBS containing 0.1% Tween 20 for 5 min. Before visualizing the complexes on an Odyssey Infrared Imager (Li-Cor Biosciences), the washing was repeated without addition of Tween.

4.7 5-LO activity assay

3×10^6 differentiated MM6 cells were harvested, washed with PBS and resuspended in PBS containing 1 mg/ml glucose. For optimal activity, $CaCl_2$ was applied to a final concentration of 1 nM before the reaction was started by adding AA (Cayman chemicals) and calcium ionophore A23187 (Sigma Aldrich) in a final concentration of 20 µM and 2.5 µM, respectively. Incubation was performed at 37°C for 10 min and stopped by the addition of 1 ml cooled methanol. As internal standard, 10 µl of a prostaglandin B_1 (PGB_1) solution with a known concentration was added, accompanied by 30 µl of 1 M HCl and 500 µl 1 × PBS pH 7.4. To get rid of cell debris, the samples were centrifuged at 800 g for 10 min before applying the supernatants to C-18 solid phase extraction columns (preconditioned with 1 ml methanol and 1 ml distilled water). The columns were washed once with 25% methanol before bound 5-LO metabolites were extracted with 300 µl pure methanol. For better separation and detection the samples were diluted with 120 µl distilled water, applied to a HPLC machine and analyzed as previously described [260]. 5-LO product formation was normalized to 1×10^6 cells and includes 5-HETE, LTB_4, and its all-trans isomers.

4.8 Fractionation of MM6 cells

Around 10×10^6 cells were harvested as described in 4.1.2. The cell pellet was resuspended in NP40 buffer (Tris pH 7.4, NaCl, $MgCl_2$, EDTA, and NP40), supplemented with Leupeptin, Phenylmethylsulfonylfluoride (PMSF), and soybean trypsin inhibitor (STI) as protease inhibitors. To separate cytoplasmic from nuclear fraction, the suspension was centrifuged for 10 min at 10,000 g/4°C. The supernatant contained the cytoplasmic fraction, which was separated and centrifuged again to dispose possible contaminations from the nuclear fraction. However, the major part of the nuclear fraction was present in the pellet derived from the first centrifugation step, which was subsequently resuspended in TKM-buffer (Tris pH 7.4, sucrose, KCl, $MgCl_2$, and EDTA) supplemented with the same protease inhibitors as indicated before. To disrupt the nuclear membrane, the samples were

sonicated (3 × 10 sec) on ice. The resulting homogenates were ultracentrifuged (250,000 g, 70 min, 4°C) to separate nuclear (supernatant) and membrane fraction (pellet). Finally all three protein fractions were resuspended in or diluted with loading buffer according to chapter 4.6.2 and analysed upon 5-LO protein expression by Northern Blot (chapter 4.6.3).

4.9 5-LO over expression

4.9.1 Plasmid construction

Six mutations were inserted into pT3 wild type and W13/75/102A triple mutant 5-LO plasmids. The original pT3 plasmids were obtained from the group of Prof. Olof Rådmark [261]. The required base mutations were inserted in two steps, by performing mutagenesis-PCR following the QuikChange™ protocol from Stratagene in series with DpnI digestion. The sequence in which the mutations are supposed to be introduced as well as the respective base mutations are listed below (Figure 8).

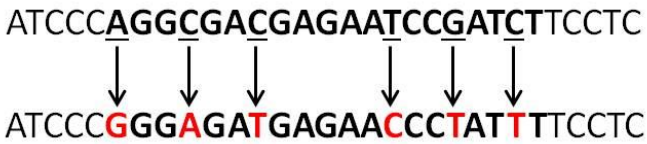

Figure 8: Mutated 5-LO sequence

The sequence in which the mutations are supposed to be inserted is written in bold while the respective bases are additionally underlined. The arrows mark the replacement of the bases and the lower sequence displays the mutated sequence with the changes marked in red.

The used primer pairs are listed in Table 9.

For the first generation primer pairs (a, Table 9), the mutagenesis protocol needed to be adapted. Phusion- instead of Pfu-Polymerase was used and 2 µl $MgCl_2$ (25 mM), 5 µl DMSO, and 10 µl betaine (5 M) were supplemented. Hence, shorter primer pairs (b, Table 9) were designed and tested. They worked out in the standard mutagenesis PCR protocol without any changes. The resulting plasmid was transformed into *E. coli* DH5α, which were cultivated overnight on ampicillin containing agar-plates. Single clones were

amplified in lysogeny broth (LB) medium and the plasmid was extracted using the GenElute™ Plasmid Miniprep Kit (Sigma Aldrich). To confirm mutations, sequencing was performed by SRD (Scientific Research and Development GmbH).

Table 9: Mutagenesis primer

Name	Sequence (5'-3')
5-LO shRNA_mut1_fwd_a	GCTCAACCAAATCCCAGGCGACGAGAACCCTATTTTCCTCCCTTCGG
5-LO shRNA_mut1_rev_a	CCGAAGGGAGGAAAATAGGGTTCTCGTCGCCTGGGATTTGGTTGAGC
5-LO shRNA_mut2_fwd_a	ACCAAATCCCAGGCGACGAGAATCCGATCTTCCTCCCTTCGGATG
5-LO shRNA_mut2_rev_a	CATCCGAAGGGAGGAAGATCGGATTCTCGTCGCCTGGGATTTGGT
5-LO shRNA_mut1_fwd_b	CAACCAAATCCCAGGCGACGAGAACCCTATTTTCCTC
5-LO shRNA_mut1_rev_b	GAGGAAAATAGGGTTCTCGTCGCCTGGGATTTGGTTG
5-LO shRNA_mut2_fwd_b	CCAGGCGACGAGAATCCGATCTTCCTCCCTTC
5-LO shRNA_mut2_rev_b	GAAGGGAGGAAGATCGGATTCTCGTCGCCTGG

In the next step, the mutated 5-LO cDNA fragments were cut out using *Eco*RI and *Sal* I, and inserted into the lentiviral expression vector pLenti-III-EF1α (Applied Biological Materials (ABM) Inc.). This vector carries a puromycin resistance gene for selection in human cells. As the shRNA expressing constructs also carries a puromycin resistance, the

Table 10: Primer for neomycin resistance gene

Name	Sequence
Neo_res_MluI_fwd	TAGGCAACGCGTGTGGAATGTGTGTCAGTTAGGGTGTGG
Neo_res_MluI_rev	TAGGCAACGCGTTCAGAAGAACTCGTCAAGAAGGCGATAG

pLenti-III-EF1α resistance was substituted with a neomycin resistance gene, which confers resistance against geneticin (G418 sulphate). The pcDNA3.1D-Topo-FLAG-Ago2cds-STOP vector was used as template for the neomycin resistance gene including the upstream SV40 promoter. Primers were designed to gain a PCR product (Table 10), containing promoter and resistance gene, flanked by *Mlu*I restriction sites. The amplified product was then ligated into the *Mlu*I digested pLenti-III-EF1α vector.

4.9.2 Lentiviral overexpression of 5-LO

HEK-293T cells were transfected by the calcium phosphate method for lentiviral overexpression [262]. One day prior transfection, 1×10^6 cells were seeded in a 15 cm tissue culture plate. For transfection, 10 µg pLenti expression plasmid and 7.5 µg each P2A and P2B (Applied Biological Materials (ABM) Inc.) as packaging plasmids were mixed with 2.5 M $CaCl_2$ and autoclaved MQ water to get a final concentration of 250 mM of Ca^{2+}. The mixture was slowly applied to 2 × HeBS buffer (NaCl, KCl, $Na_2HPO_4 \times 7\ H_2O$, dextrose, and Hepes (free acid)) under constant air supply. After short incubation for DNA-complex formation, the solution was applied little by little to the HEK-293T cells. After 6 h of incubation at 37°C/ 5% CO_2, the supernatant was replaced by fresh medium. After 24 h, 48 h, and 72 h respectively, the supernatant, containing the infectious viruses, was collected and fresh medium was applied. The viruses can be kept at 4°C for short term or at -80°C for long term storage.

For transduction, 4×10^6 MM6 cells/ml were seeded in 24 well plates and supplemented with 4 µg/ml protamine sulphate. Afterwards, 10 µl, 50 µl, 100 µl or 1 ml of the collected viruses was added to the cells. Further 6 h later, 20 µl fresh MM6 medium was applied and cells were kept for 72 h at 37°C, 5% CO_2 and subsequently selected by addition of geneticin for 21 days. Overexpression was tested on RNA-level (see chapter 4.3.3 and 4.4.3).

4.10 MicroRNA silencing

4.10.1 MiRNA-silencing in MM6 cells

The miRNA silencing of miR-99b-5p and miR-125a-5p in MM6 cells was performed using antagomiRs, designed as described in [263]. A complementary sequence to GFP was used as a control (for sequences see Table 11).

MM6 cells were differentiated for 48 h with 1 ng/ml TGFβ and 50 nM calcitriol before applying a final concentration of 25 nM of the respective antagomiRs. The cells were further treated and harvested as already described in chapter 4.1.2. For detection of knockdown efficiency, miRNA levels were detected as described in chapter 4.4.1. For miR-99b-5p level this resulted in a 95% reduction and a 75% decrease in miR-125a-5p expression.

Table 11: Antagomirs against GFP, miR-99b-5p, and miR-125a-5p

Target	Sequence (5'-3')
GFP	AAG GCA AGC UGA CCC UGA AGUU
miR-99b-5p	TCA CAG GTT AAA GGG TCT CAG GGA
miR-125a-5p	CGCA AGG TCG GTT CTA CGG GTG

4.10.2 MiRNA-silencing in polarized macrophages

In primary cells the method for miRNA-silencing as described in chapter 4.10.1 did not result in an adequate downregulation of miR-99b-5p and miR-125a-5p. Hence, the cells were transfected using the siPORT™ NeoFX™ Transfection Agent (Invitrogen) and Anti-miR™ miRNA Inhibitors (Ambion), following the standard protocol. The macrophages were detached by Trypsin and 1.5-2 × 10^5 cells were incubated with 30 to 50 nM miR-inhibitor and 5 to 8 µl transfection reagent. After 24 h, the cells were adherent again, thus the supernatant was removed and cells were rinsed once with PBS. In the next step the cells were detached using QIAzol® lysis reagent and RNA was extracted

using miRNeasy mini kit or by miRNeasy micro kit (Qiagen), if the cell number was less than 1×10^5 living cells.

4.11 Cytoplasmic Bead Array (CBA)

To determine TNFα and IL-6 formation simultaneously, CBAs were performed. MM6 cells were differentiated using 1 ng/ml TGFβ and 50 nM calcitriol. After 72 h, 100 µl supernatant of either antagomiR-treated cells or Δ5-LO and ΔFLAP cells respectively was collected. The cells were subsequently treated with LPS and further samples were taken after 4 h, 6 h, 8 h, and 24 h after stimulation. To stabilize TNFα, the samples were snap-frozen and prior assay performance diluted 1:1 with PBS. Half of the recommended amount of Capture beads (BD Biosciences) against TNFα and IL-6 were mixed and diluted following the manufacturer's manual. In the next step 5 µl of each sample was incubated with the respective beads for 1 h at room temperature. Meanwhile, Detection Reagent (BD Biosciences) was mixed and transferred to the samples. After another two hours of incubation at room temperature in the dark, the beads were washed with Wash Buffer (BD Biosciences) and subsequently centrifuged. The supernatant was discarded and the beads were resuspended in 300 µl Wash Buffer. The samples were measured by flow cytometry.

4.12 Pull down by pre-miRNA

The pull down experiment was performed using Dynabeads Streptavidin M270 (Life Technologies) coupled with pre-miR-125a, pre-miR-125b-1, pre-miR-125b-2, pre-let-7e, and pre-miR-21 either stem or loop adapted. The beads were designed and prepared by Dr. Nora Treiber and Dr. Thomas Treiber from the group of Prof. Gunter Meister, University of Regensburg. MM6 cells, U2OS and BL-41 cells were used to perform the pull down. Around 450×10^6 differentiated MM6 cells, 850×10^6 untreated BL-41 cells, and 130×10^6 U2OS cells stimulated with 5 nM actinomycin D were lysed in 8 ml lysis buffer supplemented with 1 mM 4-(2-Aminoethyl)benzenesulfonylfluoride (AEBSF) and 1 mM DTT before the twice performed sonification with 30 pulses. To dispose cell debris,

centrifugation was performed for 10 min at 20,000 g/4°C. The supernatant was subsequently incubated at 4°C over night under constant movement with 360 µl unbound hook-beads. The beads were discarded afterwards and an aliquot of the lysate was used as loading control. In the next step, each sample was splitted to 8 fresh vials and further incubated over night with the respective RNA-bound beads. The following day supernatants were discarded and the beads were washed three times with: First with lysis buffer supplemented with 0.1% (v/v) Triton X-100, second with lysis buffer supplemented with 150 mM NaCl, and third just with lysis buffer. Finally, the beads were incubated with SDS-loading dye at 95°C for 5 min to elute bound proteins and subsequently centrifuged for sedimentation of the beads. Of each supernatant, 30 µl was taken, and applied to a SDS-polyacrylamide gel. SDS-PAGE and Western Blot were performed as described in chapter 4.6.2 and 4.6.3.

4.13 Immunofluorescence microscopy

Cover slips were prepared in 6 well plates. They were incubated with 500 µl of a watery solution of 1 mg/10 ml poly-D-lysine hydrobromide (Sigma Aldrich) for 1 h to increase cell attachment. Afterwards, the slips were washed once with the same amount of PBS and left to try for 10 min. Finally a super PAP pen (Life technologies) circle was drawn around the slips to keep the watery cell suspension in a droplet.

For differentiation, 2 10^6 MM6 cells transfected with control non-target shRNA or FLAP knockdown shRNA, respectively, were supplemented for 4 days with 1 µg/ml TGFβ and 50 nM calcitriol. Afterwards the cells were harvested and resuspended in 1 ml PBS containing 1 mg/ml glucose. Around 200 µl of the cell-suspension was subsequently applied to the cover slips and kept in the fridge for 1 h. In the next step the supernatant was removed and the slips were washed with 500 µl PBS prior fixing the cells with methanol at -20°C for 4 min. Afterwards, the cells were gently rinsed with TBS, followed by blocking and permeabilisation for 45 min at room temperature with 5% nonfat dried milk powder in TBS, supplemented with 2% Triton X-100. Finally the cover slips were incubated with anti-Dicer (mouse; 1:50) and anti-5-LO (rabbit; 1:150) antibodies

overnight. The next day, the cells were washed three times with TBS and were in turn incubated for 1 h at room temperature with Alexa Fluor® 488 goat anti-mouse IgG and Alexa Fluor® 594 goat anti-rabbit IgG (Life Technologies; 1:1000) protected from light. Afterwards, the slips were washed twice with TBS and once with water, prior to light-protected incubation with 4′,6-diamidine-2-phenylindol (DAPI; 1:1000 in PBS) for a maximum of 5 min. Finally, the cells were washed with TBS and MQ water twice.

Object plates were cleaned with ethanol and one droplet of Mowiol (Sigma Aldrich) was applied. The cover slips were subsequently mounted with the cell side on top of the mowiol drop, left to try for 45 min, and the slips were sealed with nail polish. Until measurement, slides can be kept in the refrigerator, if protected from light. Microscopy was finally performed using a Leica TCS SP5, located at the Frankfurt Center for Advanced Light Miroscopy (FCAM) and analysis was executed using the Fiji software.

5 RESULTS

5.1 Microarray analysis & validation

A microarray was performed to discover miRNAs whose expression is dependent on the presence of 5-LO. The miRNA levels were determined in MM6 cells transfected with Δ5-LO shRNA and a control shRNA. Three different cell conditions were analyzed: undifferentiated cells as well as cells differentiated with TGFβ and calcitriol for two and for four days, respectively (a complete list of the microarray results is attached in the supplement, chapter 10.1).

Compared to control MM6 cells, seven miRNAs were identified which were lower expressed in Δ5-LO cells after four days of differentiation. The threshold ratio was 0.7 (miRNA expression in Δ5-LO cells : miRNA expression in control cells). The 30 miRNAs which were higher expressed in Δ5-LO cells compared to control cells (threshold ratio 1.3) are displayed as heat map in Figure 9 and as bar graphs in the supplement, chapter 10.2. It is remarkable that out of the 30 listed miRNAs up to now only 13 emerge in publications. This can be potentially attributed to their late discovery recognizable by their high given numbers. However, the majority of available publications are discussing the involvement in various types of cancer. Furthermore, miR-4485 and miR-1246 correlate with inflammatory processes. For example miR-4485 is a target of NF-κB upon TNFα stimulation while miR-1246 is involved in B cell activation and is inducible by p53. But they are not further discussed in the course of this study.

The microarray results of the seven miRNAs downregulated in Δ5-LO cells are displayed as a heatmap in Figure 10 and as bar graphs in Figure 11. These miRNAs were supplemented by miR-19a-3p, which is involved in the LT pathway (see also chapter 2.1.3). In addition, let-7e-5p was included as it is organized in a common cluster with miR-99b-5p and miR-125a-5p (compared to chapter 2.3.8).

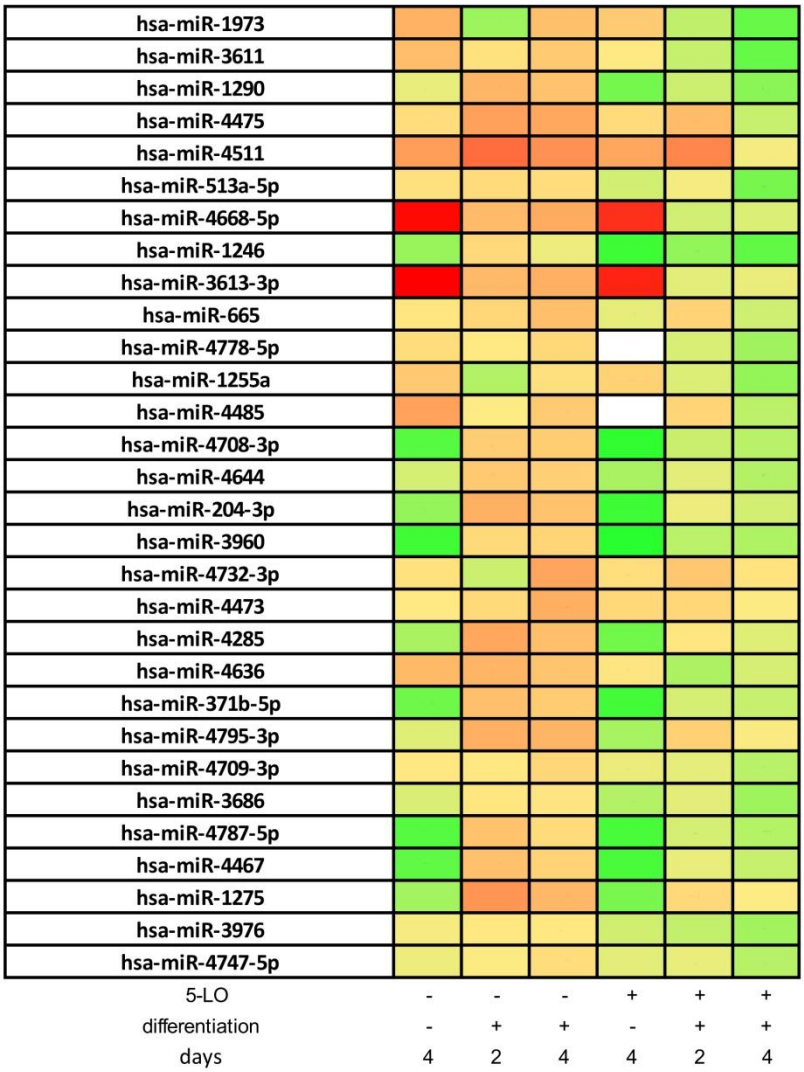

Figure 9: Microarray of upregulated miRNAs as heat map

The miRNA expression levels in control *vs.* Δ5-LO cells were determined as a function of their differentiation status. On day zero differentiation was performed using 1 ng/ml TGFβ and 50 nM calcitriol [n=3]. Undifferentiated cells were kept unstimulated [n=2]. Cells were harvested after 2 or after 4 days and RNA was extracted. Red indicates low miRNA expression and green indicates high expression.

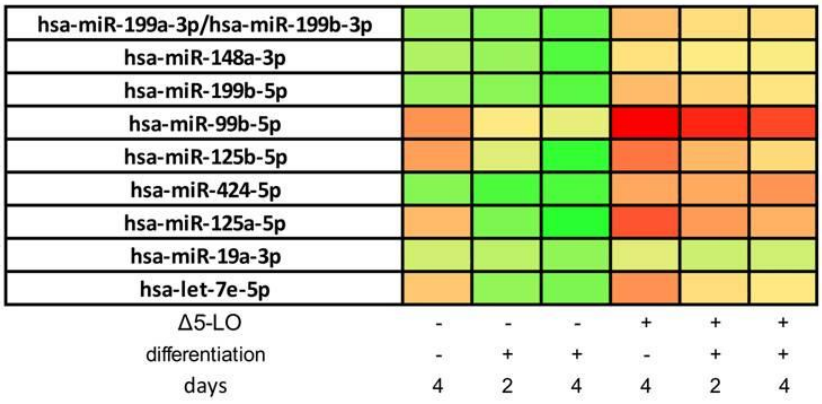

Figure 10: Microarray results of downregulated miRNAs as heat map

The miRNA expression levels in control *vs.* Δ5-LO cells were determined as a function of their differentiation status. On day zero differentiation was performed using 1 ng/ml TGFβ and 50 nM calcitriol [n=3]. Undifferentiated cells were kept unstimulated [n=2]. Cells were harvested after 2 or after 4 days and RNA was extracted. Red indicates low miRNA expression and green indicates high expression.

The microarray determined relative miRNA levels, hence a direct comparison of the expression levels of the different miRNAs was not possible. But in the microarray data of control MM6 cells, an increase in the expression of the in Figure 11 displayed miRNAs was observed upon differentiation. Furthermore, the miRNA levels in Δ5-LO cells were constantly lower as in control cells. In absence of 5-LO, the miRNA expression hardly increased upon stimulation with TGFβ and calcitriol.

In the following, the four miRNAs with the most pronounced differences in their expression level in differentiated control and differentiated Δ5-LO cells were validated by qRT-PCR (miR-125a-5p, miR-424-5p, miR-125b-5p, and miR-99b-5p). As mentioned before, miR-125a-5p and miR-99b-5p belong to the same cluster as let-7e-5p. Hence, this member of the let-7 family was included in the validation process. MiR-19a-3p was omitted in this experiment. It was formerly shown that its expression is not dependent on 5-LO expression [23].

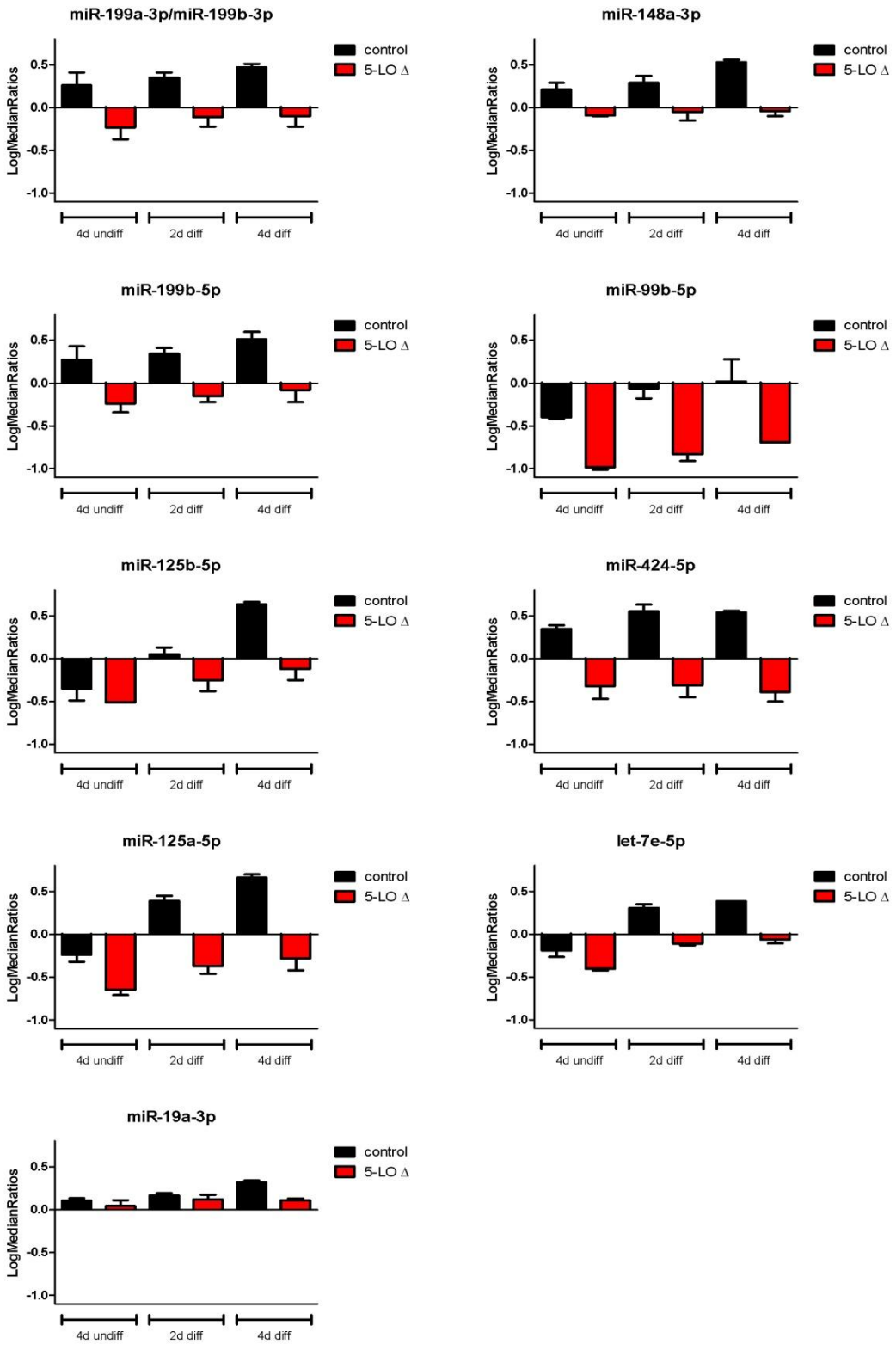

Figure 11: Microarray results of downregulated miRNAs as bar graphs

The miRNA expression levels in control (black panels) *vs.* Δ5-LO (red panels) cells were determined as a function of their differentiation status. On day zero differentiation (diff) was performed using 1 ng/ml TGFβ and 50 nM calcitriol [n=3]. Undifferentiated cells were kept unstimulated (undiff) [n=2]. Cells were harvested after 2 or after 4 days and RNA was extracted. Values are shown as log median ratios +/- SEM

The miRNA expression was monitored in undifferentiated and differentiated cells transfected with 5-LO knockdown shRNA or non-target control shRNA for four days. Undifferentiated cells reveal a similar expression pattern for miR-125a-5p (n=4), miR-424-5p (n=2), miR-125b-5p (n=3), miR-99b-5p (n=4), and let-7e-5p (n=3) in presence and absence of 5-LO at any time (Figure 12). The microarray data indicated an increased expression of the selected miRNAs after differentiation with TGFβ and calcitriol. However, this could not be confirmed for miR-125b-5p (n=3) while the expression profile of miR-424-5p was only observed twice. Both miRNAs showed strong fluctuations in the qRT-PCR experiments. Furthermore, miR-125b-5p did not increase in the control cells upon differentiation (Figure 13) whereas the qRT-PCR data for miR-125a-5p, miR-99b-5p, and let-7e-5p confirmed the microarray data obtained in differentiated MM6 cells. In control MM6 cells, the expression levels of miR-125a-5p and miR-99b-5p were around two-fold increased after four days of differentiation, compared to the expression levels in these cells at day zero. For let-7e-5p, the same trend was observed. However, the levels of let-7e-5p increased only 1.5-fold. In contrast, no enhanced expression of miR-125a-5p, miR-99b-5p, and let-7e-5p was observed in Δ5-LO cells (displayed in Figure 13). Upon differentiation, miR-125a-5p, miR-99b-5p, and let-7e-5p level were hardly changing in Δ5-LO cells.

Taken together, a microarray analysis indicated that 72 miRNAs were affected by Δ5-LO in differentiated MM6 cells. Among them, miR-99b-5p, let-7e-5p, miR-125a-5p, miR-424-5p, and miR-125b-5p were chosen to be validated by qRT-PCR. For the miRNAs belonging to the miR-99b/let-7e/miR-125a cluster, a reduced biosynthesis in absence of 5-LO could be confirmed. In contrast, no significant difference for miR-424-5p and miR-125b-5p was observed in control MM6 and Δ5-LO cells. Hence, miR-424-5p and miR-125b-5p were not employed in the subsequent experiments, while miR-99b-5p, let-7e-5p, and miR-125a-5p were further investigated.

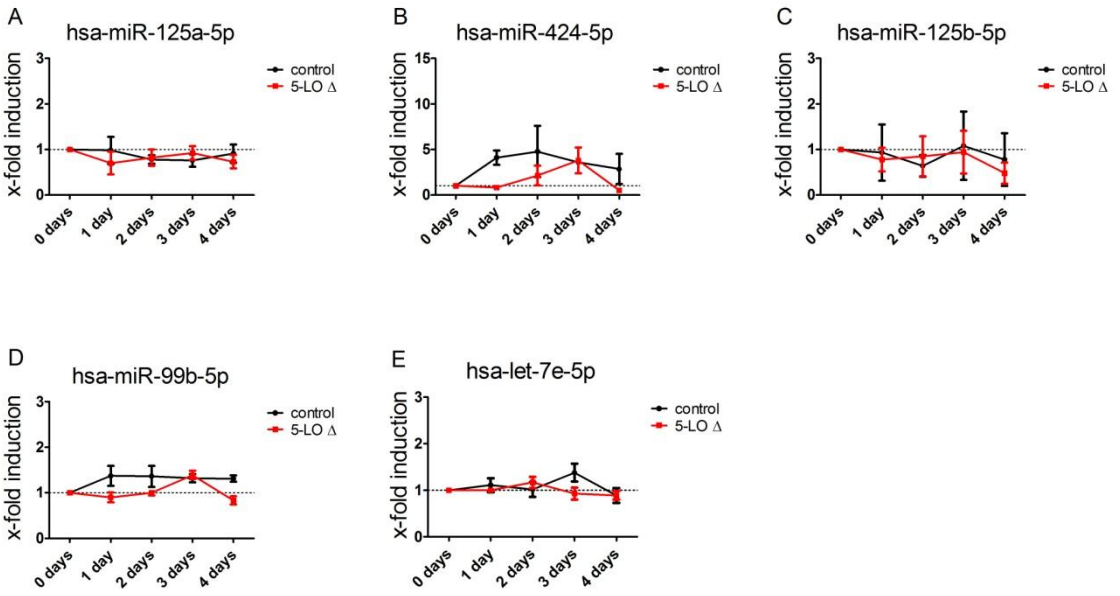

Figure 12: Time course of miR-expression in undifferentiated MM6 cells

For A) miR-125a-5p, B) miR-424-5p, C) miR-125b-5p, D) miR-99b-5p, and E) let-7e-5p. MM6 Δ5 LO (red lines) and control cells (black lines) were kept in culture for 4 days. Cells were harvested after 0 h, 24 h, 48 h, 72 h and 96 h. MiRNA expression level were determined by qRT-PCR. Fold induction based on expression level ($2^{-\Delta Ct}$ normalized to U48) on day zero. Mean ± SEM [n=2-4].

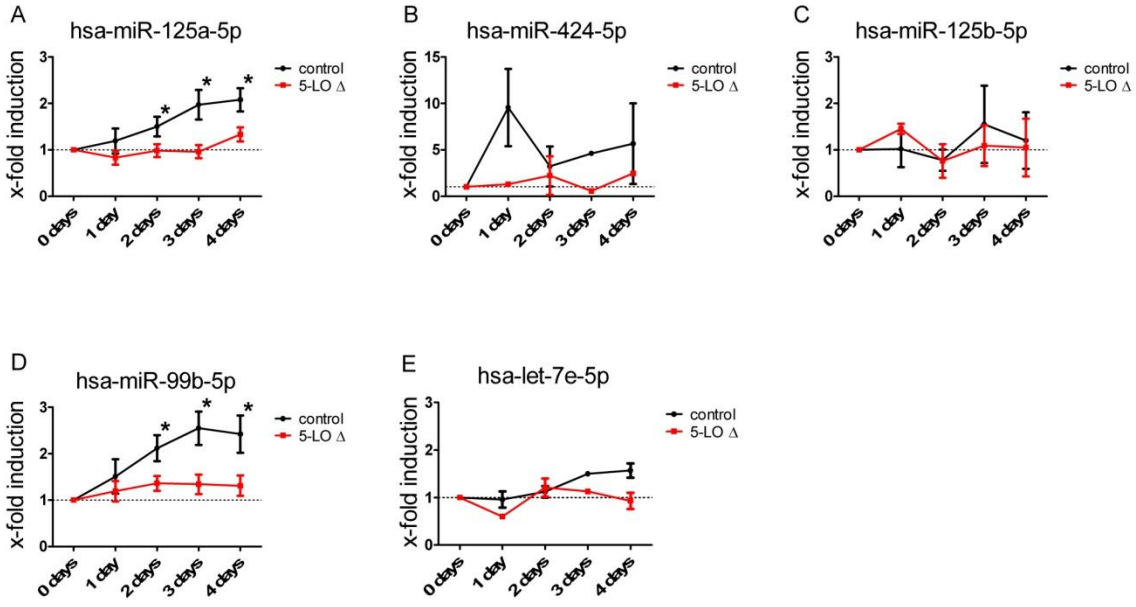

Figure 13: Time course of of miR-expression in presence of TGFβ and calcitriol

For A) miR-125a-5p, B) miR-424-5p, C) miR-125b-5p, D) miR-99b-5p, and E) let-7e-5p. MM6 Δ5-LO (red lines) and control cells (black lines) were differentiated with 1 ng/ml TGFβ and 50 nM calcitriol for 4 days. Cells were harvested before differentiation, after 24 h, 48 h, 72 h and 96 h. MiRNA expression level ($2^{-\Delta Ct}$ normalized to U48) were determined by qRT-PCR. Fold induction based on expression on day zero. Mean ± SEM [n=2-4]; analyzed by two way ANOVA and Bonferroni's post test (*p<0.05).

5.2 Quest after common miRNA characteristics

The microarray data indicated a slight effect of Δ5-LO on expression of miR-99b-5p, let-7e-5p, miR-125a-5p, miR-424-5p, and miR-125b-5p in undifferentiated cells. Hence, the selection criteria were expanded to miRNAs that showed no difference in their expression level in undifferentiated cells, but are increased (threshold ratio 1.3) or decreased (threshold ratio 0.7) in fully (four days) differentiated Δ5-LO cells compared to fully differentiated control MM6 cells. The 22 hits are displayed in the supplement, Figure 45, chapter 10.6. For further investigations, miR-181a-5p and miR-20b-3p were chosen as both exhibit low standard deviations within the different cell conditions. Furthermore, miR-181a-5p and miR-20b-3p are regarded as representative of the miR-181 and the miR-20 family, respectively. Both families were represented in the list of the 22 hits which were not affected by Δ5-LO in undifferentiated MM6 cells several times.

The microarray data indicated similar expression profiles of miR-181a-5p and the in chapter 5.1 mentioned miRNAs of the cluster miR-99b/let-7e/miR-125a. In control cells, the expression of miR-181a-5p was enhanced upon stimulation with TGFβ and calcitriol. In Δ5-LO cells, miR-181a-5p expression was slightly enhanced after differentiation. On the other hand, analysis of the microarray indicated that miR-20b-3p expression was steady in control cells during differentiation. In contrast, differentiation of Δ5-LO cells led to a decrease in miR-20b-3p expression (Figure 14).

To summarize, the microarray indicated 22 miRNAs which are comparably expressed in undifferentiated control and Δ5-LO cells. MiR-181a-5p and miR-20b-3p were chosen as representatives as the analysis of the microarray revealed that they are affected by Δ5-LO in differentiated MM6 cells. The expression of miR-181a-5p and miR-20b-3p are decreased in absence of 5-LO.

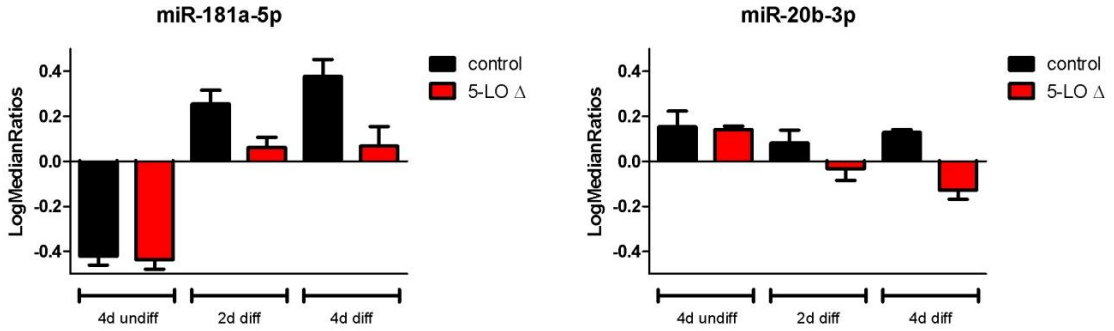

Figure 14: Microarray results for miR-181a-5p and miR-20b-3p
MiRNA expression levels for A) miR-181a-5p and B) miR-20b-3p were determined as a function of their differentiation status. Black panels: control MM6 cells transfected with nontarget shRNA; Red panels: MM6 cells transfected with Δ5-LO shRNA. On day zero, cells were differentiated using 1 µg/ml TGFβ and 50 nM calcitriol [n=3]. Undifferentiated cells were kept unstimulated [n=2]. Cells were harvested after 2 or after 4 days, followed by RNA extraction. Values are shown as log median ratios + SEM.

The microarray indicated that the absence of 5-LO reduces the expression of the mature miRNAs miR-99b-5p, let-7e-5p, miR-125a-5p, miR-125b-5p, miR-424-5p, and miR-181a-5p. Hence, common motifs or common structures in their respective precursors are probable which act as recognition signals for 5-LO controlled processing. To identify potential common regulatory mechanism, sequence alignments and structural comparisons were conducted for the precursors of miR-99b, let-7e, miR-125a, miR-125b, miR-424, miR-181a, and miR-20a. The sequence alignment was performed using MEME Suite [264]. The respective pre-miRNA sequences were obtained from miRBase [106] and were applied to the MEME software. But the alignment did not show a common motif which could act as an attractant for 5-LO controlled miRNA processing.

Unfortunately, no suitable software was available to perform structural alignments among miRNAs. Hence, the seven precursors were manually analyzed. The focus was laid on the size and the number of loops, but no analogies were observed among their structures.

In conclusion, although seven 5-LO controlled precursor miRNAs were analyzed upon common motifs and structures, no similarities were identified.

5.3 Effect of 5-LO on miRNA expression and Drosha procession

MiR-99b-5p, let-7e-5p, and miR-125a-5p were found to be affected by Δ5-LO in MM6 cells. As mentioned in chapter 2.3.8, these miRNAs are co-transcribed. Hence, it is possible that 5-LO controls the expression of the complete miR-99b/let-7e/miR-125a cluster. That would imply a 5-LO controlled regulation of pri-miRNA biosynthesis, which is independent of the interaction between 5-LO and Dicer.

To study this possibility, the levels of the pri- miR-99b/let-7e/miR-125a in dependence of the 5-LO status was analyzed by qRT-PCR.

In undifferentiated cells, the pri-miR-99b/let-7e/miR-125a level was similar in Δ5-LO and control cells. Upon differentiation with TGFβ and calcitriol, both cell types exhibited an around two-fold increase in the expression of the pri-miR-99b/let-7e/miR-125a transcript (Figure 15 A).

To sum up, the expression of pri-miR-99b/let-7e/miR-125a mRNA is not affected by Δ5-LO neither in undifferentiated nor in differentiated 5-LO expressing MM6 cells. Hence, 5-LO affects the maturation of miR-99b-5p, let-7e-5p, and miR-125a-5p and not the transcription or the expression of their common primary transcript.

After transcription of the miRNA gene encoding the cluster, the pri-miRNA is further processed by Drosha and Dicer (displayed in Figure 4, chapter 2.3.2). Drosha is responsible for forming pre-miRNAs from pri-miRNAs and acts prior to Dicer. To investigate, if the cleavage by Drosha is affected by Δ5-LO, the pre-miRNA level of miR-99b, let-7e, and miR-125a were analyzed by qRT-PCR. Since Drosha cleaves the pre-miRNA out of the corresponding pri-miRNA, the sequences of the pre-miRNAs are also present in the pri-miRNA. Hence, a specific detection of pre-miR-99b, pre-let-7e, and pre-miR-125a by qRT-PCR is not possible and the results shown in Figure 15 B-E represent the pre-miRNA as well as the corresponding pri-miRNA (referred to as pre-miRNAs). Pre-miR-19a was included in the experiments as negative control. Its level should not be affected by Δ5-LO as the expression of its predominantly occurring mature miRNA, miR-19a-3p, is stably expressed in 5-LO positive and negative MM6 cells. Pre-miR-19a is clustered with pre-miR-17, pre-miR-18a, pre-miR-19b-1, pre-miR-20a, and pre-miR-92a-1.

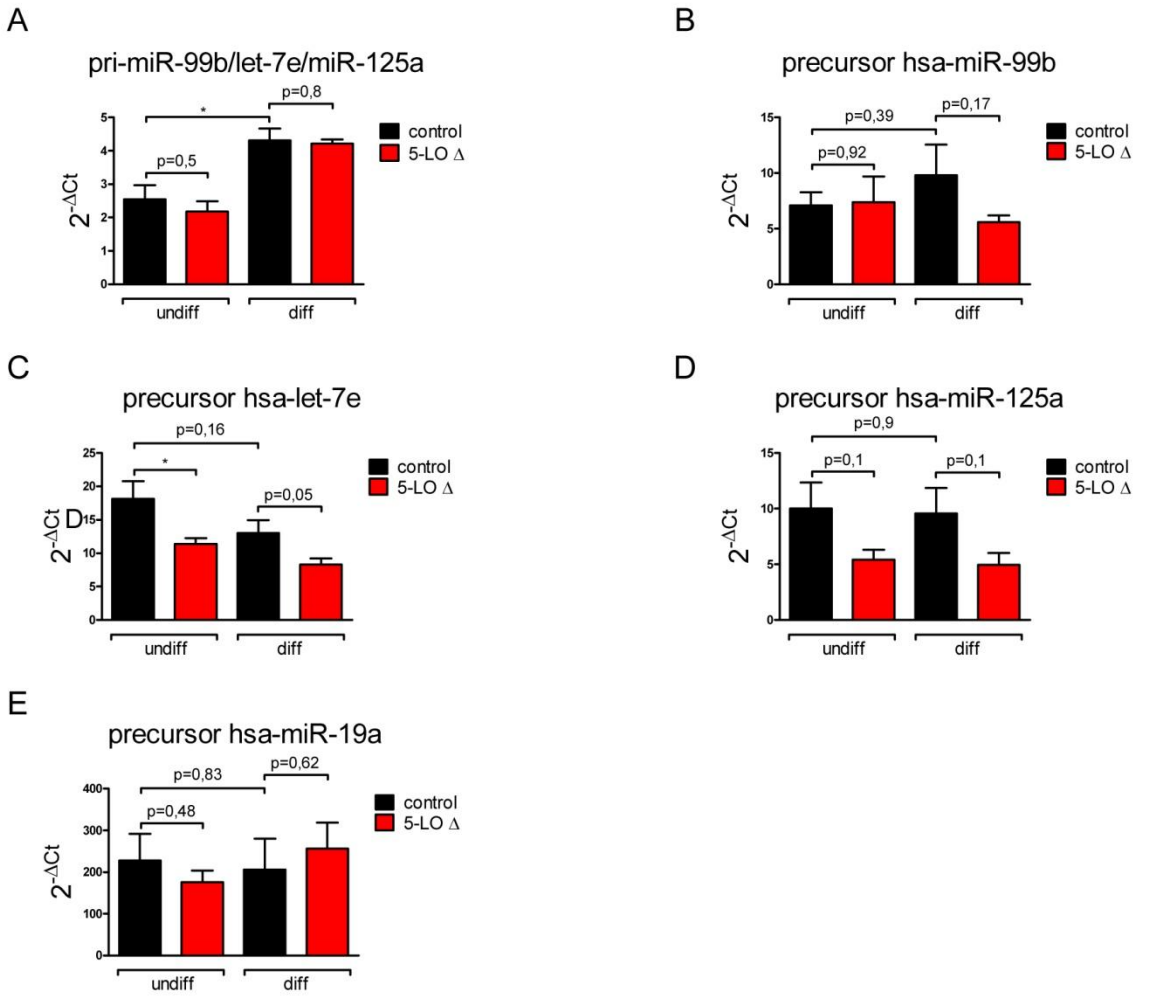

Figure 15: Effect of 5-LO on expression of the miRNA precursors

Expression levels of A) pri-miR-99b/let-7e/miR-125a, B) miR-99b precursor, C) let-7e precursor, D) miR-125a precursor, and E) miR-19a precursor were determined as a function of their differentiation status. Black panels: MM6 cells transfected with nontarget shRNA; red panels: MM6 cells transfected with Δ5-LO shRNA. On day zero, cells were differentiated using 1 µg/ml TGFβ and 50 nM calcitriol. Undifferentiated cells were kept unstimulated. Cells were harvested after four days followed by RNA extraction. Expression levels ($2^{-\Delta Ct}$ normalized to RNU6-2 expression) were determined using qRT-PCR. Data are given for A as $2^{-\Delta Ct}$ values or as fold-induction for B-E. Induction is based on expression level on day 4 of undifferentiated cells. Values represent mean + SEM [n=5] and statistical significance was determined by t-test (*$p<0.05$).

The expression of pre-miR-19a was similar in undifferentiated and differentiated MM6 cells independent of Δ5-LO. Pre-let-7e and pre-miR-125a were similarly expressed. Both precursor levels were reduced in Δ5-LO cells compared to control cells. This applied for undifferentiated and differentiated cells. Furthermore, no TGFβ and calcitriol mediated increase was observed for neither pre-let-7e nor pre-miR-125a in control and Δ5-LO cells. Pre-miR-99b appeared to have similar expression levels in undifferentiated control cells and undifferentiated Δ5-LO cells. Upon differentiation, the expression of pre-miR-99b increased around 1.5-fold in

control cells. In contrast, differentiated Δ5-LO cells displayed a slightly decreased expression of pre-miR-99b compared to undifferentiated Δ5-LO cells.

In summary, these results revealed an effect of Δ5-LO on Drosha cleavage of pre-miR-99b, pre-let-7e, and pre-miR-125a. In contrast to the data obtained for the corresponding mature miRNAs miR-99b-5p, let-7e-5p, and miR-125a-5p, the effect is in case of pre-let-7e and pre-miR-125a additionally existent in undifferentiated cells.

5.4 Pull-down of 5-LO by pre-miRNA as bait

It is known that Dicer binds to 5-LO [38]. Furthermore, this study showed an involvement of 5-LO in maturation of miR-99b, let-7e, and miR-125a. To evaluate if this is a result of direct binding of 5-LO to the miRNA-precursors pre-miR-99b, pre-let-7e, and pre-miR-125a, a pull down experiment was performed. The pull down was performed with cell lysates from differentiated MM6 cells, BL41 cells, and actinomycin stimulated U2OS cells. All cells express high levels of 5-LO. Pre-miR-125a, pre-miR-125a-1 and -2, as well as pre-let-7e were used as baits. Pre-miR-21 was applied as negative control which was tested before in another independent experiment. The precursor can potentially interact with 5-LO via its loop or its stem region. Hence, the RNA was attached to the beads via their loop or their stem region.

After performing the pull down experiment, the different samples were screened for 5-LO by immunoblot. Samples derived from differentiated MM6 cells (Figure 16 A) displayed strong 5-LO bands throughout all lanes. That implied a binding of 5-LO to the precursor of miR-125b, let-7e, miR-125a, and miR-21. However, no difference between the investigated pre-miRNAs (pre-miR-125a, pre-miR-125b-1 and -2, pre-let-7e) and the control (pre-miR-21) was detected. In addition, the 5-LO pull down efficiency was independent of loop or stem adapted pre-miRNA immobilization. Hence, these results implicate an unspecific binding of 5-LO to RNA or some technical problems with unspecific interactions.

In contrast, samples originated from BL41 cells and U2OS cells, displayed only slight or no visible bands (Figure 16 B/C). However, fewer cells and less volume of cell lysate were applied compared to MM6 cells.

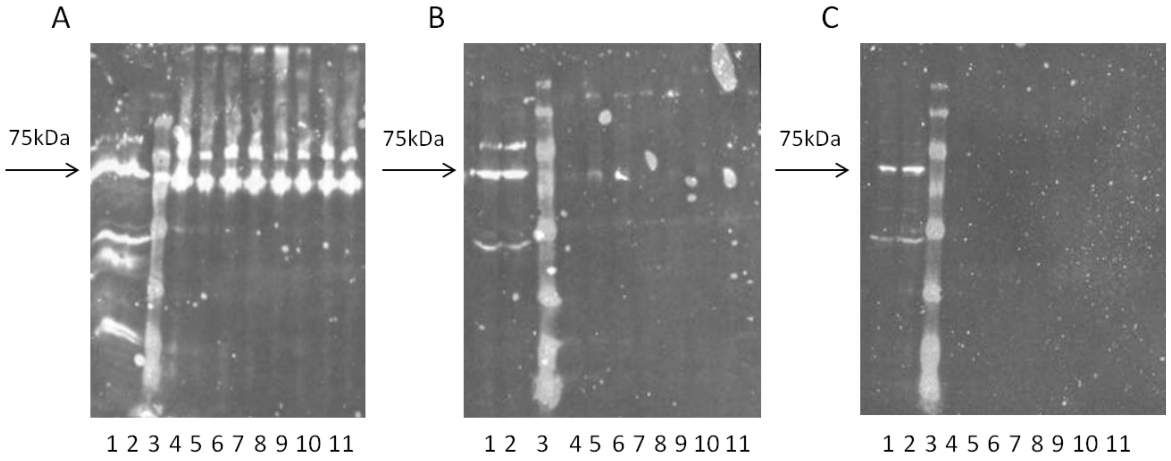

Figure 16: Pull down of 5-LO by pre-miRNA

Pull down experiment was performed using cell lysates from A) MM6 cells differentiated with 1 ng/ml TGFβ and 50 nM calcitriol for four days (45 × 10^6 cells), B) untreated BL41 cells (42.5 × 10^6 cells), and C) actinomycin stimulated U2OS cells (6.5 × 10^6 cells) and subsequently analyzed by immunoblot. 1) untreated cell lysates 2) cell lysates preincubated with uncoupled beads 3) size marker (Precision Plus Protein™ Standards, Bio-Rad) 4) cell lysates incubated with stem coupled pre-miR-125a beads 5) cell lysates incubated with stem coupled pre-miR-125b-1 beads 6) cell lysates incubated with stem coupled pre-miR-125b-2 beads 7) cell lysates incubated with stem coupled pre-let-7e beads 8) cell lysates incubated with stem coupled pre-miR-21 beads 9) cell lysates incubated with loop coupled pre-miR-125a beads 10) cell lysates incubated with loop coupled pre-miR-125b-1 beads 11) cell lysates incubated with loop coupled pre-miR-21 beads. Western blot was performed once.

Taken together, 5-LO seems to bind nonspecifically to all pre-miRs in this experiment so that no final conclusion on direct 5-LO-miRNA interaction can be drawn. But besides, a regulation of miRNA expression via direct binding of its corresponding precursor to 5-LO cannot be excluded.

5.5 The influence of 5-LO inhibitors and LTs on miRNA formation

The binding to Dicer influences 5-LO activity, resulting in an enhanced generation of LTs [38]. 5-LO knockdown, in turn, inhibited generation of miR-99b-5p, let-7e-5p, and miR-125a-5p in differentiated MM6 cells, as shown in Figure 13, chapter 5.1. To assess if LTs can regulate Dicer activity, the effect of LTs on the expression of miR-99b-5p and miR-125a-5p was analyzed. Control shRNA transfected MM6 cells were differentiated in presence of 5-HETE, LTC_4, and LTB_4 for four days. Next, the expression levels of miR-99b-5p and miR-125a-5p were analyzed by qRT-PCR. But the addition of 5-LO

metabolites did not alter the formation of miR-99b-5p and miR-125a-5p (Figure 17 A/B black staples).

In addition, it was investigated whether 5-LO needs to be active to support miRNA processing, or if the presence of 5-LO protein is sufficient for controlling miR-99b-5p and miR-125a-5p maturation. Hence, differentiated MM6 cells were treated with the 5-LO inhibitors Zileuton and MK-886. None of the inhibitors reduced formation of miR-99b-5p and miR-125a-5p (Figure 17 A/B red and white staples).

To summarize, increasing LT levels did not affect generation of miR-99b-5p and miR-125a-5p. Furthermore, inhibition of LT formation did not inhibit expression of miR-99b-5p and miR-125a-5p comparable to knockdown of 5-LO (Figure 17 A/B grey staples). Hence, these results indicate a LT independent regulation of miR-99b-5p and miR-125a-5p by 5-LO.

Figure 17: Effect of 5-LO products and 5-LO inhibitors on miRNA expression

MM6 cells were differentiated with 1 ng/ml TGFβ and 50 nM calcitriol for 4 days. Zileuton (1 µM; red panels) or MK-886 (100 nM; white panels) were added twice (at day zero and day two of the differentiation period). Alternatively a mixture of 5-LO products (100 nM 5-HETE, 100 nM LTB_4, and 100 nM LTC_4; black panels) was daily applied starting on day zero. Expression level ($2^{-\Delta Ct}$ normalized to U48 expression) were determined for A) miR-99b-5p and B) miR-125a-5p by qRT-PCR [n=3]. Data are given as fold induction based on expression levels of differentiated cells on day 4 as mean + SEM [n=3-4] and were analyzed by two way ANOVA and Bonferroni's post test (**p<0.01)

5.6 The effect of FLAP knockdown on the maturation of miR-99b-5p and miR-125a-5p

FLAP is a 5-LO interacting protein which is essential for transferring AA to 5-LO. To investigate the potential role of FLAP in 5-LO controlled miRNA processing of miR-99b-5p, let-7e-5p, and miR-125a-5p, the expression levels of these three miRNAs were analyzed by qRT-PCR in differentiated control shRNA and ΔFLAP transfected MM6 cells. As shown in

Figure 18, the level of all three miRNAs was steady in undifferentiated control and ΔFLAP cells. In control MM6 cells the expression of miR-99b-5p and miR-125a-5p increased upon differentiation. On the contrary, ΔFLAP cells did not display a significant change of miR-99b-5p and miR-125a-5p expression. Let-7e-5p was not affected by ΔFLAP.

Taken together, these results resemble the data obtained in Δ5-LO cells (see Figure 13, chapter 5.1 for comparison). In contrast to differentiated control MM6 cells, differentiated ΔFLAP cells exhibited a decreased formation of miR-99b-5p, miR-125a-5p, and let-7e-5p to a less extent. However, compared to Δ5-LO cells, the tendency in ΔFLAP cells was less pronounced, but reproducible.

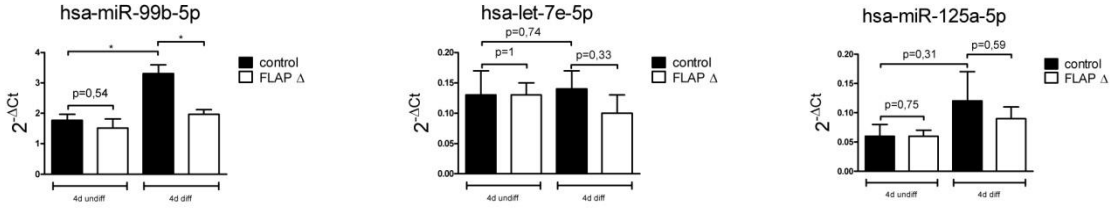

Figure 18: Effect of FLAP knockdown on miRNA expression

MM6 control cells (transfected with control non-target shRNA; black panel) and MM6 cells transfected with FLAP knockdown shRNA (white panel) were differentiated with 1 ng/ml TGFβ and 50 nM calcitriol for 4 days (4d diff) or kept untreated (4d undiff). The influence of ΔFLAP on expression level ($2^{-\Delta Ct}$ normalized to U48 expression) of A) miR-99b-5p, B) let-7e-5p, and C) miR-125a-5p was determined by qRT-PCR. Data are given as means + SEM [n=3] and were analyzed by t-test (*p<0.05)

In analogy to chapter 5.3, the influence of ΔFLAP on the transcription and the Drosha processing of the miRNA-cluster miR-99b/let-7e/miR-125a were investigated next. Therefore, control and ΔFLAP MM6 cells were differentiated with TGFβ and calcitriol for four days. Their respective levels of pri-miR-99b/let-7e/miR-125a as well as pre-miR-99b, pre-let-7e, and pre-miR-125a were analyzed by qRT-PCR. Pre-miR-19a was included in the experiments as negative control (in analogy to chapter 5.3).

The primary transcript showed a steady expression in undifferentiated control and ΔFLAP cells. Upon differentiation, the level increased about two-fold, independent of the FLAP status (Figure 19 A). These results are comparable with the data obtained in Δ5-LO cells (Figure 15, chapter 5.3). The level of pre-let-7e, pre-miR-125a, and pre-miR-19a were also rather steadily expressed in undifferentiated control and ΔFLAP cells. Furthermore, the expression of the

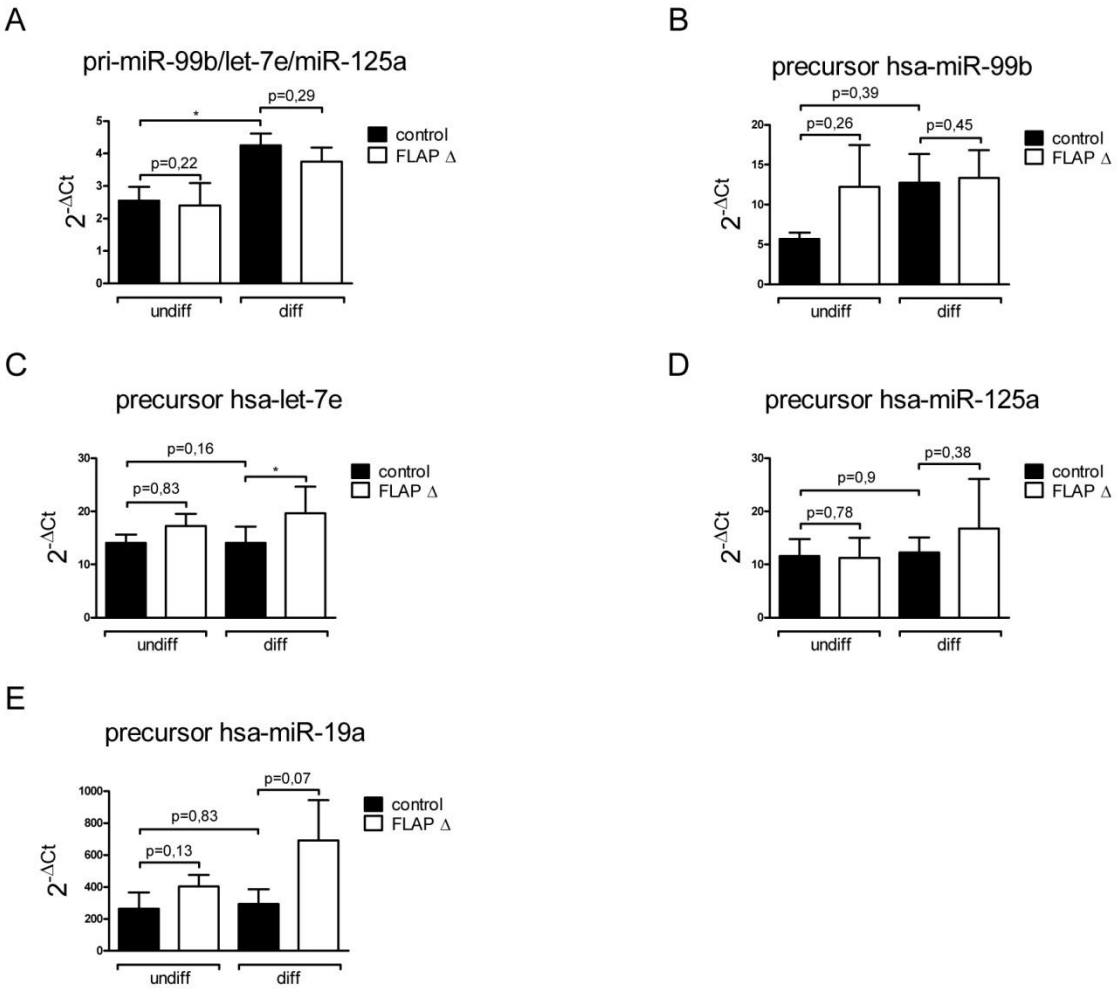

Figure 19: Effect of FLAP on expression of miRNA presursor

Expression levels of A) pri-miR-99b/let-7e/miR-125a, B) miR-99b precursor, C) let-7e precursor, D) miR-125a precursor, and E) miR-19a precursor were determined as a function of their differentiation status. Black panels: MM6 cells transfected with non-target shRNA; white panels: MM6 cells transfected with ΔFLAP shRNA. On day zero, cells were differentiated using 1 µg/ml TGFβ and 50 nM calcitriol. Undifferentiated cells were kept unstimulated. Cells were harvested after 4 days followed by RNA extraction. Expression level ($2^{-\Delta Ct}$ normalized to β-actin (A) or RNU6-2 (B-E) were determined using qRT-PCR. Data are given as $2^{-\Delta Ct}$ values. Values represent the mean + SEM [n=3] and statistical significance was determined by t-test (*p<0.05).

listed precursors was not stimulated upon differentiation in control MM6 cells. On the contrary, in TGFβ and calcitriol stimulated ΔFLAP cells the expression of pre-let-7e, pre-miR-125a, and pre-let-19a is slightly higher than in control cells (Figure 19 C-E). Actually, the precursor of let-7e-5p was significantly increased in differentiated ΔFLAP cells. Pre-miR-99b is lower expressed than pre-miR-125a and pre-let-7e in undifferentiated control MM6 cells. However, upon differentiation, the expression reached a level similar to undifferentiated and differentiated ΔFLAP cells (Figure 19 B).

To summarize, ΔFLAP did not affect expression of the pri-miR-99b/let-7e/miR-125a. However, the qRT-PCR data achieved for pre-miR-99b, pre-let-7e, and pre-miR-125a contrast the data obtained in Δ5-LO cells (Figure 15, chapter 5.3). Compared to differentiated control cells, the precursor of let-7e was rather up- than downregulated in differentiated ΔFLAP cells. The same tendency applied for pre-miR-19a. These results imply a FLAP independent performance of Drosha on pre-miR-99b, pre-let-7e, and pre-miR-125a.

5.7 Northern Blot analysis

By common PCR methods, it is not possible to determine solely pre-miRNA without detecting pri-miRNA. Hence, the only available method to analyze pre-miRNA independently, is the visualization by Northern blot analysis where mature, pre-, as well as pri-miRNAS can be detected together on one gel. Northern blots were performed to validate the qRT-PCR data obtained for miR-125a and let-7e (Figure 15, chapter 5.3 and Figure 18, chapter 5.6). The analysis was done in cooperation with Dr. Thomas Treiber, University of Regensburg.

Total RNA extracted from control, Δ5-LO, and ΔFLAP MM6 cells was analyzed. The cells were differentiated with TGFβ and calcitriol for 96h or kept untreated. The different samples were separated by gel electrophoresis, blotted onto nylon membranes and subsequently incubated with the respective radiolabelled probes. The data of one out of three independent experiments is shown in Figure 20.

The Northern blot of miR-99b-5p is displayed in Figure 20 A. The probe was able to detect all three processing states, the pri-, the pre-, and the mature miRNA. Interestingly, the probes against let-7e-5p (Figure 20 B) and miR-125a-5p (Figure 20 C) bound predominantly to the

mature miRNAs and less to the respective precursor. Unfortunately, due to the lack of a loading control quantification was not possible.

Only a tendency similar to the previous qRT-PCRs and the microarray data can be observed for the mature formof miR-99b-5p which were slightly stronger expressed in control cells compared to Δ5-LO cells, however a clear statement is not possible due to the lack of the loading control. In ΔFLAP cells, the expression of miR-99b-5p, let-7e-5p, and miR-125a-5p was comparable with the expression in control cells.

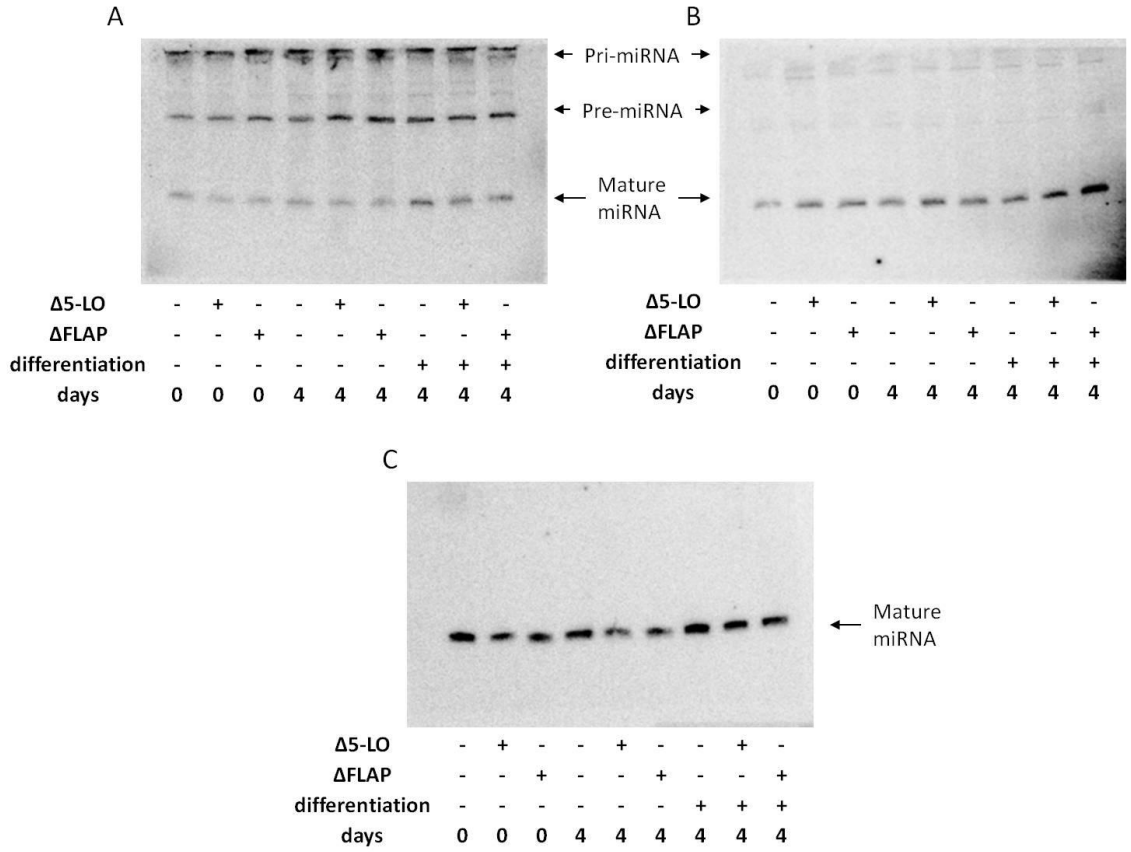

Figure 20: Northern Blot analysis of mature-, pre-, and pri-miRNAs

MM6 control cells (transfected with control non-target shRNA), MM6 cells transfected with Δ5-LO shRNA, and MM6 cells transfected with ΔFLAP shRNA were differentiated as indicated on day zero for four days with 1 ng/ml TGFβ and 50 nM calcitriol. Undifferentiated cells were just left in culture for further four days. Cells were harvested at day zero or after four days (undiff/diff) followed by RNA extraction. 10 µg of total RNA was applied and blotted onto nylon membranes, which were incubated with radioactive labeled probes against A) miR-99b-5p, B) let-7e-5p, and C) miR-125a-5p. The results from three independent experiments are shown.

The results for pre-miR-99b were inconsistent and no tendency was observed. The same applied for the pri-miR-99b/let-7e/miR-125a, detected by the same probe.

Taken together, the Northern Blots display a comparable image to the qRT-PCR data and the microarray. At least, expression of mature miR-99b-5p and miR-125a-5p seemed to be suppressed in Δ5-LO cells. MiRNA expression profiles in ΔFLAP cells did not display any difference compared to control cells. Nevertheless, no loading control was applied. Thus, the Northern Blot data should not be employed in the following.

5.8 Involvement of FLAP in co-localisation of Dicer and 5-LO

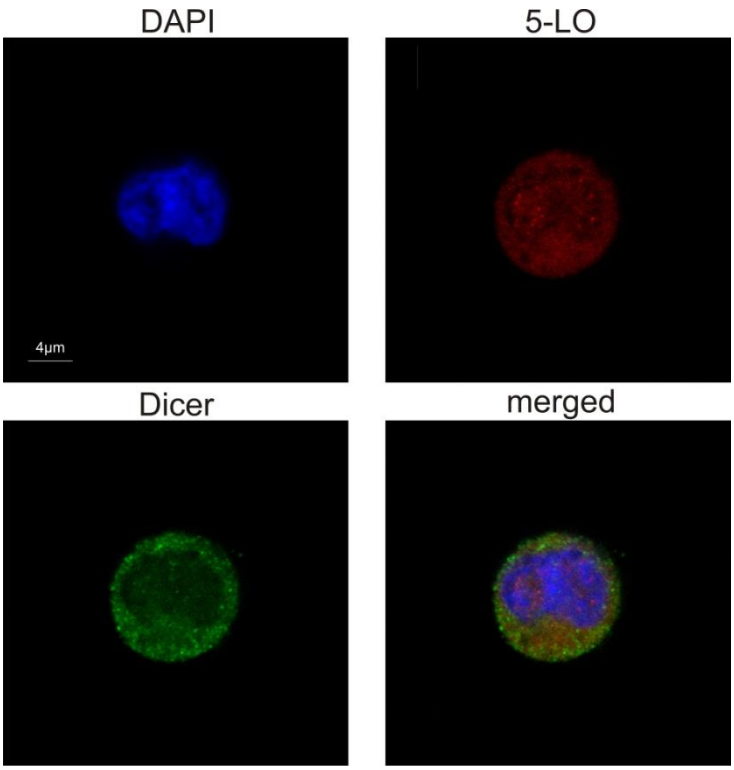

Figure 21: Immunocytochemistry of 5-LO and Dicer MM6 control cells.
MM6 cells transfected with control non-target shRNA were differentiated with 1 ng/ml TGFβ and 50 nM calcitriol for four days. Afterwards, cells were fixed and stained as described in chapter 4.13. The pictures show single staining for DAPI (nucleus; blue), 5-LO (red), Dicer (green), and merged images (Scale bar corresponds to 4 µm).

An involvement of FLAP in processing of miR-99b-5p and miR-125a-5p was discovered in this study (Figure 18, chapter 5.6), but the maturation of the listed miRNAs was not affected by the FLAP inhibitor MK-886 (Figure 17, chapter 5.5). These observations contributed to the idea of the involvement of a multi-protein complex (Dicer/5-LO/FLAP) in monitoring

miR-99b-5p and miR-125a-5p formation. Thus, it was investigated next whether the FLAP protein influences the colocalization of 5-LO and Dicer. Immunocytochemistry of 5-LO and Dicer was performed in differentiated MM6 cells transfected with non-target control and ΔFLAP shRNA, respectively.

According to previously published data [31, 265], 5-LO and Dicer were mainly located in the cytoplasm of control cells, whereas the localization inside the nucleus was secondary (Figure 21). On the contrary, 5-LO relocated in ΔFLAP cells into the nucleus while Dicer remained in the cytoplasm (Figure 22).

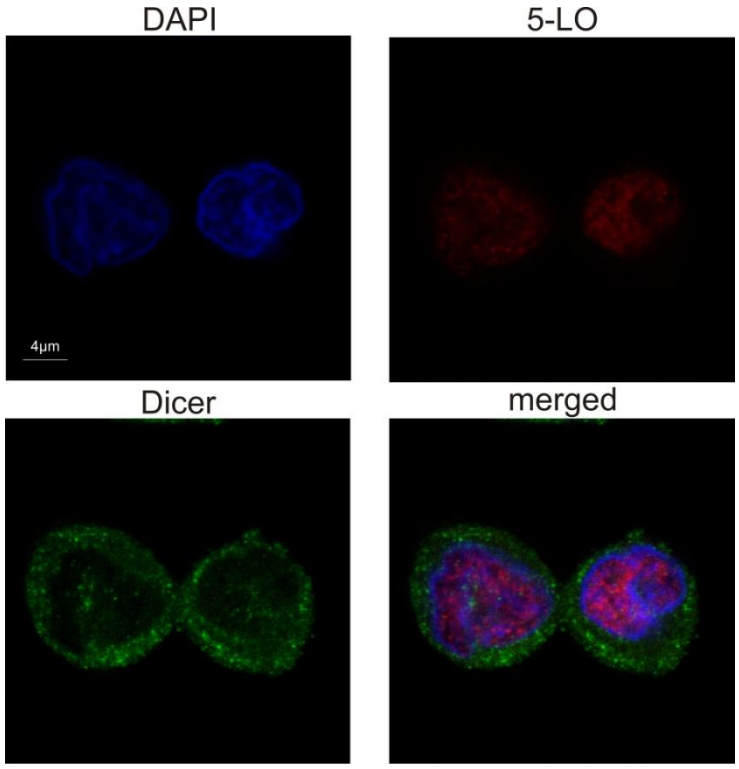

Figure 22: Immunocytochemistry of 5-LO and Dicer in ΔFLAP cells.
MM6 cells transfected with ΔFLAP shRNA were differentiated with 1 ng/ml TGFβ and 50 nM calcitriol for four days. Afterwards, cells were fixed and stained as described in chapter 504.13. The pictures show single staining for DAPI (nucleus; blue), 5-LO (red), Dicer (green), and merged images (Scale bar corresponds to 4 µm).

Taken these data together, FLAP did not seem to influence the localization of Dicer whereas the localization of 5-LO was altered by FLAP in favor of the cytosol. This implies a potential involvement of FLAP in maintaining the 5-LO protein inside the cytoplasm where 5-LO is

able to regulate maturation of miR-99b-5p, let-7e-5p, and miR-125a-5p by interacting with Dicer.

5.9 Ago2 expression is independent of 5-LO

Besides binding to 5-LO, Dicer also interacts with Ago2 [266]. This member of the Argonaute protein family is the only representative with own nuclease activity [267]. By regulating the cleavage activity of Ago2, 5-LO could be capable of controlling mRNA-silencing capacity and to a lesser extent of regulating expression of miR-99b-5p, let-7e-5p, and miR-125a-5p. To evaluate this possibility, Western Blot analysis was performed to determine Ago2 protein levels in undifferentiated and differentiated control, Δ5-LO and ΔFLAP cells.

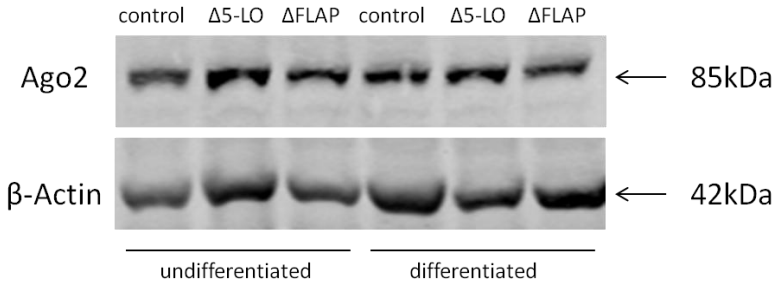

Figure 23: Ago2 expression

MM6 control cells transfected with control non-target shRNA, MM6 cells transfected with Δ5-LO shRNA and MM6 cells transfected with ΔFLAP shRNA were differentiated with 1 ng/ml TGFβ and 50 nM calcitriol for four days. Undifferentiated cells were kept untreated. After four days cells were harvested and Ago2 protein expression was determined via Western blotting. For each lane 150 µg total protein lysate was applied. The result from one out of two independent experiments is shown.

Ago2 was basally expressed in undifferentiated and differentiated MM6 cells. However, upon knockdown of 5-LO and FLAP, no impact on the protein level of Ago2 was detectable (Figure 23). Taken together, Ago2 expression was neither inhibited nor enforced by treatment with TGFβ and calcitriol. Furthermore, Ago2 expression was also independent of 5-LO and FLAP expression. Hence, Ago2 protein expression seems not to be linked to 5-LO regulated maturation of miR-99b-5p, let-7e-5p, and miR-125a-5p.

5.10 Reconstitution of 5-LO in Δ5-LO cells

In this study, MM6 cells transfected with non-target control shRNA and Δ5-LO shRNA were employed. In case of integrating the shRNA carrying plasmids within important regulatory regions of the cell, insert independent side effects can occur. To exclude unspecific side effects caused by transfection, the expression of 5-LO was reestablished in MM6 Δ5-LO cells. Finally, the resulting cell line should exhibit a reversal of the observations made in Δ5-LO cells. Therefore, the cells were transduced with a wt5-LO (Δ5-LO-oe-wt5-LO) plasmid and a control plasmid devoid of the 5-LO insert (Δ5-LO-oe-control). Prior to transduction six silent mutations were inserted in the shRNA binding region of the Δ5-LO-oe-wt5-LO plasmid as shown in Figure 8, chapter 4.9.

After a final selection with geneticin for at least 2 weeks, the transduced cells were tested for their 5-LO mRNA level (Figure 24). The 5-LO mRNA level in undifferentiated Δ5-LO-oe-wt5-LO cells resembled the 5-LO mRNA level in differentiated control cells. Hence, the transfection was successful.

Δ5-LO-oe-wt5-LO cells express 5-LO with an independent SV40 promoter. Thus, these cells did not need to be stimulated with TGFβ and calcitriol to express 5-LO. To study the effect of 5-LO relocation, the expression of miR-99b-5p and miR-125a-5p was analyzed and compared in differentiated control and Δ5-LO cells as well as in unstimulated Δ5-LO-oe-control and Δ5-LO-oe-wt5-LO cells (Figure 25).

Differentiated control cells exhibited the highest miR-99b-5p and miR-125a-5p levels. In accordance with Figure 13 in chapter 5.1, the levels were reduced to around one half in Δ5-LO cells. However, miRNA expression was not recovered simply by relocation of 5-LO in Δ5-LO cells. This suggests an involvement of TGFβ and calcitriol treatment in the generation of miR-99b-5p and miR-125a-5p. However, as the cells transfected with the wt5-LO plasmid rapidly started to pass away in culture, it was not possible to test the influence of differentiation and the 5-LO protein level in these cells.

To summarize, the 5-LO protein alone was not sufficient to increase miRNA expression. However, it was not possible in the course of this study to differentiate stable 5-LO overexpressing cells to analyze whether co-factors activated by TGFβ and calcitriol contribute to maturation of miR-99b-5p and miR-125a-5p.

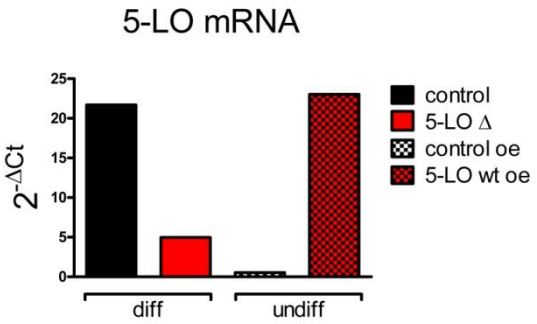

Figure 24: 5-LO expression after reconstitution

MM6 cells transfected with Δ5-LO shRNA were further transfected with a wt5-LO overexpressing plasmid (black/white checkered panels) or a control plasmid carrying no insert (black/red checkered panels), respectively. Cells were just kept in culture. MM6 control cells (transfected with control non-target shRNA; black panels) and MM6 cells transfected with Δ5-LO shRNA (red panels) were differentiated with 1 ng/ml TGFβ and 50 nM calcitriol for 4 days. Afterwards cells were harvested followed by RNA extraction. Expression levels ($2^{-\Delta Ct}$ normalized to Actin expression) for 5-LO mRNA were determined using qRT-PCR. Data are given as $2^{-\Delta Ct}$ values and represent one single experiment

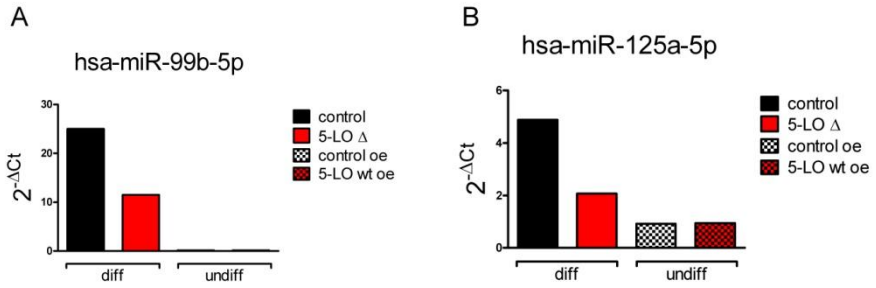

Figure 25: Influence of reconstitution of wt5-LO on miRNA expression

MM6 cells transfected with Δ5-LO shRNA were further transfected with a wt5-LO overexpressing plasmid (black/white checkered panels) or a control plasmid carrying no insert (black/red checkered panels), respectively. Cells were just kept in culture. MM6 control cells (transfected with control non-target shRNA; black panels) and MM6 cells transfected with Δ5-LO shRNA (red panels) were differentiated with 1 ng/ml TGFβ and 50 nM calcitriol for 4 days. Afterwards cells were harvested followed by RNA extraction. Expression levels ($2^{-\Delta Ct}$ normalized to U48 expression) for A) miR-99b-5p and B) miR-125a-5p were determined using qRT-PCR. Data are given as $2^{-\Delta Ct}$ values and represent one single experiment.

Furthermore, as mentioned in chapter 2.1.4, it is known that the 5-LO W13/75/102A mutant is incapable of interacting with Dicer in vitro. Unfortunately it was not possible to generate cells expressing the 5-LO mutant to investigate its effect on the maturation of miR-99b-5p and miR-125a-5p.

5.11 LPS stimulates expression of miR-99b-5p and miR-125a-5p

LPS activates Toll-like receptors and activates the transcription factor NF-κB. This transcription factor is known to activate the transcription of the miR-99b/let-7e/miR-125a cluster (see chapter 2.3.8). Hence, it is likely that LPS increases the expression of miR-99b-5p, let-7e-5p, and miR-125a-5p in MM6 cells.

To investigate this probability, control, Δ5-LO, and ΔFLAP cells were differentiated or were kept unstimulated for four days. After 48 h of differentiation, all cells were stimulated with LPS and subsequently kept growing. The miRNA expression levels were distinguished by qRT-PCR.

Let-7e-5p was steady expressed in LPS treated undifferentiated control, Δ5-LO, and ΔFLAP cells. Compared to undifferentiated control and ΔFLAP cells, miR-99b-5p and miR-125a-5p were lower expressed in undifferentiated LPS treated Δ5-LO cells. Upon differentiation, the analysis of LPS treated cells displayed an induction of miR-99b-5p, let-7e-5p and miR-125a-5p expression (Figure 26 A, D, G). In comparison to the data obtained in LPS untreated control cells, the differentiation effect was more pronounced in presence of LPS (Figure 26 B, E, H). However, differentiated Δ5-LO cells displayed a minor increase in miRNA expression upon LPS stimulation compared to control and ΔFLAP cells.

When evaluating the differentiation effect in LPS treated and untreated control, ΔFLAP, and Δ5-LO cells it is noticeable that TGFβ and calcitriol have a stronger effect in LPS treated cells (Figure 26 C, F, I). Moreover Δ5-LO seems to inhibit expression of miR-99b-5p and let-7e-5p upon differentiation in LPS treated cells, while the expression of miR-125a-5p in these cells is comparable to control transfected cells. The miRNA status of undifferentiated Δ5-LO and ΔFLAP cells is already discussed in chapter 5.3 and chapter 5.6 and shows no increase in let-7e-5p expression upon differentiation while miR-99b-5p and miR-125a-5p slightly increased.

To sum up, LPS activates the expression of miR-99b-5p, let-7e-5p, and miR-125a-5p in differentiated control and ΔFLAP cells. The absence of 5-LO inhibits expression of miR-99b-5p and let-7e-5p upon differentiation. Furthermore, FLAP seems to be involved in the maturation of the pri-miR-99b/let-7e/miR-125a cluster as the absolute values for the respective mature miRNAs in LPS treated as well as LPS untreated ΔFLAP cells are slightly

depressed in comparison to control transfected cells. However, the mean induction upon differentiation and LPS treatment is comparable to control cells.

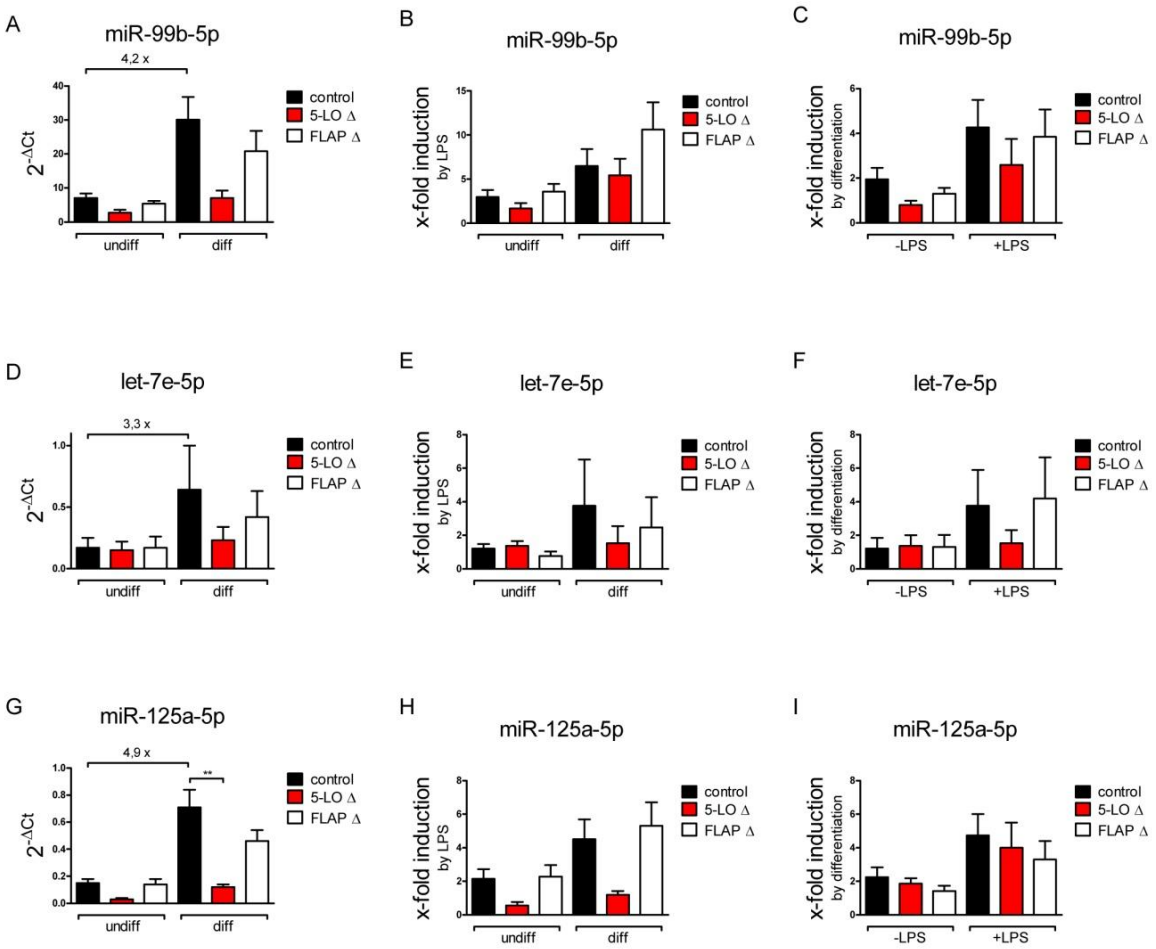

Figure 26: Effect of LPS on miRNA expression

MM6 control cells (transfected with control non-target shRNA; black panels), MM6 cells transfected with Δ5-LO shRNA (red panels), and MM6 cells transfected with ΔFLAP shRNA (white panels) were differentiated on day zero with 1 ng/ml TGFβ and 50 nM calcitriol. Undifferentiated cells were just left in culture. After 48 h 1 µg/ml LPS was added to differentiated and undifferentiated cells. Further 48 h later the cells were harvested and RNA was extracted. The effect of LPS was determined using qRT-PCR. Data are shown in three different ways for each miRNA. A), D), and G) expression levels ($2^{-\Delta Ct}$) of the indicated miRNAs normalized to U48 [n=3-5]. B), E), and H) x-fold induction of the indicated miRNAs by LPS compared to the respective cells without LPS. C), F), and I) x-fold induction of the indicated miRNAs in differentiated cells compared to the respective undifferentiated cells.Data are given as expression level ($2^{-\Delta Ct}$) normalized to U48. Values represent mean + SEM. Statistical analysis was performed by t-test (*<0.05, **p<0.01).

As mentioned above, LPS activates the transcription factor NF-κB, which is capable of stimulating expression of miR-99b-5p, let-7e-5p, and miR-125a-5p. Hence, it is probable that NF-κB activates the transcription of the miR-cluster containing miR-99b, let-7e, and miR-125a.

In this study, it was investigated whether the cluster miR-99b/let-7e/miR-125a was subjected to regulation via LPS. Thus the pri-miR-99b/let-7e/miR-125a level was analyzed in undifferentiated and differentiated control, Δ5-LO, and ΔFLAP cells subjected to LPS. Figure 27 A displays the results of the qRT-PCRs. Compared to control and ΔFLAP cells, the expression of pri-miR-99b/let-7e/miR-125a was considerably lower in LPS treated undifferentiated Δ5-LO cells. Upon differentiation, the pri-miR-99b/let-7e/miR-125a level increased around two-fold in control cells. In Δ5-LO and ΔFLAP cells the absolute pri-miRNA expression increased, but significantly less compared to control cells.

Figure 27 B displays the comparison between untreated and LPS treated cells in undifferentiated and differentiated control, Δ5-LO, and ΔFLAP cells. In absence of 5-LO, the induction of pri-miR-99b/let-7e/miR-125a expression was comparably low in differentiated and undifferentiated cells upon LPS stimulation. In control and ΔFLAP cells, the expression of pri-miR-99b/let-7e/miR-125a increased upon LPS stimulation. However, the induction was independent of the differentiation status.

Figure 27 C displays the induction upon differentiation in LPS stimulated and unstimulated control, Δ5-LO, and ΔFLAP cells and shows that the expression of the miR-99b/let-7e/miR-125a cluster was two-fold induced upon differentiation independent of LPS treatment.

In summary, LPS leads to an increase in pri-miRNA expression, dependent on the 5-LO status. However, this induction is independent of the differentiation status and thus not linked to the induction of 5-LO protein biosynthesis. The involvement of FLAP in pri-miR-99b/let-7e/miR-125a expression is only visible at the absolute expression level. It seems as FLAP reduces the expression of the pri-miRNA in a manner independent of differentiation and LPS. Hence, the induction upon treatment with TGFβ/calcitriol and LPS is comparable to control transfected cells.

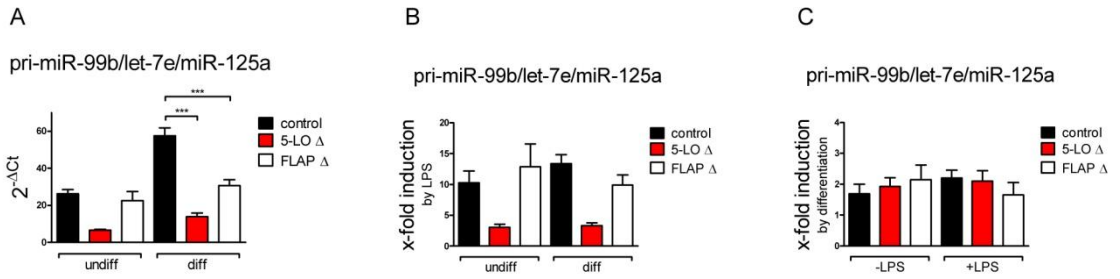

Figure 27: Effect of LPS on pri-miR-99b/let-7e/miR-125a expression
MM6 control cells (transfected with control non-target shRNA; black panels), MM6 cells transfected with Δ5-LO shRNA (red panels), and MM6 cells transfected with ΔFLAP shRNA (white panels) were differentiated on day zero with 1 ng/ml TGFβ and 50 nM calcitriol. Undifferentiated cells were just left in culture. After 48 h 1 µg/ml LPS was added to differentiated and undifferentiated cells. Further 48 h later the cells were harvested and RNA was extracted. The effect of LPS was determined using qRT-PCR. Data are shown in three different ways. A) Expression levels ($2^{-\Delta Ct}$) normalized to U48, B) x-fold induction by LPS compared to the respective cells without LPS, and C) x-fold induction in differentiated cells compared to the respective undifferentiated cells. Values represent mean + SEM with n=5. Statistical analysis was performed by one way ANOVA and Bonferroni post test (***p<0.001).

5.12 Influence of LPS on 5-LO expression

Compared to Figure 26 in chapter 5.11, an effect of LPS on transcriptional regulation of the miR-99b/let-7e/125a cluster was observed in presence of 5-LO. Hence, an involvement of LPS in regulation of 5-LO protein expression was assumed, which, in turn, could be able to enhance the expression of the pri-miR-99b/let-7e/125a. This hypothesis was investigated by Immunoblot. In line with previous experiments displayed in chapter 5.11, MM6 cells were differentiated to induce 5-LO expression. After 48h the cells were additionally stimulated with LPS and kept in culture for further 48h or kept unstimulated after start of differentiation. Finally, 5-LO expression was determined in presence and absence of LPS (Figure 28). However, compared to unstimulated MM6, no obvious difference of the 5-LO expression level was detectable upon stimulation with LPS.

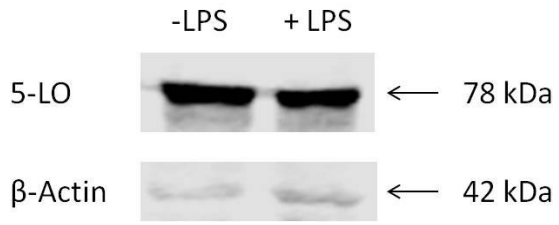

Figure 28: 5-LO expression in dependence on LPS

MM6 cells were differentiated with 1 ng/ml TGFβ and 50 nM calcitriol. After 48 h 1 µg/ml LPS was added as indicated. Further 48 h later the cells were harvested and the LPS effect on 5-LO protein expression was determined by immunoblot. Anti-β-Actin was applied as loading control. The result from one of two independent experiments is shown.

Taken together, LPS does not influence the protein expression of 5-LO in MM6 cells. Hence, the inducing effect of LPS on the expression of pri-miR-miR-99b/let-7e/125a was not mediated by higher 5-LO protein level.

Another possible explanation of 5-LO dependent upregulation of pri-miR-99b/let-7e/125a upon LPS treatment could be a LPS mediated relocation of 5-LO. In unstimulated MM6 cells, Dicer and 5-LO are mainly localized in the cytoplasm, but both happen to be located inside the nucleus as well (Figure 21 and [24, 268]). Due to the fact that total 5-LO protein expression was independent of LPS treatment (Figure 28), the effect of LPS on 5-LO localization was analyzed. An accumulation of 5-LO inside the nucleus would make the pri-miR-miR-99b/let-7e/125a accessible for 5-LO mediated transcriptional activation. Therefore differentiated MM6 cells were fractionated into the cytoplasmic, the nuclear, and the membrane section. Each fraction was analyzed by immunoblot with regard on 5-LO expression. Inside the membrane fraction (Figure 29 C), no 5-LO protein was detectable. Samples originated from the nuclear fraction (Figure 29 B) displayed a faint 5-LO band in unstimulated MM6 cells, but no intensification was observed upon LPS treatment. Inside the cytoplasmic fraction (Figure 29 A), 5-LO was highly present. But again, no change of 5-LO expression was observed due to the LPS treatment.

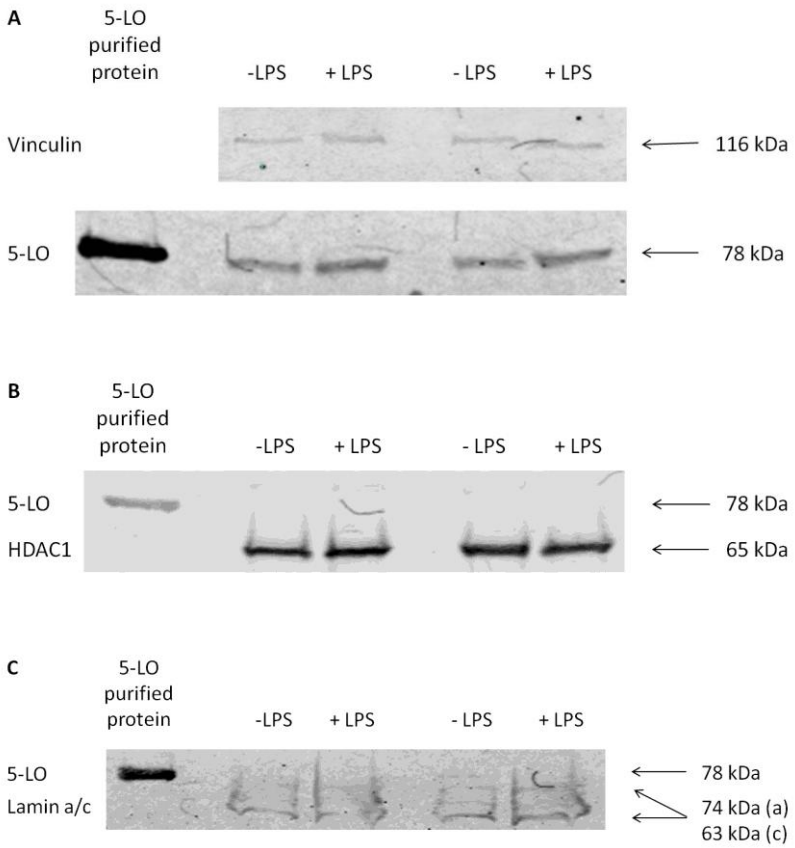

Figure 29: 5-LO localization in dependence on LPS

MM6 cells were differentiated with 1 ng/ml TGFβ and 50 nM calcitriol. After 48 h 1 µg/ml LPS was added as indicated and after further 48 h cells were harvested. Cells were separated into A) cytoplasmic fraction, B) nuclear fraction, and C) membrane fraction. As indicated anti-Vinculin, anti-HDAC1, and anti-Lamin a/c served as loading controls. The results from two of four independent experiments are shown.

To summarize, LPS did not affect neither 5-LO protein amount, nor 5-LO localization. Hence, the 5-LO dependent increase in pri-miR-miR-99b/let-7e/125a after stimulation with LPS is not mediated by enhanced 5-LO protein level or altered cytoplasmic concentrations of 5-LO.

5.13 Target validation for miR-99b-5p and miR-125a-5p

5.13.1 Mono Mac 6 cells

MiR-99b-5p and miR-125a-5p are located in close proximity and are transcribed simultaneously (see Figure 7, chapter 2.3.8). On the basis of their co-expression, it is likely

that both miRNAs act on similar targets or pathways [269]. To predict potential miRNA-target interactions, the bioinformatic prediction program miRTarBase for experimentally validated targets was used [270].

Two targets with strong evidence were declared for miR-99b-5p, 16 announced targets were found for miR-125a-5p. Among them were tumor necrosis factor alpha-induced protein 3 (TNFAIP3) [208] and tumor protein 53 (TP53 or p53) [196, 200]. The latter protein functions as tumor suppressor and is known to interact with 5-LO [201]. Hence, the interaction between 5-LO and PT53 might be regulated by the 5-LO controlled expression of miR-99b-5p and miR-125a-5p via a feedback loop mechanism.

To investigate this possibility in MM6 cells, miR-125-5p and miR-99b-5p expression was silenced. As control, an antagomiR against GFP was used. Since up to now no target of miR-99b-5p and miR-125a-5p was validated in MM6 cells, the knockdown efficiency was tested by measuring the miRNA level (Figure 30).

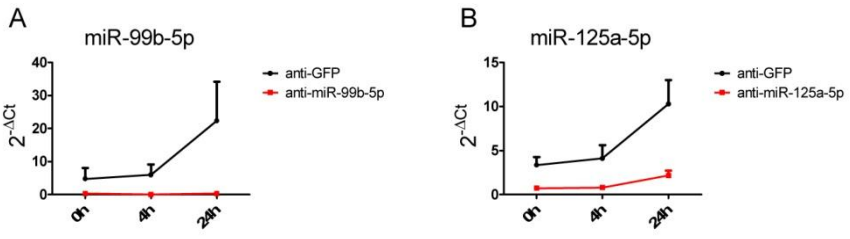

Figure 30: Efficiency of antagomiR treatment in MM6 cells

MM6 cells were differentiated with 1 ng/ml TGFβ and 50 nM calcitriol for 4 days. After 48h 25 nM antagomiR against A) miR-99b-5p and B) miR-125a-5p (red graphs) was added. As control differentiated MM6 cells were treated with antagomiR against GFP (black graphs). After further 24h cells were incubated with 1 µg/ml LPS. At time of addition, after 4h, and after 24h cells were harvested followed by RNA extraction. The LPS dependent antagomiR effect was determined using qRT-PCR. Data are given as expression level ($2^{-\Delta Ct}$) normalized to U48. Data are given as mean + SEM [n=4]

Subsequently, the mRNA level of TP53 in differentiated MM6 cells was measured by qRT-PCR (Figure 31 A). It was observed that TP53 mRNA is expressed in differentiated MM6 cells. However, its expression was independent of miRNA silencing.

Next, an Immunoblot was performed to determine the TP53 protein level in differentiated MM6 cells (Figure 31 B). The Western Blot displayed a high basal expression of PT53 in differentiated MM6 cells, but no stimulation or inhibition of PT53 protein expression was observed upon silencing of miR-99b-5p and miR-125a-5p.

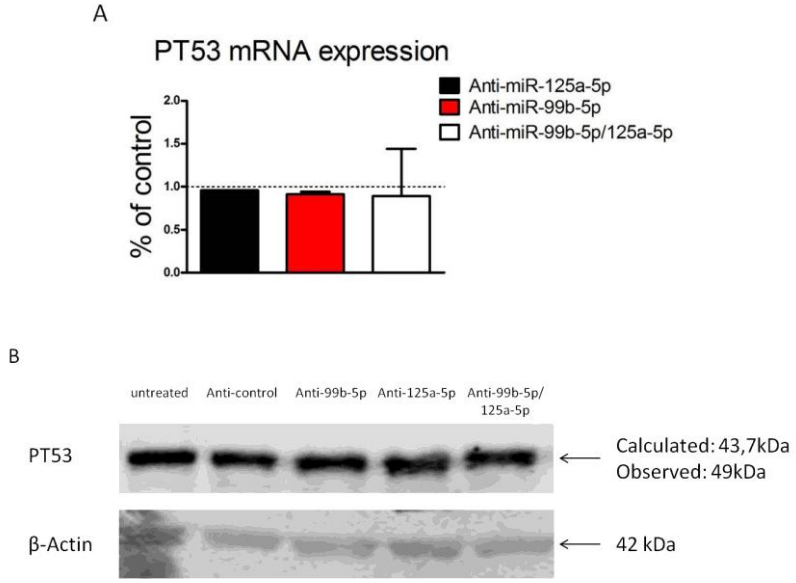

Figure 31: PT53 expression in miRNA silenced MM6 cells

MM6 cells were differentiated with 1 ng/ml TGFβ and 50 nM calcitriol. After 48 h 25 nM control antagomiR against GFP, 25 nM anti-miR-99b-5p antagomiR, 25 nM anti-miR-125a-5p antagomiR, or alternatively a mixture of 12.5 nM anti-miR-99b-5p and 12.5 nM anti-miR-125a-5p was added as indicated. After further 48 h cells were harvested. A) PT53 mRNA level changes in MM6 cells after silencing of miR-125a-5p (black panel), miR-99b-5p (red panel), and miR-125a-5p together with miR-99b-5p (white panel). Expression levels ($2^{-\Delta Ct}$) were determined by qRT-PCR with induction based on differentiated MM6 cells treated with control antagomiR, Mean + SD [n=2-3]. B) PT53 protein level in MM6 cells after silencing of miR-125a-5p, miR-99b-5p, or miR-125a-5p together with miR-99b-5p determined by immunoblot. β-Actin served as loading control. The result of one single experiment is shown.

Taken together, TP53 mRNA and TP53 protein are detectable in MM6 cells. However, in contrasts to previous reports the TP53 mRNA as well as the TP53 protein level stayed unaffected by silencing of miR-99–5p and miR-125a-5p [196]. Since TP53 and miR-125a-5p are both present in MM6 cells, another mechanism, controlling the association of PT53 and miR-125a-5p, seems to be involved.

TNFAIP3 activates NF-ϰB and inhibits TNFα induced apoptosis [271]. Since the latter cytokine is induced by LPS [272] and is associated with increased 5-LO activity [60], TNFα

expression is potentially affected by miR-99b-5p and miR-125a-5p expression. Besides, IL-6 release is also regulated by NF-κB [273] and induced by LPS [272]. Hence, the dependence of TNFα and IL-6 release on miR-99b-5p and miR-125a-5p expression was analyzed in differentiated MM6 cells by Cytoplasmatic Bead Array (CBA). Both TNFα and IL-6 have low basal expression level in MM6 cells. Therefore, the cells were stimulated with LPS to enhance their cytokine release. After LPS stimulation, IL-6 and TNFα level were tracked for 24 h in the supernatant of MM6 cells. The maximum TNFα level was reached after 4 h following LPS addition with around 2000 pg/ml in the supernatant. Within 24 h the level declined to almost baseline values. Otherwise, IL-6 levels were continuously increasing to around 440 pg/ml supernatant after 24 h (Figure 32).

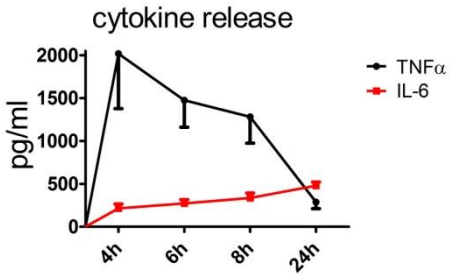

Figure 32: Release of TNFα and IL-6 with time upon LPS stimulation

MM6 cell were differentiated with 1 ng/ml TGFβ and 50 nM calcitriol for four days. After 48 h 25 nM antagomiR against GFP was added. After further 24 h 1 µg/ml LPS was applied. At time of addition and after 4 h, 6 h, 8 h, and 24 h 100 µl supernatant was collected and diluted 1:2with PBS. Samples were snap frozen and subjected to CBA analysis. The black graph shows TNFα release, the red graph IL-6 release. Values represent mean +/- SEM [n=3].

Since this clear difference in the expression profiles of IL-6 and TNFα, it is possible that miRNAs fine tune the expression of TNFα and IL-6 to adapt their availability to current needs. Hence, the impact of miR-99b-5p and miR-125a-5p silencing on the release of TNFα and IL-6 was analyzed as a function of time. In cells treated with antagomiR against miR-125a-5p (anti-miR-125a-5p), cytokine expression levels were significantly increased after 6 h compared to cells treated with a GFP targeted control antagomiR. After 4 h, 8 h, and 24 h, no significant effect of anti-miR-125a-5p on TNFα and IL-6 release was observed (Figure 33 A). Treatment with anti-miR-99b-5p increased the cytokine expression after 6 h compared to control treated cells (TNFα p=0.08; IL-6 p=0.2), but displayed no effect after 4 h, 8 h, and 24 h (Figure 33 B).

To sum up, anti-miR-99b-5p and anti-miR-125a-5p slightly increase the IL-6 and TNFα release 6 h after stimulation with LPS.

In chapter 5.1, Figure 13, it was shown that miR-99b-5p and miR-125a-5p increase with time after stimulation with TGFβ and calcitriol. Both miRNAs affect the release of TNFα and IL-6, which have different expression profiles upon stimulation with LPS. Hence, the miRNA release as a function of time was next monitored after LPS stimulation to compare their expression profile with the expression profile of TNFα and IL-6. According to cells stimulated with TGFβ and calcitriol, a continuous increase over 24 h for both miR-99b-5p and miR-125a-5p was observed (Figure 26). Compared to antagomiR treated cells, expression of miR-125a-5p was 25 times higher in control cells 6 h after LPS stimulation. The knockdown of miR-99b-5p was in turn as effective as its expression was underneath the detection limit.

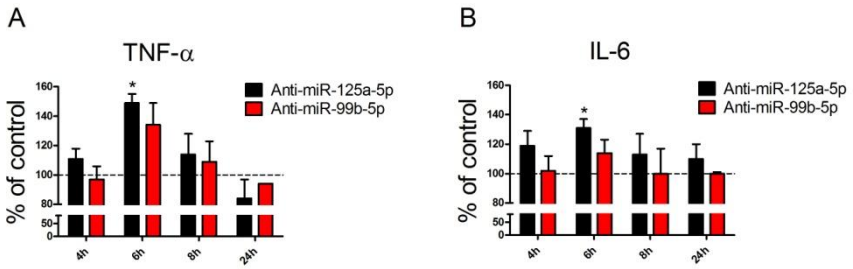

Figure 33: Effect of antagomiR treatment on TNFα and IL-6 level

MM6 cell were differentiated with 1 ng/ml TGFβ and 50 nM calcitriol for four days. After 48 h 25 nM antagomiR against miR-125a-5p (black staples) and miR-99b-5p (red staples) were added. After further 24 h cells were treated with 1 µg/ml LPS. At time of addition and after 4 h, 6 h, 8 h, and 24 h 100 µl supernatant was collected and diluted 1:2 with PBS. Samples were snap frozen and subjected to CBA analysis. Expression of A) TNFα and B) IL-6 was detected. Values are shown as % of control in comparison to differentiated, LPS stimulated cells treated with antagomiR against GFP at the respective time points (Figure 32). Mean + SEM [n=3]; analyzed by one way ANOVA and Bonferroni post test; statistical significance shown as * with $p<0.05$.

In summary, miR-99b-5p and miR-125a-5p are slowly ascending in MM6 cells upon stimulation with LPS. These expression profiles resemble the profile of IL-6 expression in LPS stimulated MM6 cells, whereas TNFα release escalates quickly and subsequently drops. The effect of miR-99b-5p and miR-125a-5p on TNFα as well as on IL-6 release, are most pronounced 6 h after treatment with LPS, although the cytokine expression profiles are totally

different. Hence, it can be suggested that miR-99b-5p and miR-125a-5p act to arrest TNFα release, while they fine tune expression of IL-6.

5.13.2 Primary monocytes

Banerjee *et al.* observed an involvement of miR-125a-5p in differential activation of mouse macrophages [205]. Furthermore, they showed a dependency of TNFα release upon miR-125a-5p expression in LPS stimulated cells. To test whether this is also relevant in humans, monocytes were isolated from buffy coats, as described in 4.1.3 and polarized towards M1 or M2 macrophages, respectively. After six days, cells were stimulated with LPS and further 24 h later, when the cells were fully differentiated by M-CSF or GM-CSF respectively, their miRNA expression levels were measured. MiR-125a-5p was according to Banerjee *et al.* relatively low expressed in unstimulated control macrophages and increased upon differentiation towards M2. Compared to M2 activated macrophages, miR-125a-5p expression was less enhanced in cells differentiated towards M1 (Figure 34 A). MiR-99b-5p was comparably low expressed in control and M1 differentiated macrophages, but increased upon stimulation towards M2 (Figure 34 B).

Taken together, the differential activation of monocytes towards M2 macrophages promotes the expression of miR-99b-5p and miR-125a-5p.

Banerjee *et al.* also showed a dependence of regular macrophage differentiation on miR-125a-5p expression in mice. Upon overexpression of miR-125a-5p, the M1 phenotype expression was diminished, whereas M2 marker expression was promoted [205]. Hence, the function of miR-125a-5p and miR-99b-5p in human macrophage polarization was characterized in the next step. Therefore, miR-99b-5p and miR-125a-5p were silenced in the differential activated human macrophages. However, the method of Krutzfeldt *et al.* [263], which was used in chapter 5.13.1, did not work for primary cells (tested by qRT-PCR). Hence, the cells were transfected with siPORT™ NeoFX™ Transfection Agent and Anti-miR™ miRNA Inhibitors as described in Methods, chapter 4.10.2. (efficiency shown in Figure 35).

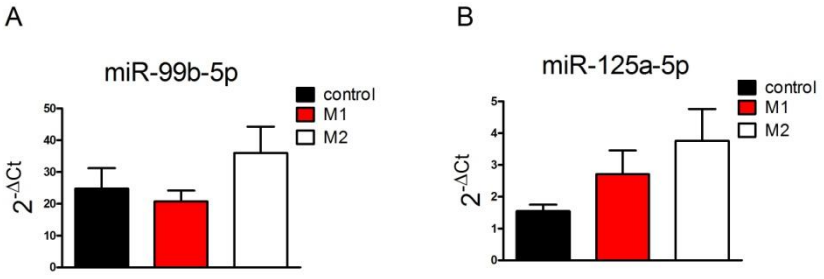

Figure 34: MiRNA expression level in M1 and M2 macrophages

Monocytes were isolated from buffy coats. Control monocytes cells were just left in culture (black staples). Macrophages differentiated towards M1 were stimulated with 10 ng/ml GM-CSF, followed five days later by addition of 10 ng/ml IFNγ (red staples). M2 macrophages were differentiated using 10 ng/ml M-CSF. After five days 10 ng/ml IL-4 was added (white staples). The next day, all cells were stimulated with 10 ng/ml LPS and harvested further 24 h later. RNA was extracted and miRNA level for A) miR-99b-5p [n=3] and B) miR-125a-5p [n=4] were determined using qRT-PCR. Data are given as expression level ($2^{-\Delta Ct}$) normalized to U48; mean + SEM.

MiR-99b-5p expression was stimulated by increasing amounts of transfection reagent and antagomiR, thus transfection was performed with 8 µl transfection reagents plus 30 nM antagomiR. The amount was required for sufficient miRNA silencing and at the same time affected miRNA expression the least in control antagomiR treated cells. The transfection agent itself led to an around two-fold increase in miR-99b-5p expression in cells transfected with

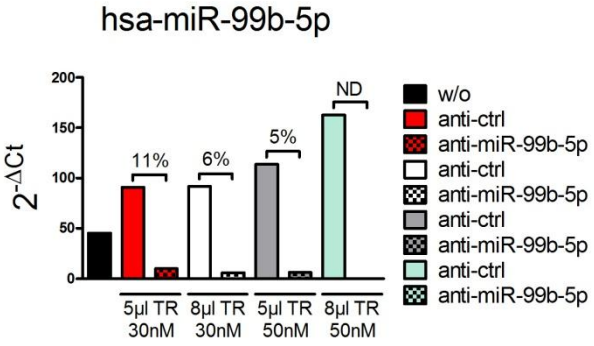

Figure 35: AntagomiR efficiency in primary macrophages

Monocytes were isolated from buffy coats and kept in culture. After 6 days adherent cells were trypsinized and $1.5x10^5$ cells were: black staple: resuspended in normal culture medium, red staples: incubated with 5 µl transfection reagent and 30 nM anti-control (plain red staple) or anti-miR-99b-5p (tiled staple), white staples: incubated with 8 µl transfection reagent and 30 nM anti-control (plain white staple) or anti-miR-99b-5p (tiled staple), grey staples: incubated with 5 µl transfection reagent and 50 nM anti-control (plain grey staple) or anti-miR-99b-5p (tiled staple), blue staples: incubated with 8 µl transfection reagent and 50 nM anti-control (plain blue staple) or anti-miR-99b-5p (tiled staple). MiR-99b-5p expression levels were determined by qRT-PCR. Data are given as expression level ($2^{-\Delta Ct}$) normalized to U48. Results show one single experiment.

control antagomiR compared to untreated cells. However, transfection of miR-99b-5p inhibitor led to a reduction down to 6% of the miR-99b-5p level observed in cells treated with anti-control. In the next step, the differential activated macrophages were supposed to be classified upon their cluster of differentiation. Unfortunately, due to the stress of trypsinization and transfection, not enough cells were obtained for reliable FACS data. Hence, in the course of this study it was not investigated whether miRNA silencing leads to a shift from M2 activated macrophages towards M1 macrophages in humans.

To sum up, miR-99b-5p and miR-125a-5p expression was enhanced upon differential activation of monocytes towards M2 macrophages. But data concerning the role of these miRNAs in the differentiation process are missing.

A potential link between macrophage polarization and the increase in miR-99b-5p and miR-125a-5p expression is 5-LO, as 5-LO was shown to control the release of the listed miRNAs. To investigate if 5-LO is involved in macrophage polarization by regulating miR-99b-5p and miR-125a-5p expression, 5-LO mRNA levels in differentially activated macrophages were analyzed. The same samples as for miRNA detection were used, but an opposing expression profile for miR-125a-5p/miR-99b-5p and 5-LO was found. The mRNA level of 5-LO was induced more than ten-fold in M1 macrophages compared to control

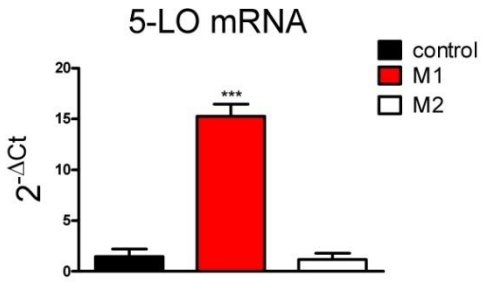

Figure 36: 5-LO mRNA expression level in M1 and M2 macrophages

Monocytes were isolated from buffy coats. Control monocytes cells were left in culture (black staples). Macrophages differentiated towards M1 were stimulated with 10 ng/ml GM-CSF, followed five days later by addition of 10 ng/ml IFNγ (red staples). M2 macrophages were differentiated using 10 ng/ml M-CSF. After five days, 10 ng/ml IL-4 was added (white staples). The next day, all cells were stimulated with 10 ng/ml LPS and harvested further 24 h later. RNA was extracted and 5-LO mRNA level were determined using qRT-PCR. Data are given as expression level ($2^{-\Delta Ct}$) normalized to β2 microglobulin (B2M). Data are given as mean + SEM; analyzed by one way ANOVA and Bonferroni post test; statistical significance shown as *** with $p<0.001$.

differentiated cells, whereas M-CSF/IL-4 treatment (M2) rather led to a decrease in 5-LO expression (Figure 36). Immunoblot experiments showed comparable results (data not shown).

In summary, polarization towards M2 is accompanied by increased expression of miR-99b-5p and miR-125a-5p. Furthermore, it is in question if 5-LO is involved in the upregulation of these miRNAs upon differentiation in macrophages.

5.14 Role of miR-125a-5p and miR-99b-5p on 5-LO activity

TNFα is known to induce 5-LO activity, what as a consequence leads to an increased generation of reactive oxygen species (ROS) [58]. Woo *et al.* found LTB_4 to be responsible for this increase in ROS. To understand the role of miR-99b-5p and miR-125a-5p in this interplay, 5-LO activity assays were performed in LPS stimulated and anti-miR-99b-5p and anti-miR-125a-5p transfected differentiated MM6. The difference to control antagomiR transfected cells was investigated. However, no increase in 5-LO product formation in miR-99b-5p and miR-125a-5p silenced cells was observed upon LPS treatment (Figure 37 A). Performing the same experiment in absence of LPS, 5-HETE and LTB_4 formation significantly increased in miR-125a-5p silenced cells compared to control cells. Anti-miR-99b-5p treatment and a combination of anti-miR-99b-5p and anti-miR-125a-5p appeared to enhance 5-LO activity in a less, but reproducible, extent (Figure 37 B). However, the results for anti-miR-99b-5p and anti-miR-125a-5p treated cells is in question as the antagomiR concentration should be 25 nM each to be comparable to the mono treated cells.

To sum up, silencing of miR-99b-5p and miR-125a-5p had no impact on the generation of LTB_4 and 5-HETE in differentiated LPS stimulated MM6 cells. In contrast, absence of those miRNAs in differentiated MM6 cells without further stimuli resulted in increased 5-LO activity. The treatment with anti-miR-125a-5p leads to a significantly enhanced release of LTB4 and 5-HETE. That implies a TNFα independent regulation of 5-LO activity, as MM6 cells only release TNFα upon stimulation with LPS.

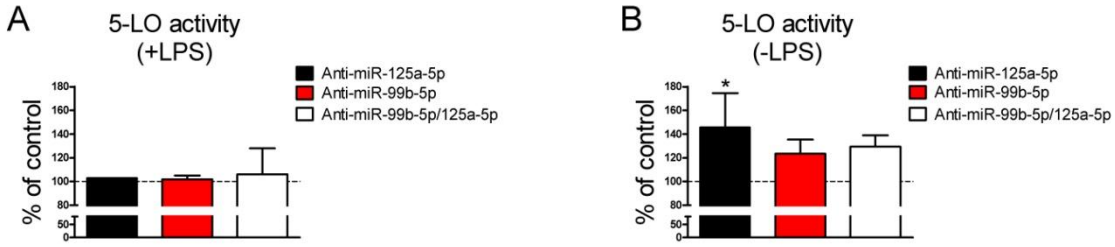

Figure 37: Effect of antagomiR treatment on 5-LO activity

MM6 cells were differentiated with 1 ng/µl TGFβ and 50 nM calcitriol. After 48 h 25 nM antagomiR against miR-125a-5p (black staples), miR-99b-5p (red staples), or both in combination (white staples) were added. Further 24 h later, the cells were A) treated with 1 µg/ml LPS or B) just left in culture. The following day cells were harvested and resuspended in PBS containing 1 mg/ml glucose. Activity assay was performed using 20 µM AA and 2.5 µM calcium ionophore A23187 according to chapter 4.7. 5-LO activity was determined by HPLC. Fold induction based on product formation in differentiated MM6 cells treated with 25 nM control antagomiR against GFP (absolute activity A) 278,44 ng 5-LO products/1 × 10^6 cells and B) 126,90 ng 5-LO products/1 × 10^6 cells. Data are given as mean + SEM [n=2-6]; analyzed by one way ANOVA and Bonferroni's post test (*p<0.05).

In general, miRNAs regulate protein biosynthesis. Since miR-99b-5p and miR-125a-5p affect the activity of 5-LO, it is likely that silencing of the respective miRNAs also affect the 5-LO mRNA and/or the 5-LO protein expression level. Hence, an immunoblot analysis of 5-LO protein expression (Figure 38) and a qRT-PCR for 5-LO mRNA expression (Figure 39) in dependency of antagomiR treatment were performed next. In differentiated MM6 cells, a high 5-LO protein expression was detected. The expression did not change upon control antagomiR treatment. Furthermore, neither silencing of miR-99b-5p nor miR-125a-5p did significantly affect 5-LO protein expression. Comparable results were obtained for 5-LO mRNA expression in anti-miR-125a-5p and anti-miR-99b-5p treated cells.

In summary, miR-99b-5p and miR-125a-5p influence 5-LO activity. However, neither 5-LO protein expression nor 5-LO mRNA level were affected by silencing miR-99b-5p and miR-125a-5p. That implies an indirect effect of miR-99b-5p and miR-125a-5p on 5-LO activity. The effect of the combined inhibition of miR-99b-5p and miR-125a-5p on 5-LO expression stays in question as the concentration of each antagomiR was to low.

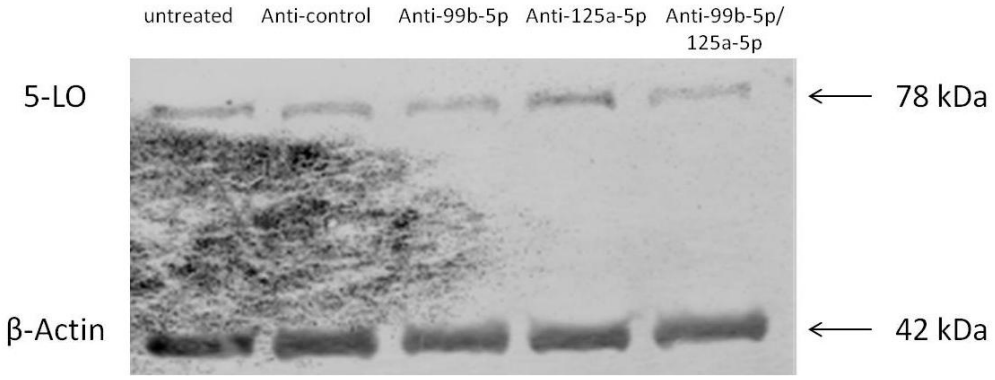

Figure 38: Effect of antagomiR treatment on 5-LO protein expression

MM6 cells were differentiated with 1 ng/ml TGFβ and 50 nM calcitriol. After 48 h 25 nM control antagomiR against GFP, 25 nM anti-miR-99b-5p antagomiR, 25 nM anti-miR-125a-5p antagomiR, or alternatively a mixture of 12.5 nM anti-miR-99b-5p and 12.5 nM anti-miR-125a-5p was added as indicated. After further 48 h cells were harvested. A) 5-LO protein level in MM6 cells after silencing of miR-125a-5p, miR-99b-5p, or miR-125a-5p together with miR-99b-5p determined by immunoblot. β-Actin served as loading control. The result of one single experiment is shown.

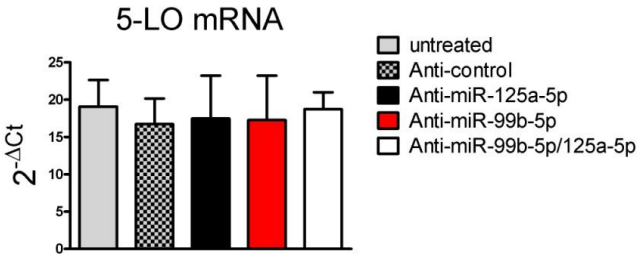

Figure 39: Effect of antagomiR treatment on 5-LO mRNA expression

MM6 cells were differentiated with 1 ng/ml TGFβ and 50 nM calcitriol. After 48 h 25 nM control antagomiR against GFP, 25 nM anti-miR-99b-5p antagomiR, 25 nM anti-miR-125a-5p antagomiR, or alternatively a mixture of 12.5 nM anti-miR-99b-5p and 12.5 nM anti-miR-125a-5p was added as indicated. After further 48 h cells were harvested. RNA was extracted and 5-LO mRNA level were determined using qRT-PCR. Data are given as expression level ($2^{-\Delta Ct}$) normalized to Actin. Data are given as mean + SEM [n=3].

5.15 Expression of IL-6 and TNFα in Δ5-LO and ΔFLAP cells

As repeatedly published and observed, IL-6 and TNFα are targets of miR-99b-5p and miR-125a-5p. Furthermore, both miRNAs are regulated in a 5-LO and FLAP dependent manner (Figure 13, chapter 5.1 and Figure 18, chapter 5.6). Hence, it is likely that Δ5-LO and ΔFLAP affect IL-6 and TNFα release, mediated by miR-99b-5p and miR-125a-5p.

Hence, the cytokine level in LPS stimulated Δ5-LO and ΔFLAP cells were measured by CBA. The respective expression levels were determined after 4 h, 6 h, and 8 h of LPS stimulation (Figure 40). The knockdown of 5-LO led to a significant decrease in the expression of TNFα and IL-6, independent of time. FLAP did not alter TNFα expression, whereas IL-6 release was significantly increased. The boosting effect of ΔFLAP on IL-6 expression appeared to slightly increase with time in analogy to the regular expression profile of IL-6 (see Figure 32).

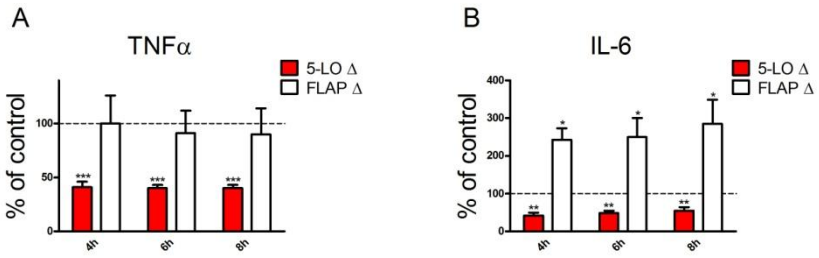

Figure 40: Effect of Δ5-LO and ΔFLAP on TNFα and IL-6 release

MM6 Δ5-LO cells (red staples), ΔFLAP cells (white staples), and control cells transfected with non-target shRNA were differentiated with 1 ng/ml TGFβ and 50 nM calcitriol. After 72 h cells were stimulated with 1 µg/ml LPS. Further 4 h, 6 h, and 8 h later, 100 µl supernatant was collected and diluted 1:2 with PBS. Samples were snap frozen and subjected to CBA analysis. Release of A) TNFα and B) IL-6 was detected. Values are shown as % of control in comparison to differentiated control cells at the respective time points. Data are given as mean + SEM [n=3]; analyzed by paired, two tailed t test; statistical significance shown as * with $p<0.05$, ** with $p<0.01$, and *** with $p<0.001$.

Taken together, Δ5-LO and ΔFLAP affect the release of the inflammatory cytokines TNFα and IL-6. However, these results stand in contrast to the data obtained in miR-99b-5p and miR-125a-5p silenced MM6 cells (Figure 33 in chapter 5.13.1). Hence, the effects on TNFα and IL-6 release in Δ5-LO and ΔFLAP cells are not mediated by miR-99b-5p and miR-125a-5p.

6 DISCUSSION

The results of the present thesis reveal that 5-LO and FLAP influence miRNA maturation. Using a lentivirus mediated shRNA transfection, 5-LO was knocked down in the human monocytic cell line MM6 [31]. These cells were subsequently analyzed by a microarray for miRNA expression. Out of a total of 2082 tested miRNAs, 30 miRNAs were found to be upregulated upon Δ5-LO (factor 1.3), while 7 appeared to be downregulated (factor 0.7). The majority of upregulated miRNAs are not yet associated or studied in relation to inflammatory events. Hence the study further focused on the miRNAs downregulated in Δ5-LO cells, including miR-199a-3p/miR-199b-3p, miR-148-3p, miR-199b-5p, miR-99b-5p, miR-125b-5p, miR-424-5p, and miR-125a-5p. Among these miRNAs, the study focused on miR-99b-5p and miR-125a-5p. They are organized in a common cluster which in addition includes let-7e.

The other miRNAs showing altered expression profiles in Δ5-LO cells in the microarray are left to be analyzed.

6.1 5-LO affects cleaving activity of human Dicer

Provost *et al.* published in 1999 an interaction of 5-LO with the ΔK12H4.8 homologue which was later identified as Dicer [33]. Dincbas-Renqvist *et al.* were further able to assign the required binding sites to the C-terminus of Dicer and the Trp residues 13, 75, and 102 in the N-terminal C2-like domain of 5-LO. Furthermore they were able to show the influence of Dicer and 5-LO protein on the respective activities [38]. *In vitro* assays revealed that the interaction between 5-LO and Dicer changes the product pattern to be steering away from the regular 22 nt long RNA molecules, leading to longer (~55nt) and shorter (10-12nt) RNA strands. This was shown for the miRNA precursor pre-let-7a-3. However, the emerging Dicer products of pre-let7a-3, let-7a-3p and let-7a-5p (highlighted in grey in chapter 10), did not show an effect in the microarray upon Δ5-LO. Hence, a repetition of the *in vitro* cleavage assay for newly identified regulated miRNAs like miR-99b-5p and miR-125a-5p in the Δ5-LO cells would give a more detailed insight into 5-LO dependent cleavage capacity of Dicer.

Another interesting question left to answer is whether the RNA fragments, emerging from the *in vitro* cleavage in presence of 5-LO, have a biological function and how they are formed. However, this study focused on the mature miRNAs primarily depending on the presence of 5-LO. Therefore, this study concentrated on the four miRNAs which showed the strongest decrease in the Δ5-LO cells according to the microarray (chapter 5.1, Figure 10). Among them was miR-424-5p, a miRNA already known to be related to inflammatory processes and cancer [274-276]. Due to high fluctuations between different RNA samples, the microarray data could not be reproduced by qRT-PCR. The same applies for miR-125b-5p, a miRNA recently shown by Busch *et al.* to directly regulate 5-LO expression. However, they observed a independent expression of miR-125b-5p and 5-LO upon differentiation in MM6 cells [23]. Under these circumstances, and since miR-99a and miR-100, members of the two miR-125b clusters, did not appear in the microarray data, the study subsequently focused on the cluster containing miR-99b, let-7e, and miR-125a.

In order to find common structural properties or common recognition motives, the selection criteria for 5-LO controlled miRNAs were slightly changed, to explain the specific regulation of scattered miRNAs by 5-LO. MiR-181a-5p, for example, was included as it is implicated in the motility of hepatocellular carcinomas [277] and the inhibition of differentiation in human bone marrow precursor B cells [278]. Moreover, miR-20b-5p was incorporated, as it shows a promotion of cell growth in breast cancer cells [279] and contributes to autoimmune demyelization in multiple sclerosis patients [280].Unfortunately, it was not possible for me to identify common features which could qualify these miRNA for regulation by 5-LO. An enlarged bioinformatical approach could be more successful to unravel common features. Another possibility is a mutational approach, shown by Auyeung *et al.* [140], in combination with the Dicer *in vitro* cleavage assay. However, a direct binding of Dicer educts (pre-miRNAs) to 5-LO and a subsequent transfer to the processing machinery could not be determined, as unspecific binding of 5-LO in one single pull-down experiment was observed. 5-LO bound to any kind of pre-miRNA irrespective of their place of adaption to the beads (chapter 5.4).

6.2 Expression of miR-99b-5p and miR-125a-5p is regulated by 5-LO

Differentiation of MM6 cells with TGFβ and calcitriol strongly upregulates 5-LO expression (about 100-fold), with a high, detectable protein level after 2-4 days. Simultaneously, expression of miR-99b-5p and miR-125a-5p was two times stronger upon differentiation in 5-LO positive MM6 cells, compared to Δ5-LO cells (Figure 13). This implies a role of 5-LO in the regulation of miRNA expression. Up to now, several Dicer interaction partners are identified. Among them are TRBP, PACT, and ADAR1. All of them affect Dicer processing [163, 165, 169, 266]. However, none of them regulate specific miRNAs, they rather have overall inducing implications on Dicer performance.

Insertion of a shRNA can lead to secondary and off-target effects. An elegant way to exclude these due to random insertion of 5-LO shRNA is to reexpress 5-LO in the Δ5-LO cells and, subsequently, observe a recovery of miRNA expression. In this context, it is interesting that the 5-LO triple mutant W13/75/102A lacks binding capacity to Dicer [38]. Hence, a failed recovery of miRNA generation after expressing this mutant in the Δ5-LO cells would contribute to the observations of the interaction between 5-LO and Dicer (chapter 5.10).

Unfortunately, re-expression of 5-LO in the 5-LO silenced cells was not successful. On one hand the size of the final expression vector with more than 11,000 bp could result in a hindered uptake and integration. However, the introduction of the wt5-LOoe vector was at first successful, hence this possibility can be neglected. On the other hand, the constant expression of 5-LO in successfully transduced cells leads to enhanced cell stress and as a consequence, the majority of cells die in the early recovery phase. The integration of the 5-LO cDNA into a smaller expression vector and the usage of a weaker promotor, compared to the used SV40, could help to overcome the problem. For example Ubiquitin C promoter exhibits a lower basic activity in mammalian cells compared to the employed one [281].

6.3 5-LO does not affect expression of the miR-99b/let-7e/miR-125a cluster in unstimulated cells

While analyzing the effect of Δ5-LO on the expression of the primary transcript of the cluster miR-99b/let-7e/miR-125a, this study showed that the expression of the pri-miRNA is

independent of the presence of 5-LO as well as of its metabolites LTB_4, 5-HETE, and LTC_4 (chapter 5.3 and 5.5). These findings show that 5-LO affects maturation of miR-99b-5p, let-7e-5p, and miR-125a-5p in MM6 cells and not the expression of the pri-miRNA of the cluster.

6.4 LTB_4 is not involved in miRNA maturation

In the year 2014, Wang *et al.* proposed that LTB_4 increases expression of miR-155, miR-146b, and miR-125b [175]. Compared with the microarray results, all listed miRNAs are to a greater or lesser extent, but significantly, down regulated in Δ5-LO cells (highlighted in turquoise in chapter 10). However, at least in MM6 cells, miR-125b-5p expression did not seem to be affected by LTB_4 (data not shown). This observation can possibly be explained by cell specific characteristics, as discussed in chapter 6.3. Another possible explanation is that the different data are attributed to a rapid upregulation of miRNA expression upon LTB_4 stimulation followed by an autoregulated decline. Since the cells were treated for 96 h with the LT, the rapid upregulation might be already vanished by the time the cells were tested for their miRNA expression level. A miRNA expression profile over time would detect such a pattern.
The effect of different LTs on the expression of miRNAs was analyzed next, including LTB_4, 5-HETE, and LTC_4, which are according to the microarray data more dominantly regulated by 5-LO. But as already observed for miR-125b-5p, the three members of the miRNA-cluster miR-99b/let-7e/miR-125a did not show an increased expression upon stimulation with LTs.
Taken together, neither addition of LTB_4, 5-HETE, LTC_4 to Δ5-LO cells rescued miR-99b-5p or miR-125a-5p production, nor did the presence of 5-LO inhibitors inhibit the expression of the respective miRNAs in control shRNA treated MM6 cells (chapter 5.5). As mentioned before, a fast and short lasting effect of LTs on miRNA expression level might be missed due to the experimental set up. LTB_4 without stimulation is hardly present in the cell culture model, therefore, a 5-LO product independent regulation of miRNA maturation seems logic.

6.5 LPS induces formation of miR-99b-5p, let-7e-5p, and miR-125a-5p

This study showed that, LPS stimulates miR-99b-5p, miR-125a-5p, and let-7e-5p expression in MM6 cells. However, the enhancing LPS effect on miRNA expression is absent in Δ5-LO cells. In contrast to these findings, the homolog of miR-125a, miR-125b, which is also regulated by NF-κB [282, 283], is upregulated, in absence and presence of 5-LO after stimulation with LPS (data not shown).

It is already known, that the TLR4 ligand LPS induces activity of NF-κB [284] which, in turn, enhances the transcription of the miR-99b/let-7e/miR-125a cluster [216].

In accordance with that, LPS was shown to activate the expression of miR-125a-5p [205, 212] as well as let-7e in murine macrophages. MiR-155 and miR-125b, in contrast, were shown to be decreased in primary murine macrophages upon LPS stimulation [285]. These data are not consistent with the observations in this study, probably due to species specific differences in miRNA expression.

Apart from that, Lindner *et al.* showed an approximately two-fold increase in 5-LO activity upon LPS treatment [286]. However, total 5-LO protein expression and its localization stayed unaffected by the LPS treatment (chapter 5.12). Additionally, as already known, miR-99b-5p, let-7e-5p, and miR-125a-5p induction is independent of 5-LO activity (chapter 5.5) and the increase in miRNA expression upon LPS treatment was in average two times higher than the increase of 5-LO activity (Figure 26 compared to [286]). Furthermore, the LPS effect on miRNA expression is more pronounced in differentiated control and ΔFLAP cells whereas the induction is similarly low in undifferentiated and differentiated Δ5-LO cells. This supports the theory of 5-LO dependence together with the observation that the miRNA induction by differentiation is also stronger in LPS treated control and ΔFLAP cells than in undifferentiated cells and Δ5-LO cells. Hence, LPS seems to regulate miRNA expression in a 5-LO-dependent manner.

The transcription of the mir-99b/let-7e/mir-125a gene depends on the presence of LPS. The induction upon LPS treatment is independent of the cellular differentiation status. However, in control and ΔFLAP cells the overall expression of the pri-miRNA is up to 10 times higher upon stimulation with LPS. Interestingly, in Δ5-LO cells, only a minor increase in

transcription of the miR-99b/let-7e/miR-125a cluster was observed after stimulation with LPS (Figure 27).

Taken together, two independent mechanisms for controlling miRNA expression by 5-LO were found.

1) LPS independent two-fold increase controlled by 5-LO protein expression and TGFβ/calcitriol stimulation.
2) A strong, LPS dependent induction which is 5-LO but not FLAP dependent.

6.6 Drosha processing is affected by 5-LO

Drosha activity is known to be controlled by several proteins connected to 5-LO. Among them are SMADs, which facilitate the pri-miRNA processing of miR-21 and miR-199a [151], as well as p53 [153]. However, no direct protein interactions between the microprocessor complex and Dicer or the microprocessor complex and 5-LO have been described to date. Nevertheless, pre-miR-99b, pre-let-7e, and pre-miR-125a were found to be expressed on a lower level in Δ5-LO cells, while pre-miR-19a as precursor of a miRNA, which is not controlled by 5-LO, is unaffected (chapter 5.3, Figure 15). This indicates an additional involvement of 5-LO in nuclear Drosha performance regarding the miR-99b/let-7e/miR-125a containing pri-miRNA.

Apart from that, the precursor level in ΔFLAP cells of the respective miRNAs are rather expressed on a higher level compared to control cells (Figure 19). This is in line with our data showing that FLAP stimulates cytosolic localization of 5-LO. In contrast, in ΔFLAP cells, 5-LO seems to accumulate in the nucleus. As a consequence, pre-miRNA formation increases, whereas formation of mature miRNAs decreases thus explaining the opposite effects of ΔFLAP effects on the pre- and the mature miRNAs. However, these are speculative statements and they need further confirmation as the formation of a tripartite complex, consisting of Dicer, 5-LO, and FLAP, is could be also part of this model system.

6.7 5-LO knockdown does not influence Ago2 expression

Ago2 is the only member of the Ago protein family, which exhibits own catalytical activity and which is capable of bypassing Dicer cleavage to independently form mature miRNAs, for example, miR-451 [287]. But neither ΔFLAP nor Δ5-LO affected Ago2 protein amount (Figure 23). Hence, an effect of 5-LO or FLAP on Ago-expression, which in turn controls miRNA-targeting and in a less extent miRNA-processing, can be excluded.

Ago2 is involved in miRNA guide strand selection. Its performance can be enhanced in association with Dicer, PACT, and TRBP. Interestingly, strand selection for a few specific miRNAs is enhanced in presence of PACT, whereas TRBP has no influence. Furthermore, TRBP containing RISC has a lower affinity towards mRNA compared to RISC including PACT [288].

To summarize, the increase of miR-99b-5p and miR-125a-5p in MM6 cells, absent in Δ5-LO cells, was independent of Ago2 expression.

6.8 Silencing of miR-99b-5p and miR-125a-5p increases release of TNFα and IL-6 in MM6 cells

LPS stimulates the expression of TNFα and IL-6 in monocytic cells by binding to TLR4 what leads to an activation of MyD88 and NF-κB subsequently [284]. A quick onset of TNFα release in the human monocytic cell line MM6 was observed, whereas IL-6 level were only slowly ascending (Figure 32). These findings reflect the biological signal transduction, where TNFα activates T cells and macrophages to release IL-6 [289], and IL-6, in turn, inhibits TNFα secretion [290].

MiRNAs are involved in the regulation of the immune system to control and fine-tune this sensitive interplay [291] For example, miR-155 and miR-125b directly target TNFα-mRNA [292], whereas miR-125b and miR-146b regulate IL-6 expression in *Heliobacter pylori* infected gastroduodenal ulcer [293]. As expected, the homolog of miR-125b, miR-125a, regulates TNFα and IL-6 release (chapter 6.8) in MM6 cells. Silencing of the miRNA led to a significant decrease in TNFα and IL-6 levels. However, contrary tendencies concerning miR-125a-5p and its activity towards TNFα have been observed in different cell

lines. According to Kim *et al.*, miR-125a-5p downregulates LPS-induced TNFα expression in mouse bone-marrow derived macrophages [205]. The monocytic cell line THP-1 shows the opposite, here expression of miR-125a-5p upregulates a basal TNFα mRNA level [207]. Apart from this, steady expression of miR-125a reduces TNFAIP3 level in diffuse large B-cell lymphoma cell lines [208]. TNFAIP3 in turn is induced by TNFα and inhibits NF-ϰB activity. Hence, the effect of TNFAIP3 inhibition is comparable to the TNFα upregulation in THP-1 cells. Additionally, this conclusion is supported by the observation that in HEK293 cells a luciferase reporter containing the 3´-UTR of TNFAIP3 was downregulated after co-transfection with a plasmid encoding pGFP-125a [207].

Apart from miR-125a-5p, miR-99b-5p is also able to downregulate TNFα in MM6 cells (chapter 6.8). However, the impact is minor compared to the effect of miR-125a-5p.

The same applies for TNFα protein in murine bone-marrow derived dendritic cells, infected with *M. tuberculosis*. In addition, miR-99b-5p decreases IL-6, IL-12p40, IL-12p70, and IL-1ß expression [223].

Taken together, the data suggest that miR-125a-5p and miR-99b-5p play an inhibitory role in inflammation.

Besides the discussed involvement of miR-125a-5p in inflammatory responses via TNFα, this miRNA-target interaction plays a role in the lipid uptake. In addition to miR-9, miR-155, miR-146b-5p, and miR-146a, miR-125a-5p is also upregulated in oxLDL stimulated primary peripheral blood monocytes [294]. Furthermore, it was shown that this increased miRNA-level is associated with reduced lipid uptake, reduction in oxysterol binding protein-like 9 (ORP9), and decreased release of inflammatory cytokines like IL-6 and TNFα. Taken into account that both, 5-LO and FLAP, are found in lipid bodies inside foam cells [89], enhanced miR-125a-5p expression is a potential factor to reduce inflammation at the atherosclerotic side and to delay further foam cell formation. However, this needs to be confirmed.

6.9 PT53 is not affected by reduced miR-99b-5p and miR-125a-5p expression

Apart from the regulation of cytokines, miR-125a-5p and miR-99b-5p are mainly published to be important during cancer development and cancer spreading. PT53, also called p53, is

one of the most extensive investigated tumor suppressor proteins. However, an effect of miR-125a-5p silencing upon p53 release, neither on RNA nor on protein level was not observed in MM6 cells. In contrast, PT53 was previously described to be targeted by miR-125a-5p in HEK293T cells [295], in human bronchial epithelial cells [296], in human hepatocellular carcinoma [297], and multiple myeloma cells [298]. Besides, the overexpression of the passenger strand of miR-125a-5p, miR-125a-3p, activates p53 [299]. Since p53 and miR-125a-5p are present in MM6 cells, further regulatory elements seem to hinder the binding of the miR-125a-5p guided RISC to the p53 mRNA. A potential explanation is a protection of the miR-125a-5p binding sequence within the p53 mRNA by a RNA binding protein. Up to now, the best characterized representative is the human antigen R (HuR). This protein is known to bind, amongst others, to p53 mRNA and thereby blocking the access of, for example, the ncRNA 7SL [300]. As a consequence, the translation is blocked. Interestingly, HuR can be activated upon 5-, 12-, and 15-HETEs treatment in human colonic myofibroblasts. Thereby it is able to stabilize IL-1 induced COX-2 mRNA to improve COX-2 translation [301].

6.10 Silencing of miR-99b-5p and miR-125a-5p affects 5-LO activity

5-LO activity depends on several factors. According to Lindner *et al.*, LPS stimulation of MM6 cells leads to a two-fold increase in LT biosynthesis [286]. By activating TLR4, LPS induces TNFα release [302] which, in turn, increases 5-LO activity [57, 58]. Thereupon, an enhanced 5-LO activity after silencing of miR-99b-5p and miR-125a-5p in LPS treated cells was expected. But inhibition of these miRNA had no influence on 5-LO activity (chapter 5.14). In contrast, silencing of miR-125a-5p and miR-99b-5p increased production of LTB_4 and 5-HETE in differentiated MM6 cells without further LPS stimulation. Apart from that, the 5-LO mRNA levels (data not shown) and the 5-LO protein level as shown in Figure 38 were not affected by miR-99b-5p and miR-125a-5p knockdown. Unexpectedly, the combination of both antagomirs did not enhance the effects observed in cells treated solely with anti-miR-99b-5p and anti-miR-125a-5p. It is possible that the individual antagomir concentration in the combinatory experiment was too low, as the total antagomir

concentration was kept constant. Twice the amount of the respective antagomirs should further enhance 5-LO activity.

Taken together, these results imply a role for the listed miRNAs in the regulation of 5-LO activity. The extent of TNFα involvement in this regulation needs to be investigated. But it seems that LPS masks the weak effect of miRNA controlled regulation of 5-LO activity.

6.11 TNFα and IL-6 expression is significantly altered by 5-LO and FLAP knockdown

Several studies show the impact of cytokines on 5-LO expression and 5-LO activity [54-56, 303]. This study monitored the changes in IL-6 and TNFα release in Δ5-LO and ΔFLAP shRNA treated MM6 cells, compared to control cells. Both cytokines were significantly altered upon 5-LO and FLAP knockdown (Figure 33). Taking into account that knockdown of 5-LO and FLAP led to a decreased expression of miR-99b-5p and miR-125a-5p and silencing of these miRNAs furthermore increased TNFα and IL-6 expression, it was expected to detect increasing cytokine level in the Δ5-LO and ΔFLAP cells. However, unlike the assumption, TNFα and IL-6 were expressed on a lower level in absence of 5-LO. In contrast, FLAP knockdown showed a different impact on TNFα and IL-6 expression. While the TNFα level is independent of FLAP, the release of IL-6 increased in ΔFLAP cells (Figure 40). These observations suggest a miRNA independent regulation of cytokine release.

6.12 Expression of miR-125a-5p and miR-99b-5p varies with differential activation of macrophages

MiR-125a-5p and miR-99b-5p were found to be upregulated in human primary macrophages activated by M-CSF. Additionally, miR-125a-5p showed the same tendency upon M2 activation (Figure 34). These results are consistent with the data obtained in M2 activated murine bone marrow-derived macrophages for miR-125a-5p [205]. In contrast, Graff *et al.* found miR-125a-5p constantly expressed upon differential activation, while its passenger strand miR-125a-3p was more than three-fold induced in M1 macrophages, compared to untreated controls [207].

A possible explanation for these controversial results is the usage of different activation stimuli. The group of Graff *et al.*, for example, performed, prior to cytokine stimulation, a CD14 positive cell selection of human monocyte derived macrophages. Furthermore, they applied double the amount of IFNγ (referred to as M2a) and IL-4 (M1) for polarization. However, the usage of LPS for M1 polarization implicates the strongest differences. The group of Banerjee *et al.* only applied LPS for M1 polarization, which induces miR-125a-5p expression independently of former GM-CSF or M-CSF stimulation. Furthermore, they performed their experiments in murine macrophages [205]. The limited transferability of data observed in mice onto humans is illustrated by the fact that two classical M2 murine macrophage markers, arginase-1 and YM-1, cannot be used as macrophage markers in humans [304].

To conclude, it is difficult to compare miRNA expression profiles in different species and, in particular, after activation with different stimuli. Therefore, it is necessary to further analyze the impact of miR-125a-5p and miR-99b-5p on M1 and M2 macrophage properties in humans. Unfortunately, it was not possible to transfect enough cells to analyze the consequences of miR-99b-5p and miR-125a-5p silencing on differential activation of macrophages. However, since the transfection of anti-miR-99b-5p and anti-miR-125a-5p into primary macrophages was successful in a small scale, this should be an easy follow up experiment.

Additionally, with regard to 5-LO, it is likely that differential activation of macrophages has a major impact on 5-LO protein expression. However, in contrast to the expression of the 5-LO controlled miRNAs, the 5-LO protein is significantly increased in M1 polarized macrophages, while the expression level in untreated control cells and M2 polarized macrophages are comparably low (Figure 36). Thus it is unlikely that 5-LO is the missing link between miR-99b-5p and miR-125a-5p expression and differential activation of macrophages.

7 SUMMARY

LTs are important inflammatory mediators. One of the key components in the LT metabolism is the 5-Lipoxygenase enzyme (5-LO). Via its N-terminal domain 5-LO is able to interact with several proteins. Among them are Coactosin-like protein (CLP) and Dicer. The latter mentioned enzyme is responsible for the last step of microRNA (miRNA/miR) maturation. It cleaves precursor miRNAs (pre-miRNAs) to form mature miRNAs. These short non-coding RNAs are involved in the posttranscriptional regulation of protein biosynthesis.

Already 1999, Dincbas-Renqvist *et al.* studied the relationship between miRNA maturation and LT biosynthesis on the basis of the interaction between Dicer and 5-LO. They found 5-LO activity to be enhanced in the presence of Dicer *in vitro*. On the other hand, although turnover of the pre-miRNA let-7a-3 by Dicer was unaffected in the presence of 5-LO, they observed a product shift with increasing 5-LO concentrations. In absence of 5-LO, the regular Dicer product size of around 23 nt was detected, whereas longer (~55 nt) and shorter (~10-12 nt) RNA fragments were found in presence of 5-LO [38].

In this study we worked mainly with the monocytic cell line Mono Mac 6 (MM6). In their undifferentiated state, they hardly express 5-LO, but after a 4 days differentiation with TGFβ and calcitriol, 5-LO protein expression is strongly induced. With this study, we intended to figure out whether 5-LO affects maturation and expression of distinct miRNAs in these cells. This question was addressed by performing a microarray in 5-LO knockdown (Δ) MM6 cells and control cells, to detect the respective miRNA expression levels. In Δ5-LO cells, 30 miRNAs which were upregulated (threshold ratio 1.3) and 7 miRNAs which were downregulated (threshold ratio 0.7) were found and the decrease of miR-99b-5p and miR-125a-5p in absence of 5-LO was subsequently analyzed. Interestingly, these two miRNAs are organized in a common miRNA-cluster, which also includes let-7e-5p. Hence, this study focused on these three miRNAs, originated from one single transcript.

Next, it was investigated if either the transcription of the miRNA-cluster or the maturation of the respective miRNAs is specifically controlled by 5-LO. It was found that the primary transcript (pri-miRNA) is unaffected by Δ5-LO, whereas the pre-miRNA levels are lowered in absence of 5-LO. This shows that besides Dicer, Drosha activity to process certain miRNAs might be

regulated by 5-LO. Drosha is besides Dicer responsible for the maturation of miRNAs and converts the pri-miRNA into the respective pre-miRNAs. However, up to now, there is no evidence that 5-LO is also able to directly interact with Drosha, thus further studies dealing with their mutual influence are necessary.

Next it was tested whether LTs or 5-LO pathway inhibitors affect miRNA expression and it was found that expression of miR-99b-5p and miR-125a-5p is independent of the respective LT levels. But in contrast, expression of both miRNAs is altered by 5-LO activating protein (FLAP), another 5-LO binding partner. This protein is necessary for 5-LO activity *in vivo*. Unlike 5-LO, it is assumed that FLAP only controls Dicer specificity towards pre-miR-99b and pre-miR-125a, as these precursors are unaffected by ΔFLAP, whereas the expression of mature miRNAs decreased. To confirm this assumption, immunofluorescence microscopy including 5-LO and Dicer was performed in presence and absence of FLAP. [31]. In absence of FLAP, 5-LO is localized inside the nucleus and not in the cytoplasm, while, according to former results, FLAP positive cells show a primary localization of 5-LO inside the cytoplasm. Dicer is localized in the cytoplasm, independently of the presence of FLAP. This distinct localization can be an explanation for the different expression profiles of pre-miRNAs in Δ5-LO and ΔFLAP cells. It is probable that FLAP maintains 5-LO inside the cytoplasm and as a consequence 5-LO is predominantly localized in the nucleus of ΔFLAP cells. By means of higher nuclear 5-LO level in ΔFLAP cells the Drosha activity towards pri-miR-99b/let-7e/miR-125a increases what eventually explains the high level of pre-miR-99b and pre-miR-125a in these cells. In presence of FLAP 5-LO is localized inside the cytoplasm where it probably changes the Dicer specificity towards pre-miR-99b and pre-miR-125a. Additionally, the nuclear 5-LO is most likely to change the Drosha specificity towards the respective pri-miRNA.

To further characterize the importance of miR-99b-5p and miR-125a-5p in inflammation, the effect of strong immune responses on miRNA expression was analyzed next by means of lipopolysaccharides (LPS) stimulation. Compared to unstimulated cells, expression of miR-99b-5p and miR-125a-5p was found to be enhanced. Interestingly this effect is much stronger in differentiated, 5-LO expressing cells, than in undifferentiated cells. Furthermore Δ5-LO cells display a minor increase of miR-99b-5p and miR-125a-5p expression. When next

the expression level of the corresponding pri-miRNA was analyzed, the same tendency was observed. However, after classification of the increase in pri-miRNA level according to 'effect based on differentiation' and 'effect based on LPS', it was discovered that miR-125a-5p and miR-99b-5p expression is always 2-fold increased upon stimulation with TGFβ and calcitriol, independent of LPS treatment and independent of Δ5-LO or ΔFLAP. In contrast, LPS stimulates miRNA expression independently of the differentiation status, but not in Δ5-LO cells. This suggests an additional, 5-LO dependent, regulatory mechanism on miRNA expression upon LPS stimulation. But LPS does neither alter localization of 5-LO nor 5-LO expression in MM6 cells. Hence, further studies dealing with the effect of LPS on 5-LO in connection with Dicer and miRNA expression are necessary.

Next, potential targets of miR-99b-5p and miR-125a-5p were tested by silencing their respective expression. The amount of the cytokines IL-6 and TNFα increased upon miRNA-silencing.

TNFα is an interesting target as it enhances 5-LO activity [58], but although TNFα expression is enhanced after inhibition of miR-99b-5p and miR-125a-5p, 5-LO activity in MM6 cells stays unaffected in LPS-treated and miR-99b-5p/miR-125a-5p silenced cells. In contrast, unstimulated cells which do not express TNFα show an increased 5-LO activity upon miRNA silencing. At the same time, the 5-LO protein level is unaffected. This suggests that miR-99b-5p and miR-125a-5p are involved in the regulation of 5-LO activity whereas LPS masks or reverses this effect.

Furthermore, differentiated Δ5-LO cells exhibit significantly reduced TNFα levels compared to differentiated control cells. Hence, the absence of 5-LO seems to affect further pathways, which regulate cytokine release.

Taken together, the results of the present study could show a regulatory function of 5-LO on the maturation of miR-99b-5p and miR-125a-5p. This effect could be due to the previously observed direct interaction between 5-LO and Dicer, while the influence of 5-LO on the miRNA-processing by Drosha is not completely determined yet. Furthermore, it could be shown that regulation of miRNA-expression by 5-LO does not depend on its canonical enzymatic activity. These results strike a new path in 5-LO research. In the future, this knowledge is able to contribute to characterize so far not known effects, which are based on the presence of 5-LO.

8 ZUSAMMENFASSUNG

Die 5-Lipoxygenase (5-LO) zählt zu einer Klasse von Enzymen, welche für die Umsetzung von Arachidonsäure (arachidonic acid, AA) zu LTn zuständig ist. Diese entstehen hierbei in einer zweistufigen Reaktion. Zu den wichtigsten Vertretern dieser Substanzklasse zählen Leukotrien B_4-E_4 (LTB_4-E_4), die wichtige Funktionen bei entzündlichen Prozessen besitzen [305]. Mittlerweile konnten mehrere 5-LO interagierende Proteine identifiziert werden, welche die Aktivität der 5-LO beeinflussen [33]. Dazu zählen unter anderem das 5-LO aktivierende Protein (5-LO activating protein, FLAP) [43], das Coactosin-ähnliche Protein (coactosine-like protein, CLP) [40] und Dicer [38]. Letzteres ist an der Reifung kleiner, nicht-kodierender RNAs beteiligt, die an der post-transkriptionellen Regulation der Proteinbiosynthese beteiligt sind und als microRNAs (miRNA/miR) bezeichnet werden. Bei der Bildung von miRNAs wird zuerst das jeweilige miRNA-Gen transkribiert. Das entstandene primäre Transkript (pri-miRNA) wird anschließend im Nukleus vom Mikroprozessorkomplex, bestehend aus dem RNA-bindenden Protein DGCR8 (DiGeorge syndrome chromosomal region 8) und Drosha, erkannt und prozessiert. Die resultierende Vorläufer-miRNA (precursor-miRNA, pre-miRNA) besteht aus einer einzelnen Stammschleifen-Struktur und wird mit Hilfe von Exportin 5 in das Zytoplasma exportiert. Dort wird die pre-miRNA von Dicer erkannt und zu etwa 23 nt langen doppelsträngigen (ds) miRNAs prozessiert. Im letzten Schritt wird schließlich der ds-miRNA-Strang entwunden. Während der thermodynamisch instabilere Einzelstrang degradiert wird, kann der Andere als reife miRNA regulatorisch wirken. Dafür bindet die generierte miRNA über ihre sogenannte seed-Sequenz, welche die Basen 2-8 einschließt, an die 3‘ untranslatierte Region (UTR) der Ziel mRNA und verhindert dadurch die Translation jener mRNA, beziehungsweise initiiert deren Degradation [306].

Bereits im Jahr 1999 haben Dincbas-Renqvist *et al.* den Einfluss der Interaktion zwischen Dicer und 5-LO untersucht. Dabei stellten sie fest, dass beide Proteine über die N-terminale Domäne der 5-LO und drei Tryptophanen des C-Terminus von Dicer interagieren. Darüber hinaus konnten sie zeigen, dass die *in-vitro* Aktivität der 5-LO in Gegenwart von Dicer in geringem Maße ansteigt. Hingegen ist die Umsetzung der pre-miRNA pre-let-7a-3 durch Dicer 5-LO unabhängig. Allerdings veränderte sich die Länge des entstandenen Produktes nach der

Dicer-Prozessierung mit steigender 5-LO-Konzentration. In Gegenwart von 5-LO verschiebt sich die Produktverteilung von der normalen durchschnittlichen miRNA-Länge zu längeren, etwa 55 nt langen RNA-Strängen und zu kürzeren, etwa 10-12 nt langen Strängen [38]. Gegenstand der vorliegenden Dissertation ist die Frage, ob neben der Prozessierung der pre-let-7a-3 die Reifung weiterer miRNAs durch die 5-LO kontrolliert wird und inwiefern diese Beobachtungen auf zelluläre Systeme übertragbar sind. Im Rahmen dieser Arbeit wurde mit der monozytischen Zelllinie Mono Mac 6 (MM6) gearbeitet- Dieses zelluläre Modellsystem exprimiert im undifferenzierten Zustand nur geringe Mengen an 5-LO. Nach viertägiger Inkubation mit dem transformierenden Wachstumsfaktor β (TGFβ) und Calcitriol kommt es zu einer starken Induktion des mRNA-Niveaus und einer etwa 100-fachen Induktion [16] der 5-LO Proteinexpression. Basavajarappa *et al.* etablierten eine MM6 Zelllinie, in der die Expression der 5-LO mittels RNA-Interferenz stark reduziert ist [31]. Diese Zelllinie wurde verwendet, um mittels Microarray deren miRNA-Expression mit dem Expressionsmuster in Kontroll-MM6 Zellen zu vergleichen.

In dem Array zeichnete sich ab, dass die Expression spezifischer miRNAs durch den Knockdown der 5-LO beeinflusst ist. Interessanterweise wurden zwei miRNAs identifiziert, miR-99b-5p und miR-125a-5p, die simultan transkribiert werden. Man kann erkennen, dass die beiden miRNAs eine weitere miRNA flankieren: die let-7e-5p. Aus diesem Grund lag der Fokus im Verlauf dieser Arbeit auf den miRNAs miR-99b-5p, let-7e-5p und miR-125a-5p, die dem gleichen Cluster entstammen. In Übereinstimmung mit den Mikroarray-Daten konnte gezeigt werden, dass nach Differenzierung der Zellen mit TGFβ und Calcitriol die Expression von miR-99b-5p und miR-125a-5p in Gegenwart der 5-LO etwa zweifach induziert wird. Im Gegensatz dazu ist keine Induktion in 5-LO-Knockdown-Zellen zu beobachten. Eine vergleichbare Tendenz weist ebenfalls let-7e-5p auf.

Da die drei vornehmlich aus dem Cluster miR-99b/let-7e/miR-125a resultierenden reifen miRNA, auch guide miRNA genannt, durch 5-LO reguliert werden, liegt die Vermutung nahe, dass bereits die Transkription von miR-99b-5p, let-7e-5p und miR-125a-5p durch 5-LO reguliert wird. Allerdings konnte kein Unterschied zwischen der Expression der pri-miRNA in Kontroll-, beziehungsweise 5-LO Knockdown-Zellen beobachtet werden. Daraus resultiert, dass

die 5-LO erst nach der Transkription in die Reifung der miRNA eingreift. Ferner stellte sich heraus, dass die nukleäre Prozessierung bestimmter miRNAs durch Drosha durch die 5-LO eventuell moduliert wird. Bisher konnte allerdings keine direkte Interaktion zwischen 5-LO und Drosha belegt werden. Aus diesem Grund sind zusätzliche Studien, die sich mit dem Thema des Einflusses der 5-LO auf Drosha-Ebene beschäftigen, notwendig.

Weiterhin konnte gezeigt werden, dass Produkte der 5-LO, insbesondere LTB_4, LTC_4 und 5-Hydroxyeicosatetraensäure (5-Hydroxyicosatetraenoic acid; 5-HETE), keinerlei Einfluss auf die Expression von miR-99b-5p und miR-125a-5p haben. Das gleiche Resultat wurde im Umkehr-Experiment durch Zugabe von 5-LO-Signalweg-Inhibitoren, wie Zileuton und MK-886, erzielt. Daraus lässt sich schließen, dass die 5-LO-Proteinexpression, nicht jedoch deren Aktivität die miRNA-Prozessierung reguliert. Im Gegensatz dazu konnte gezeigt werden, dass für die Leukotrien-Biosynthese *in vivo* essentielles FLAP einen mit 5-LO vergleichbaren Effekt auf die Dicer-vermittelte pre-miRNA Prozessierung hat. Die Aktivität von Drosha ist hingegen FLAP unabhängig. Daher wird angenommen, dass FLAP die zytoplasmatische Interaktion zwischen Dicer und 5-LO fördert, während die Regulierung von Drosha durch 5-LO unabhängig von FLAP stattfindet. Diese Ergebnisse stehen zudem in Einklang mit Protein-Lokalisationsstudien mittels Immunofluoreszenz. Darin zeigte sich, dass wie bereits publiziert [31], innerhalb von Kontroll-MM6 Zellen sowohl 5-LO als auch Dicer bevorzugt innerhalb des Zytoplasmas lokalisiert sind. In Abwesenheit von FLAP scheint 5-LO hingegen innerhalb des Nukleus‘ zu akkumulieren, während Dicer bevorzugt im Zytoplasma lokalisiert ist. Dies ist eine mögliche Erklärung für die Besonderheit, dass die Expression von miR-99b-5p und miR-125a-5p in FLAP Knockdown-Zellen reduziert ist, da das Niveau an 5-LO innerhalb des Zytoplasmas nicht ausreicht um die akkumulierende pre-miRNA mittels Dicer zu prozessieren.

Des Weiteren wurden die Auswirkungen pro-inflammatorischer Faktoren auf die Expression der Mitglieder des miRNA-Clusters miR-99b/let-7e/miR-125a ermittelt. Insbesondere wurde der Einfluss der als Antigen wirkenden Lipopolysacchariden (LPS) getestet. LPS stammen aus der äußeren Zellmembran gramnegativer Bakterien und binden im humanen Organismus an den Membranrezeptor CD14, der unter Anderem auf der Oberfläche von Monozyten lokalisiert ist. Dieser Komplex aus LPS und CD14 aktiviert wiederum den Toll-like Rezeptor 4 (TLR4),

welcher im Allgemeinen Pathogen-assoziierte molekulare Muster (PAMPs) erkennt. Im weiteren Verlauf wird durch die Aktivierung des TLR4 die Expression des Transkriptionsfaktors nukleärer Faktor 'kappa-light-chain-enhancer' aktivierter B-Zellen (NF-κB) induziert. NF- κB hat eine relativ geringe Spezifität und ist an vielfältigen entzündlichen Prozessen beteiligt, unter Anderem durch eine Aktivierung des proinflammatorischen Zytokins TNFα.

Bei der Untersuchung des Einflusses von LPS auf die Expression von miR-99b-5p, let-7e-5p und miR-125a-5p stellte sich heraus, dass sich die Expression der reifen miRNA in differenzierten im Vergleich zu undifferenzierten MM6 Zellen in etwa vervierfachte. In 5-LO Knockdown-Zellen ist diese Induktion hingegen nicht zu beobachten. Bei der Betrachtung des primären Transkriptes zeigt sich auf den ersten Blick ein ähnliches Bild. Die Expression der pri-miRNA in differenzierten Zellen verglichen mit undifferenzierten Zellen ist ebenfalls deutlich erhöht. Betrachtet man gezielt den LPS vermittelten Effekt erkennt man, dass das primäre Transkript unabhängig vom Differenzierungsstatus und unabhängig vom Zelltyp (Kontrolle/Δ5-LO/ΔFLAP) etwa zweifach induziert wird. Im Gegensatz dazu zeigt sich bei der Betrachtung des reinen Differenzierungseffektes, dass LPS die Expression von pri-miR-99b/let-7e/miR-125a in Gegenwart von 5-LO um den Faktor 10 erhöht. In 5-LO Knockdown-Zellen ist dieser Effekt deutlich minimiert. Es lässt sich sagen, dass LPS einen differenzierungs-unabhängigen Einfluss auf die Transkription des besagten Clusters besitzt. Interessanterweise ist diese Induktion 5-LO abhängig.

Zusammengefasst ist die Expression des primären Transkriptes von miR-99b, let-7e und miR-125a nach Stimulation mit LPS in Abwesenheit von 5-LO deutlich reduziert, allerdings sind weder das Niveau an mRNA noch die 5-LO-Protein Expression von Relevanz. LPS scheint über einen weiteren, bisher unbekannten Mechanismus, die miRNA-Expression zu beeinflussen.

Im dritten Teil dieser Arbeit wurde die biologische Rolle der 5-LO regulierten miRNAs behandelt. Literaturrecherchen zeigten einerseits den Einfluss von miR-99b-5p und miR-125a-5p auf die Hematopoese und andererseits Verknüpfungen zu Entzündungsprozessen. Insbesondere die Zytokine Interleukin 6 (IL-6) und Tumornekrosefaktor α (TNFα) sowie der Tumorsuppressor p53 erschienen wiederholt in diesem Zusammenhang. In Gegenwart von Antagomiren, die komplementär zu den jeweiligen miRNAs sind, kommt es zur Degradation der

jeweiligen miRNAs und einer damit einhergehenden Inhibition ihrer Funktionen. Übereinstimmend mit vorherigen Daten konnte mittels dieser Methode gezeigt werden, dass nach Differenzierung von MM6 Zellen und in Gegenwart der Antagomire gegen miR-99b-5p und miR-125a-5p die Expression der Zytokine IL-6 und TNFα erhöht ist. Deren Expression ist jedoch nur nach vorheriger Stimulation mittels LPS messbar, wobei die stärksten Unterschiede 6 h nach Zugabe von LPS zu beobachten waren.

Nach Identifizierung von TNFα und IL-6 als Targets der durch 5-LO kontrollierten miRNAs, stellte sich weiterhin die Frage, inwiefern die entsprechenden Zytokine in Δ5-LO- beziehungsweise ΔFLAP-Zellen herunter reguliert sind. Es zeigte sich, dass in Abwesenheit von 5-LO sowohl die Expression von TNFα als auch die Freisetzung von IL-6 signifikant reduziert ist. Im Falle eines miRNA-vermittelten Effektes müsste die Zytokin-Freisetzung durch die erniedrigten miR-99b-5p und miR-125a-5p Spiegel in Δ5-LO Zellen dahingegen erhöht sein. Aufgrund dessen kann in diesem Fall davon ausgegangen werden, dass die Inhibierung der Zytokin-Freisetzung in Abwesenheit der 5-LO miRNA unabhängig stattfindet. Dies wird durch die Beobachtung unterstützt, dass im Gegensatz zu 5-LO-Knockdown-Zellen, FLAP Knockdown-Zellen eine konstante TNFα-Freisetzung aufwiesen, während sich die Menge an freigesetztem IL-6 in etwa verdoppelte. Die miRNA Expression ist jedoch in beiden Zelllinien vergleichbar. Aufgrund dessen kann man zusammenfassend sagen, dass der relativ schwache miRNA-vermittelte Effekt überlagert wird. Außerdem legen die Daten nahe, dass lediglich 5-LO aber nicht FLAP an der LPS-vermittelten Stimulation der Freisetzung der beiden Zytokine beteiligt ist.

Darüber hinaus stellte sich die Frage inwiefern die Inhibition von miR-99b-5p und miR-125a-5p die Aktivität der 5-LO durch Stimulation der TNFα-Sekretion positiv beeinflusst wird. Übereinstimmend mit vorherigen Resultaten zeigte sich hierbei, dass die Gabe von LPS die 5-LO-Aktivität erhöht. Die zelluläre 5-LO-Aktivität konnte allerdings durch den Einsatz von Antagomiren nicht weiter gesteigert werden. Im Gegensatz dazu führte die Hemmung von miR-125a-5p in LPS unstimulierten Zellen zu einer signifikanten Aktivitätssteigerung. Diese Resultate lassen vermuten, dass die miRNA lediglich die basale 5-LO-Aktivität beeinflussen kann während LPS den miRNA-vermittelten Effekt überlagert.

Der letzte Abschnitt dieser Arbeit beschäftigt sich mit der biologischen Rolle von miR-99b-5p und miR-125a-5p in Primärzellen. Es konnte gezeigt werden, dass die Expression beider miRNAs durch die Differenzierung von Monozyten zu Makrophagen beeinflusst wird. Unterschieden werden kann dabei zwischen M1-Makrophagen, die hauptsächlich an der akuten Immunantwort beteiligt sind, und M2-Makrophagen, denen Zuständigkeiten sowohl während der Gewebeerneuerung als auch während der Wundheilung zugesprochen werden. Dabei zeigt sich, dass durch die Differenzierung zu M2-Makrophagen die Expression von miR-99b-5p und miR-125a-5p erhöht ist. Dies lässt auf eine anti-inflammatorische Funktion der beiden miRNAs schließen und würde zu einer regulatorischen Rolle in Bezug zur 5-LO passen. Im Gegensatz dazu wird die 5-LO allerdings hauptsächlich in M1-Makrophagen exprimiert. Diese Ergebnisse legen nahe, dass die Induktion von miR-99b-5p und miR-125a-5p in Primärzellen 5-LO unabhängig erfolgt und in dem Falle einer Beteiligung von 5-LO an der Differenzierung von Monozyten diese nicht miRNA vermittelt erfolgt.

Zusammenfassend konnte in dieser Arbeit gezeigt werden, dass 5-LO eine regulierende Funktion auf die Reifung der beiden miRNAs miR-99b-5p und miR-125a-5p aufweist. Dieser Effekt könnte einer direkten Interaktion zwischen der 5-LO und Dicer zuzuschreiben sein. Des Weiteren konnte gezeigt werden, dass die Regulierung der Expression bestimmter miRNAs mittels 5-LO nicht auf deren kanonischer enzymatischer Aktivität beruht. Diese Ergebnisse schlagen eine neue Richtung der 5-LO-Forschung ein und können in Zukunft dazu beitragen 5-LO vermittelte Effekte besser charakterisieren zu können.

9 REFERENCES

1. Radmark, O. and B. Samuelsson, *Regulation of the activity of 5-lipoxygenase, a key enzyme in leukotriene biosynthesis.* Biochem Biophys Res Commun, 2010. **396**(1): p. 105-10.
2. Samuelsson, B., *An elucidation of the arachidonic acid cascade. Discovery of prostaglandins, thromboxane and leukotrienes.* Drugs, 1987. **33 Suppl 1**: p. 2-9.
3. Rosenthal, M.D., et al., *Cellular regulation of arachidonate mobilization and metabolism.* Prostaglandins Leukot Essent Fatty Acids, 1995. **52**(2-3): p. 93-8.
4. Borgeat, P., M. Hamberg, and B. Samuelsson, *Transformation of arachidonic acid and homo-gamma-linolenic acid by rabbit polymorphonuclear leukocytes. Monohydroxy acids from novel lipoxygenases.* J Biol Chem, 1976. **251**(24): p. 7816-7820.
5. Borgeat, P. and B. Samuelsson, *Transformation of arachidonic acid by rabbit polymorphonuclear leukocytes. Formation of a novel dihydroxyeicosatetraenoic acid.* J Biol Chem, 1979. **254**(8): p. 2643-6.
6. Murphy, R.C., S. Hammarstrom, and B. Samuelsson, *Leukotriene C: a slow-reacting substance from murine mastocytoma cells.* Proc Natl Acad Sci U S A, 1979. **76**(9): p. 4275-9.
7. Uderhardt, S. and G. Kronke, *12/15-lipoxygenase during the regulation of inflammation, immunity, and self-tolerance.* J Mol Med (Berl), 2012. **90**(11): p. 1247-56.
8. Funk, C.D., et al., *Characterization of the human 5-lipoxygenase gene.* Proc Natl Acad Sci U S A, 1989. **86**(8): p. 2587-91.
9. Carlberg, C., *Mechanisms of nuclear signalling by vitamin D3. Interplay with retinoid and thyroid hormone signalling.* Eur J Biochem, 1995. **231**(3): p. 517-27.
10. Sorg, B.L., et al., *Analysis of the 5-lipoxygenase promoter and characterization of a vitamin D receptor binding site.* Biochim Biophys Acta, 2006. **1761**(7): p. 686-97.
11. Katryniok, C., et al., *Role of DNA methylation and methyl-DNA binding proteins in the repression of 5-lipoxygenase promoter activity.* Biochim Biophys Acta, 2010. **1801**(1): p. 49-57.
12. Yu, V.C., et al., *RXR beta: a coregulator that enhances binding of retinoic acid, thyroid hormone, and vitamin D receptors to their cognate response elements.* Cell, 1991. **67**(6): p. 1251-66.
13. Radmark, O., et al., *5-Lipoxygenase: regulation of expression and enzyme activity.* Trends Biochem Sci, 2007. **32**(7): p. 332-41.
14. Seuter, S., et al., *Functional characterization of vitamin D responding regions in the human 5-Lipoxygenase gene.* Biochim Biophys Acta, 2007. **1771**(7): p. 864-72.
15. Stoffers, K.L., et al., *Calcitriol upregulates open chromatin and elongation markers at functional vitamin D response elements in the distal part of the 5-lipoxygenase gene.* J Mol Biol, 2010. **395**(4): p. 884-96.
16. Brungs, M., et al., *Sequential induction of 5-lipoxygenase gene expression and activity in Mono Mac 6 cells by transforming growth factor β and 1,25-dihydroxyvitamin D3.* Proc Natl Acad Sci U S A, 1995. **92**: p. 107-111.
17. Seuter, S., B.L. Sorg, and D. Steinhilber, *The coding sequence mediates induction of 5-lipoxygenase expression by Smads3/4.* Biochem Biophys Res Commun, 2006. **348**(4): p. 1403-10.

18. Massague, J., J. Seoane, and D. Wotton, *Smad transcription factors.* Genes Dev, 2005. **19**(23): p. 2783-810.
19. Löms Ziegler-Heitbrock, H.W., et al., *Establishment of a human cell line (Mono Mac 6) with characteristics of mature monocytes.* Int. J. Cancer, 1988. **41**(3): p. 456-461.
20. Boado, R.J., et al., *Differential expression of arachidonate 5-lipoxygenase transcripts in human brain tumors: evidence for the expression of a multitranscript family.* Proc Natl Acad Sci U S A, 1992. **89**(19): p. 9044-8.
21. Ochs, M.J., et al., *Post-transcriptional regulation of 5-lipoxygenase mRNA expression via alternative splicing and nonsense-mediated mRNA decay.* PLoS One, 2012. **7**(2): p. e31363.
22. Boudreau, L.H., et al., *Novel 5-lipoxygenase isoforms affect the biosynthesis of 5-lipoxygenase products.* FASEB J, 2011. **25**(3): p. 1097-105.
23. Busch, S., et al., *5-Lipoxygenase Is a Direct Target of miR-19a-3p and miR-125b-5p.* J Immunol, 2015.
24. Brock, T.G., R. Paine, 3rd, and M. Peters-Golden, *Localization of 5-lipoxygenase to the nucleus of unstimulated rat basophilic leukemia cells.* J Biol Chem, 1994. **269**(35): p. 22059-66.
25. Chamulitrat, W., R.P. Mason, and D. Riendeau, *Nitroxide metabolites from alkylhydroxylamines and N-hydroxyurea derivatives resulting from reductive inhibition of soybean lipoxygenase.* J Biol Chem, 1992. **267**(14): p. 9574-9.
26. Gillard, J., et al., *L-663,536 (MK-886) (3-[1-(4-chlorobenzyl)-3-t-butyl-thio-5-isopropylindol-2-yl]-2,2 - dimethylpropanoic acid), a novel, orally active leukotriene biosynthesis inhibitor.* Can J Physiol Pharmacol, 1989. **67**(5): p. 456-64.
27. Evans, J.F., et al., *5-Lipoxygenase-activating protein is the target of a quinoline class of leukotriene synthesis inhibitors.* Mol Pharmacol, 1991. **40**(1): p. 22-7.
28. Miller, D.K., et al., *Identification and isolation of a membrane protein necessary for leukotriene production.* Nature, 1990. **343**(6255): p. 278-81.
29. Jakobsson, P.J., et al., *Membrane-associated proteins in eicosanoid and glutathione metabolism (MAPEG). A widespread protein superfamily.* Am J Respir Crit Care Med, 2000. **161**(2 Pt 2): p. S20-4.
30. Mandal, A.K., et al., *The nuclear membrane organization of leukotriene synthesis.* Proc Natl Acad Sci U S A, 2008. **105**(51): p. 20434-9.
31. Basavarajappa, D., et al., *Roles of coactosin-like protein (CLP) and 5-lipoxygenase-activating protein (FLAP) in cellular leukotriene biosynthesis.* Proc Natl Acad Sci U S A, 2014.
32. Hafner, A.K., et al., *Characterization of the interaction of human 5-lipoxygenase with its activating protein FLAP.* Biochim Biophys Acta, 2015. **1851**(11): p. 1465-72.
33. Provost, P., O. Radmark, and B. Samuelsson, *Interaction of 5-lipoxygenase with cellular proteins.* Proc Natl Acad Sci U S A, 1999. **96**: p. 1881-1885.
34. Feisst, C., et al., *Hyperforin is a novel type of 5-lipoxygenase inhibitor with high efficacy in vivo.* Cell Mol Life Sci, 2009. **66**(16): p. 2759-71.
35. Rakonjac, M., et al., *Coactosin-like protein supports 5-lipoxygenase enzyme activity and up-regulates leukotriene A4 production.* Proc Natl Acad Sci U S A, 2006. **103**(35): p. 13150-5.
36. Kulkarni, S., et al., *Molecular basis of the specific subcellular localization of the C2-like domain of 5-lipoxygenase.* J Biol Chem, 2002. **277**(15): p. 13167-74.

37. Esser, J., et al., *Coactosin-like protein functions as a stabilizing chaperone for 5-lipoxygenase: role of tryptophan 102.* Biochem J, 2010. **425**(1): p. 265-74.
38. Dincbas-Renqvist, V., et al., *Human Dicer C-terminus functions as a 5-lipoxygenase binding domain.* Biochim Biophys Acta, 2009. **1789**(2): p. 99-108.
39. Provost, P., et al., *Coactosin-like protein, a human F-actin-binding protein: critical role of lysine-75.* Biochem J, 2001. **359**(Pt 2): p. 255-63.
40. Provost, P., et al., *5-Lipoxygenase interacts with coactosin-like protein.* J Biol Chem, 2001. **276**(19): p. 16520-7.
41. Bonventre, J.V. and M. Swidler, *Calcium dependency of prostaglandin E2 production in rat glomerular mesangial cells. Evidence that protein kinase C modulates the Ca2+-dependent activation of phospholipase A2.* J Clin Invest, 1988. **82**(1): p. 168-76.
42. Alonso, F., P.M. Henson, and C.C. Leslie, *A cytosolic phospholipase in human neutrophils that hydrolyzes arachidonoyl-containing phosphatidylcholine.* Biochim Biophys Acta, 1986. **878**(2): p. 273-80.
43. Mancini, J.A., et al., *5-lipoxygenase-activating protein is an arachidonate binding protein.* FEBS Lett, 1993. **318**(3): p. 277-81.
44. Brock, T.G., R.W. McNish, and M. Peters-Golden, *Translocation and leukotriene synthetic capacity of nuclear 5-lipoxygenase in rat basophilic leukemia cells and alveolar macrophages.* J Biol Chem, 1995. **270**(37): p. 21652-8.
45. Lepley, R.A. and F.A. Fitzpatrick, *Inhibition of mitogen-activated protein kinase kinase blocks activation and redistribution of 5-lipoxygenase in HL-60 cells.* Arch Biochem Biophys, 1996. **331**(1): p. 141-4.
46. Werz, O., et al., *5-lipoxygenase is phosphorylated by p38 kinase-dependent MAPKAP kinases.* Proc Natl Acad Sci U S A, 2000. **97**(10): p. 5261-6.
47. Markoutsa, S., et al., *Analysis of 5-lipoxygenase phosphorylation on molecular level by MALDI-MS.* FEBS J, 2014. **281**(8): p. 1931-47.
48. Werz, O., et al., *Arachidonic acid promotes phosphorylation of 5-lipoxygenase at Ser-271 by MAPK-activated protein kinase 2 (MK2).* J Biol Chem, 2002. **277**(17): p. 14793-800.
49. Werz, O., et al., *Phorbol ester up-regulates capacities for nuclear translocation and phosphorylation of 5-lipoxygenase in Mono Mac 6 cells and human polymorphonuclear leukocytes.* Blood, 2001. **97**(8): p. 2487-95.
50. Luo, M., et al., *Protein kinase A inhibits leukotriene synthesis by phosphorylation of 5-lipoxygenase on serine 523.* J Biol Chem, 2004. **279**(40): p. 41512-20.
51. Luo, M., et al., *Phosphorylation by protein kinase a inhibits nuclear import of 5-lipoxygenase.* J Biol Chem, 2005. **280**(49): p. 40609-16.
52. Straif, D., et al., *Glutathione peroxidase-1 but not -4 is involved in the regulation of cellular 5-lipoxygenase activity in monocytic cells.* Biochem J, 2000. **349**(Pt 2): p. 455-61.
53. Burkert, E., et al., *The C2-like beta-barrel domain mediates the Ca2+-dependent resistance of 5-lipoxygenase activity against inhibition by glutathione peroxidase-1.* J Biol Chem, 2003. **278**(44): p. 42846-53.
54. Pacheco, P., et al., *Lipopolysaccharide-induced leukocyte lipid body formation in vivo: innate immunity elicited intracellular Loci involved in eicosanoid metabolism.* J Immunol, 2002. **169**(11): p. 6498-506.

55. Surette, M.E., et al., *Priming of human peripheral blood mononuclear cells with lipopolysaccharides for enhanced arachidonic acid release and leukotriene synthesis.* J Leukoc Biol, 1996. **59**(5): p. 709-15.
56. Plociennikowska, A., et al., *Co-operation of TLR4 and raft proteins in LPS-induced pro-inflammatory signaling.* Cell Mol Life Sci, 2015. **72**(3): p. 557-81.
57. Roubin, R., et al., *Recombinant human tumour necrosis factor (rTNF)2 enhances leukotriene biosynthesis in neutrophils and eosinophils stimulated with the Ca2+ ionophore A23187.* Clin Exp Immunol, 1987. **70**(2): p. 484-90.
58. Woo, C.H., et al., *Tumor necrosis factor- α generates reactive oxygen species via a cytosolic phospholipase A2-linked cascade.* Journal of Biological Chemistry, 2000. **275**(41): p. 32357-32362.
59. Steinhilber, D., O. Radmark, and B. Samuelsson, *A heat stable serum factor upregulates 5-lipoxygenase activity in HL-60 cells, modulation by TNF alpha or GM-CSF.* Biochem Biophys Res Commun, 1993. **193**(3): p. 1083-90.
60. Lin, H.C., et al., *5-Lipoxygenase Inhibitors Attenuate TNF-alpha-Induced Inflammation in Human Synovial Fibroblasts.* PLoS One, 2014. **9**(9): p. e107890.
61. Stanke-Labesque, F., et al., *Leukotriene B4 pathway activation and atherosclerosis in obstructive sleep apnea.* J Lipid Res, 2012. **53**(9): p. 1944-51.
62. Zhang, Z., et al., *[Leukotriene D4 activates BV2 microglia in vitro].* Zhejiang Da Xue Xue Bao Yi Xue Ban, 2013. **42**(3): p. 253-60.
63. Ford-Hutchinson, A.W., et al., *Leukotriene B, a potent chemokinetic and aggregating substance released from polymorphonuclear leukocytes.* Nature, 1980. **286**(5770): p. 264-5.
64. Palmer, R.M., et al., *Chemokinetic activity of arachidonic and lipoxygenase products on leucocyctes of different species.* Prostaglandins, 1980. **20**(2): p. 411-8.
65. Yokomizo, T., et al., *A G-protein-coupled receptor for leukotriene B4 that mediates chemotaxis.* Nature, 1997. **387**(6633): p. 620-4.
66. Peters-Golden, M. and W.R. Henderson, Jr., *Leukotrienes.* N Engl J Med, 2007. **357**(18): p. 1841-54.
67. Okunishi, K., et al., *A Novel Role of Cysteinyl Leukotrienes to Promote Dendritic Cell Activation in the Antigen-Induced Immune Responses in the Lung.* The Journal of Immunology, 2004. **173**(10): p. 6393-6402.
68. Robbiani, D.F., et al., *The Leukotriene C4 Transporter MRP1 Regulates CCL19 (MIP-3beta, ELC)–Dependent Mobilization of Dendritic Cells to Lymph Nodes* Cell Pre, 2000. **103**: p. 757–768.
69. Yokomizo, T., et al., *A second leukotriene B(4) receptor, BLT2. A new therapeutic target in inflammation and immunological disorders.* J Exp Med, 2000. **192**(3): p. 421-32.
70. Yokomizo, T., *Two distinct leukotriene B4 receptors, BLT1 and BLT2.* J Biochem, 2015. **157**(2): p. 65-71.
71. Okuno, T., et al., *12(S)-Hydroxyheptadeca-5Z, 8E, 10E-trienoic acid is a natural ligand for leukotriene B4 receptor 2.* J Exp Med, 2008. **205**(4): p. 759-66.
72. Peres, C.M., et al., *Specific leukotriene receptors couple to distinct G proteins to effect stimulation of alveolar macrophage host defense functions.* J Immunol, 2007. **179**(8): p. 5454-61.

73. Mancuso, P., et al., *5-Lipoxygenase reaction products modulate alveolar macrophage phagocytosis of Klebsiella pneumoniae.* Infect Immun, 1998. **66**(11): p. 5140-6.
74. Lynch, K.R., et al., *Characterization of the human cysteinyl leukotriene CysLT1 receptor.* Nature, 1999. **399**(6738): p. 789-93.
75. Sarau, H.M., et al., *Identification, molecular cloning, expression, and characterization of a cysteinyl leukotriene receptor.* Mol Pharmacol, 1999. **56**(3): p. 657-63.
76. Heise, C.E., et al., *Characterization of the human cysteinyl leukotriene 2 receptor.* J Biol Chem, 2000. **275**(39): p. 30531-6.
77. Kanaoka, Y. and J.A. Boyce, *Cysteinyl leukotrienes and their receptors: cellular distribution and function in immune and inflammatory responses.* J Immunol, 2004. **173**(3): p. 1503-10.
78. Coleman, R.A., et al., *Prostanoid and leukotriene receptors: a progress report from the IUPHAR working parties on classification and nomenclature.* Adv Prostaglandin Thromboxane Leukot Res, 1995. **23**: p. 283-5.
79. Coffey, M. and M. Peters-Golden, *Extending the understanding of leukotrienes in asthma.* Curr Opin Allergy Clin Immunol, 2003. **3**(1): p. 57-63.
80. Funk, C.D., *Leukotriene modifiers as potential therapeutics for cardiovascular disease.* Nat Rev Drug Discov, 2005. **4**(8): p. 664-72.
81. Steele, V.E., et al., *Lipoxygenase inhibitors as potential cancer chemopreventives.* Cancer Epidemiol Biomarkers Prev, 1999. **8**(5): p. 467-83.
82. Strachan, D.P. and D.G. Cook, *Health effects of passive smoking .5. Parental smoking and allergic sensitisation in children.* Thorax, 1998. **53**(2): p. 117-23.
83. Sutherland, E.R., et al., *Comparative effect of body mass index on response to asthma controller therapy.* Allergy Asthma Proc, 2010. **31**(1): p. 20-5.
84. Hsieh, F.H., et al., *T helper cell type 2 cytokines coordinately regulate immunoglobulin E-dependent cysteinyl leukotriene production by human cord blood-derived mast cells: profound induction of leukotriene C(4) synthase expression by interleukin 4.* J Exp Med, 2001. **193**(1): p. 123-33.
85. Thivierge, M., J. Stankova, and M. Rola-Pleszczynski, *IL-13 and IL-4 up-regulate cysteinyl leukotriene 1 receptor expression in human monocytes and macrophages.* J Immunol, 2001. **167**(5): p. 2855-60.
86. Jones, T.R., et al., *Pharmacology of montelukast sodium (Singulair), a potent and selective leukotriene D4 receptor antagonist.* Can J Physiol Pharmacol, 1995. **73**(2): p. 191-201.
87. Bundesamt, S., *https://www.destatis.de/DE/ZahlenFakten/GesellschaftStaat/Gesundheit/Todesursachen/Todesursachen.html*, 2013.
88. Dahlen, S.E., et al., *Leukotrienes promote plasma leakage and leukocyte adhesion in postcapillary venules: in vivo effects with relevance to the acute inflammatory response.* Proc Natl Acad Sci U S A, 1981. **78**(6): p. 3887-91.
89. Silva, A.R., et al., *Lipid bodies in oxidized LDL-induced foam cells are leukotriene-synthesizing organelles: a MCP-1/CCL2 regulated phenomenon.* Biochim Biophys Acta, 2009. **1791**(11): p. 1066-75.
90. Dwyer, J.H., et al., *Arachidonate 5-lipoxygenase promoter genotype, dietary arachidonic acid, and atherosclerosis.* N Engl J Med, 2004. **350**(1): p. 29-37.

91. Helgadottir, A., et al., *Association between the gene encoding 5-lipoxygenase-activating protein and stroke replicated in a Scottish population.* Am J Hum Genet, 2005. **76**(3): p. 505-9.
92. Helgadottir, A., et al., *The gene encoding 5-lipoxygenase activating protein confers risk of myocardial infarction and stroke.* Nat Genet, 2004. **36**(3): p. 233-9.
93. Tardif, J.C., et al., *Treatment with 5-lipoxygenase inhibitor VIA-2291 (Atreleuton) in patients with recent acute coronary syndrome.* Circ Cardiovasc Imaging, 2010. **3**(3): p. 298-307.
94. Reid, J.J., *ABT-761 (Abbott).* Curr Opin Investig Drugs, 2001. **2**(1): p. 68-71.
95. Gaztanaga, J., et al., *A phase 2 randomized, double-blind, placebo-controlled study of the effect of VIA-2291, a 5-lipoxygenase inhibitor, on vascular inflammation in patients after an acute coronary syndrome.* Atherosclerosis, 2015. **240**(1): p. 53-60.
96. Steinhilber, D. and B. Hofmann, *Recent advances in the search for novel 5-lipoxygenase inhibitors.* Basic Clin Pharmacol Toxicol, 2014. **114**(1): p. 70-7.
97. Ghosh, J. and C.E. Myers, *Arachidonic acid stimulates prostate cancer cell growth: critical role of 5-lipoxygenase.* Biochem Biophys Res Commun, 1997. **235**(2): p. 418-23.
98. Takayama, H., et al., *Altered arachidonate metabolism by leukocytes and platelets in myeloproliferative disorders.* Prostaglandins Leukot Med, 1983. **12**(3): p. 261-72.
99. Chen, Y., et al., *Loss of the Alox5 gene impairs leukemia stem cells and prevents chronic myeloid leukemia.* Nat Genet, 2009. **41**(7): p. 783-92.
100. Roos, J., et al., *5-Lipoxygenase is a candidate target for therapeutic management of stem cell-like cells in acute myeloid leukemia.* Cancer Res, 2014. **74**(18): p. 5244-55.
101. Hodgkin, J., et al., *A new kind of informational suppression in the nematode Caenorhabditis elegans.* Genetics, 1989. **123**(2): p. 301-13.
102. Lee, R.C., R.L. Feinbaum, and V. Ambros, *The C. elegans heterochronic gene lin-4 encodes small RNAs with antisense complementarity to lin-14.* Cell, 1993. **75**(5): p. 843-54.
103. Reinhart, B.J., et al., *The 21-nucleotide let-7 RNA regulates developmental timing in Caenorhabditis elegans.* Nature, 2000. **403**(6772): p. 901-6.
104. Pasquinelli, A.E., et al., *Conservation of the sequence and temporal expression of let-7 heterochronic regulatory RNA.* Nature, 2000. **408**(6808): p. 86-9.
105. Ambros, V., et al., *A uniform system for microRNA annotation.* RNA, 2003. **9**(3): p. 277-9.
106. Kozomara, A. and S. Griffiths-Jones, *miRBase: annotating high confidence microRNAs using deep sequencing data.* Nucleic Acids Res, 2014. **42**(Database issue): p. D68-73.
107. Lagos-Quintana, M., et al., *Identification of novel genes coding for small expressed RNAs.* Science, 2001. **294**(5543): p. 853-8.
108. Aravin, A.A., et al., *The small RNA profile during Drosophila melanogaster development.* Dev Cell, 2003. **5**(2): p. 337-50.
109. Lagos-Quintana, M., et al., *New microRNAs from mouse and human.* RNA, 2003. **9**(2): p. 175-9.
110. Lee, Y., et al., *MicroRNA genes are transcribed by RNA polymerase II.* The EMBO Journal, 2004. **23**(20): p. 4051-4060.
111. Lee, Y., et al., *The nuclear RNase III Drosha initiates microRNA processing.* Nature, 2003. **425**(6956): p. 415-9.

112. Yi, R., et al., *Exportin-5 mediates the nuclear export of pre-microRNAs and short hairpin RNAs.* Genes Dev, 2003. **17**(24): p. 3011-6.
113. Bernstein, E., et al., *Role for a bidentate ribonuclease in the initiation step of RNA interference.* Nature, 2001. **409**(6818): p. 363-6.
114. Haase, A.D., et al., *TRBP, a regulator of cellular PKR and HIV-1 virus expression, interacts with Dicer and functions in RNA silencing.* EMBO Rep, 2005. **6**(10): p. 961-7.
115. Chendrimada, T.P., et al., *TRBP recruits the Dicer complex to Ago2 for microRNA processing and gene silencing.* Nature, 2005. **436**(7051): p. 740-4.
116. Kawamata, T., H. Seitz, and Y. Tomari, *Structural determinants of miRNAs for RISC loading and slicer-independent unwinding.* Nat Struct Mol Biol, 2009. **16**(9): p. 953-60.
117. Meister, G., et al., *Human Argonaute2 mediates RNA cleavage targeted by miRNAs and siRNAs.* Mol Cell, 2004. **15**(2): p. 185-97.
118. Wang, B., et al., *Recapitulation of short RNA-directed translational gene silencing in vitro.* Mol Cell, 2006. **22**(4): p. 553-60.
119. Lim, J., et al., *Uridylation by TUT4 and TUT7 marks mRNA for degradation.* Cell, 2014. **159**(6): p. 1365-76.
120. Fukao, A., et al., *MicroRNAs trigger dissociation of eIF4AI and eIF4AII from target mRNAs in humans.* Mol Cell, 2014. **56**(1): p. 79-89.
121. Bethune, J., C.G. Artus-Revel, and W. Filipowicz, *Kinetic analysis reveals successive steps leading to miRNA-mediated silencing in mammalian cells.* EMBO Rep, 2012. **13**(8): p. 716-23.
122. Djuranovic, S., A. Nahvi, and R. Green, *miRNA-mediated gene silencing by translational repression followed by mRNA deadenylation and decay.* Science, 2012. **336**(6078): p. 237-40.
123. Kwak, P.B. and Y. Tomari, *The N domain of Argonaute drives duplex unwinding during RISC assembly.* Nat Struct Mol Biol, 2012. **19**(2): p. 145-51.
124. Schirle, N.T. and I.J. MacRae, *The crystal structure of human Argonaute2.* Science, 2012. **336**(6084): p. 1037-40.
125. Elkayam, E., et al., *The structure of human argonaute-2 in complex with miR-20a.* Cell, 2012. **150**(1): p. 100-10.
126. Zipprich, J.T., et al., *Importance of the C-terminal domain of the human GW182 protein TNRC6C for translational repression.* RNA, 2009. **15**(5): p. 781-93.
127. Chen, C.Y., et al., *Ago-TNRC6 triggers microRNA-mediated decay by promoting two deadenylation steps.* Nat Struct Mol Biol, 2009. **16**(11): p. 1160-6.
128. Piao, X., et al., *CCR4-NOT deadenylates mRNA associated with RNA-induced silencing complexes in human cells.* Mol Cell Biol, 2010. **30**(6): p. 1486-94.
129. Li, S., et al., *TRIM65 regulates microRNA activity by ubiquitination of TNRC6.* Proc Natl Acad Sci U S A, 2014. **111**(19): p. 6970-5.
130. Rybak, A., et al., *The let-7 target gene mouse lin-41 is a stem cell specific E3 ubiquitin ligase for the miRNA pathway protein Ago2.* Nat Cell Biol, 2009. **11**(12): p. 1411-20.
131. Qi, H.H., et al., *Prolyl 4-hydroxylation regulates Argonaute 2 stability.* Nature, 2008. **455**(7211): p. 421-4.
132. Zeng, Y., et al., *Phosphorylation of Argonaute 2 at serine-387 facilitates its localization to processing bodies.* Biochem J, 2008. **413**(3): p. 429-36.

133. Rudel, S., et al., *Phosphorylation of human Argonaute proteins affects small RNA binding.* Nucleic Acids Res, 2011. **39**(6): p. 2330-43.
134. Gregory, R.I., et al., *The Microprocessor complex mediates the genesis of microRNAs.* Nature, 2004. **432**(7014): p. 235-40.
135. Denli, A.M., et al., *Processing of primary microRNAs by the Microprocessor complex.* Nature, 2004. **432**(7014): p. 231-5.
136. Blaszczyk, J., et al., *Crystallographic and modeling studies of RNase III suggest a mechanism for double-stranded RNA cleavage.* Structure, 2001. **9**(12): p. 1225-36.
137. Han, J., et al., *The Drosha-DGCR8 complex in primary microRNA processing.* Genes Dev, 2004. **18**(24): p. 3016-27.
138. Han, J., et al., *Posttranscriptional crossregulation between Drosha and DGCR8.* Cell, 2009. **136**(1): p. 75-84.
139. Yeom, K.H., et al., *Characterization of DGCR8/Pasha, the essential cofactor for Drosha in primary miRNA processing.* Nucleic Acids Res, 2006. **34**(16): p. 4622-9.
140. Auyeung, V.C., et al., *Beyond secondary structure: primary-sequence determinants license pri-miRNA hairpins for processing.* Cell, 2013. **152**(4): p. 844-58.
141. Zahler, A.M., et al., *Human SR proteins and isolation of a cDNA encoding SRp75.* Mol Cell Biol, 1993. **13**(7): p. 4023-8.
142. Huang, Y. and J.A. Steitz, *Splicing factors SRp20 and 9G8 promote the nucleocytoplasmic export of mRNA.* Mol Cell, 2001. **7**(4): p. 899-905.
143. Swartz, J.E., et al., *The shuttling SR protein 9G8 plays a role in translation of unspliced mRNA containing a constitutive transport element.* J Biol Chem, 2007. **282**(27): p. 19844-53.
144. Lou, H., et al., *Regulation of alternative polyadenylation by U1 snRNPs and SRp20.* Mol Cell Biol, 1998. **18**(9): p. 4977-85.
145. Mori, M., et al., *Hippo signaling regulates microprocessor and links cell-density-dependent miRNA biogenesis to cancer.* Cell, 2014. **156**(5): p. 893-906.
146. Tang, X., et al., *Glycogen synthase kinase 3 beta (GSK3beta) phosphorylates the RNAase III enzyme Drosha at S300 and S302.* PLoS One, 2011. **6**(6): p. e20391.
147. Herbert, K.M., et al., *Phosphorylation of DGCR8 Increases Its Intracellular Stability and Induces a Progrowth miRNA Profile.* Cell Reports, 2013. **5**(4): p. 1070-1081.
148. Tang, X.L., et al., *Acetylation of Drosha on the N-Terminus Inhibits Its Degradation by Ubiquitination.* Plos One, 2013. **8**(8).
149. Wada, T., J. Kikuchi, and Y. Furukawa, *Histone deacetylase 1 enhances microRNA processing via deacetylation of DGCR8.* Embo Reports, 2012. **13**(2): p. 142-149.
150. Fuller-Pace, F.V., *The DEAD box proteins DDX5 (p68) and DDX17 (p72): multi-tasking transcriptional regulators.* Biochim Biophys Acta, 2013. **1829**(8): p. 756-63.
151. Davis, B.N., et al., *SMAD proteins control DROSHA-mediated microRNA maturation.* Nature, 2008. **454**(7200): p. 56-61.
152. Davis, B.N., et al., *Smad proteins bind a conserved RNA sequence to promote microRNA maturation by Drosha.* Mol Cell, 2010. **39**(3): p. 373-84.
153. Suzuki, H.I., et al., *Modulation of microRNA processing by p53.* Nature, 2009. **460**(7254): p. 529-33.

154. Dews, M., et al., *Augmentation of tumor angiogenesis by a Myc-activated microRNA cluster.* Nat Genet, 2006. **38**(9): p. 1060-5.
155. Onnis, A., et al., *Alteration of microRNAs regulated by c-Myc in Burkitt lymphoma.* PLoS One, 2010. **5**(9).
156. O'Donnell, K.A., et al., *c-Myc-regulated microRNAs modulate E2F1 expression.* Nature, 2005. **435**(7043): p. 839-43.
157. Wang, X., et al., *c-Myc modulates microRNA processing via the transcriptional regulation of Drosha.* Sci Rep, 2013. **3**: p. 1942.
158. Kuchenreuther, M.J. and J.D. Weber, *The ARF tumor-suppressor controls Drosha translation to prevent Ras-driven transformation.* Oncogene, 2014. **33**(3): p. 300-7.
159. Zhang, H., et al., *Single processing center models for human Dicer and bacterial RNase III.* Cell, 2004. **118**(1): p. 57-68.
160. Tsutsumi, A., et al., *Recognition of the pre-miRNA structure by Drosophila Dicer-1.* Nat Struct Mol Biol, 2011. **18**(10): p. 1153-8.
161. Park, J.E., et al., *Dicer recognizes the 5' end of RNA for efficient and accurate processing.* Nature, 2011. **475**(7355): p. 201-5.
162. Tian, Y., et al., *A phosphate-binding pocket within the platform-PAZ-connector helix cassette of human Dicer.* Mol Cell, 2014. **53**(4): p. 606-16.
163. Gregory, R.I., et al., *Human RISC couples microRNA biogenesis and posttranscriptional gene silencing.* Cell, 2005. **123**(4): p. 631-40.
164. Lau, P.W., et al., *Structure of the human Dicer-TRBP complex by electron microscopy.* Structure, 2009. **17**(10): p. 1326-32.
165. Lee, H.Y., et al., *Differential roles of human Dicer-binding proteins TRBP and PACT in small RNA processing.* Nucleic Acids Res, 2013. **41**(13): p. 6568-76.
166. Guo, L. and F. Chen, *A challenge for miRNA: multiple isomiRs in miRNAomics.* Gene, 2014. **544**(1): p. 1-7.
167. Tomaselli, S., F. Locatelli, and A. Gallo, *The RNA editing enzymes ADARs: mechanism of action and human disease.* Cell Tissue Res, 2014. **356**(3): p. 527-32.
168. Ma, E., et al., *Autoinhibition of human dicer by its internal helicase domain.* J Mol Biol, 2008. **380**(1): p. 237-43.
169. Ota, H., et al., *ADAR1 forms a complex with Dicer to promote microRNA processing and RNA-induced gene silencing.* Cell, 2013. **153**(3): p. 575-89.
170. Tokumaru, S., et al., *let-7 regulates Dicer expression and constitutes a negative feedback loop.* Carcinogenesis, 2008. **29**(11): p. 2073-7.
171. Helwak, A., et al., *Mapping the human miRNA interactome by CLASH reveals frequent noncanonical binding.* Cell, 2013. **153**(3): p. 654-65.
172. Cochrane, D.R., et al., *MicroRNAs link estrogen receptor alpha status and Dicer levels in breast cancer.* Horm Cancer, 2010. **1**(6): p. 306-19.
173. Fredman, G., et al., *Self-limited versus delayed resolution of acute inflammation: temporal regulation of pro-resolving mediators and microRNA.* Sci Rep, 2012. **2**: p. 639.
174. Serezani, C.H., et al., *Leukotriene B4 amplifies NF-kappaB activation in mouse macrophages by reducing SOCS1 inhibition of MyD88 expression.* J Clin Invest, 2011. **121**(2): p. 671-82.

175. Wang, Z., et al., *Leukotriene B4 enhances the generation of proinflammatory microRNAs to promote MyD88-dependent macrophage activation.* J Immunol, 2014. **192**(5): p. 2349-56.
176. Gonsalves, C.S. and V.K. Kalra, *Hypoxia-mediated expression of 5-lipoxygenase-activating protein involves HIF-1alpha and NF-kappaB and microRNAs 135a and 199a-5p.* J Immunol, 2010. **184**(7): p. 3878-88.
177. Sun, Y.M., K.Y. Lin, and Y.Q. Chen, *Diverse functions of miR-125 family in different cell contexts.* J Hematol Oncol, 2013. **6**: p. 6.
178. Zhang, H., et al., *Upregulation of microRNA-125b contributes to leukemogenesis and increases drug resistance in pediatric acute promyelocytic leukemia.* Mol Cancer, 2011. **10**: p. 108.
179. Klusmann, J.H., et al., *miR-125b-2 is a potential oncomiR on human chromosome 21 in megakaryoblastic leukemia.* Genes Dev, 2010. **24**(5): p. 478-90.
180. Fernando, T.R., N.I. Rodriguez-Malave, and D.S. Rao, *MicroRNAs in B cell development and malignancy.* J Hematol Oncol, 2012. **5**: p. 7.
181. Zeng, Q.H., et al., *[miR-125b promotes proliferation of human acute myeloid leukemia cells by targeting Bak1].* Zhonghua Xue Ye Xue Za Zhi, 2013. **34**(12): p. 1010-4.
182. Daschkey, S., et al., *MicroRNAs distinguish cytogenetic subgroups in pediatric AML and contribute to complex regulatory networks in AML-relevant pathways.* PLoS One, 2013. **8**(2): p. e56334.
183. Chung, S.S., W. Hu, and C.Y. Park, *The Role of MicroRNAs in Hematopoietic Stem Cell and Leukemic Stem Cell Function.* Ther Adv Hematol, 2011. **2**(5): p. 317-34.
184. Bousquet, M., et al., *Myeloid cell differentiation arrest by miR-125b-1 in myelodysplastic syndrome and acute myeloid leukemia with the t(2;11)(p21;q23) translocation.* J Exp Med, 2008. **205**(11): p. 2499-506.
185. Perez-Novo, C.A., et al., *Prostaglandin, leukotriene, and lipoxin balance in chronic rhinosinusitis with and without nasal polyposis.* J Allergy Clin Immunol, 2005. **115**(6): p. 1189-96.
186. Al-Shemari, H., et al., *Influence of leukotriene gene polymorphisms on chronic rhinosinusitis.* BMC Med Genet, 2008. **9**: p. 21.
187. Zhang, X.H., et al., *Overexpression of miR-125b, a novel regulator of innate immunity, in eosinophilic chronic rhinosinusitis with nasal polyps.* Am J Respir Crit Care Med, 2012. **185**(2): p. 140-51.
188. Reijerkerk, A., et al., *MicroRNAs regulate human brain endothelial cell-barrier function in inflammation: implications for multiple sclerosis.* J Neurosci, 2013. **33**(16): p. 6857-63.
189. Raaby, L., et al., *Changes in mRNA expression precede changes in miRNA expression in lesional psoriatic skin during treatment with adalimumab.* Br J Dermatol, 2015.
190. Zhao, X., et al., *MicroRNA-125a contributes to elevated inflammatory chemokine RANTES levels via targeting KLF13 in systemic lupus erythematosus.* Arthritis Rheum, 2010. **62**(11): p. 3425-35.
191. Alam, R., et al., *RANTES is a chemotactic and activating factor for human eosinophils.* J Immunol, 1993. **150**(8 Pt 1): p. 3442-8.
192. Ooi, A.G., et al., *MicroRNA-125b expands hematopoietic stem cells and enriches for the lymphoid-balanced and lymphoid-biased subsets.* Proc Natl Acad Sci U S A, 2010. **107**(50): p. 21505-10.

193. O'Connell, R.M., et al., *MicroRNAs enriched in hematopoietic stem cells differentially regulate long-term hematopoietic output.* Proc Natl Acad Sci U S A, 2010. **107**(32): p. 14235-40.
194. Gerrits, A., et al., *Genetic screen identifies microRNAcluster 99b/let-7e/125a as a regulator of primitive hematopoietic cells.* Blood, 2012. **119**(2): p. 377-387.
195. Rossi, R.L., et al., *Distinct microRNA signatures in human lymphocyte subsets and enforcement of the naive state in CD4+ T cells by the microRNA miR-125b.* Nat Immunol, 2011. **12**(8): p. 796-803.
196. Zhang, Y., et al., *MicroRNA 125a and its regulation of the p53 tumor suppressor gene.* FEBS Letters, 2009. **583**(22): p. 3725-3730.
197. Le, M.T., et al., *MicroRNA-125b is a novel negative regulator of p53.* Genes Dev, 2009. **23**(7): p. 862-76.
198. Lane, D.P., *Cancer. p53, guardian of the genome.* Nature, 1992. **358**(6381): p. 15-6.
199. Torosyan, Y., et al., *Distinct effects of annexin A7 and p53 on arachidonate lipoxygenation in prostate cancer cells involve 5-lipoxygenase transcription.* Cancer Res, 2006. **66**(19): p. 9609-16.
200. Gilbert, B., et al., *5-Lipoxygenase is a direct p53 target gene in humans.* Biochim Biophys Acta, 2015. **1849**(8): p. 1003-1016.
201. Catalano, A., et al., *5-lipoxygenase antagonizes genotoxic stress-induced apoptosis by altering p53 nuclear trafficking.* FASEB J, 2004. **18**(14): p. 1740-2.
202. Catalano, A., et al., *5-Lipoxygenase regulates senescence-like growth arrest by promoting ROS-dependent p53 activation.* EMBO J, 2005. **24**(1): p. 170-9.
203. Lee, A.J., K.J. Cho, and J.H. Kim, *MyD88-BLT2-dependent cascade contributes to LPS-induced interleukin-6 production in mouse macrophage.* Exp Mol Med, 2015. **47**: p. e156.
204. Rajaram, M.V., et al., *Mycobacterium tuberculosis lipomannan blocks TNF biosynthesis by regulating macrophage MAPK-activated protein kinase 2 (MK2) and microRNA miR-125b.* Proc Natl Acad Sci U S A, 2011. **108**(42): p. 17408-13.
205. Banerjee, S., et al., *miR-125a-5p regulates differential activation of macrophages and inflammation.* J Biol Chem, 2013. **288**(49): p. 35428-36.
206. Tsuchiya, S., et al., *Establishment and characterization of a human acute monocytic leukemia cell line (THP-1).* Int J Cancer, 1980. **26**(2): p. 171-6.
207. Graff, J.W., et al., *Identifying functional microRNAs in macrophages with polarized phenotypes.* J Biol Chem, 2012. **287**(26): p. 21816-25.
208. Kim, S.W., et al., *MicroRNAs miR-125a and miR-125b constitutively activate the NF-kappaB pathway by targeting the tumor necrosis factor alpha-induced protein 3 (TNFAIP3, A20).* Proc Natl Acad Sci U S A, 2012. **109**(20): p. 7865-70.
209. Song, H.Y., M. Rothe, and D.V. Goeddel, *The tumor necrosis factor-inducible zinc finger protein A20 interacts with TRAF1/TRAF2 and inhibits NF-kappaB activation.* Proc Natl Acad Sci U S A, 1996. **93**(13): p. 6721-5.
210. Tili, E., et al., *Modulation of miR-155 and miR-125b levels following lipopolysaccharide/TNF-alpha stimulation and their possible roles in regulating the response to endotoxin shock.* J Immunol, 2007. **179**(8): p. 5082-9.
211. Huang, H.C., et al., *miRNA-125b regulates TNF-alpha production in CD14+ neonatal monocytes via post-transcriptional regulation.* J Leukoc Biol, 2012. **92**(1): p. 171-82.

212. Monk, C.E., G. Hutvagner, and J.S. Arthur, *Regulation of miRNA transcription in macrophages in response to Candida albicans.* PLoS One, 2010. **5**(10): p. e13669.
213. Hamilton, T.A., et al., *Myeloid colony-stimulating factors as regulators of macrophage polarization.* Front Immunol, 2014. **5**: p. 554.
214. Shaham, L., et al., *MiR-125 in normal and malignant hematopoiesis.* Leukemia, 2012. **26**(9): p. 2011-8.
215. Lionetti, M., et al., *Identification of microRNA expression patterns and definition of a microRNA/mRNA regulatory network in distinct molecular groups of multiple myeloma.* Blood, 2009. **114**(25): p. e20-6.
216. de la Rica, L., et al., *NF-kappaB-direct activation of microRNAs with repressive effects on monocyte-specific genes is critical for osteoclast differentiation.* Genome Biol, 2015. **16**(1): p. 2.
217. Boyce, B.F., et al., *NF-kappaB-Mediated Regulation of Osteoclastogenesis.* Endocrinol Metab (Seoul), 2015. **30**(1): p. 35-44.
218. Endale Ahanda, M.L., et al., *The hsa-miR-125a/hsa-let-7e/hsa-miR-99b cluster is potentially implicated in Cystic Fibrosis pathogenesis.* J Cyst Fibros, 2015.
219. Riordan, J.R., et al., *Identification of the cystic fibrosis gene: cloning and characterization of complementary DNA.* Science, 1989. **245**(4922): p. 1066-73.
220. Rozmahel, R., et al., *Modulation of disease severity in cystic fibrosis transmembrane conductance regulator deficient mice by a secondary genetic factor.* Nat Genet, 1996. **12**(3): p. 280-7.
221. Zielenski, J., et al., *Detection of a cystic fibrosis modifier locus for meconium ileus on human chromosome 19q13.* Nat Genet, 1999. **22**(2): p. 128-9.
222. Wei, F., et al., *miR-99b-targeted mTOR induction contributes to irradiation resistance in pancreatic cancer.* Mol Cancer, 2013. **12**: p. 81.
223. Singh, Y., et al., *Mycobacterium tuberculosis controls microRNA-99b (miR-99b) expression in infected murine dendritic cells to modulate host immunity.* J Biol Chem, 2013. **288**(7): p. 5056-61.
224. Johansson, J., et al., *TGF-beta1-Induced Epithelial-Mesenchymal Transition Promotes Monocyte/Macrophage Properties in Breast Cancer Cells.* Front Oncol, 2015. **5**: p. 3.
225. Turcatel, G., et al., *MIR-99a and MIR-99b modulate TGF-beta induced epithelial to mesenchymal plasticity in normal murine mammary gland cells.* PLoS One, 2012. **7**(1): p. e31032.
226. Yu, F., et al., *let-7 regulates self renewal and tumorigenicity of breast cancer cells.* Cell, 2007. **131**(6): p. 1109-23.
227. Yu, J., et al., *Induced pluripotent stem cell lines derived from human somatic cells.* Science, 2007. **318**(5858): p. 1917-20.
228. Hatfield, S. and H. Ruohola-Baker, *microRNA and stem cell function.* Cell Tissue Res, 2008. **331**(1): p. 57-66.
229. Wu, M., et al., *Genetic variations of microRNAs in human cancer and their effects on the expression of miRNAs.* Carcinogenesis, 2008. **29**(9): p. 1710-6.
230. Sorrentino, A., et al., *Role of microRNAs in drug-resistant ovarian cancer cells.* Gynecol Oncol, 2008. **111**(3): p. 478-86.

231. Ragusa, M., et al., *Specific alterations of microRNA transcriptome and global network structure in colorectal carcinoma after cetuximab treatment.* Mol Cancer Ther, 2010. **9**(12): p. 3396-409.
232. Nymark, P., et al., *Integrative analysis of microRNA, mRNA and aCGH data reveals asbestos- and histology-related changes in lung cancer.* Genes Chromosomes Cancer, 2011. **50**(8): p. 585-97.
233. Buechner, J., et al., *Tumour-suppressor microRNAs let-7 and mir-101 target the proto-oncogene MYCN and inhibit cell proliferation in MYCN-amplified neuroblastoma.* Br J Cancer, 2011. **105**(2): p. 296-303.
234. Mitra, D., et al., *Jumonji/ARID1 B (JARID1B) protein promotes breast tumor cell cycle progression through epigenetic repression of microRNA let-7e.* J Biol Chem, 2011. **286**(47): p. 40531-5.
235. Guan, H., et al., *MicroRNA let-7e is associated with the pathogenesis of experimental autoimmune encephalomyelitis.* Eur J Immunol, 2013. **43**(1): p. 104-14.
236. Suojalehto, H., et al., *MicroRNA profiles in nasal mucosa of patients with allergic and nonallergic rhinitis and asthma.* Int Forum Allergy Rhinol, 2013. **3**(8): p. 612-20.
237. Suojalehto, H., et al., *Altered microRNA expression of nasal mucosa in long-term asthma and allergic rhinitis.* Int Arch Allergy Immunol, 2014. **163**(3): p. 168-78.
238. Bernstein, E., et al., *Dicer is essential for mouse development.* Nat Genet, 2003. **35**(3): p. 215-7.
239. De Tullio, G., et al., *Challenges and opportunities of microRNAs in lymphomas.* Molecules, 2014. **19**(9): p. 14723-81.
240. Saki, N., et al., *Involvement of MicroRNA in T-Cell Differentiation and Malignancy.* Int J Hematol Oncol Stem Cell Res, 2015. **9**(1): p. 33-49.
241. Lu, Y., et al., *Transgenic over-expression of the microRNA miR-17-92 cluster promotes proliferation and inhibits differentiation of lung epithelial progenitor cells.* Dev Biol, 2007. **310**(2): p. 442-53.
242. Etheridge, A., et al., *Extracellular microRNA: a new source of biomarkers.* Mutation research, 2011. **717**(1-2): p. 85-90.
243. Zheng, J., et al., *Serum microRNA-125a-5p, a useful biomarker in liver diseases, correlates with disease progression.* Mol Med Rep, 2015. **12**(1): p. 1584-90.
244. Min, W., et al., *The expression and significance of five types of miRNAs in breast cancer.* Med Sci Monit Basic Res, 2014. **20**: p. 97-104.
245. Hsieh, T.H., et al., *miR-125a-5p is a prognostic biomarker that targets HDAC4 to suppress breast tumorigenesis.* Oncotarget, 2015. **6**(1): p. 494-509.
246. Gattolliat, C.H., et al., *MicroRNA and targeted mRNA expression profiling analysis in human colorectal adenomas and adenocarcinomas.* Eur J Cancer, 2015. **51**(3): p. 409-20.
247. Shang, H., et al., *A germline mutation in the miR125a coding region reduces miR125a expression and is associated with human gastric cancer.* Mol Med Rep, 2014. **10**(4): p. 1839-44.
248. Zhu, W.Y., et al., *Differential expression of miR-125a-5p and let-7e predicts the progression and prognosis of non-small cell lung cancer.* Cancer Invest, 2014. **32**(8): p. 394-401.
249. Ha, M. and V.N. Kim, *Regulation of microRNA biogenesis.* Nat Rev Mol Cell Biol, 2014. **15**(8): p. 509-24.

250. Shimizu, T., O. Radmark, and B. Samuelsson, *Enzyme with dual lipoxygenase activities catalyzes leukotriene A4 synthesis from arachidonic acid.* Proc Natl Acad Sci U S A, 1984. **81**(3): p. 689-93.
251. Lu, L.F. and A. Liston, *MicroRNA in the immune system, microRNA as an immune system.* Immunology, 2009. **127**(3): p. 291-8.
252. Lin, Y.C., et al., *Genome dynamics of the human embryonic kidney 293 lineage in response to cell biology manipulations.* Nat Commun, 2014. **5**: p. 4767.
253. Werz, O., D. Szellas, and D. Steinhilber, *Reactive oxygen species released from granulocytes stimulate 5-lipoxygenase activity in a B-lymphocytic cell line.* Eur J Biochem, 2000. **267**(5): p. 1263-9.
254. Werz, O., M. Brungs, and D. Steinhilber, *Purification of transforming growth factor beta 1 from human platelets.* Pharmazie, 1996. **51**(11): p. 893-6.
255. Varkonyi-Gasic, E., et al., *Protocol: a highly sensitive RT-PCR method for detection and quantification of microRNAs.* Plant Methods, 2007. **3**: p. 12.
256. Livak, K.J. and T.D. Schmittgen, *Analysis of relative gene expression data using real-time quantitative PCR and the 2(-Delta Delta C(T)) Method.* Methods, 2001. **25**(4): p. 402-8.
257. Pall, G.S. and A.J. Hamilton, *Improved northern blot method for enhanced detection of small RNA.* Nat Protoc, 2008. **3**(6): p. 1077-84.
258. Pall, G.S., et al., *Carbodiimide-mediated cross-linking of RNA to nylon membranes improves the detection of siRNA, miRNA and piRNA by northern blot.* Nucleic Acids Res, 2007. **35**(8): p. e60.
259. Bradford, M.M., *A rapid and sensitive method for the quantitation of microgram quantities of protein utilizing the principle of protein-dye binding.* Anal Biochem, 1976. **72**: p. 248-54.
260. Steinhilber, D., T. Herrmann, and H.J. Roth, *Separation of lipoxins and leukotrienes from human granulocytes by high-performance liquid chromatography with a Radial-Pak cartridge after extraction with an octadecyl reversed-phase column.* J Chromatogr, 1989. **493**(2): p. 361-6.
261. Zhang, Y.Y., O. Rådmark, and B. Samuelsson, *Mutagenesis of some conserved residues in human 5-lipoxygenase: Effects on enzyme activity.* Proc Natl Acad Sci U S A, 1992. **89**: p. 485-489.
262. Graham, F.L.e.a., *A New Technique for the Assay of Infectivity of Human Adenovirus 5 DNA.* Journal of Virology, 1973. **52**(2): p. 456-467.
263. Krutzfeldt, J., et al., *Silencing of microRNAs in vivo with 'antagomirs'.* Nature, 2005. **438**(7068): p. 685-9.
264. Bailey, T.L., et al., *MEME Suite: tools for motif discovery and searching.* Nucleic Acids Research, 2009. **37**(suppl 2): p. W202-W208.
265. Ando, Y., et al., *Nuclear pore complex protein mediated nuclear localization of dicer protein in human cells.* PLoS One, 2011. **6**(8): p. e23385.
266. Tahbaz, N., et al., *Characterization of the interactions between mammalian PAZ PIWI domain proteins and Dicer.* EMBO Rep, 2004. **5**(2): p. 189-94.
267. Iosue, I., et al., *Argonaute 2 sustains the gene expression program driving human monocytic differentiation of acute myeloid leukemia cells.* Cell Death Dis, 2013. **4**: p. e926.
268. Gagnon, K.T., et al., *RNAi factors are present and active in human cell nuclei.* Cell Rep, 2014. **6**(1): p. 211-21.

269. Servin-Gonzalez, L.S., A.J. Granados-Lopez, and J.A. Lopez, *Families of microRNAs Expressed in Clusters Regulate Cell Signaling in Cervical Cancer.* Int J Mol Sci, 2015. **16**(6): p. 12773-90.
270. Hsu, S.D., et al., *miRTarBase update 2014: an information resource for experimentally validated miRNA-target interactions.* Nucleic Acids Res, 2014. **42**(Database issue): p. D78-85.
271. Heyninck, K., et al., *The zinc finger protein A20 inhibits TNF-induced NF-kappaB-dependent gene expression by interfering with an RIP- or TRAF2-mediated transactivation signal and directly binds to a novel NF-kappaB-inhibiting protein ABIN.* J Cell Biol, 1999. **145**(7): p. 1471-82.
272. Huang, C.J., et al., *LPS-stimulated tumor necrosis factor-alpha and interleukin-6 mRNA and cytokine responses following acute psychological stress.* Psychoneuroendocrinology, 2011. **36**(10): p. 1553-61.
273. Libermann, T.A. and D. Baltimore, *Activation of interleukin-6 gene expression through the NF-kappa B transcription factor.* Mol Cell Biol, 1990. **10**(5): p. 2327-34.
274. Takahashi, N., T. Nakaoka, and N. Yamashita, *Profiling of immune-related microRNA expression in human cord blood and adult peripheral blood cells upon proinflammatory stimulation.* Eur J Haematol, 2012. **88**(1): p. 31-8.
275. Min, M., et al., *Aquaporin 8 expression is reduced and regulated by microRNAs in patients with ulcerative colitis.* Chin Med J (Engl), 2013. **126**(8): p. 1532-7.
276. Zhang, D., et al., *Hypoxia-induced miR-424 decreases tumor sensitivity to chemotherapy by inhibiting apoptosis.* Cell Death Dis, 2014. **5**: p. e1301.
277. Korhan, P., E. Erdal, and N. Atabey, *MiR-181a-5p is downregulated in hepatocellular carcinoma and suppresses motility, invasion and branching-morphogenesis by directly targeting c-Met.* Biochem Biophys Res Commun, 2014. **450**(4): p. 1304-12.
278. Jensen, K., et al., *Transcriptional profiling of mRNAs and microRNAs in human bone marrow precursor B cells identifies subset- and age-specific variations.* PLoS One, 2013. **8**(7): p. e70721.
279. Zhou, W., et al., *MicroRNA-20b promotes cell growth of breast cancer cells partly via targeting phosphatase and tensin homologue (PTEN).* Cell Biosci, 2014. **4**(1): p. 62.
280. Ingwersen, J., et al., *Natalizumab restores aberrant miRNA expression profile in multiple sclerosis and reveals a critical role for miR-20b.* Ann Clin Transl Neurol, 2015. **2**(1): p. 43-55.
281. Qin, J.Y., et al., *Systematic Comparison of Constitutive Promoters and the Doxycycline-Inducible Promoter.* PLoS ONE, 2010. **5**(5): p. e10611.
282. Zhou, F., et al., *NF-kappaB target microRNAs and their target genes in TNFalpha-stimulated HeLa cells.* Biochim Biophys Acta, 2014. **1839**(4): p. 344-54.
283. Tan, G., et al., *NF-kappaB-dependent microRNA-125b up-regulation promotes cell survival by targeting p38alpha upon ultraviolet radiation.* J Biol Chem, 2012. **287**(39): p. 33036-47.
284. Andreakos, E., et al., *Distinct pathways of LPS-induced NF-kappa B activation and cytokine production in human myeloid and nonmyeloid cells defined by selective utilization of MyD88 and Mal/TIRAP.* Blood, 2004. **103**(6): p. 2229-37.

285. Androulidaki, A., et al., *The kinase Akt1 controls macrophage response to lipopolysaccharide by regulating microRNAs.* Immunity, 2009. **31**(2): p. 220-31.
286. Lindner, S.C., et al., *TLR2 ligands augment cPLA2alpha activity and lead to enhanced leukotriene release in human monocytes.* J Leukoc Biol, 2009. **86**(2): p. 389-99.
287. Cheloufi, S., et al., *A dicer-independent miRNA biogenesis pathway that requires Ago catalysis.* Nature, 2010. **465**(7298): p. 584-9.
288. Noland, C.L. and J.A. Doudna, *Multiple sensors ensure guide strand selection in human RNAi pathways.* RNA, 2013. **19**(5): p. 639-48.
289. Wolf, J., S. Rose-John, and C. Garbers, *Interleukin-6 and its receptors: A highly regulated and dynamic system.* Cytokine, 2014. **70**(1): p. 11-20.
290. Aderka, D., J.M. Le, and J. Vilcek, *IL-6 inhibits lipopolysaccharide-induced tumor necrosis factor production in cultured human monocytes, U937 cells, and in mice.* J Immunol, 1989. **143**(11): p. 3517-23.
291. Jeker, L.T. and R. Marone, *Targeting microRNAs for immunomodulation.* Curr Opin Pharmacol, 2015. **23**: p. 25-31.
292. Kim, J.K., et al., *Fascin Regulates TLR4/PKC-mediated Translational Activation Through miR-155 and miR-125b, which Targets the 3' Untranslated Region of TNF-alpha mRNA.* Immunol Invest, 2015. **44**(3): p. 309-20.
293. Cheng, S.F., L. Li, and L.M. Wang, *miR-155 and miR-146b negatively regulates IL6 in Helicobacter pylori (cagA+) infected gastroduodenal ulcer.* Eur Rev Med Pharmacol Sci, 2015. **19**(4): p. 607-13.
294. Chen, T., et al., *MicroRNA-125a-5p partly regulates the inflammatory response, lipid uptake, and ORP9 expression in oxLDL-stimulated monocyte/macrophages.* Cardiovasc Res, 2009. **83**(1): p. 131-9.
295. Zhang, Y., et al., *MicroRNA 125a and its regulation of the p53 tumor suppressor gene.* FEBS Letters, 2009. **583**(22): p. 3725-3730.
296. Jiang, L., et al., *MicroRNA HSA-miR-125a-5p induces apoptosis by activating p53 in lung cancer cells.* Exp Lung Res, 2011. **37**(7): p. 387-98.
297. Kim, J.K., et al., *Sirtuin7 oncogenic potential in human hepatocellular carcinoma and its regulation by the tumor suppressors MiR-125a-5p and MiR-125b.* Hepatology, 2013. **57**(3): p. 1055-67.
298. Leotta, M., et al., *A p53-dependent tumor suppressor network is induced by selective miR-125a-5p inhibition in multiple myeloma cells.* J Cell Physiol, 2014. **229**(12): p. 2106-16.
299. Jiang, L., et al., *MicroRNA hsa-miR-125a-3p activates p53 and induces apoptosis in lung cancer cells.* Cancer Invest, 2013. **31**(8): p. 538-44.
300. Abdelmohsen, K., et al., *7SL RNA represses p53 translation by competing with HuR.* Nucleic Acids Res, 2014. **42**(15): p. 10099-111.
301. Di Mari, J.F., et al., *HETEs enhance IL-1-mediated COX-2 expression via augmentation of message stability in human colonic myofibroblasts.* Am J Physiol Gastrointest Liver Physiol, 2007. **293**(4): p. G719-28.
302. Satomi, N., K. Haranaka, and O. Kunii, *Research on the production site of tumor necrosis factor (TNF).* Jpn J Exp Med, 1981. **51**(6): p. 317-22.

303. Takahashi, H., et al., *In vivo effect of lipopolysaccharide on alveolar and peritoneal macrophages of rats: superoxide anion generation and 5-lipoxygenase metabolism of arachidonic acid.* Am J Respir Cell Mol Biol, 1993. **8**(3): p. 291-8.
304. Raes, G., et al., *Arginase-1 and Ym1 are markers for murine, but not human, alternatively activated myeloid cells.* J Immunol, 2005. **174**(11): p. 6561; author reply 6561-2.
305. Rådmark, O., et al., *5-Lipoxygenase, a key enzyme for leukotriene biosynthesis in health and disease.* Biochimica et Biophysica Acta (BBA) - Molecular and Cell Biology of Lipids, 2015. **1851**(4): p. 331-339.
306. Bartel, D.P., *MicroRNAs: Genomics, Biogenesis, Mechanism, and Function.* Cell Pre, 2004. **116**(2): p. 281–297.

10 SUPPLEMENT

10.1 List of miRNAs detected in MM6 cells

Table 12: Microarray data for differentiated samples.
X-fold induction calculated based on miRNA expression in differentiated Δ5-LO cells : expression in differentiated control cells.

Annotation	p-value	x-fold
hsa-let-7a-2-3p	0,801	0,985
hsa-let-7a-3p		0,934
hsa-let-7a-5p	0,303	0,871
hsa-let-7b-3p		1,020
hsa-let-7b-5p	0,200	1,249
hsa-let-7c	0,587	1,077
hsa-let-7d-3p	0,963	0,999
hsa-let-7d-5p	0,055	0,906
hsa-let-7e-5p	0,009	0,734
hsa-let-7f-1-3p	0,500	0,982
hsa-let-7f-5p	0,218	0,795
hsa-let-7g-5p	0,167	0,860
hsa-let-7i-5p	0,134	0,882
hsa-miR-101-3p	0,143	0,796
hsa-miR-103a-3p	0,112	0,777
hsa-miR-106a-5p	0,149	0,814
hsa-miR-106b-3p	0,149	0,893
hsa-miR-106b-5p	0,297	0,910
hsa-miR-107	0,056	0,752
hsa-miR-1184		
hsa-miR-1207-3p	0,332	0,932

hsa-miR-1207-5p		
hsa-miR-1227-3p		
hsa-miR-1228-5p	0,924	0,992
hsa-miR-1236-3p	0,147	0,930
hsa-miR-124-3p	0,623	1,123
hsa-miR-124-5p	0,897	0,994
hsa-miR-1246	0,194	1,466
hsa-miR-1247-5p	0,154	0,925
hsa-miR-1248	0,275	0,862
hsa-miR-1249	0,492	0,919
hsa-miR-1255a	0,118	1,423
hsa-miR-1255b-2-3p	0,487	1,102
hsa-miR-1258		
hsa-miR-125a-5p	0,004	0,522
hsa-miR-125b-5p	0,006	0,597
hsa-miR-1260a	0,373	0,947
hsa-miR-1260b	0,387	0,954
hsa-miR-1264	0,184	0,919
hsa-miR-1265	0,269	0,877
hsa-miR-1268b		0,875
hsa-miR-1270	0,356	1,031
hsa-miR-1273e		1,264
hsa-miR-1273f		
hsa-miR-1273g-3p	0,264	0,886
hsa-miR-1275	0,530	1,341
hsa-miR-128	0,073	0,952
hsa-miR-1281	0,147	0,898
hsa-miR-1282	0,588	0,952

hsa-miR-1285-3p	0,845	1,022
hsa-miR-1285-5p		
hsa-miR-129-1-3p	0,030	0,825
hsa-miR-1290	0,194	1,692
hsa-miR-1293		
hsa-miR-1297	0,036	0,735
hsa-miR-1299	0,462	1,049
hsa-miR-1301	0,018	0,872
hsa-miR-1304-5p	0,306	1,160
hsa-miR-1307-3p	0,195	0,816
hsa-miR-1307-5p	0,018	0,773
hsa-miR-130b-3p	0,049	0,858
hsa-miR-1321	0,328	1,077
hsa-miR-138-2-3p	0,086	0,868
hsa-miR-140-3p	0,097	0,889
hsa-miR-140-5p	0,275	0,825
hsa-miR-142-3p	0,247	0,815
hsa-miR-142-5p	0,235	0,909
hsa-miR-143-3p		
hsa-miR-145-5p		
hsa-miR-1469	0,714	1,173
hsa-miR-146a-5p	0,015	0,706
hsa-miR-146b-5p	0,034	0,778
hsa-miR-147a	0,516	0,958
hsa-miR-148a-3p	0,001	0,675
hsa-miR-148b-3p	0,017	0,767
hsa-miR-149-3p	0,732	1,186
hsa-miR-150-5p	0,275	1,092

hsa-miR-152	0,012	0,738
hsa-miR-153	0,028	0,787
hsa-miR-155-3p		0,840
hsa-miR-155-5p	0,005	0,773
hsa-miR-1587	0,500	1,063
hsa-miR-15a-5p	0,373	0,865
hsa-miR-15b-5p	0,268	0,844
hsa-miR-16-1-3p		0,990
hsa-miR-16-2-3p	0,091	0,915
hsa-miR-16-5p	0,113	0,807
hsa-miR-17-3p	0,025	0,830
hsa-miR-17-5p	0,066	0,786
hsa-miR-181a-2-3p		0,971
hsa-miR-181a-5p	0,079	0,810
hsa-miR-181b-5p	0,204	0,904
hsa-miR-181c-5p	0,192	0,838
hsa-miR-181d	0,101	0,876
hsa-miR-1825		
hsa-miR-1827	0,461	1,110
hsa-miR-183-3p		1,023
hsa-miR-183-5p	0,755	1,043
hsa-miR-185-5p	0,713	1,022
hsa-miR-186-5p	0,013	0,867
hsa-miR-18a-3p	0,044	0,930
hsa-miR-18a-5p	0,057	0,801
hsa-miR-18b-5p	0,127	0,818
hsa-miR-1908	0,577	1,233
hsa-miR-190a		0,904

hsa-miR-191-5p	0,238	0,888
hsa-miR-1913	0,048	0,841
hsa-miR-1914-5p		
hsa-miR-1915-3p		1,120
hsa-miR-193a-3p	0,375	0,902
hsa-miR-193a-5p	0,493	0,945
hsa-miR-195-5p	0,077	0,805
hsa-miR-196a-3p	0,436	0,962
hsa-miR-196a-5p	0,200	0,804
hsa-miR-196b-5p	0,077	0,767
hsa-miR-197-3p		0,993
hsa-miR-1973	0,011	1,888
hsa-miR-1976		0,991
hsa-miR-199a-3p/ hsa-miR-199b-3p	0,009	0,677
hsa-miR-199b-5p	0,012	0,667
hsa-miR-19a-3p	0,016	0,867
hsa-miR-19a-5p	0,317	0,934
hsa-miR-19b-1-5p	0,188	0,863
hsa-miR-19b-3p	0,037	0,849
hsa-miR-203a		1,042
hsa-miR-204-3p	0,329	1,366
hsa-miR-205-3p	0,191	1,202
hsa-miR-205-5p		
hsa-miR-206		
hsa-miR-20a-3p	0,048	0,802
hsa-miR-20a-5p	0,195	0,790
hsa-miR-20b-3p	0,016	0,837
hsa-miR-20b-5p	0,112	0,762

hsa-miR-21-3p		0,809
hsa-miR-21-5p	0,324	0,774
hsa-miR-210	0,670	0,953
hsa-miR-2113		1,244
hsa-miR-2115-3p	0,346	0,951
hsa-miR-2115-5p	0,198	0,900
hsa-miR-2116-5p	0,521	1,082
hsa-miR-214-3p		1,159
hsa-miR-22-3p	0,057	0,711
hsa-miR-22-5p		0,938
hsa-miR-221-3p	0,022	0,782
hsa-miR-221-5p		
hsa-miR-222-3p	0,044	0,802
hsa-miR-223-3p	0,099	0,776
hsa-miR-223-5p	0,459	0,926
hsa-miR-2355-3p	0,624	0,968
hsa-miR-23a-3p	0,454	0,922
hsa-miR-23b-3p	0,393	0,911
hsa-miR-23c	0,515	1,041
hsa-miR-24-2-5p	0,164	0,858
hsa-miR-24-3p	0,408	0,865
hsa-miR-25-3p	0,320	1,040
hsa-miR-25-5p	0,360	1,062
hsa-miR-2681-5p	0,513	1,227
hsa-miR-26a-5p	0,034	0,825
hsa-miR-26b-3p		0,897
hsa-miR-26b-5p	0,165	0,770
hsa-miR-27a-3p	0,351	0,872

hsa-miR-27b-3p	0,728	0,957
hsa-miR-298		1,197
hsa-miR-29a-3p	0,236	0,887
hsa-miR-29a-5p	0,213	0,921
hsa-miR-29b-1-5p	0,111	0,847
hsa-miR-29b-3p	0,919	0,985
hsa-miR-29c-3p	0,249	1,195
hsa-miR-301a-3p	0,158	0,706
hsa-miR-301b		0,809
hsa-miR-302a-3p	0,252	1,150
hsa-miR-302c-5p	0,131	0,903
hsa-miR-302e		0,943
hsa-miR-30a-5p	0,199	0,878
hsa-miR-30b-3p		0,957
hsa-miR-30b-5p	0,237	0,843
hsa-miR-30c-1-3p		1,005
hsa-miR-30c-5p	0,513	0,938
hsa-miR-30d-5p	0,074	0,913
hsa-miR-30e-3p	0,154	0,904
hsa-miR-30e-5p	0,442	0,926
hsa-miR-3124-3p	0,377	1,223
hsa-miR-3127-3p		1,138
hsa-miR-3133	0,744	1,056
hsa-miR-3136-3p	0,189	1,250
hsa-miR-3142	0,036	0,887
hsa-miR-3148		1,153
hsa-miR-3149	0,149	1,254
hsa-miR-3156-3p	0,696	0,972

hsa-miR-3158-5p	0,392	1,258
hsa-miR-3161		1,127
hsa-miR-3162-3p		
hsa-miR-3164	0,346	0,946
hsa-miR-3175	0,396	0,978
hsa-miR-3178	0,032	1,221
hsa-miR-3182	0,311	1,130
hsa-miR-3183		1,248
hsa-miR-3184-3p		
hsa-miR-3190-5p		
hsa-miR-3195		1,124
hsa-miR-3196	0,574	1,153
hsa-miR-32-3p	0,100	1,280
hsa-miR-32-5p	0,113	0,833
hsa-miR-3201		
hsa-miR-3202	0,468	1,287
hsa-miR-320a	0,154	0,890
hsa-miR-320b	0,145	0,884
hsa-miR-320c	0,048	0,863
hsa-miR-320d	0,189	0,884
hsa-miR-320e		0,918
hsa-miR-323b-5p		0,945
hsa-miR-324-3p	0,291	0,950
hsa-miR-331-3p	0,100	0,886
hsa-miR-335-3p	0,334	1,116
hsa-miR-335-5p	0,003	0,705
hsa-miR-337-3p		
hsa-miR-338-3p	0,175	0,825

hsa-miR-339-5p	0,966	1,001
hsa-miR-33a-5p	0,207	0,895
hsa-miR-33b-5p	0,029	0,889
hsa-miR-340-3p	0,946	0,999
hsa-miR-340-5p	0,062	0,887
hsa-miR-342-3p	0,093	0,880
hsa-miR-34a-5p		
hsa-miR-3591-5p	0,344	1,102
hsa-miR-3607-3p	0,072	0,787
hsa-miR-3607-5p	0,035	0,753
hsa-miR-361-3p		1,062
hsa-miR-361-5p	0,058	0,822
hsa-miR-3611	0,027	1,801
hsa-miR-3613-3p	0,706	1,608
hsa-miR-3613-5p	0,400	0,921
hsa-miR-3614-3p	0,241	0,936
hsa-miR-362-3p	0,155	0,850
hsa-miR-3621	0,635	1,091
hsa-miR-3622a-3p		
hsa-miR-363-5p		0,838
hsa-miR-3646	0,505	1,058
hsa-miR-3648		1,228
hsa-miR-3651	0,002	0,762
hsa-miR-3653	0,818	0,991
hsa-miR-3654	0,658	0,968
hsa-miR-3656	0,576	1,104
hsa-miR-365a-3p/ hsa-miR-365b-3p	0,097	0,882
hsa-miR-3664-5p	0,777	1,035

hsa-miR-3667-5p	0,331	1,106
hsa-miR-3675-3p	0,192	0,899
hsa-miR-3676-3p	0,252	0,969
hsa-miR-3676-5p	0,299	0,949
hsa-miR-3679-3p	0,474	0,933
hsa-miR-3680-5p	0,902	1,049
hsa-miR-3685	0,187	1,177
hsa-miR-3686	0,020	1,330
hsa-miR-3687	0,348	1,098
hsa-miR-3690		
hsa-miR-371b-3p	0,167	0,898
hsa-miR-371b-5p	0,490	1,436
hsa-miR-374a-5p	0,293	0,789
hsa-miR-374b-5p	0,437	0,949
hsa-miR-374c-3p		
hsa-miR-374c-5p	0,281	0,886
hsa-miR-378a-3p	0,208	0,847
hsa-miR-378a-5p		0,887
hsa-miR-378b	0,052	0,864
hsa-miR-378c	0,193	0,823
hsa-miR-378d	0,174	0,834
hsa-miR-378e	0,031	0,819
hsa-miR-378f	0,055	0,824
hsa-miR-378g		0,862
hsa-miR-382-3p	0,527	0,934
hsa-miR-3911		1,053
hsa-miR-3915	0,303	1,267
hsa-miR-3920		

hsa-miR-3924	0,493	1,067
hsa-miR-3935	0,106	1,194
hsa-miR-3938	0,503	0,935
hsa-miR-3940-5p	0,605	1,147
hsa-miR-3941	0,494	1,141
hsa-miR-3960	0,475	1,442
hsa-miR-3976	0,186	1,299
hsa-miR-422a	0,002	0,887
hsa-miR-423-3p	0,057	0,847
hsa-miR-423-5p	0,628	1,078
hsa-miR-424-5p	0,003	0,525
hsa-miR-425-3p	0,092	0,852
hsa-miR-425-5p	0,156	0,890
hsa-miR-4258	0,836	1,028
hsa-miR-4268	0,547	1,177
hsa-miR-4274	0,107	0,855
hsa-miR-4275	0,125	0,891
hsa-miR-4279	0,433	1,266
hsa-miR-4284	0,616	0,913
hsa-miR-4285	0,444	1,392
hsa-miR-4286	0,263	0,912
hsa-miR-4288	0,047	0,818
hsa-miR-4289	0,010	0,726
hsa-miR-4290	0,452	1,185
hsa-miR-4291	0,339	0,943
hsa-miR-4292		1,166
hsa-miR-4297	0,292	1,079
hsa-miR-4299	0,018	1,199

hsa-miR-4301	0,811	0,970
hsa-miR-4306	0,279	1,248
hsa-miR-4308		
hsa-miR-431-3p	0,292	0,918
hsa-miR-431-5p		1,071
hsa-miR-4312	0,408	0,941
hsa-miR-4317	0,263	0,934
hsa-miR-432-5p		
hsa-miR-4324		0,947
hsa-miR-4329		0,918
hsa-miR-4417	0,980	0,998
hsa-miR-4419b	0,079	1,287
hsa-miR-4421	0,277	1,253
hsa-miR-4423-5p	0,182	1,270
hsa-miR-4425		1,127
hsa-miR-4429	0,690	0,979
hsa-miR-4436b-5p	0,401	1,067
hsa-miR-4443	0,897	0,995
hsa-miR-4445-5p		1,227
hsa-miR-4448		
hsa-miR-4449	0,633	1,115
hsa-miR-4450		1,091
hsa-miR-4451	0,379	1,130
hsa-miR-4454	0,591	0,941
hsa-miR-4455	0,163	1,190
hsa-miR-4456	0,457	0,913
hsa-miR-4459		1,025
hsa-miR-4467	0,433	1,345

hsa-miR-4468	0,220	1,212
hsa-miR-4472	0,811	0,977
hsa-miR-4473	0,034	1,370
hsa-miR-4475	0,212	1,758
hsa-miR-4478	0,114	1,233
hsa-miR-4484	0,662	1,231
hsa-miR-4485		1,426
hsa-miR-4488		1,126
hsa-miR-4497	0,778	1,120
hsa-miR-4500	0,479	0,931
hsa-miR-4505	0,376	1,202
hsa-miR-4507		1,015
hsa-miR-4508	0,692	1,148
hsa-miR-450b-5p		
hsa-miR-4511	0,150	1,615
hsa-miR-4516	0,696	1,254
hsa-miR-4518		0,909
hsa-miR-451b	0,183	0,929
hsa-miR-4521		
hsa-miR-4524b-5p		
hsa-miR-4530	0,689	1,258
hsa-miR-4531	0,560	1,194
hsa-miR-4532	0,344	1,254
hsa-miR-4533	0,345	1,220
hsa-miR-4534	0,705	1,157
hsa-miR-4536-3p	0,983	1,004
hsa-miR-454-3p	0,032	0,710
hsa-miR-4540		1,190

hsa-miR-4632-3p		1,008
hsa-miR-4633-5p		0,996
hsa-miR-4636		1,374
hsa-miR-4639-3p	0,217	1,254
hsa-miR-4644	0,259	1,402
hsa-miR-4646-3p		0,929
hsa-miR-4653-3p		
hsa-miR-4657	0,315	1,056
hsa-miR-4658		
hsa-miR-4667-5p	0,428	1,172
hsa-miR-4668-5p	0,661	1,758
hsa-miR-4682		0,996
hsa-miR-4687-3p	0,819	1,047
hsa-miR-4687-5p	0,222	1,251
hsa-miR-4694-3p		
hsa-miR-4695-3p	0,424	0,958
hsa-miR-4698		1,227
hsa-miR-4701-5p		0,990
hsa-miR-4707-5p	0,738	1,098
hsa-miR-4708-3p	0,445	1,474
hsa-miR-4709-3p	0,018	1,335
hsa-miR-4712-3p	0,423	1,053
hsa-miR-4714-5p	0,714	0,987
hsa-miR-4716-5p	0,633	1,017
hsa-miR-4723-3p	0,453	0,943
hsa-miR-4725-3p		
hsa-miR-4725-5p		1,292
hsa-miR-4726-5p	0,335	1,216

hsa-miR-4728-3p	0,795	1,042
hsa-miR-4732-3p	0,135	1,400
hsa-miR-4732-5p	0,510	1,292
hsa-miR-4739		1,035
hsa-miR-4742-3p	0,783	1,019
hsa-miR-4747-5p	0,061	1,302
hsa-miR-4750-5p	0,624	1,167
hsa-miR-4753-3p		
hsa-miR-4756-3p		
hsa-miR-4758-3p		
hsa-miR-4762-5p		1,313
hsa-miR-4764-3p	0,290	1,287
hsa-miR-4764-5p		
hsa-miR-4765		0,916
hsa-miR-4769-3p		
hsa-miR-4775		
hsa-miR-4777-5p		1,200
hsa-miR-4778-5p		1,437
hsa-miR-4780	0,051	0,828
hsa-miR-4784	0,199	1,267
hsa-miR-4787-5p	0,563	1,345
hsa-miR-4791	0,007	0,739
hsa-miR-4792		1,078
hsa-miR-4795-3p	0,379	1,328
hsa-miR-4795-5p	0,473	1,127
hsa-miR-4797-5p	0,277	0,922
hsa-miR-4800-3p	0,724	1,164
hsa-miR-4800-5p		

hsa-miR-4804-3p		1,092
hsa-miR-483-3p	0,431	1,206
hsa-miR-483-5p	0,301	1,182
hsa-miR-484	0,204	0,953
hsa-miR-485-3p	0,489	1,090
hsa-miR-487b	0,070	0,874
hsa-miR-491-3p	0,434	1,154
hsa-miR-492		1,086
hsa-miR-493-5p	0,015	0,931
hsa-miR-495-5p		
hsa-miR-498	0,616	0,973
hsa-miR-499a-5p		0,909
hsa-miR-5000-3p		0,927
hsa-miR-5002-3p	0,530	1,046
hsa-miR-5002-5p	0,506	1,082
hsa-miR-5004-3p		
hsa-miR-5006-3p		
hsa-miR-5007-3p		
hsa-miR-500a-3p		0,912
hsa-miR-500a-5p		
hsa-miR-501-5p	0,606	0,962
hsa-miR-502-5p	0,277	0,952
hsa-miR-505-3p		
hsa-miR-505-5p	0,390	1,038
hsa-miR-508-3p	0,834	1,012
hsa-miR-508-5p		1,114
hsa-miR-5089-5p	0,124	0,899
hsa-miR-509-3p		1,174

hsa-miR-5100	0,712	0,968
hsa-miR-513a-5p	0,152	1,602
hsa-miR-513b		1,062
hsa-miR-516b-5p		1,076
hsa-miR-5187-3p		1,140
hsa-miR-518e-5p/ hsa-miR-519a-5p/ hsa-miR-519b-5p/ hsa-miR-519c-5p/ hsa-miR-522-5p/ hsa-miR-523-5p		1,087
hsa-miR-5193	0,314	1,154
hsa-miR-5196-3p	0,569	0,955
hsa-miR-519e-3p	0,170	0,961
hsa-miR-519e-5p	0,600	1,033
hsa-miR-532-5p		
hsa-miR-542-3p	0,061	0,706
hsa-miR-542-5p	0,633	0,945
hsa-miR-548an	0,759	1,072
hsa-miR-548ap-5p/ hsa-miR-548j	0,995	1,002
hsa-miR-548as-3p	0,527	1,075
hsa-miR-548l		0,941
hsa-miR-548aa/ hsa-miR-548ap-3p/ hsa-miR-548t-3p		0,907
hsa-miR-548aa/hsa-miR-548t-3p		1,007
hsa-miR-550a-3-5p/ hsa-miR-550a-5p	0,153	0,909
hsa-miR-551a		1,001
hsa-miR-5571-5p	0,357	0,968
hsa-miR-5572	0,363	1,163
hsa-miR-5580-5p		0,997
hsa-miR-5581-3p	0,241	0,922
hsa-miR-5584-3p		

hsa-miR-5585-3p		
hsa-miR-5681b	0,248	1,107
hsa-miR-5684	0,086	0,866
hsa-miR-5701	0,143	0,862
hsa-miR-5704	0,112	1,303
hsa-miR-574-3p	0,480	0,982
hsa-miR-574-5p	0,443	1,092
hsa-miR-576-5p		0,912
hsa-miR-578		
hsa-miR-584-5p		0,984
hsa-miR-589-5p	0,296	0,906
hsa-miR-590-5p	0,343	0,842
hsa-miR-593-3p	0,680	0,976
hsa-miR-595		
hsa-miR-597		0,877
hsa-miR-598		
hsa-miR-600	0,381	0,959
hsa-miR-601		
hsa-miR-615-3p		
hsa-miR-616-3p		
hsa-miR-618		
hsa-miR-620		1,258
hsa-miR-623		
hsa-miR-625-3p		
hsa-miR-628-3p		
hsa-miR-629-3p	0,919	0,996
hsa-miR-629-5p		0,957
hsa-miR-630	0,115	1,203

hsa-miR-634	0,217	1,085
hsa-miR-636	0,066	0,859
hsa-miR-638	0,682	1,096
hsa-miR-639		
hsa-miR-642a-5p		
hsa-miR-642b-3p		1,016
hsa-miR-642b-5p	0,314	1,240
hsa-miR-647		1,153
hsa-miR-652-3p	0,053	0,817
hsa-miR-652-5p		1,246
hsa-miR-656		
hsa-miR-659-3p	0,811	1,061
hsa-miR-660-3p	0,386	1,203
hsa-miR-660-5p	0,034	0,800
hsa-miR-663a		1,245
hsa-miR-663b		
hsa-miR-664a-3p	0,289	0,949
hsa-miR-664a-5p	0,224	0,877
hsa-miR-664b-3p	0,679	1,031
hsa-miR-664b-5p	0,029	0,805
hsa-miR-665		1,452
hsa-miR-668	0,026	0,832
hsa-miR-675-5p	0,498	1,310
hsa-miR-676-5p		
hsa-miR-7-5p	0,124	0,907
hsa-miR-711	0,803	1,136
hsa-miR-718	0,925	1,010
hsa-miR-744-5p	0,795	1,059

hsa-miR-767-5p	0,061	0,923
hsa-miR-874	0,260	0,963
hsa-miR-876-3p		
hsa-miR-877-3p	0,495	1,078
hsa-miR-877-5p	0,362	0,956
hsa-miR-885-5p		0,899
hsa-miR-890	0,289	0,937
hsa-miR-892a		
hsa-miR-9-3p		1,006
hsa-miR-9-5p	0,402	0,893
hsa-miR-92a-1-5p	0,519	0,919
hsa-miR-92a-3p	0,194	0,929
hsa-miR-92b-3p	0,071	0,902
hsa-miR-93-5p	0,943	0,998
hsa-miR-934		
hsa-miR-937-3p	0,404	0,960
hsa-miR-942	0,428	1,053
hsa-miR-943	0,712	1,157
hsa-miR-98-5p	0,184	0,767
hsa-miR-99b-3p	0,436	0,931
hsa-miR-99b-5p	0,162	0,603
hsa-miRPlus-A1015	0,243	0,892
hsa-miRPlus-A1072	0,140	1,247
hsa-miRPlus-A1073	0,329	0,902
hsa-miRPlus-A1083		
hsa-miRPlus-A1086	0,883	1,308
hsa-miRPlus-A1087	0,885	0,996
hsa-miRPlus-G1246-3p	0,032	0,786

10.2 MiRNAs affected by Δ5-LO (four days of differentiation)

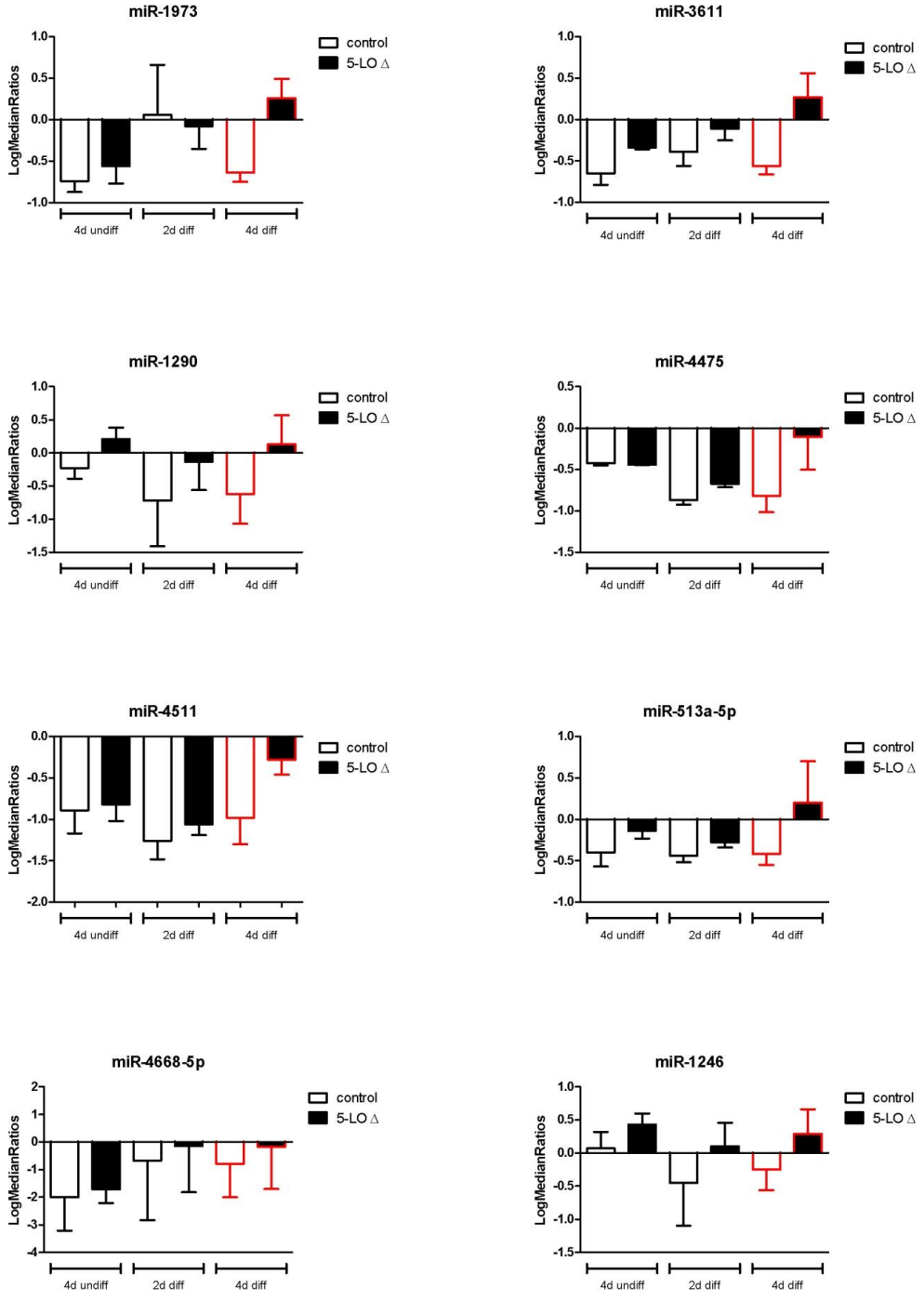

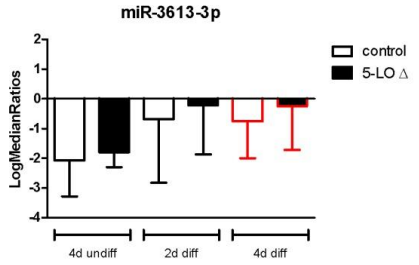
miR-3613-3p
LogMedianRatios
control
5-LO Δ
4d undiff
2d diff
4d diff

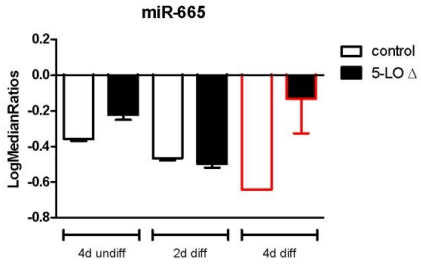
miR-665
LogMedianRatios
control
5-LO Δ
4d undiff
2d diff
4d diff

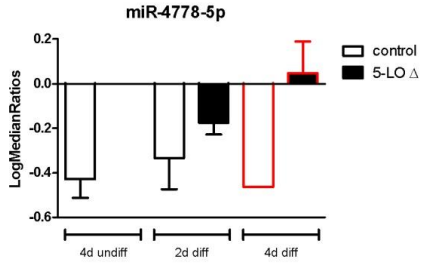
miR-4778-5p
LogMedianRatios
control
5-LO Δ
4d undiff
2d diff
4d diff

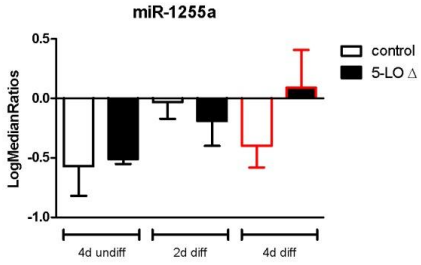
miR-1255a
LogMedianRatios
control
5-LO Δ
4d undiff
2d diff
4d diff

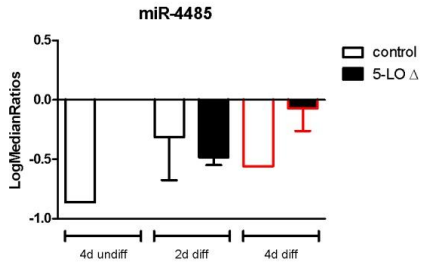
miR-4485
LogMedianRatios
control
5-LO Δ
4d undiff
2d diff
4d diff

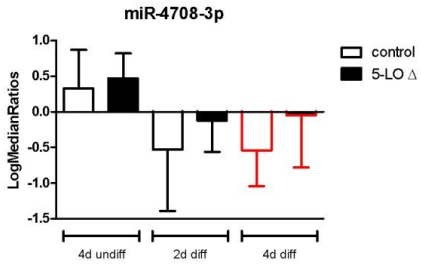
miR-4708-3p
LogMedianRatios
control
5-LO Δ
4d undiff
2d diff
4d diff

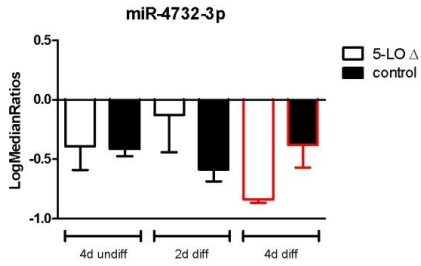
miR-4732-3p
LogMedianRatios
5-LO Δ
control
4d undiff
2d diff
4d diff

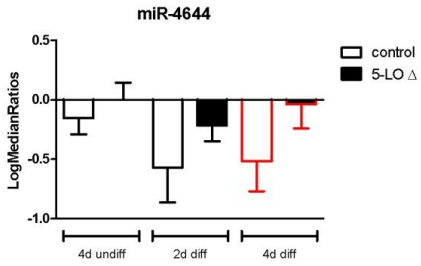
miR-4644
LogMedianRatios
control
5-LO Δ
4d undiff
2d diff
4d diff

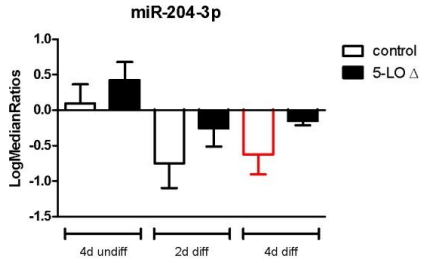
miR-204-3p
LogMedianRatios
1.0
0.5
0.0
-0.5
-1.0
-1.5
4d undiff
2d diff
4d diff
control
5-LO Δ

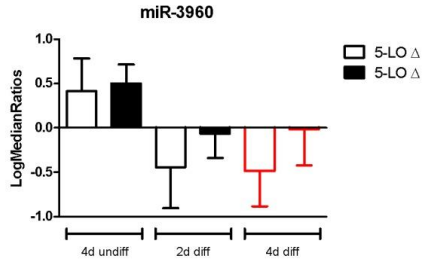
miR-3960
LogMedianRatios
1.0
0.5
0.0
-0.5
-1.0
4d undiff
2d diff
4d diff
5-LO Δ
5-LO Δ

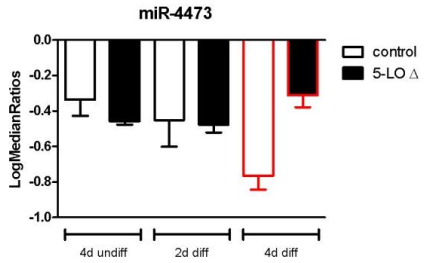
miR-4473
LogMedianRatios
0.0
-0.2
-0.4
-0.6
-0.8
-1.0
4d undiff
2d diff
4d diff
control
5-LO Δ

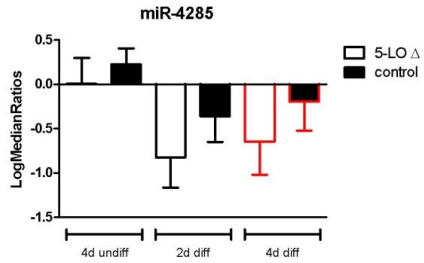
miR-4285
LogMedianRatios
0.5
0.0
-0.5
-1.0
-1.5
4d undiff
2d diff
4d diff
5-LO Δ
control

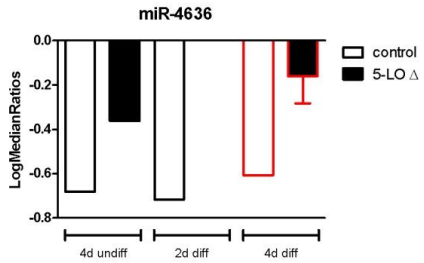
miR-4636
LogMedianRatios
0.0
-0.2
-0.4
-0.6
-0.8
4d undiff
2d diff
4d diff
control
5-LO Δ

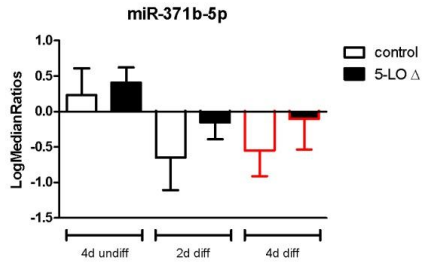
miR-371b-5p
LogMedianRatios
1.0
0.5
0.0
-0.5
-1.0
-1.5
4d undiff
2d diff
4d diff
control
5-LO Δ

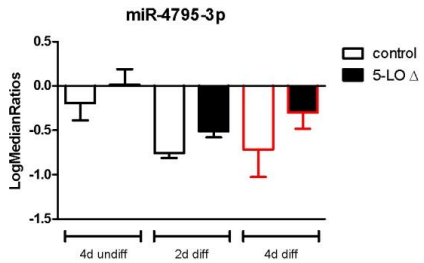
miR-4795-3p
LogMedianRatios
0.5
0.0
-0.5
-1.0
-1.5
4d undiff
2d diff
4d diff
control
5-LO Δ

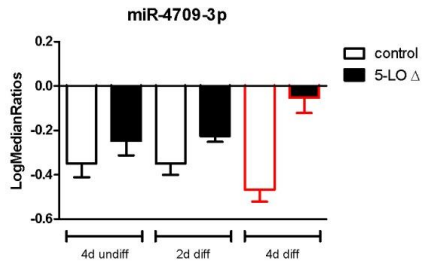
miR-4709-3p
LogMedianRatios
0.2
0.0
-0.2
-0.4
-0.6
4d undiff
2d diff
4d diff
control
5-LO Δ

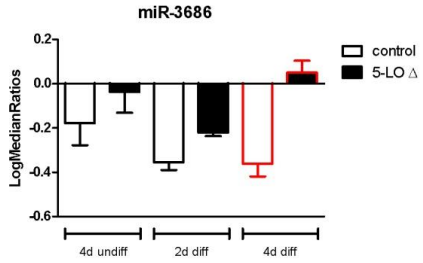
miR-3686
LogMedianRatios
0.2
0.0
-0.2
-0.4
-0.6
4d undiff
2d diff
4d diff
control
5-LO Δ

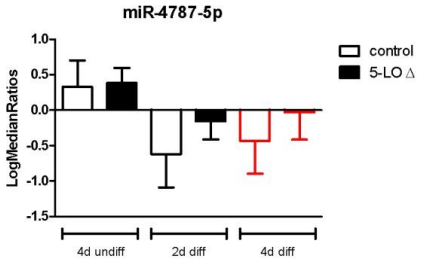
miR-4787-5p
LogMedianRatios
1.0
0.5
0.0
-0.5
-1.0
-1.5
4d undiff
2d diff
4d diff
control
5-LO Δ

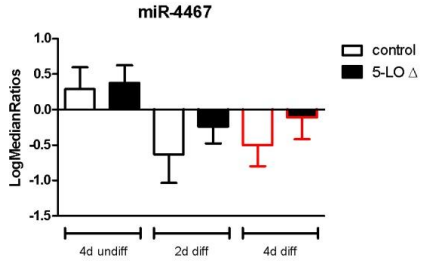
miR-4467
LogMedianRatios
1.0
0.5
0.0
-0.5
-1.0
-1.5
4d undiff
2d diff
4d diff
control
5-LO Δ

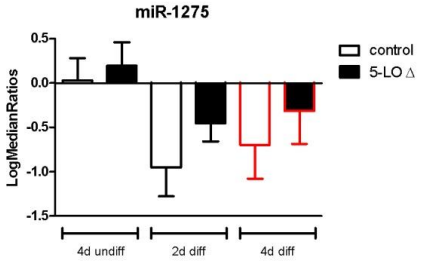
miR-1275
LogMedianRatios
0.5
0.0
-0.5
-1.0
-1.5
4d undiff
2d diff
4d diff
control
5-LO Δ

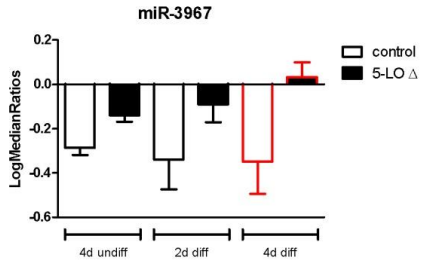
miR-3967
LogMedianRatios
0.2
0.0
-0.2
-0.4
-0.6
4d undiff
2d diff
4d diff
control
5-LO Δ

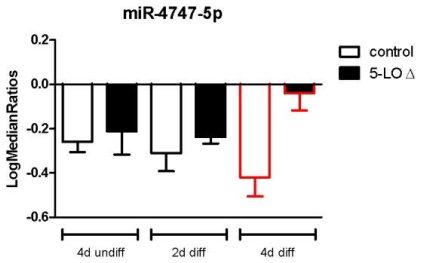
miR-4747-5p
LogMedianRatios
0.2
0.0
-0.2
-0.4
-0.6
4d undiff
2d diff
4d diff
control
5-LO Δ

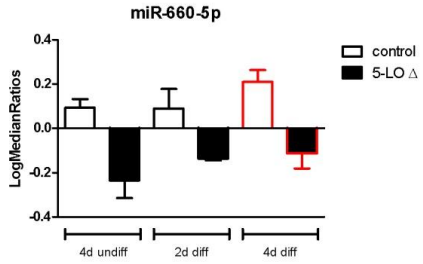
miR-660-5p
LogMedianRatios
0.4
0.2
0.0
-0.2
-0.4
4d undiff
2d diff
4d diff
control
5-LO Δ

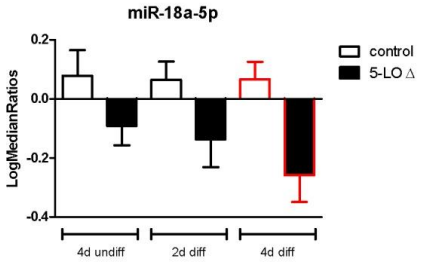
miR-18a-5p
LogMedianRatios
0.2
0.0
-0.2
-0.4
4d undiff
2d diff
4d diff
control
5-LO Δ

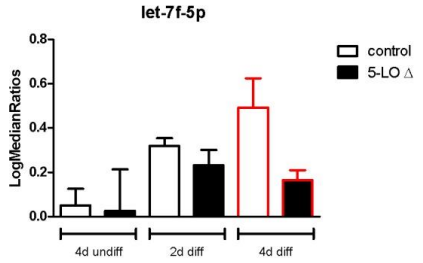
let-7f-5p
LogMedianRatios
0.8
0.6
0.4
0.2
0.0
control
5-LO Δ
4d undiff
2d diff
4d diff

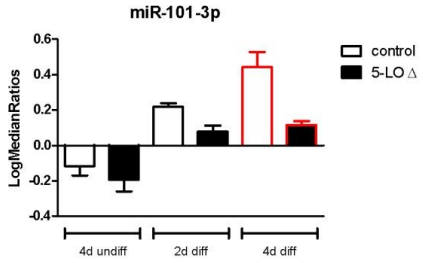
miR-101-3p
LogMedianRatios
0.6
0.4
0.2
0.0
-0.2
-0.4
control
5-LO Δ
4d undiff
2d diff
4d diff

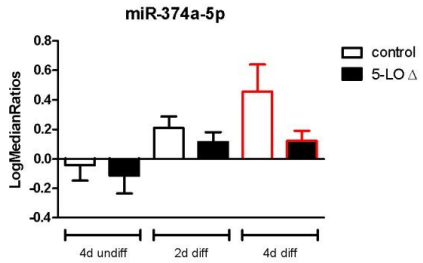
miR-374a-5p
LogMedianRatios
0.8
0.6
0.4
0.2
0.0
-0.2
-0.4
control
5-LO Δ
4d undiff
2d diff
4d diff

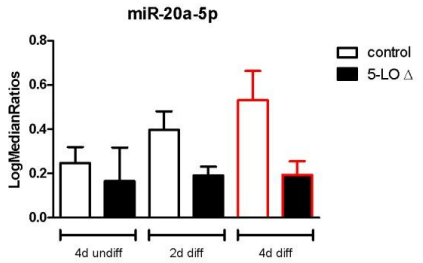
miR-20a-5p
LogMedianRatios
0.8
0.6
0.4
0.2
0.0
control
5-LO Δ
4d undiff
2d diff
4d diff

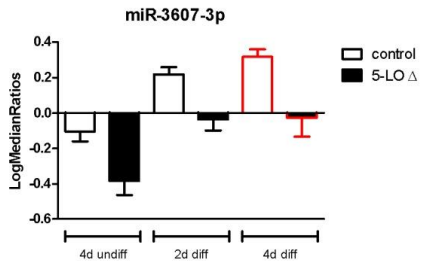
miR-3607-3p
LogMedianRatios
0.4
0.2
0.0
-0.2
-0.4
-0.6
control
5-LO Δ
4d undiff
2d diff
4d diff

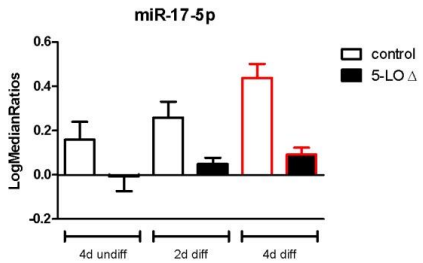
miR-17-5p
LogMedianRatios
0.6
0.4
0.2
0.0
-0.2
control
5-LO Δ
4d undiff
2d diff
4d diff

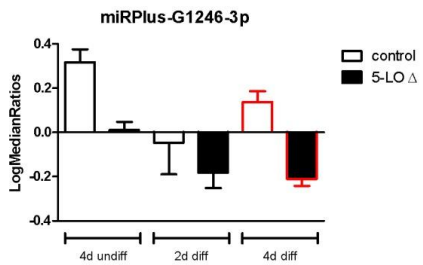
miRPlus-G1246-3p
LogMedianRatios
0.4
0.2
0.0
-0.2
-0.4
control
5-LO Δ
4d undiff
2d diff
4d diff

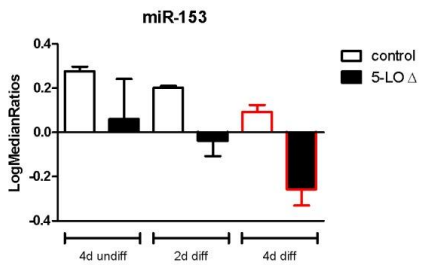
miR-153
LogMedianRatios
0.4
0.2
0.0
-0.2
-0.4
control
5-LO Δ
4d undiff
2d diff
4d diff

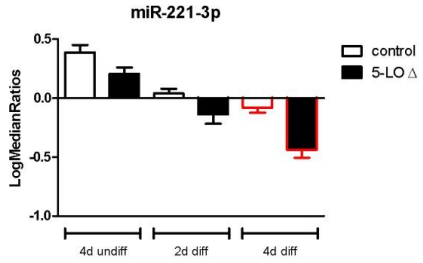
miR-221-3p
LogMedianRatios
0.5
0.0
-0.5
-1.0
4d undiff
2d diff
4d diff
control
5-LO Δ

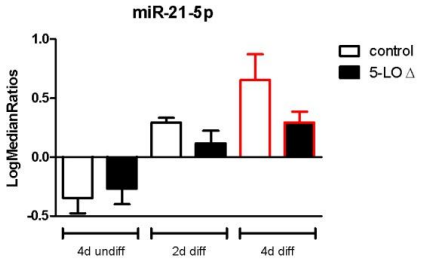
miR-21-5p
LogMedianRatios
1.0
0.5
0.0
-0.5
4d undiff
2d diff
4d diff
control
5-LO Δ

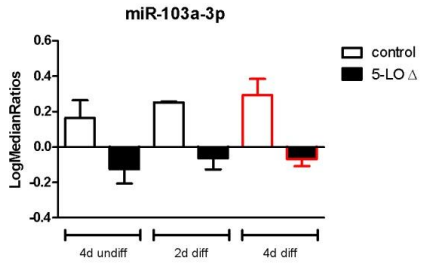
miR-103a-3p
LogMedianRatios
0.6
0.4
0.2
0.0
-0.2
-0.4
4d undiff
2d diff
4d diff
control
5-LO Δ

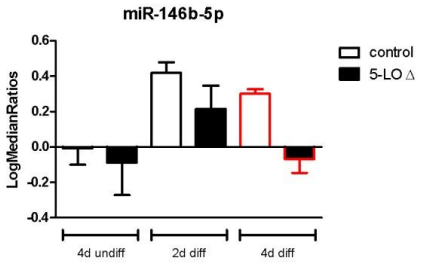
miR-146b-5p
LogMedianRatios
0.6
0.4
0.2
0.0
-0.2
-0.4
4d undiff
2d diff
4d diff
control
5-LO Δ

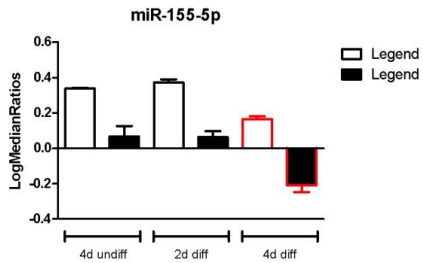
miR-155-5p
LogMedianRatios
0.6
0.4
0.2
0.0
-0.2
-0.4
4d undiff
2d diff
4d diff
Legend
Legend

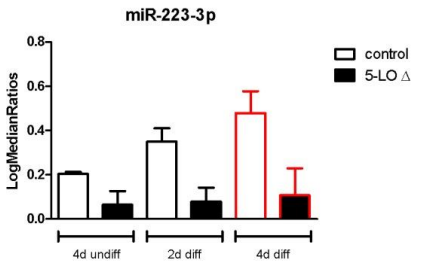
miR-223-3p
LogMedianRatios
0.8
0.6
0.4
0.2
0.0
4d undiff
2d diff
4d diff
control
5-LO Δ

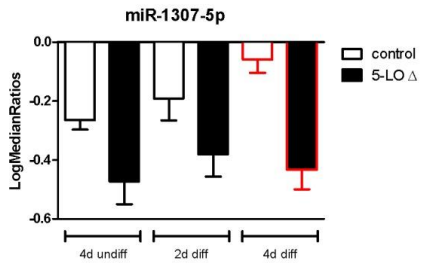
miR-1307-5p
LogMedianRatios
0.0
-0.2
-0.4
-0.6
4d undiff
2d diff
4d diff
control
5-LO Δ

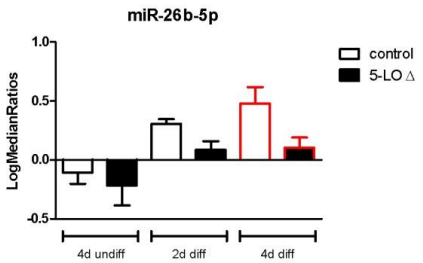
miR-26b-5p
LogMedianRatios
1.0
0.5
0.0
-0.5
4d undiff
2d diff
4d diff
control
5-LO Δ

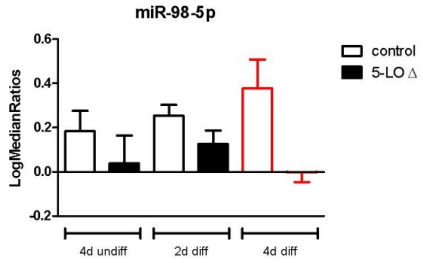
miR-98-5p
LogMedianRatios
0.6
0.4
0.2
0.0
-0.2
4d undiff
2d diff
4d diff
control
5-LO Δ

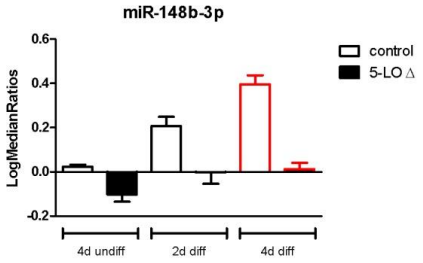
miR-148b-3p
LogMedianRatios
0.6
0.4
0.2
0.0
-0.2
4d undiff
2d diff
4d diff
control
5-LO Δ

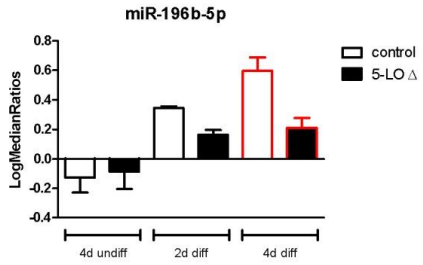
miR-196b-5p
LogMedianRatios
0.8
0.6
0.4
0.2
0.0
-0.2
-0.4
4d undiff
2d diff
4d diff
control
5-LO Δ

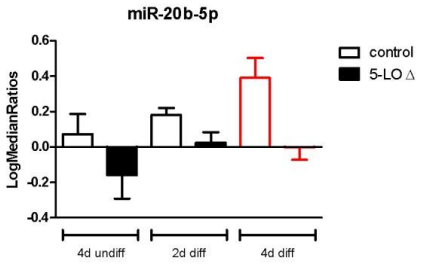
miR-20b-5p
LogMedianRatios
0.6
0.4
0.2
0.0
-0.2
-0.4
4d undiff
2d diff
4d diff
control
5-LO Δ

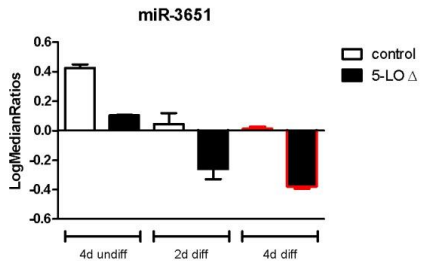
miR-3651
LogMedianRatios
0.6
0.4
0.2
0.0
-0.2
-0.4
-0.6
4d undiff
2d diff
4d diff
control
5-LO Δ

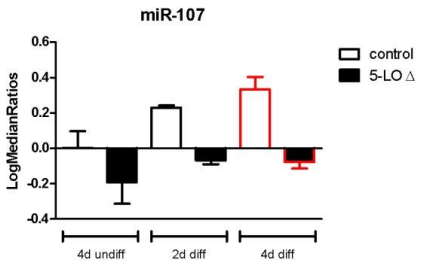
miR-107
LogMedianRatios
0.6
0.4
0.2
0.0
-0.2
-0.4
4d undiff
2d diff
4d diff
control
5-LO Δ

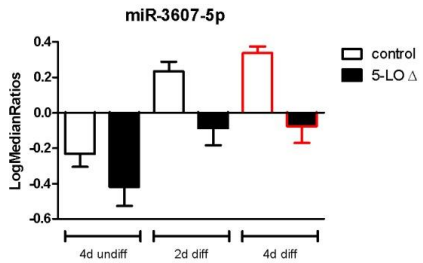
miR-3607-5p
LogMedianRatios
0.4
0.2
0.0
-0.2
-0.4
-0.6
4d undiff
2d diff
4d diff
control
5-LO Δ

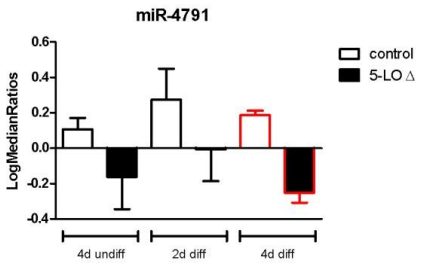
miR-4791
LogMedianRatios
0.6
0.4
0.2
0.0
-0.2
-0.4
4d undiff
2d diff
4d diff
control
5-LO Δ

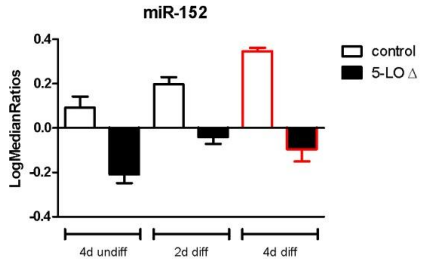
miR-152
LogMedianRatios
0.4
0.2
0.0
-0.2
-0.4
4d undiff
2d diff
4d diff
control
5-LO Δ

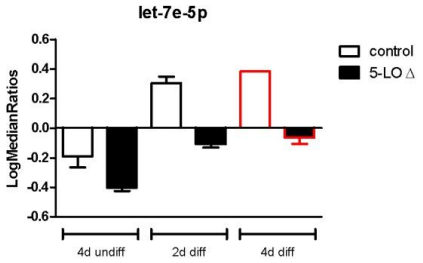
let-7e-5p
LogMedianRatios
0.6
0.4
0.2
0.0
-0.2
-0.4
-0.6
4d undiff
2d diff
4d diff
control
5-LO Δ

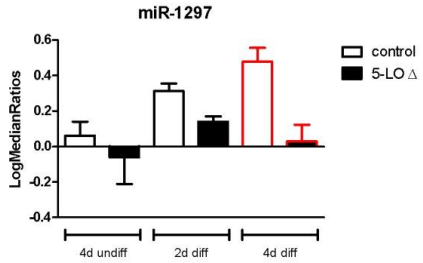
miR-1297
LogMedianRatios
0.6
0.4
0.2
0.0
-0.2
-0.4
4d undiff
2d diff
4d diff
control
5-LO Δ

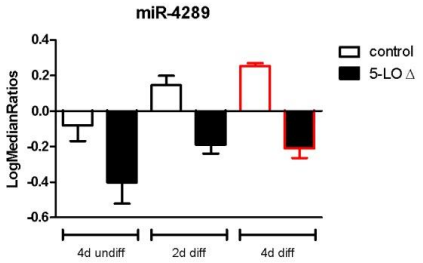
miR-4289
LogMedianRatios
0.4
0.2
0.0
-0.2
-0.4
-0.6
4d undiff
2d diff
4d diff
control
5-LO Δ

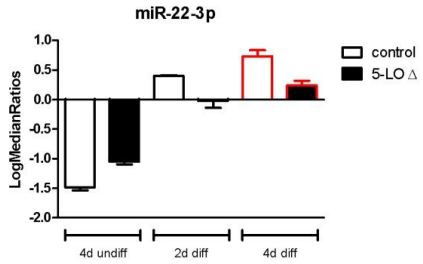
miR-22-3p
LogMedianRatios
1.0
0.5
0.0
-0.5
-1.0
-1.5
-2.0
4d undiff
2d diff
4d diff
control
5-LO Δ

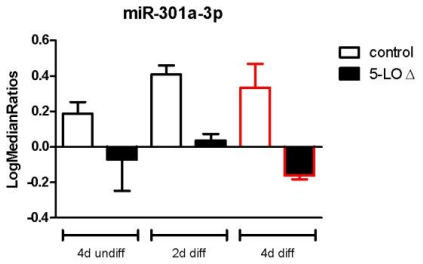
miR-301a-3p
LogMedianRatios
0.6
0.4
0.2
0.0
-0.2
-0.4
4d undiff
2d diff
4d diff
control
5-LO Δ

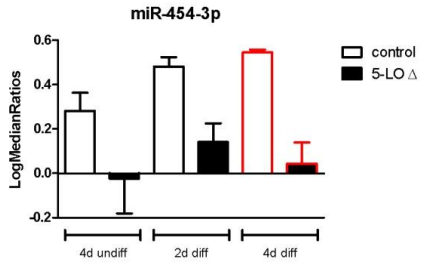
miR-454-3p
LogMedianRatios
0.6
0.4
0.2
0.0
-0.2
4d undiff
2d diff
4d diff
control
5-LO Δ

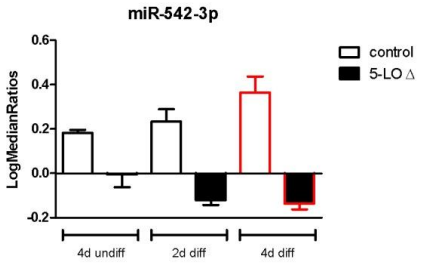
miR-542-3p
LogMedianRatios
0.6
0.4
0.2
0.0
-0.2
4d undiff
2d diff
4d diff
control
5-LO Δ

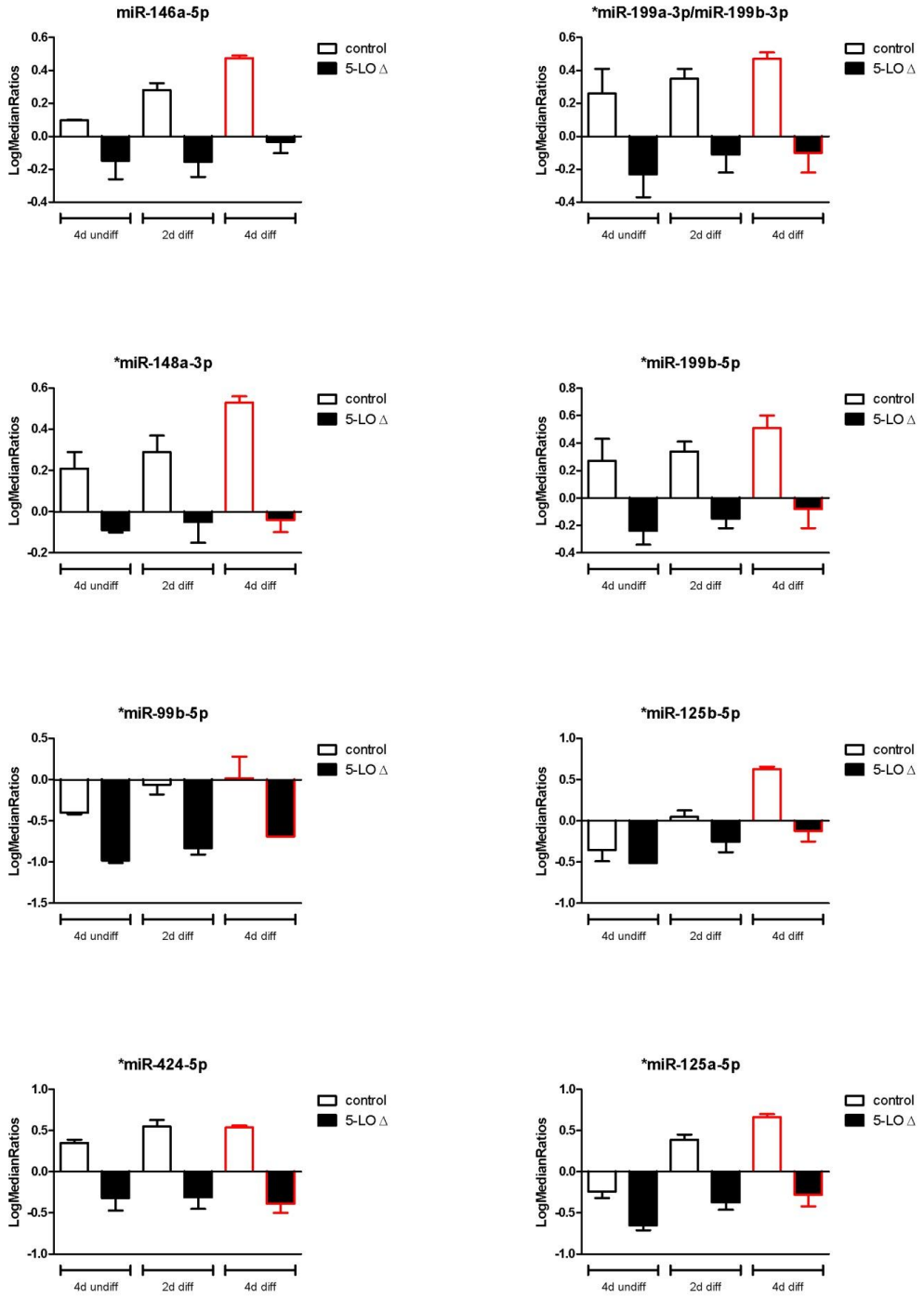

Figure 41: Microarray results of miRNAs affected by Δ5-LO

after four days of differentiation with TGFβ and calcitriol. MiRNAs with an x-fold induction <0.8 and >1.3, respectively (expression level in control transduced : expression level in Δ5-LO transduced MM6 cells) were chosen.

10.3 MiRNAs affected by Δ5-LO (two days of differentiation)

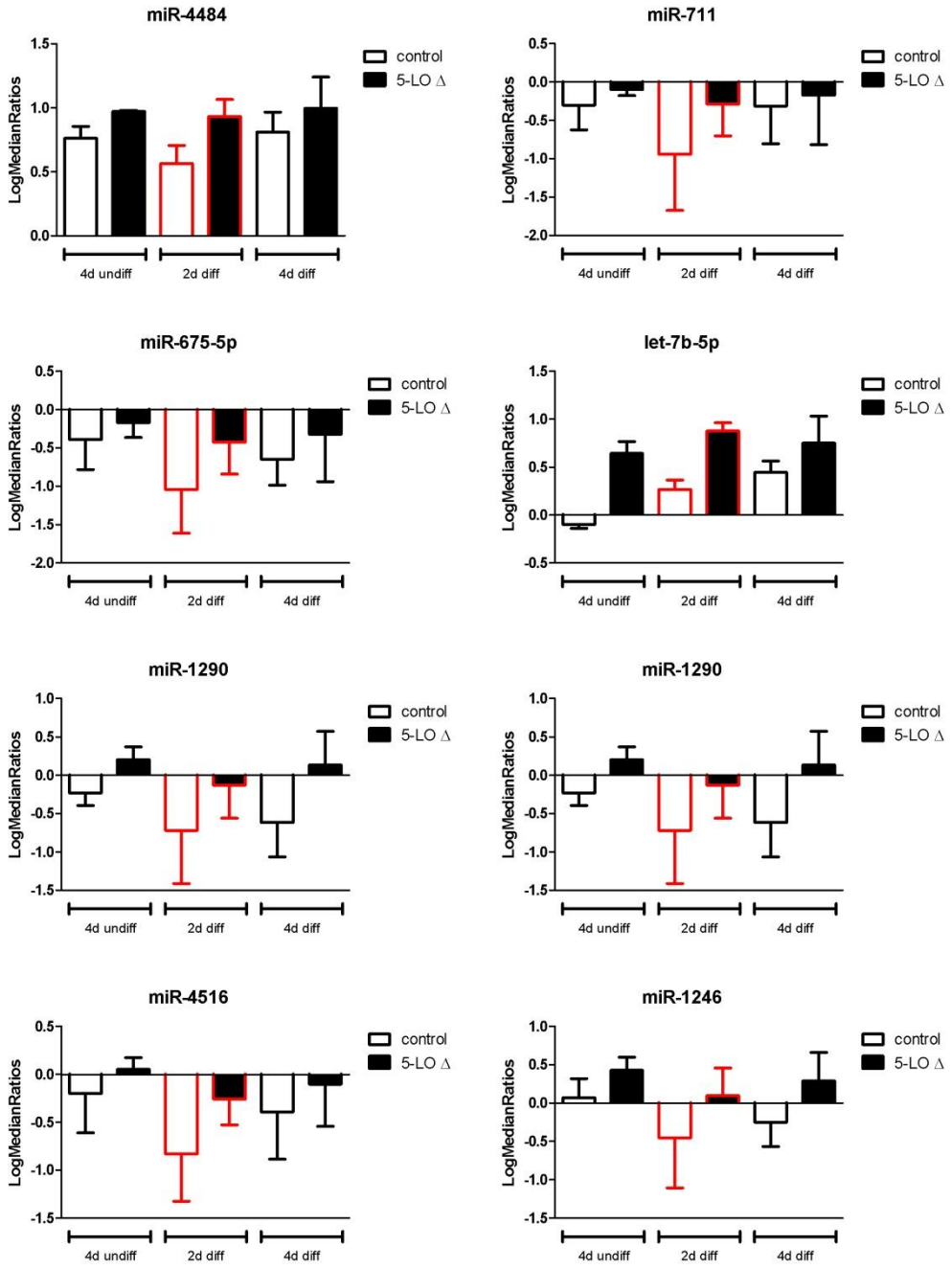

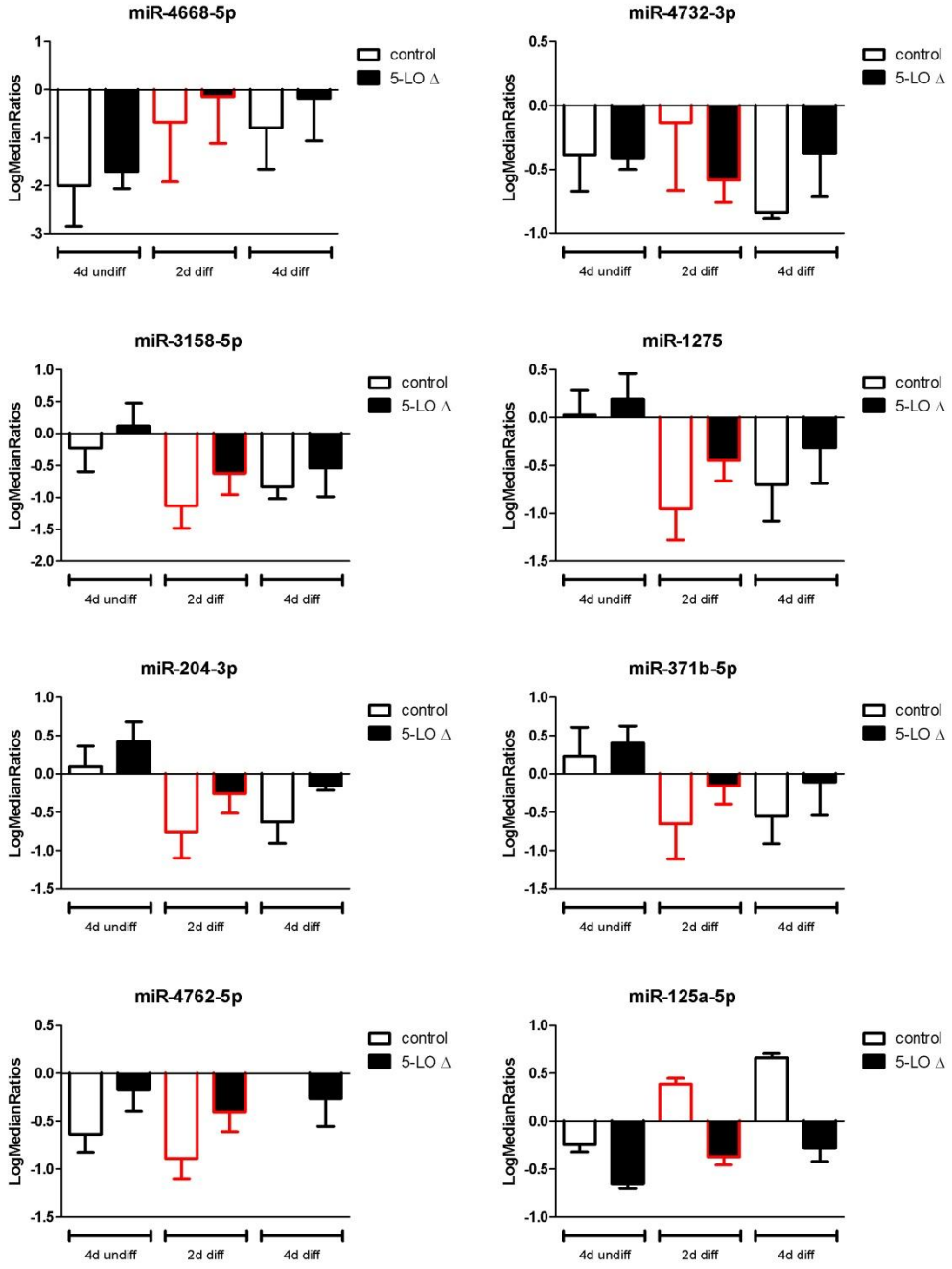
miR-4668-5p
miR-4732-3p
miR-3158-5p
miR-1275
miR-204-3p
miR-371b-5p
miR-4762-5p
miR-125a-5p
control
5-LO Δ
LogMedianRatios
4d undiff
2d diff
4d diff

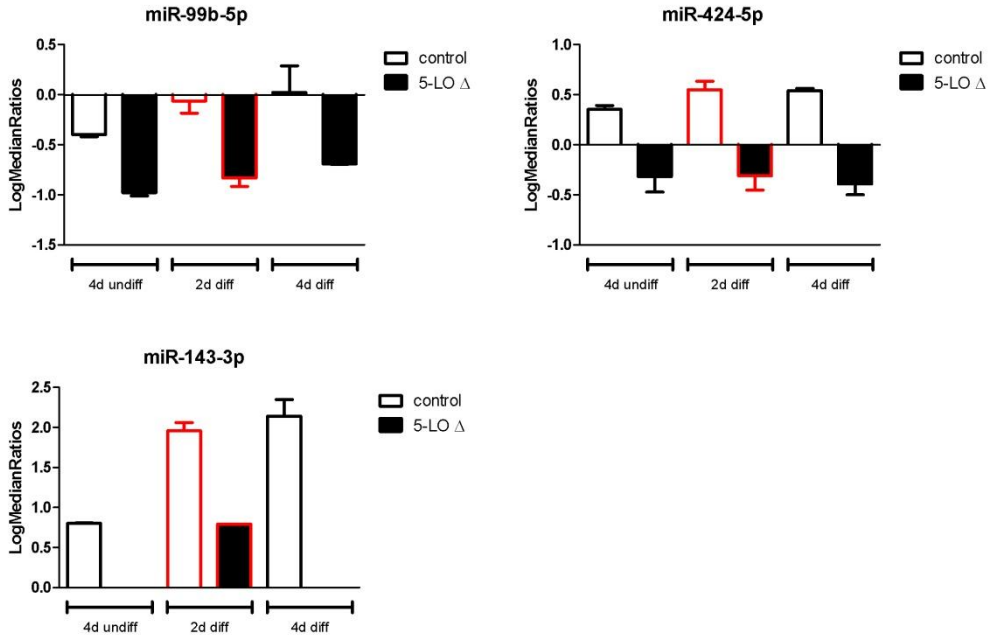

Figure 42: Microarray results of miRNAs affected by Δ5-LO

after two days of differentiation with TGFβ and calcitriol. MiRNAs with an x-fold induction <0.6 and >1.4, respectively (expression level in control transduced : expression level in Δ5-LO transduced MM6 cells) were chosen.

10.4 MiRNAs affected by Δ5-LO (undifferentiated cells)

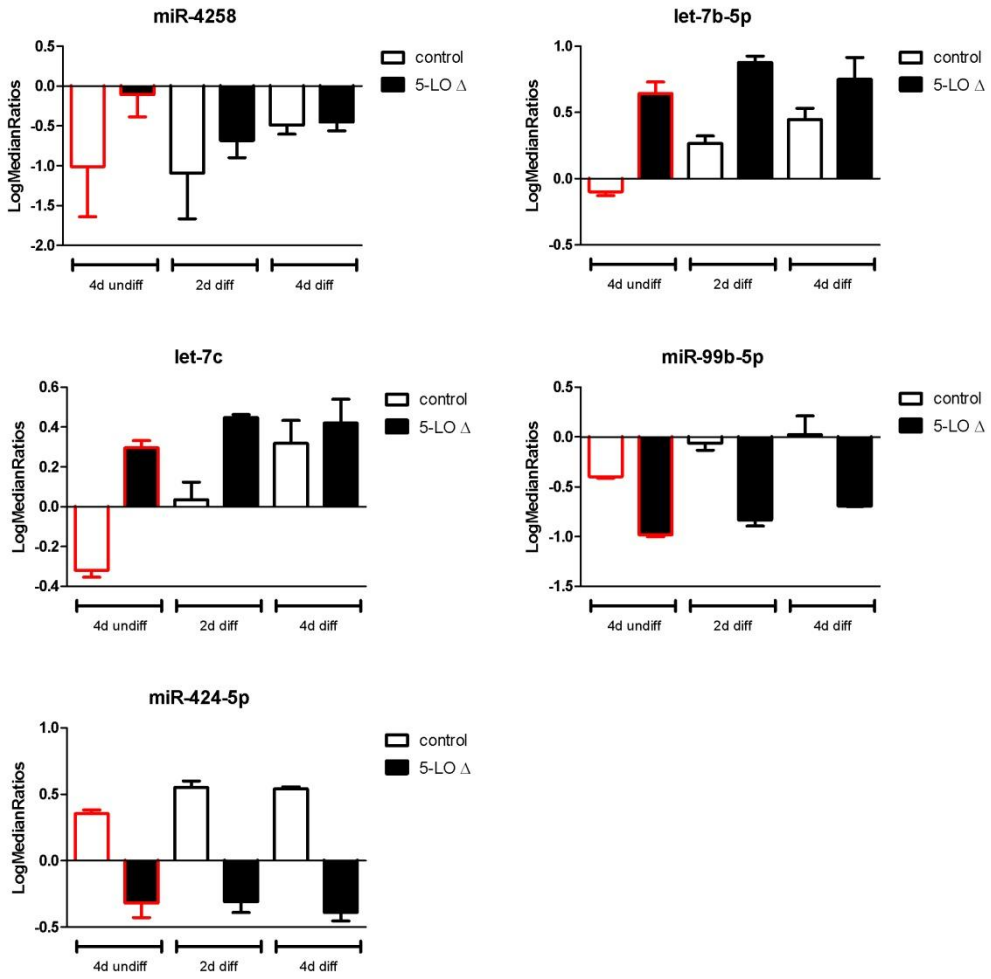

Figure 43: Microarray results of miRNAs affected by Δ5-LO in undifferentiated cells
MiRNAs with an x-fold induction <0.7 and >1.5, respectively (expression level in control transduced : expression level in Δ5-LO transduced MM6 cells) were chosen.

10.5 MiRNAs affected by TGFβ and calcitriol in control MM6 cells

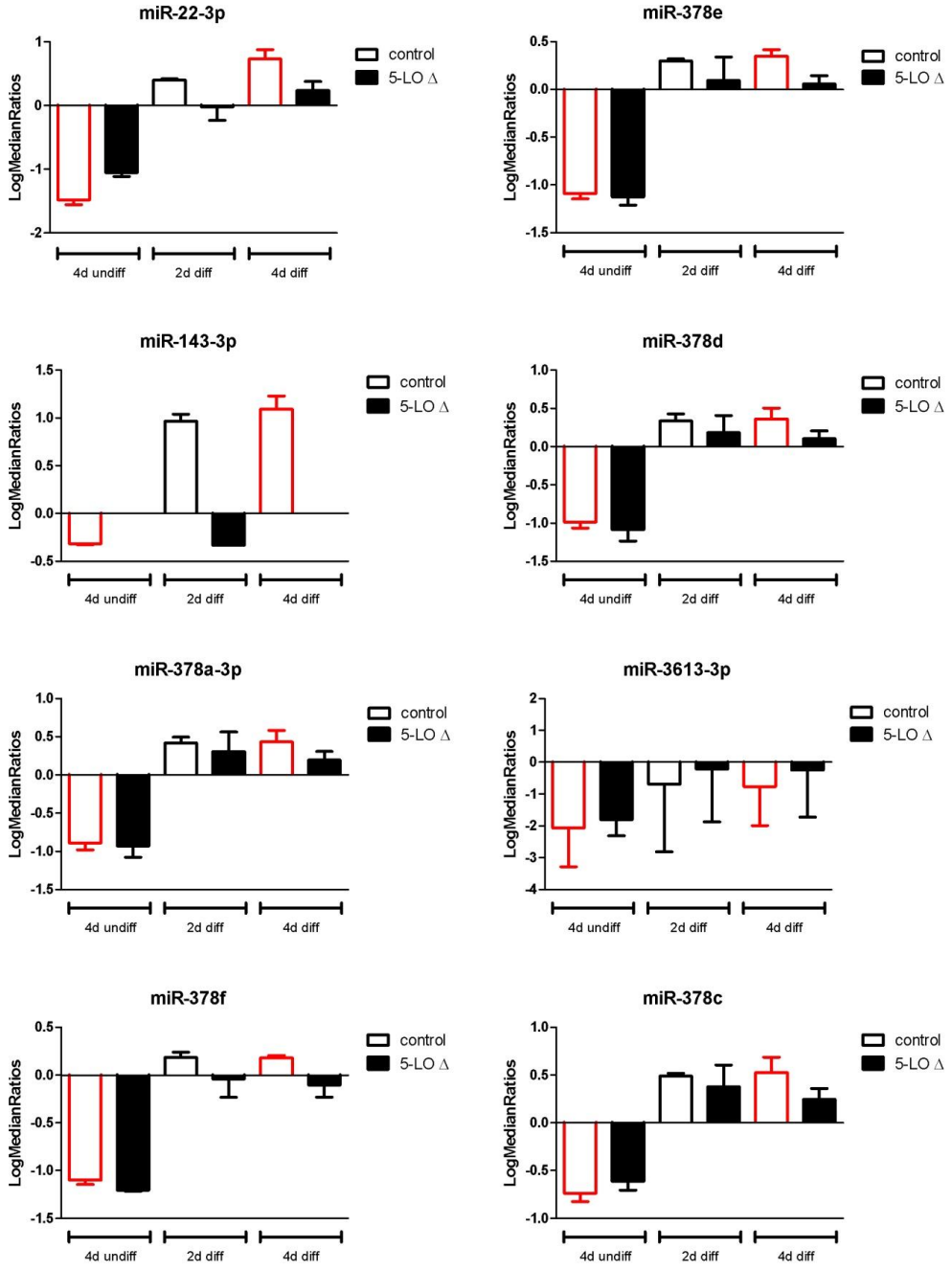

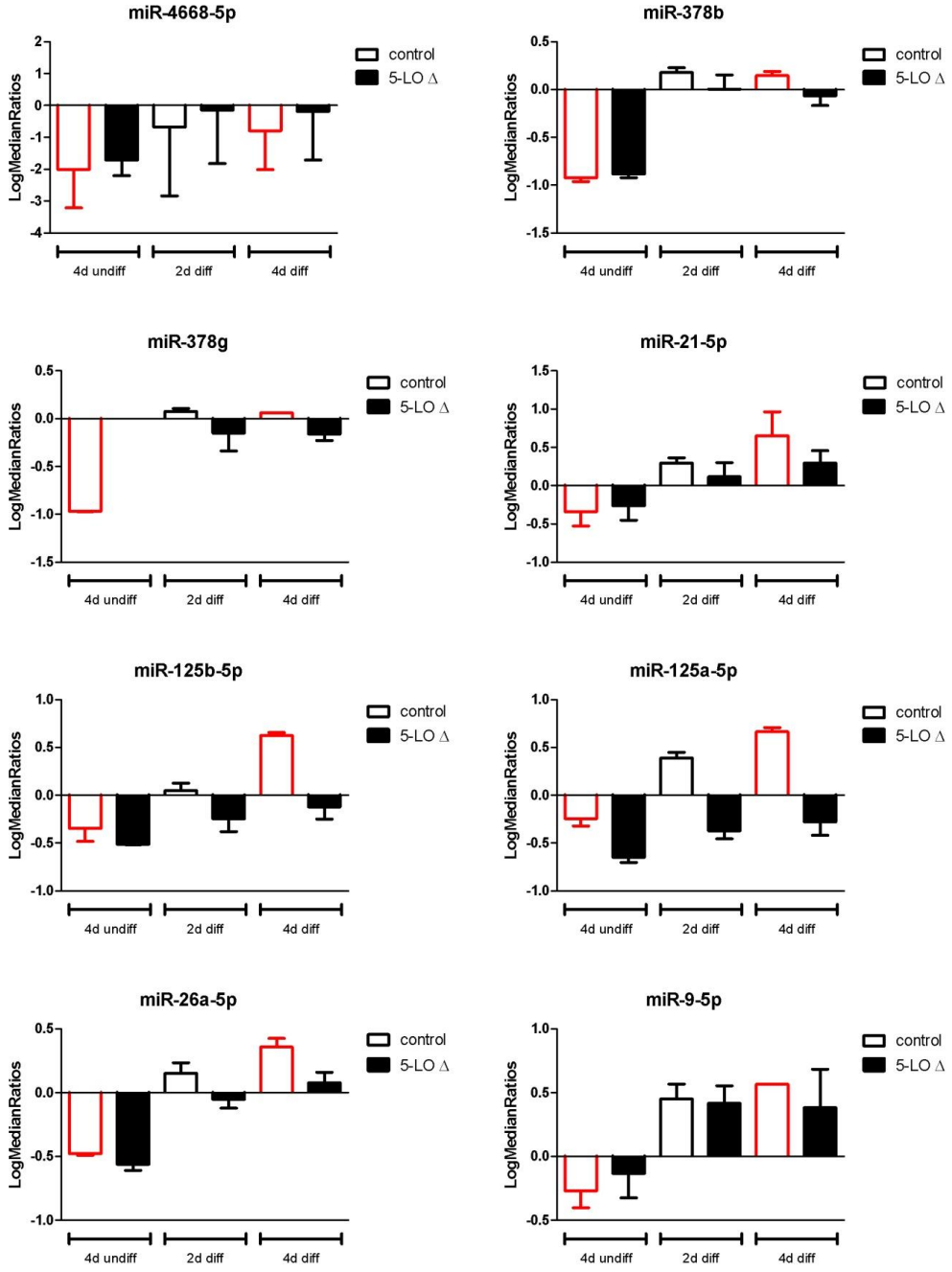
miR-4668-5p
miR-378b
miR-378g
miR-21-5p
miR-125b-5p
miR-125a-5p
miR-26a-5p
miR-9-5p
LogMedianRatios
control
5-LO Δ
4d undiff
2d diff
4d diff

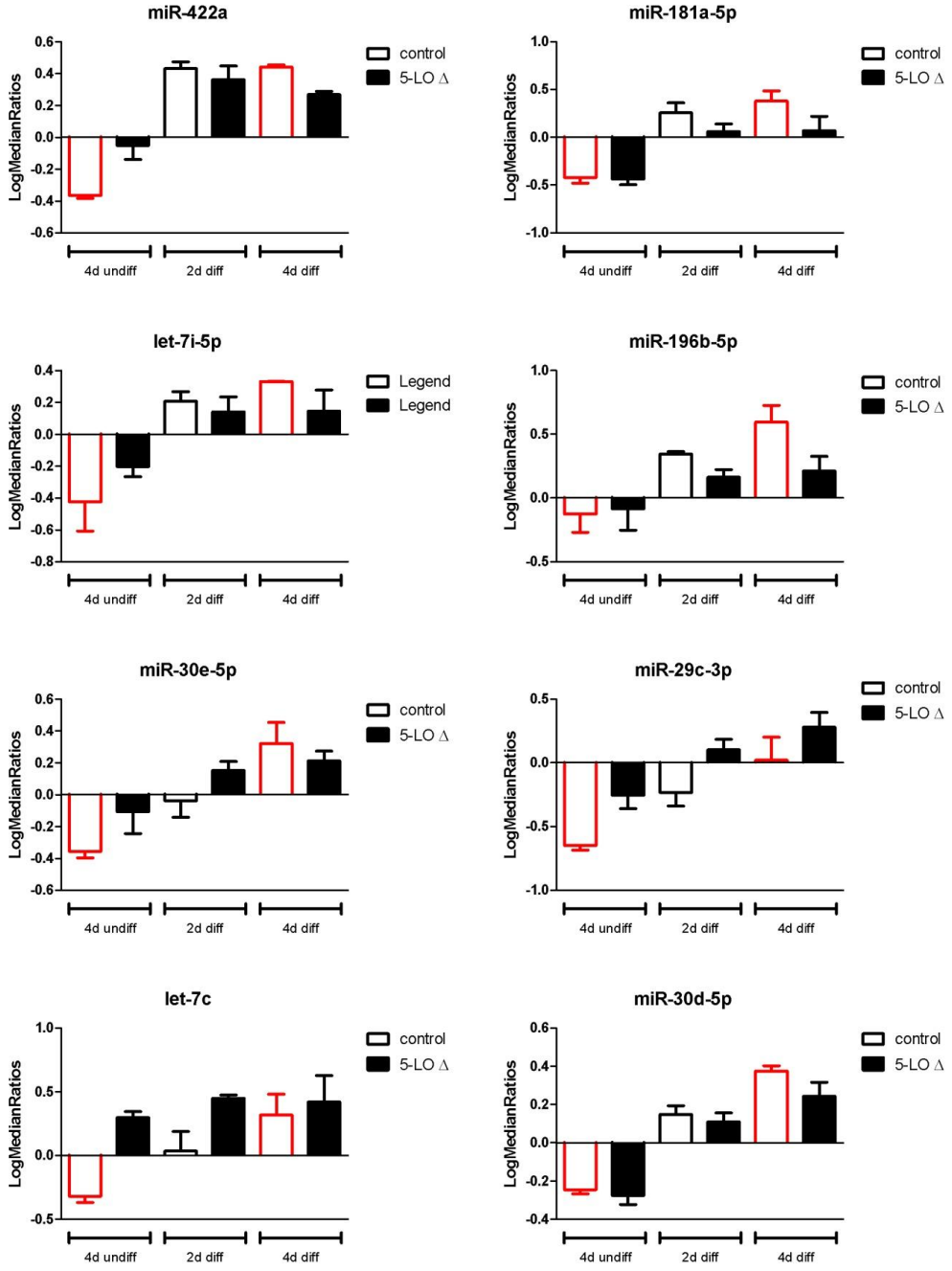
miR-422a
LogMedianRatios
0.6
0.4
0.2
0.0
-0.2
-0.4
-0.6
4d undiff
2d diff
4d diff
control
5-LO Δ
miR-181a-5p
LogMedianRatios
1.0
0.5
0.0
-0.5
-1.0
4d undiff
2d diff
4d diff
control
5-LO Δ
let-7i-5p
LogMedianRatios
0.4
0.2
0.0
-0.2
-0.4
-0.6
-0.8
4d undiff
2d diff
4d diff
Legend
Legend
miR-196b-5p
LogMedianRatios
1.0
0.5
0.0
-0.5
4d undiff
2d diff
4d diff
control
5-LO Δ
miR-30e-5p
LogMedianRatios
0.6
0.4
0.2
0.0
-0.2
-0.4
-0.6
4d undiff
2d diff
4d diff
control
5-LO Δ
miR-29c-3p
LogMedianRatios
0.5
0.0
-0.5
-1.0
4d undiff
2d diff
4d diff
control
5-LO Δ
let-7c
LogMedianRatios
1.0
0.5
0.0
-0.5
4d undiff
2d diff
4d diff
control
5-LO Δ
miR-30d-5p
LogMedianRatios
0.6
0.4
0.2
0.0
-0.2
-0.4
4d undiff
2d diff
4d diff
control
5-LO Δ

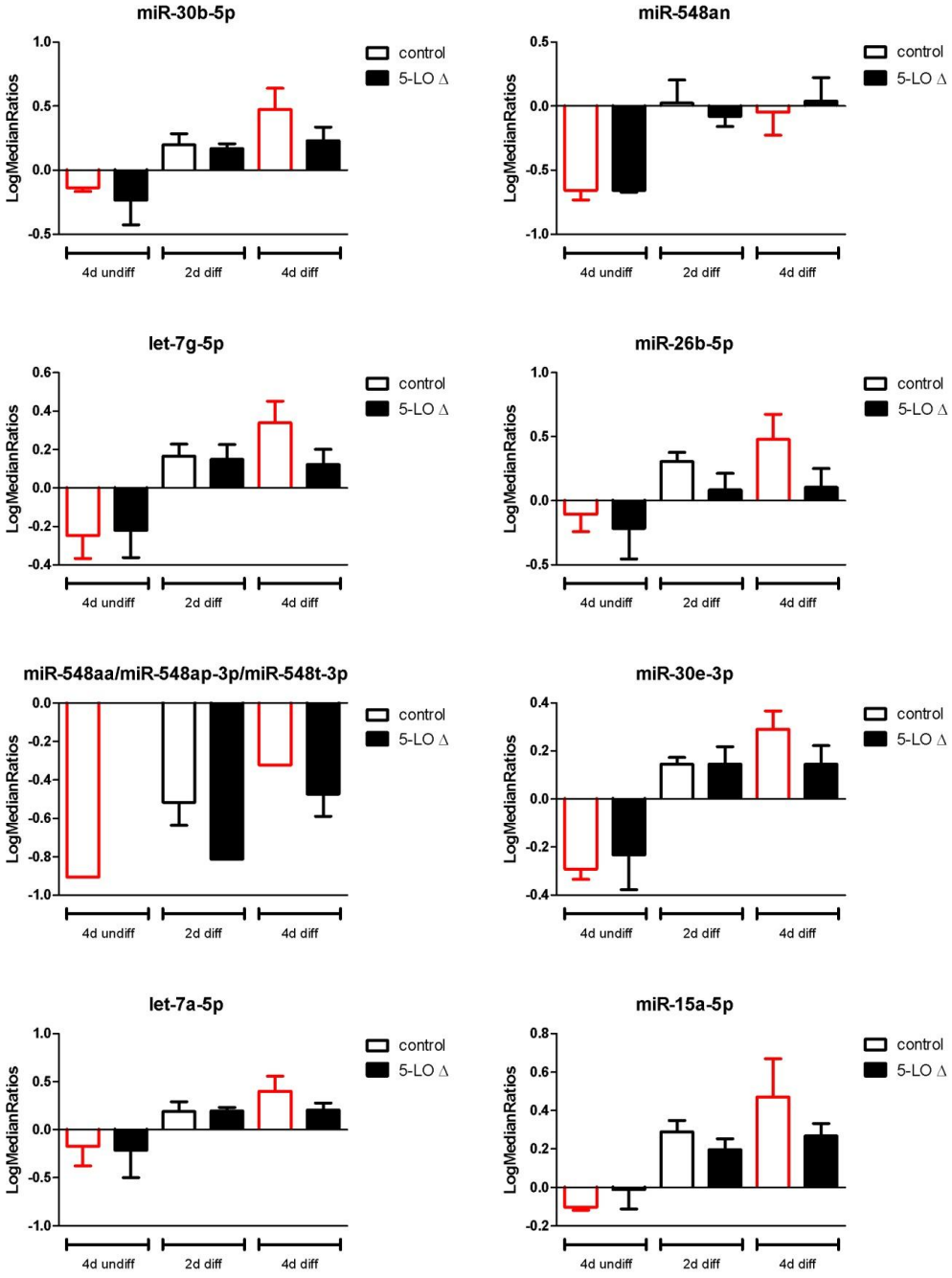
miR-30b-5p
miR-548an
let-7g-5p
miR-26b-5p
miR-548aa/miR-548ap-3p/miR-548t-3p
miR-30e-3p
let-7a-5p
miR-15a-5p
LogMedianRatios
control
5-LO Δ
4d undiff
2d diff
4d diff

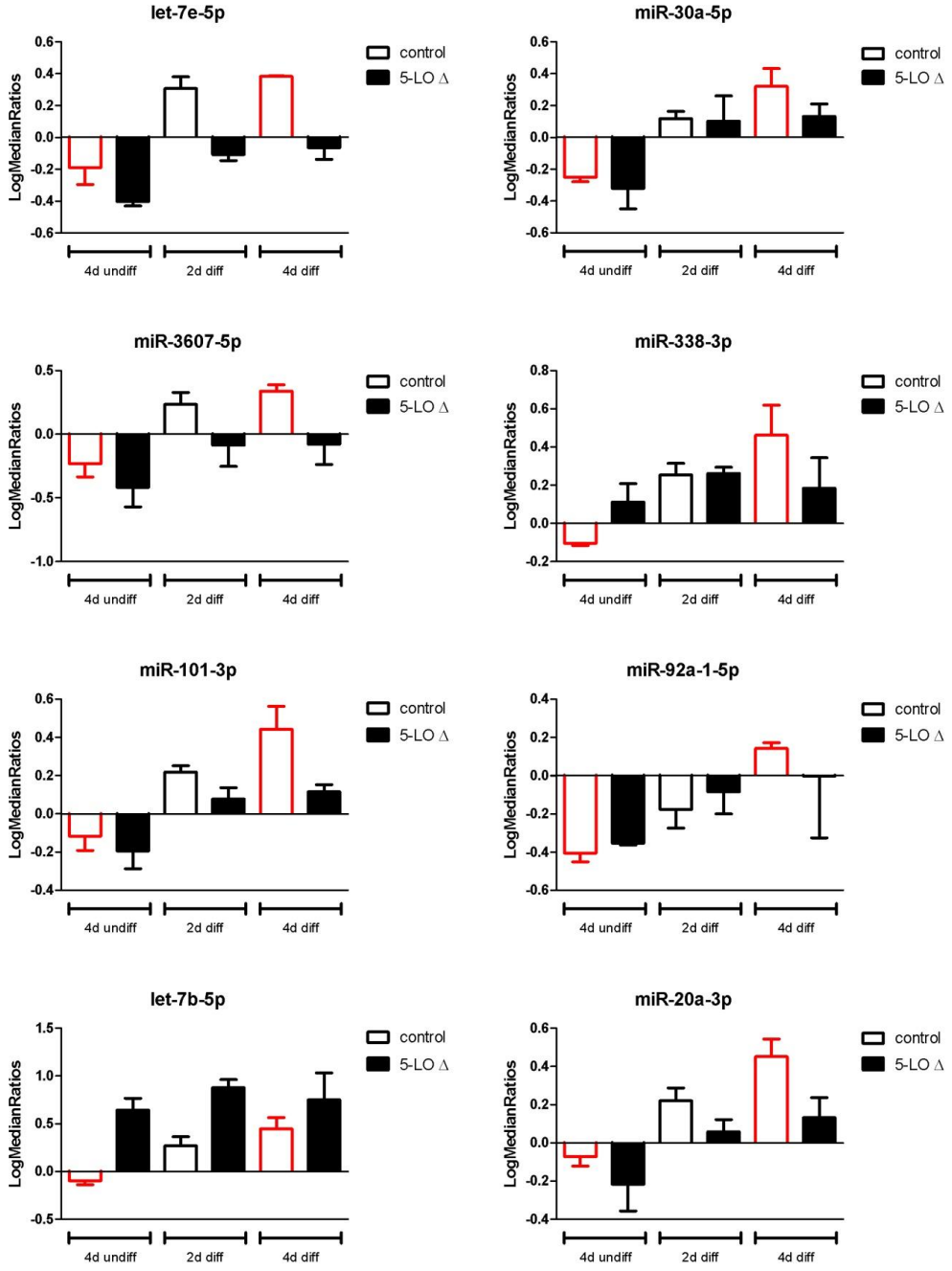
let-7e-5p
miR-30a-5p
miR-3607-5p
miR-338-3p
miR-101-3p
miR-92a-1-5p
let-7b-5p
miR-20a-3p
LogMedianRatios
control
5-LO Δ
4d undiff
2d diff
4d diff

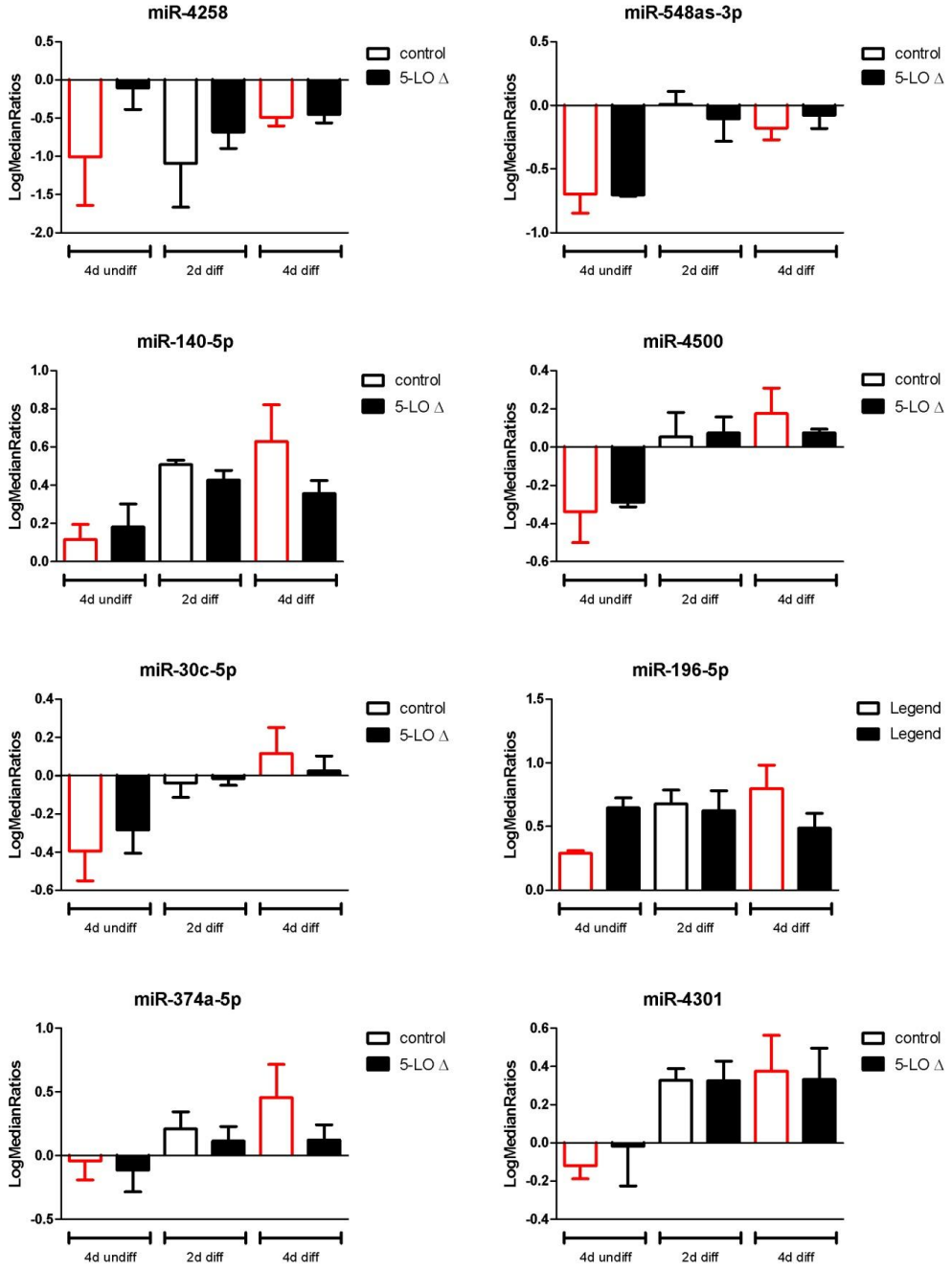
miR-4258
miR-548as-3p
miR-140-5p
miR-4500
miR-30c-5p
miR-196-5p
miR-374a-5p
miR-4301
LogMedianRatios
control
5-LO Δ
Legend
4d undiff
2d diff
4d diff

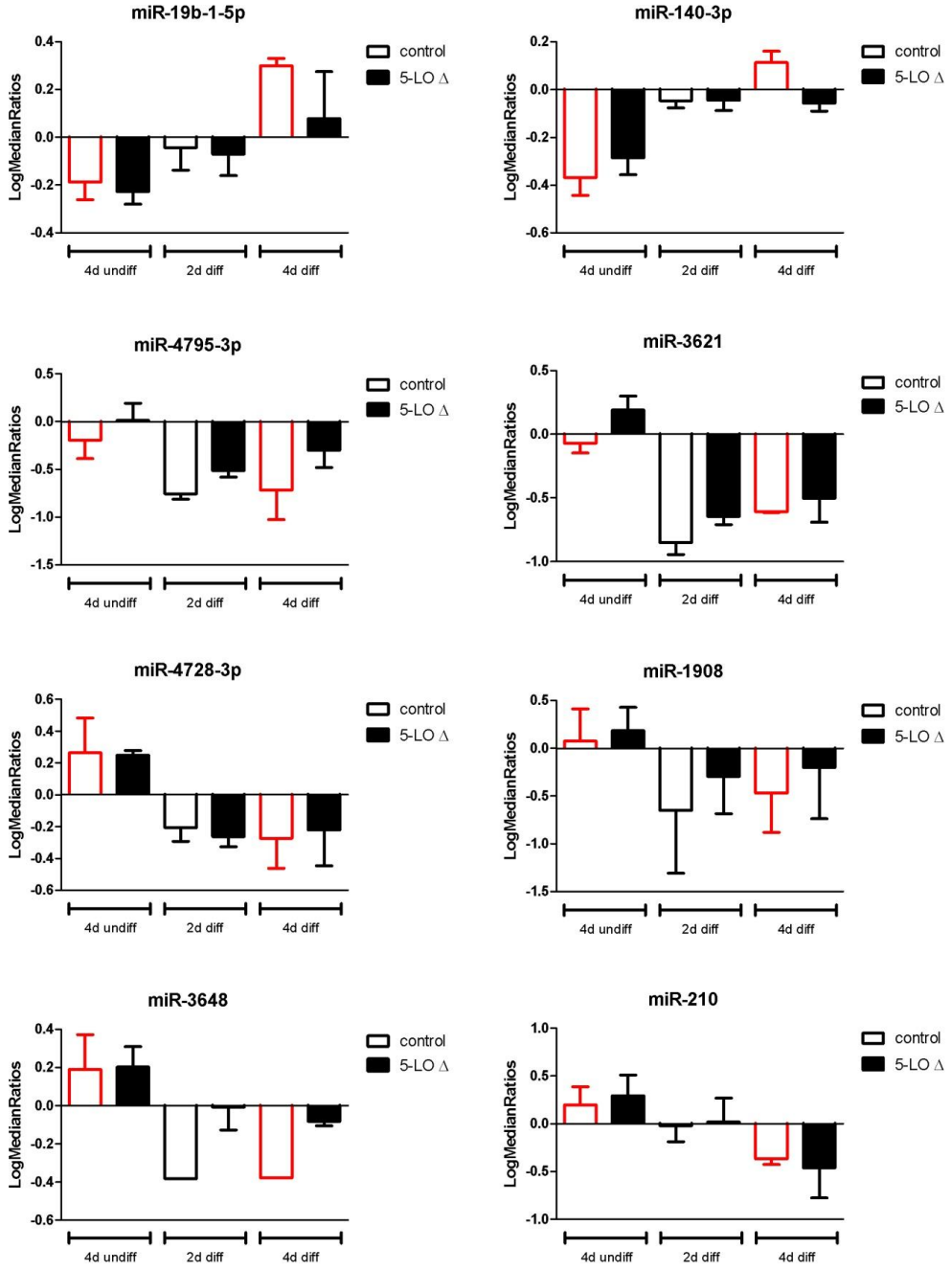
miR-19b-1-5p
miR-140-3p
miR-4795-3p
miR-3621
miR-4728-3p
miR-1908
miR-3648
miR-210
LogMedianRatios
control
5-LO Δ
4d undiff
2d diff
4d diff

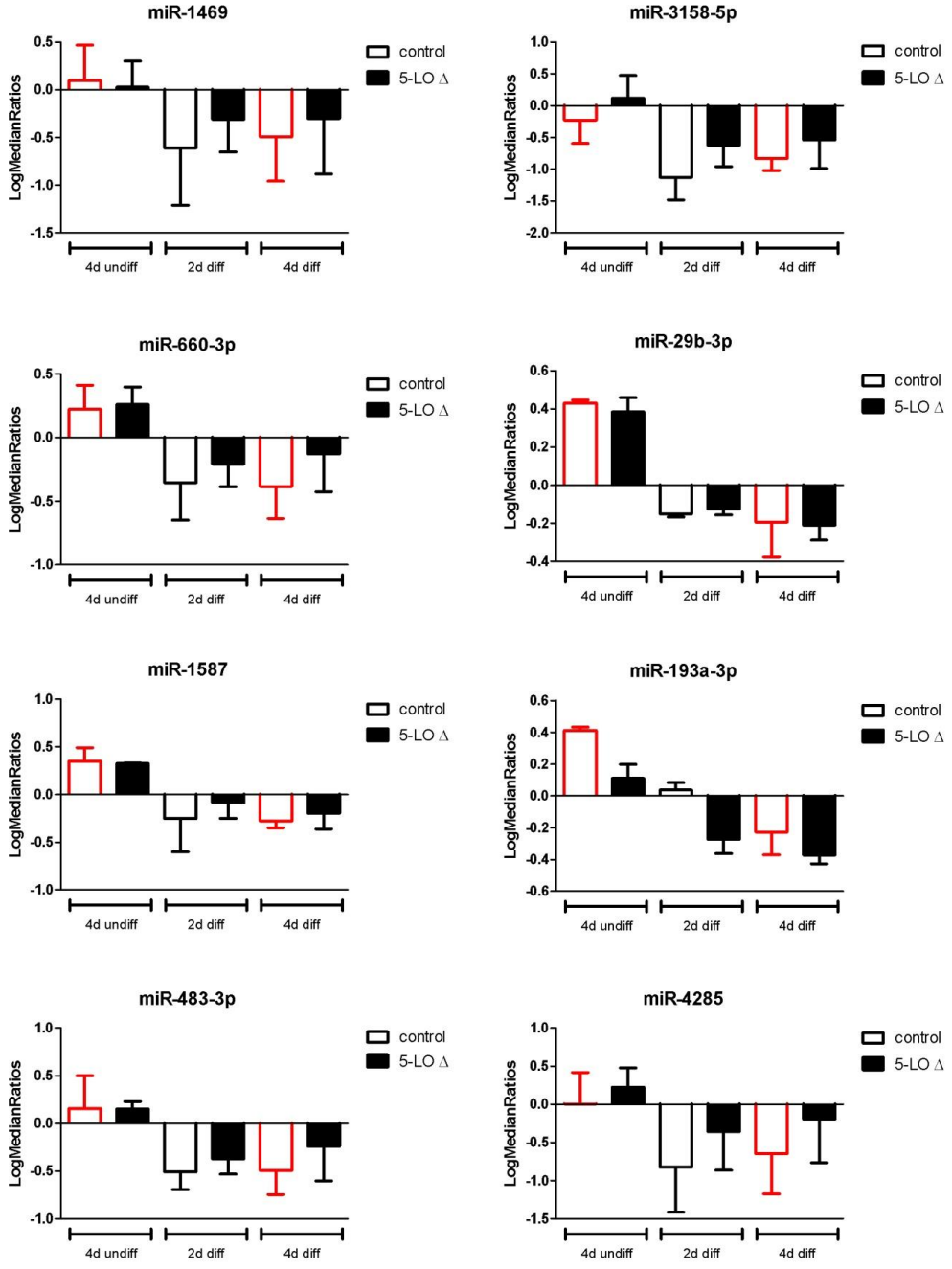
miR-1469
LogMedianRatios
0.5
0.0
-0.5
-1.0
-1.5
4d undiff
2d diff
4d diff
control
5-LO Δ
miR-3158-5p
LogMedianRatios
1.0
0.5
0.0
-0.5
-1.0
-1.5
-2.0
4d undiff
2d diff
4d diff
control
5-LO Δ
miR-660-3p
LogMedianRatios
0.5
0.0
-0.5
-1.0
4d undiff
2d diff
4d diff
control
5-LO Δ
miR-29b-3p
LogMedianRatios
0.6
0.4
0.2
0.0
-0.2
-0.4
4d undiff
2d diff
4d diff
control
5-LO Δ
miR-1587
LogMedianRatios
1.0
0.5
0.0
-0.5
-1.0
4d undiff
2d diff
4d diff
control
5-LO Δ
miR-193a-3p
LogMedianRatios
0.6
0.4
0.2
0.0
-0.2
-0.4
-0.6
4d undiff
2d diff
4d diff
control
5-LO Δ
miR-483-3p
LogMedianRatios
1.0
0.5
0.0
-0.5
-1.0
4d undiff
2d diff
4d diff
control
5-LO Δ
miR-4285
LogMedianRatios
1.0
0.5
0.0
-0.5
-1.0
-1.5
4d undiff
2d diff
4d diff
control
5-LO Δ

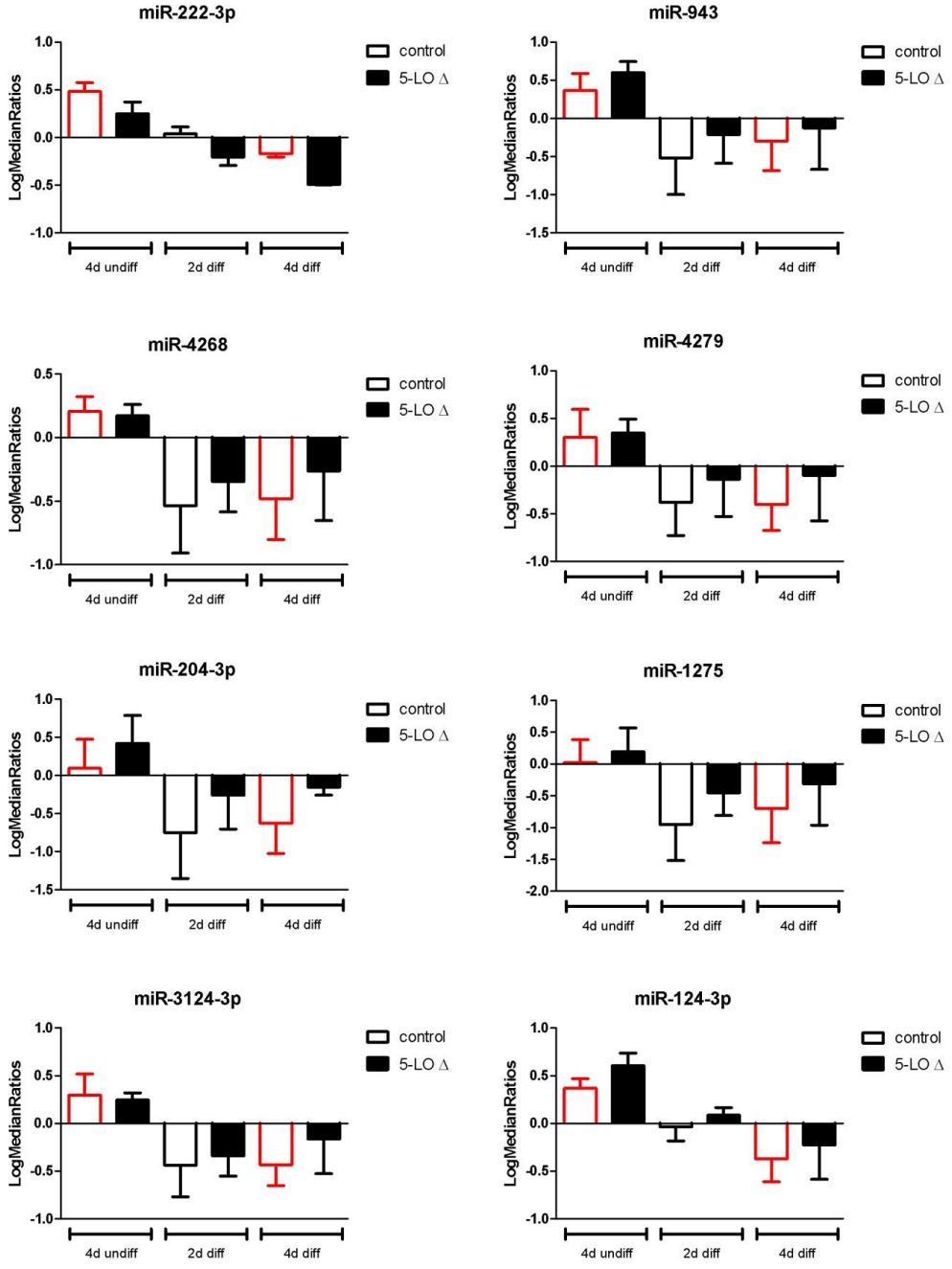
miR-222-3p
miR-943
miR-4268
miR-4279
miR-204-3p
miR-1275
miR-3124-3p
miR-124-3p
LogMedianRatios
control
5-LO Δ
4d undiff
2d diff
4d diff

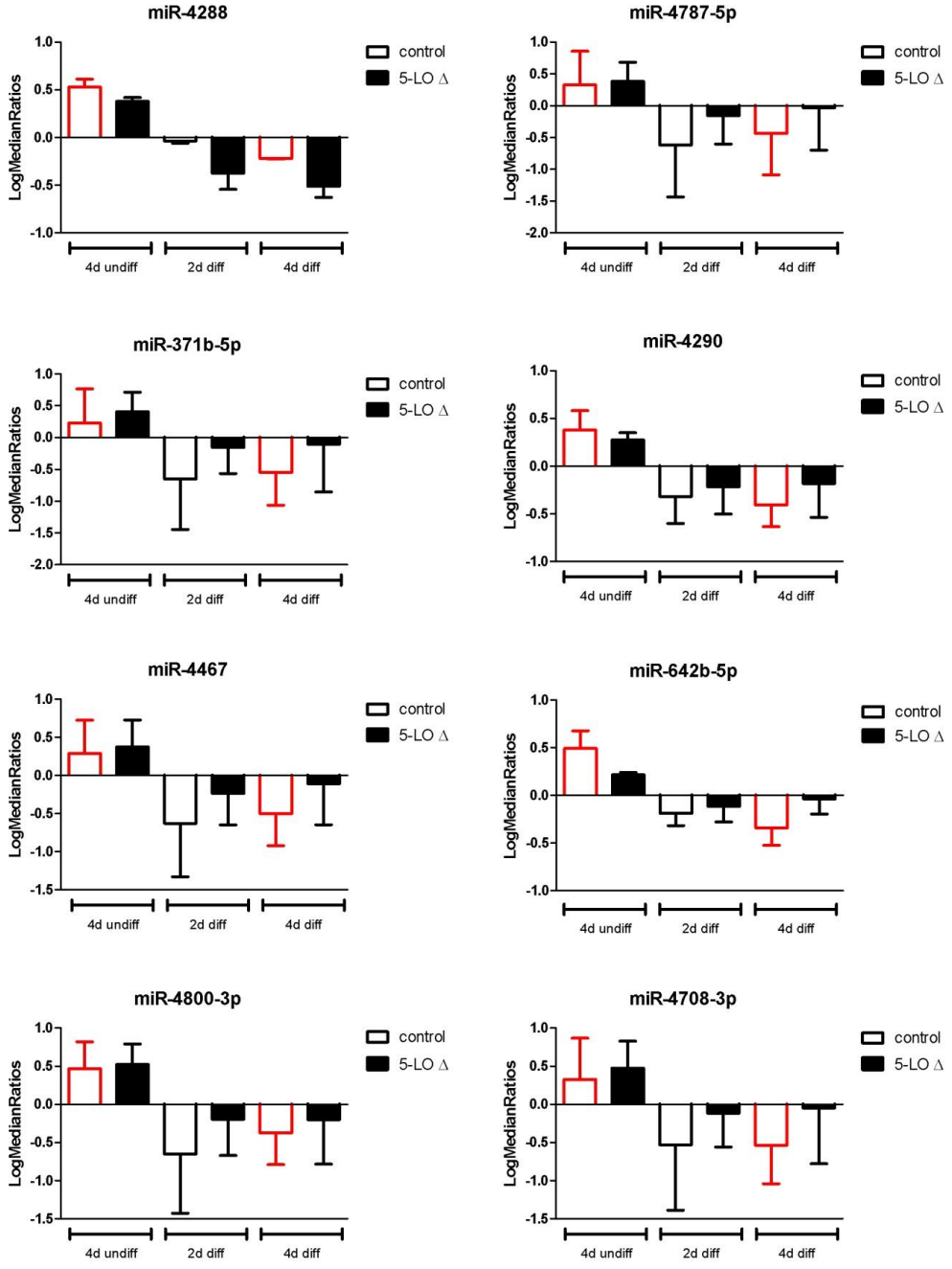
miR-4288
miR-4787-5p
miR-371b-5p
miR-4290
miR-4467
miR-642b-5p
miR-4800-3p
miR-4708-3p
LogMedianRatios
control
5-LO Δ
4d undiff
2d diff
4d diff

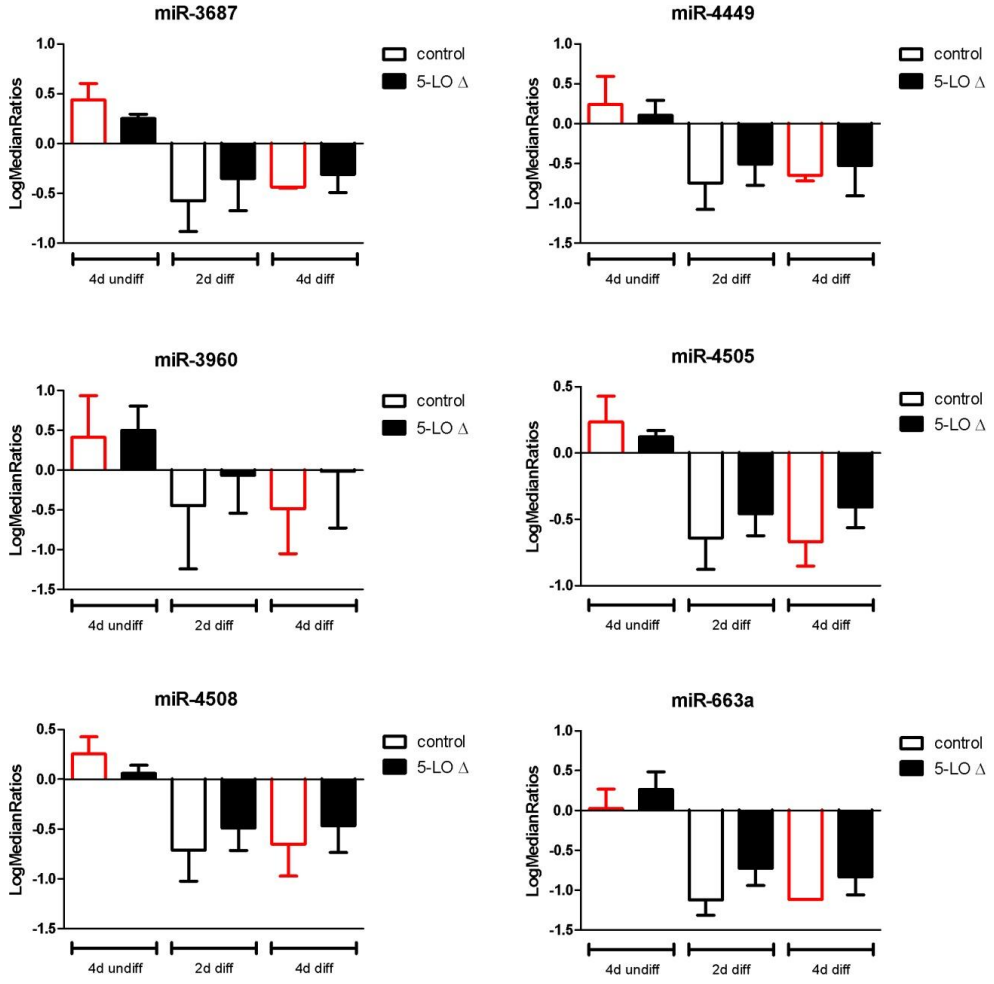

Figure 44: Microarray results of miRNAs affected by TGFβ and calcitriol
in MM6 cells. MiRNAs with an x-fold induction <0.7 and >1.4, respectively (expression level in differentiated : expression level in undifferentiated cells) were chosen.

10.6 MiRNAs similarly expressed in undifferentiated Δ5-LO and control MM6 cells

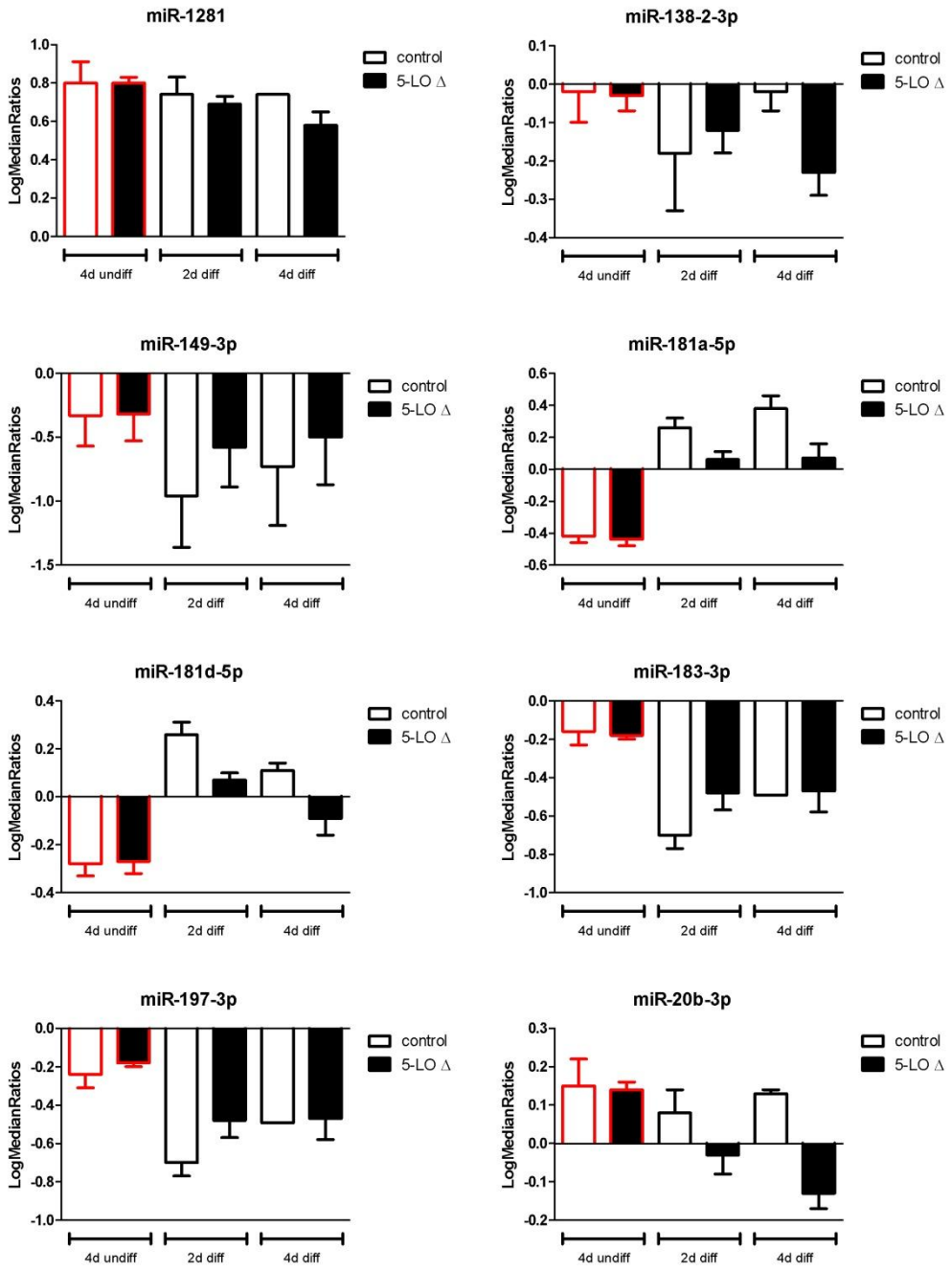

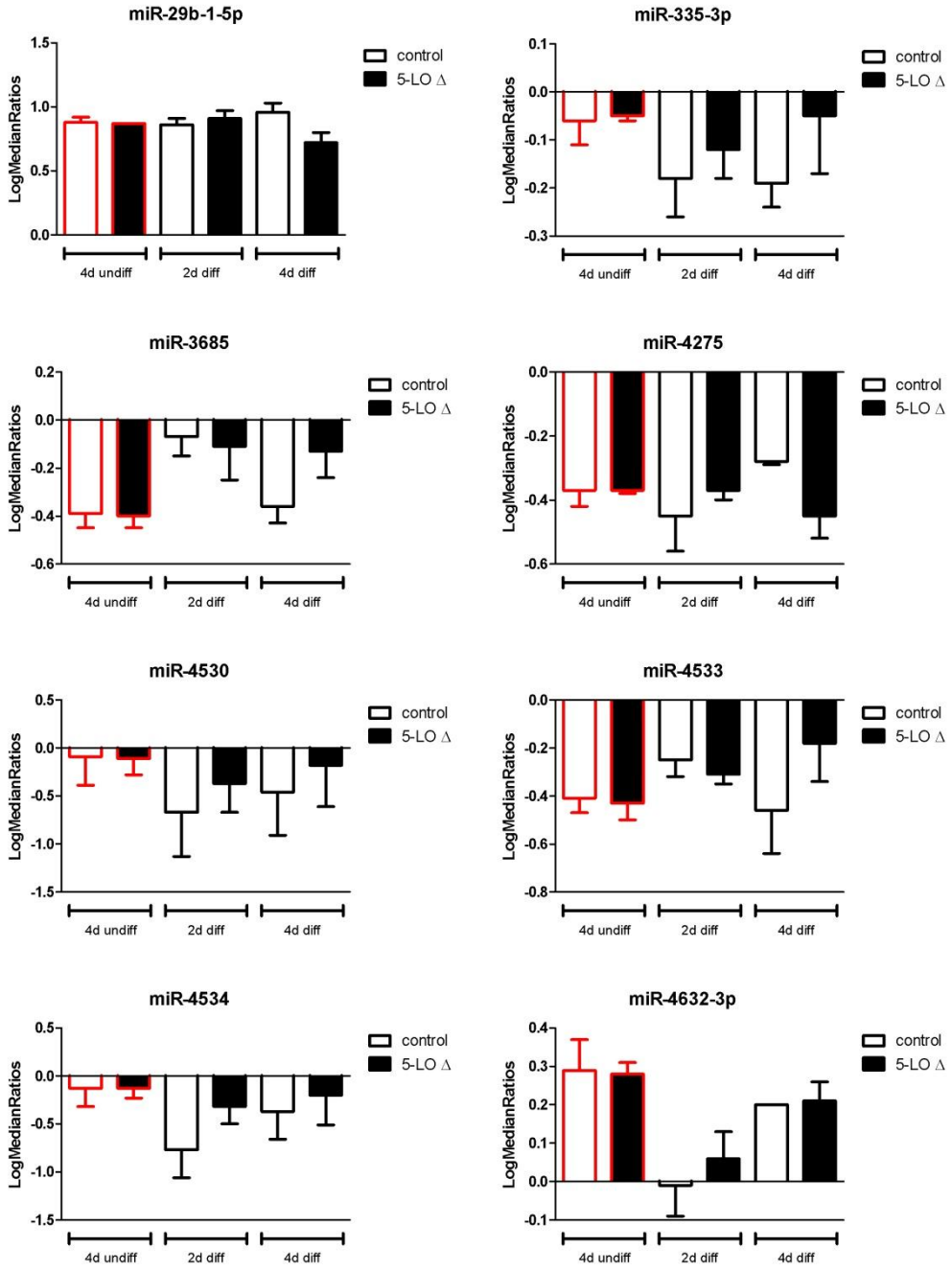
miR-29b-1-5p
miR-335-3p
miR-3685
miR-4275
miR-4530
miR-4533
miR-4534
miR-4632-3p
LogMedianRatios
control
5-LO Δ
4d undiff
2d diff
4d diff

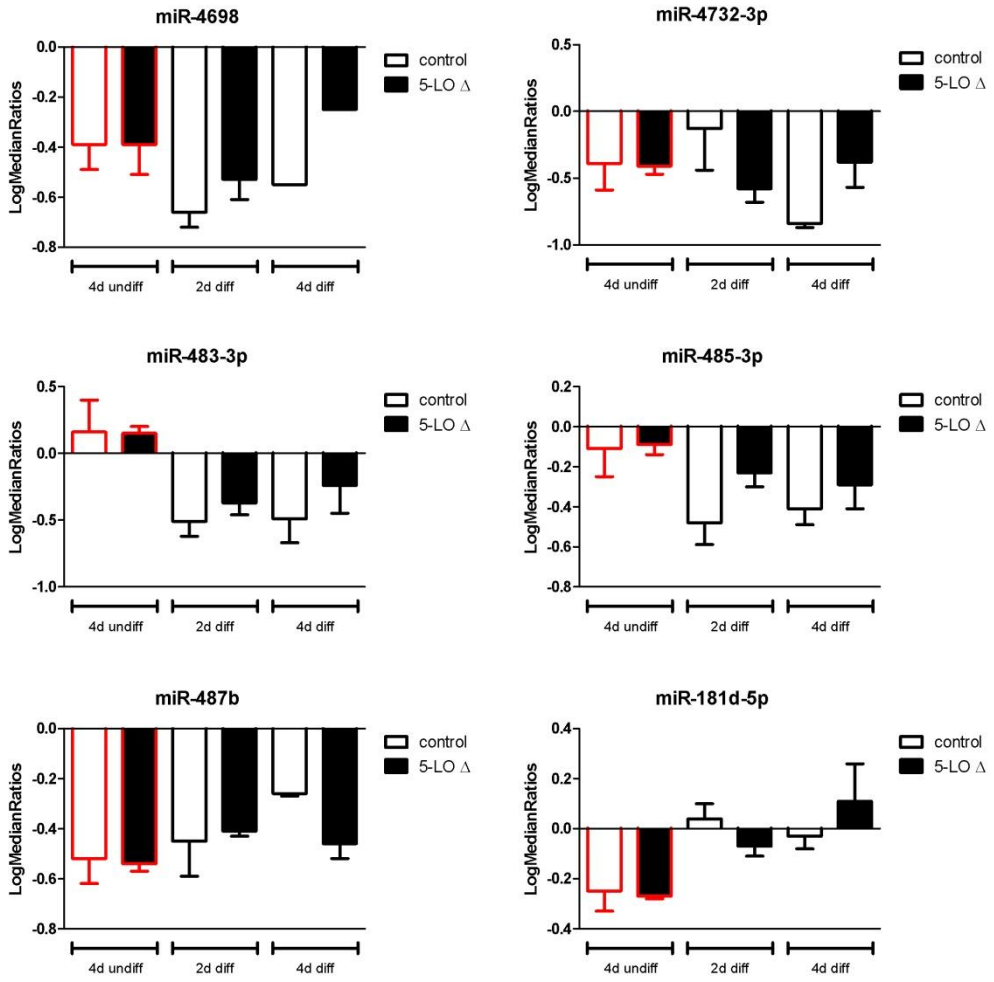

Figure 45: Microarray results of miRNAs which are similarly expressed
in control and Δ5-LO MM6 cells and differ in their expression after four days of differentiation.. MiRNAs with an x-fold induction <0.7 and >1.3, respectively (expression level in differentiated Δ5-LO cells : expression level in differentiated control cells) were chosen.

11 REGISTERS

11.1 Register of illustrations

11.2 Register of tables

14 EIDESSTAATLICHE ERKLÄRUNG

Ich erkläre hiermit eidesstattlich, dass ich die vorgelegte Dissertation selbständig angefertigt und mich nicht anderer Hilfsmittel als der in ihr angegebenen bedient habe, insbesondere, dass alle Entlehnungen aus anderen Schriften mit Angabe der betreffenden Schrift gekennzeichnet sind.
Ich versichere die Grundsätze der guten wissenschaftlichen Praxis beachtet zu haben.

Frankfurt am Main, 19. November 2014